DYNAMIC ANALYSIS OF A 1-1 SHELL AND TUBE HEAT EXCHANGER BY SUPERPOSITION OF SIMULTANEOUS FLOW RATE DISTURBANCES

by

HECTOR JOSE GUTIERREZ R.

Thesis submitted to the Senate of the University of Aston in Birmingham, in partial fulfillment of the requirements for the Degree of Doctor of Philosophy.

660.451 GUT

196313 24 AUG 1976

Department of Chemical Engineering,

Birmingham, March 1976.

TO

LIGIA

MARCELA IRENE

OSWALDO ANTONIO

ACKNOWLEDGEMENT

In recognition to the help and advice received, the author is very grateful to:

Universidad de Oriente of Venezuela, whose financial support made possible the undertaking of this project.

Mr. A.R. Cooper for his valuable supervision and suggestions during the development of the program and his patient review of the manuscript.

Dr.L.H. Hazelwood of the Computer Center and Drs. B.Gay and J.P. Fletcher of the Department of Chemical Engineering for their helpful comments and assistance during the development of the computer programs.

The technical and clerical personnel of the Department of Chemical Engineering who in many ways provided valuable assistance in solving experimental problems.

Miss N.P. Freeman for her diligent typing of this thesis.

SUMMARY

Extensive research on the dynamics of heat exchange between two fluids has been carried out in the past with orientation mainly towards the industrially important situation of a single variable process operating in the high turbulent flow region.

The need for a more general understanding of the phenomenon and the wider requirements of more recent processes justified the investigation of heat exchange under multivariable conditions and at lower Reynolds numbers, particularly in the transition and laminar regions.

Based upon the experience and results reported for the turbulent regime the techniques of analysis were extended to investigate the region of present interest. This meant treating the system as a linear one with combination of the simultaneous disturbances by superposition as required by linear system theory.

Two mathematical models were developed for the purpose, based on the description of the process by a set of four partial differential equations. The first model, representing the system in the time domain, is an explicit numerical algorithm applicable to countercurrent and parallel flow schemes under single or simultaneous flow disturbances. The effect of these disturbances on the heat transfer coefficients can be chosen as the exact ones given by the current correlations or as the corresponding linearised ones. This model also includes the dynamics of the control valves regulating the flow rates. The second method representing the system in the frequency domain is a linearised version of the same set of differential equations, expressed as a transfer function, and also applicable to the case of countercurrent and parallel flow schemes, under single or double variable operation. Both models were evaluated by

computer for relevant operating conditions.

To test the models, a liquid-liquid 1-1 shell-and-tube heat exchanger was operated under several sets of conditions, and the experimental results indicated that:

(i) The superposition of two flow disturbances in the heat exchanger can be simulated adequately by use of linear system principles in both the time domain and the frequency domain.

(ii) Although in general the data collection at low Reynolds numbers has a larger degree of uncertainty, the process dynamics in this region of the time domain can be described satisfactorily by the model proposed, for both single and double variable operation.

(iii) The quality of representation in the frequency domain was less satisfactory for the tube-side outlet temperature and had severe limitations for the shell-side outlet temperature. The fact that this representation was based on a fully linearised set of convective equations, as required for application of the Laplace transformation, makes it less useful in a region where thermal diffusion assumes greater significance.

TABLE OF CONTENTS

LIST OF TABLES

LIST OF FIGURES

Page No.

CHAPTER 1

STATEMENT OF THE PROBLEM

Extensive research has been conducted into the dynamic analysis of heat exchangers subject to single variable disturbances, but very little on the case of simultaneous disturbances. This work is an attempt to extend to the multivariable case, the principles which govern the response of liquid-liquid heat exchangers disturbed by a single variable. Thus in the same way that most of the previous analysis has been done using basically linear techniques it is thought likely that the multivariable case can be analysed by the application of the superposition principle which is also a linear concept. The present work examines this possibility.

The insight and conclusions obtained in this work can be generalized to all flow systems of the distributed parameter type which can be described by mathematical structures of the type developed here.

The specific objects are:

(1) Deduction and development of a mathematical model for a liquid-liquid, 1-1 shell-and-tube heat exchanger considering the arrangements of countercurrent flow, parallel flow, heating (hot fluid in tubes), and cooling (hot fluid in shell) for the cases of disturbances in shell flow and tube flow, either individually or simultaneously. Furthermore the work aimed to examine the superposition of these disturbances relative to their separate effects.

(2) Development of digital computer simulation for the model in both the time domain and frequency domains, versatile enough to cover

the several combinations of conditions previously mentioned.

(3) Construction and assembly of an experimental system able to realize the characteristics of the model as closely as possible within the available means.

(4) Development of experimental techniques and collection of experimental data for the different sets of conditions in order to verify the adequacy of the mathematical model.

(5) To analyse and compare experimental and simulated results, draw conclusions about the quality of the model, its implications and limitations, and to present suggestions of areas deserving further research.

The areas of work previously defined and their corresponding relationships are presented graphically in Fig.1.1 which is a block diagram of the range and sequence of analytical and experimental work achieved during this project.

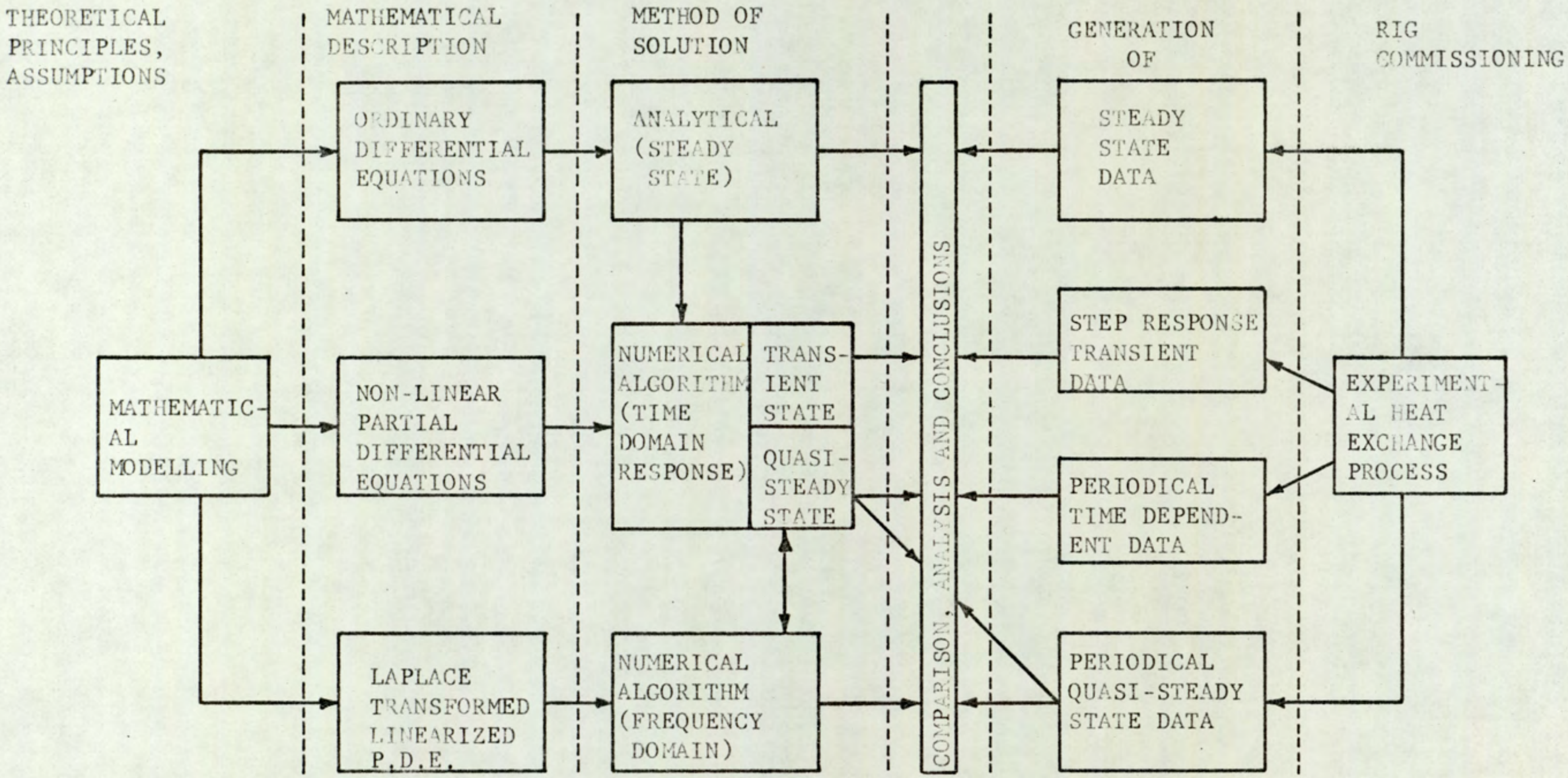

FIG.1.1. BLOCK DIAGRAM OF THE RANGE AND SEQUENCE OF ANALYTICAL AND EXPERIMENTAL WORK ACHIEVED DURING THIS PROJECT.

CHAPTER 2

INTRODUCTION

Almost every physical system of practical importance when represented by a rigorous mathematical description becomes too complicated to be thoroughly analysed. On the other hand, if the description is made too schematic, the resulting analysis may be misleading or inadequate. It is necessary then, to reach a compromise between the complexity of the model and the level of insight needed for the system.

It happens that most real systems are nonlinear when rigorously examined and therefore the well-established techniques developed to analyse ideal linear systems do not apply to them or apply only in a restricted manner. The study of such systems requires therefore, the use of the less evolved nonlinear techniques which generally lead to more complicated procedures, or the 'linearization' of the description in order to make it suitable for treatment by linear techniques. It is the requirement that any description of a real system must be solvable to render it useful that compels the analyst to compromise.

In general, the behaviour of a system is described by a set of differential equations whose nature reflects the nature of the system and whose solution allows prediction of the response of the system to a given disturbance. Unfortunately, the practical analytical solution of differential equations is, so far, restricted to a relatively few simple cases. Most current differential equation solutions require an undeserved amount of work, if solvable at all, and in many cases the solution itself is so involved that it cannot be used immediately.

The computer is then the alternative. Since the advent of computers (both digital and analog) great progress has been achieved in the solution of mathematical models which were impossible or too difficult to solve analytically or by manual numerical methods. However, since analog computers can only operate on one independent variable at a time, partial differential equations cannot be solved directly and the 'discretisation' technique must be employed. Digital computers on the other hand, by means of adequate numerical methods can solve any type of differential equation very efficiently, and though the programming takes more time and effort than the 'patching' of the same problem in an analog computer, the powerful numerical techniques introduced, very often more than offset those inconveniences.

Modelling of heat exchange equipment of the distributed parameter type has followed the general trend previously described. The relatively simple process of heat transfer that takes place in an ordinary heat exchanger has to be described imposing several simplifications of a hydrodynamic and thermodynamic type in order to obtain a tractable mathematical model. The heat transfer phenomenon in a tubular heat exchanger is, strictly speaking, a complex process since heat is transferred by the combined mechanisms of conduction, convection and radiation from and to fluids moving with non-uniform velocity profiles, with spatially varying properties, across a medium of more or less complicated geometry and whose properties also change with position. Obviously a mathematical expression that exactly fits the previous description becomes too cumbersome to be useful, so that general simplification like negligible heat transfer by radiation (and sometimes by axial conduction), constant physical properties of the media and flat velocity profiles are generally assumed, if operating conditions of the prototype reasonably allow, to attain a more practical mathematical expression.

The cause-and-effect relationship, the really useful form of mathematical description, is obtained by the solution of the model, stage at which three alternatives are available: Mathematical analytical solution, numerical solution and analog solution. In general, the simpler the model the larger the possibility of finding an analytical solution, but the more restricted the description of the system. The numerical solution, however, can cope with descriptions of variable complexity but instead makes necessary a digital computer to carry out the calculations as soon as the complexity of the model increases the number of calculations required to reach a solution. Finally, the analog solution requires the use of an analog computer or the construction of specialised analog devices, themselves very specific analog computers.

If the solution of the parameter distributed model of such a heat exchanger is attempted in an analog computer, the system has to be simulated by a series of lumped parameter modules (equivalent in some way to the use of finite differences instead of derivatives in the numerical approach). Furthermore, if the model involves some nonlinear relationships and a rather large number of modules is necessary to ensure accuracy, then the number of hardware components (operational amplifiers, multipliers, potentiometers, function generators) might be exceptionally large.

A thorough study of heat exchanger dynamics includes its analysis in the time domain and in the frequency domain since both areas yield complementary information of the general system behaviour. The frequency domain analysis makes use of the Laplace transform technique which is a linear system concept and therefore requires that any model including nonlinear relationships be linearised before the Laplace transform can be applied. Within this context, the frequency response results ought to be considered as an approximation.

The analysis in the time domain is a more direct procedure that makes use of the finite differences approach when the numerical solution is necessary. Such a solution of a set of partial differential equations, like the one developed to describe the heat exchanger used in this work can be of great versatility to represent a wide range of operating conditions and to include a considerable amount of detail.

Since one limiting factor of the quality of a model lies in the quality of its parameters, special attention was put on the choice of the film coefficient correlations, particularly the shell side correlation where no definite agreement has yet been reached.

CHAPTER 3

PREVIOUS WORK

In this chapter a comprehensive review of the literature so far generated on the dynamics of heat exchangers is presented as the foundation of the present work. The papers and reports are analysed with emphasis on the most significant contributions to the field from the point of view of mathematical treatment and experimental techniques, as well as the degree of agreement reached between these two aspects of studying the problem.

Due to the importance of finding appropriate correlations for the individual heat transfer coefficients on both sides of the heat transfer wall, a review of some important works carried out on this subject is also presented.

3.1 DYNAMIC RESPONSE

The analysis of the dynamic behaviour of a heat exchange process can be classified in several ways, by no means exclusive of each other:

(i) According to the type of thermodynamic model proposed:

- (a) Convective model, when all the heat is transferred by the convection mechanism,
- (b) Dispersion model, when part of the heat is transferred by one or several forms of diffusion mechanism, besides the convective transfer.

(ii) According to the type of mathematic structure:

- (a) Exact model, linear or nonlinear,
- (b) Linearized model.

(iii) According to the type of condition disturbed:

(a) Temperature forced, which yields linear models when the effect of temperature on the physical properties of the fluid is neglected,

(b) Flow forced, which yields varying parameter models.

(iv) According to the domain of the solutions proposed:

(a) Time domain solutions, which yield the transient response of the system,

(b) Frequency domain solutions, which yield the actual frequency response of the system.

The time domain solution can be achieved by several methods

(a) Direct analytical integration of the mathematical model proposed, if mathematical complexities allow,

(b) Analog simulation in a passive or active analog computer by 'lumping' of the distributed components of the exchanger,

(c) Digital Computer simulation by a numerical procedure based on 'discretization' of the continuous variables of the model.

The frequency domain solution is obtained by Laplace transformation of the differential equations that describe the system operation, and replacement of the Laplace operator by the complex frequency $j\omega$.

(v) According to the experimental technique used:

(a) Transient testing when a noncyclic signal is used as disturbance,

(b) Sinusoidal testing when a sinusoidal signal is used, and

(c) Pulse testing when an analytical pulse is used as disturbance.

Because many of the papers reviewed cover several classes within those defined above and analyse different types of cause-effect relationships over a wide variety of conditions, it is not possible to segregate them into groups according to a specific characteristic, without significant entanglement. It is a fact that each single work could be classified in most of the groups and therefore the review would become very repetitive and dispersed.

3.1.1 The Most Convetional Approaches

It is understandable that after the initial steps toward development of a continuous quantitative process technology by Mason (63), Haigler (40) and Bristol et al (7), the first works properly on heat exchange dynamics approached the subject by analysing the 'percolation' problem in which heat is exchanged between a solid surface and a fluid stream flowing along it. Profos and Diss (77) studied this process in the case in which the excitation of the system was the fluid inlet temperature variation.

Takahashi (87) extended the analysis to typical heat exchange processes of the parallel, counter-current and mixed types. He classified the processes into four cases:

(1) Both fluids unmixed (parallel and counter-current flows); this is the case that considers the whole system to be of the distributed parameter class;

(2) One fluid mixed (i.e. lumped);

(3) Both fluids mixed; and

(4) Percolation.

The model he formulated for the first case would consider four different solutions.

1a. Completely neglected shell and tube wall capacities;

1b. Neglected tube wall capacity only;

1c. Inclusion of both wall capacities, with conductivities considered infinite in the transverse direction and zero in the axial direction;

1d. Same as 1c but with finite shell wall conductivity.

Partial differential equations were set up to represent each stream and each wall (when not neglected) for each case; then after assuming constant system parameters, the set of partial differential equations was solved for the steady state (thus yielding a set of ordinary differential equations) and several transfer functions of the form

$$F(j\omega) = \frac{\text{OUTLET TEMPERATURE OF THE COLD FLUID}}{\text{INLET TEMPERATURE OF THE HOT FLUID}} \qquad (3.1)$$

for changes with position were obtained. The author compared the properties of the heat exchange process by the vector-loci method for the three combinations of supply, demand and velocity ratios. The effect of solid capacities was also shown and although no extensive experimental data was reported this work was a significant advance on the unified study of heat exchange process dynamics.

Shortly afterwards Gould (36) presented a thorough and systematic analysis of the behaviour and control of the heat transfer process, stressing the fact that these systems are usually described by nonlinear partial differential equations whose analytical solutions are facilitated by linearization techniques. Since procedure restricts the application of the linearized equation, he introduced a systematic lumping technique which greatly reduced the effort involved in the solution (37).

The general equations of convective heat transfer elements were deduced and applied to specific systems, their solutions appearing as transfer functions. Along with the theoretical considerations, Gould presented experimental evidence taken on a small heat exchanger, and developed analogs on a lumped basis to study the operation of various types of controls. His lumped equivalent included the system dead time by the use of the 'dead time extraction' method. A quick estimate of the number of lumped sections was found by determining the number of heat transfer units in the exchanger, defined as*

$$N = U.A./W.C \tag{3.2}$$

This worker found also that for gases and two-phase fluid systems the general equations can be solved analytically only under severe restrictions, whereas in 'composite' systems the response is dominated by the behaviour of the liquid side and dynamic effects due to the gas or the two phase flow can be ignored.

Rizika (78) developed a procedure to find the thermal lags in distributed systems, applied to the cases of a fluid (vapour phase) flowing through an insulated pipe, and the parallel flow heat exchanger. He set up partial differential equations for the components of an element of the heat exchanger and solved them by Laplace Transformation, so obtaining the response in the complex s-domain. By further inversion of the model of flow in an insulated pipe - for the case of a step

* Symbols not defined in the text conform with the nomenclature key given on page 225

function disturbance - he could present the solution in a graphical form relating the three-dimensional system of normalized temperature-time-distance. Proceeding in the same way for the case of exponential temperature disturbance to the same model, a partial plotting of the solution was obtained. Rizika's idea was to reduce the amount of calculations when solving for a particular set of conditions, as his numerical examples proved.

Rizika's solution in the time domain, obtained in terms of an infinite series using a Bessel function of the first kind, made it clear that analytical procedures even for fairly simplified systems have to resort to a great deal of numerical manipulation in order to get the final results. Therefore the contribution of Dusinberre (20) on numerical methods for the prediction of transient phenomena in pipes and heat exchangers was very appropriate. By dividing the distributed system into several lumped sub-systems, Dusinberre presented in tabular form a method of numerical solution using one of Rizika's previous examples as illustration.

At the same time Debolt (18) analysed the dynamic characteristics of a steam-water tube and shell heat exchanger by actually taking the experimental frequency response and transient data. He further constructed an electromechanical analog for simulating the heat exchanger and compared test results with those obtained from the actual exchanger. The simulation proved to be a basically sound method for predicting the performance of any prototype. Debolt's experimental results, reported up to a frequency of about 12 cycles per minute (1.26 radians per second), indicated that as the average tube side flow (water) was increased, the corresponding Bode diagrams were gradually displaced upwards, the shell side fluid (steam) being kept at the same constant pressure. All the curves were smooth and continually decreasing with the exception of those corresponding to the lowest flow (2.4 gpm) which showed one resonant peak in both gain and phase. The analog simulation run for the flow of 6.0 gpm was able to predict resonant peaks.

By this time the advantages of frequency response for analysing and synthesising chemical process control systems had been acknowledged, and the variety and frequency of works on the subject started to increase. Up to this stage the main concern of the authors was the development of transfer functions out of the differential equations describing the system, so that most of the results reported were in the frequency domain.

Cohen and Johnson (15) analysed a double pipe heat exchanger of the 'composite' type (steam in shell and water in tubes) under temperature disturbances. With moderate simplifications they represented the system by a set of two linear partial differential equations that after Laplace transformation and further simultaneous solution gave the expression

$$\bar{T}_{IL} = (\bar{T}_{Io} - (\tfrac{a}{b})\,\bar{T}_s)\, e^{-Lb/V_I} + \frac{a}{b}\,\bar{T}_s \qquad (3.3)$$

where a and b are groups enclosing the Laplace complex operator, s and the physical parameters of the system. Equation (3.3) represents the total response of the outlet water temperature at position L to the multiple disturbances of steam temperature and inlet water temperature. When each disturbance was considered separately the corresponding transfer functions were

$$\frac{\bar{T}_{IL}}{\bar{T}_s} = \frac{a}{b}\,(1 - e^{-bL/V_I}) \qquad (3.4)$$

and

$$\frac{T_{IL}}{T_{Io}} = e^{-bL/V_I} \tag{3.5}$$

from which it is clear that in the case of a single variable disturbance the transfer function is independent of the type of forcing.

They approximated the system by a dead time component and two non-interacting RC stages, and though this approximation showed a closer agreement with the experimental data, it did not predict resonant peaks as the theoretical model did.

In a contemporary paper Mozley (69) published the analysis of a concentric tube liquid-liquid heat exchanger under temperature disturbances. His approach was based on lumping the properties of the streams at their midpoint conditions so that his model was based on a set of ordinary differential equations. Mozley also developed a passive (without internal energy sources) electrical network simulation of his exchanger which included effects of the tube wall in one and five stages of lumping. Data for the response of outlet cold water temperature to changes in inlet cold (annulus) and inlet hot (tube) water temperature were compared with experimental results. The agreement of the five stage lumped simulation was, as expected, better than the totally lumped model.

Since the first attempts to simulate a distributed system by electrical analogs (Gould, Debolt and Mozley) there has been much progress leading to the present simulations in sophisticated analog computers which while keeping the same basic approach, are far more versatile and powerful.

By that time it became clear that the efforts were directed towards a compromise between the degree of complexity a model should present and the accuracy of its representation. Leonhard (61) had presented a method to find transient response from frequency response for a control loop, with a moderate amount of calculating work, and within the same context of reducing undue work Paynter and Takahashi (73) published a new method to evaluate the dynamic response of counterflow and parallel heat exchangers. Their paper provided a rigorous basis for setting up working equations for the transfer functions of heat exchangers, from design data. In their treatment, after defining the simultaneous equations of the system, the authors expanded the corresponding Laplace transform solutions in the form

$$G(s) = e^{\delta - T_m s + \frac{T_{s*}^2}{2} s^2 - \frac{T_a^3}{6} s^3 + \ldots\ldots} \qquad (3.6)$$

where δ = ln (S.S. change in output/S.S. change in input)

T_m = Mean delay of step response relative to distance-velocity lag of tube side response (L_1)

T_{s*} = Dispersion time of step response relative to L_1

T_a = Skew time of step response relative to L_1

s = Complex Laplace transform variable

the value and significance of this representation being indicated in another paper. This equation and the actual transfer function of the system are expanded in a series in terms of s and the parameters of (3.6) are determined by comparing corresponding terms. These parameters appear as functions of the partial differential equation coefficients, the simplest relationship being when the solid capacities are neglected and the thermal capacitances and velocities are equal for both fluids. By relating the new parameters in terms of conventional relative statistical measures like coefficient of variance

$$\mu = T_{s*}/T_m \qquad (3.7)$$

and coefficient of skew

$$\alpha = T_a^{\,3}/T_{s*}^{\,3} \qquad (3.8)$$

it is possible to select suitable elemental blocks or combinations of them to represent the original system.

From the original development of equation (3.6) the frequency response of the exchanger may be found after putting s = jω, by the relationships

$$\text{Ampl. } |G(j\omega)| = e^{\delta - \frac{1}{2} T_{s*}^{\,2} \omega^2 + \,.....} \qquad (3.9)$$

and

$$\text{Phase} \angle G(j\omega) = -T_m \omega + \frac{1}{6} T_a^{\,3} \omega^3 - \,.... \qquad (3.10)$$

According to the authors, although the formulae appear somewhat involved, the numerical evaluations of the parameters from design data are generally simple.

The experimental data they presented for step response and frequency response show fair agreement with their predictions, being in general on the lower side.

3.1.2 Pulse Testing

An interesting paper by Lees and Hougen (60) demonstrated how the transient response to a given pulse can yield the frequency response of a system by suitable manipulation in accordance with the Fourier transform theory. The pulse, they stated, must maintain continuity of the input and its first derivative and its duration must be comparable to the characteristic time of the system under test. They used the displaced cosine pulse function to test a small tube and shell heat exchanger with water through the U-tube bundle (two passes) and steam in the shell. Fig.3.1 shows the functional diagram used which, with small variations, is typical of most of the dynamic response experiments.

The data from the pulse disturbed system were converted to frequency response data following the method described by Drapper, Mc Kay and Lees (19). The results indicated that the pulse tests yielded smoother and more regular data than the actual sinusoidal tests. No theoretical predictions were available to check agreement.

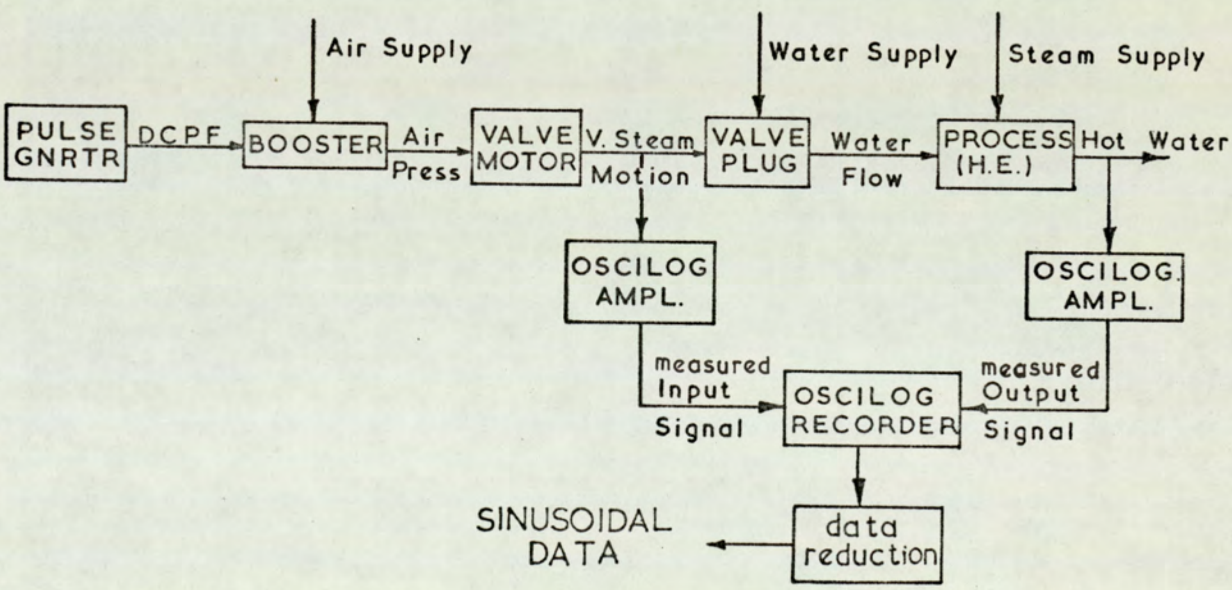

Fig. 3.1 Functional Diagram of Experimental System

The importance of the Lees and Hougen paper is in the considerable reduction of experimental work, produced by the technique presented. Later on Hougen and Walsh (44) made a comprehensive presentation of the method substantiating it by a good deal of data obtained by application of the pulse technique to several operating real systems and to two systems simulated by analog computer. It was evident that properly conducted pulse tests on real systems yielded frequency response data in excellent agreement with those obtained by direct sinusoidal forcing. From the data obtained by testing several instruments and items of process equipment it was concluded also that simple linear forms can be used to describe their dynamics within normal operating conditions.

Cima and London (13) studying the gas-turbine regenerator problem approached the transient response of the two-fluid heat exchanger via an electrical analog since the purely analytical attack was unsuccessful due to mathematical difficulties. They proposed a set of non-dimensional parameters to characterize the system: four normally used for steady state heat exchanger behaviour and four more unique to the transient problem, but all of them related to the performance of the exchanger by the following functional equation:

$$T_H, T_w, T_C, \varepsilon_H, \varepsilon_C = \Phi(\underbrace{FA, N, C_{min}/C_{max}, x^*}_{\text{S.S. Parameters}}, \underbrace{\theta^*, \theta_d, R^*, C_w^*}_{\text{Transient Parameters}(*)}) \qquad (3.11)$$

where the letters of the left hand side represent relative temperature differences corresponding to the hot (H) and cold (C) streams, and the metal wall (w). They are dimensionless, and the ε's are further defined as the generalized effectiveness for either fluid or the ratio of the actual heat transfer rate to the maximum possible as limited by thermodynamic considerations. Also

FA denotes flow arrangements

$N = A.U/C.W$, Number of transfer units

C_{min}/C_{max}, Capacity rate ratio of fluids

$x^* = x/L$, dimensionless flow length

$\theta^* = \theta/\theta_d$, dimensionless time

$\theta_d = \theta_{dmin}/\theta_{dmax}$, dwell time ratio

$R^* = R_{min}/R_{max}$, heat transfer resistance ratio

$C_w^* = C_w/C_{min}$, wall capacity ratio.

By operating on these parameters the simulation was greatly systematized and a substantial reduction of effort achieved in the analog work.

The same year Paschkis and Hlinka (72) made a detailed study of electric analogs to investigate the behaviour of heat exchangers. They presented RC circuits for steady state conditions, including the case of a three fluid exchanger, and RC circuits for transient conditions. In this last case a circuit element (module) represented one section (lump) of the exchanger. Their ensuing analysis of lumping errors gave three methods to improve the results:

(1) extrapolation procedure;

(2) uneven lumping; and

(3) treating each section as a separate heat exchanger.

This last procedure led to the estimation of a correction factor based in the use of log mean temperature rather than average temperature which produced exact answers for the steady state and improved the results for the transient conditions.

The pure crossflow heat exchanger dynamics was studied by Flaherthy (30). He set up equations of the output mean temperature as functions of the input temperatures, in the frequency domain. The Laplace transforms of the transient responses were then approximated by an inverse transformable function which had definable properties of the exact function in real time and which allowed the calculation of the time response of the output mean temperature. In this procedure he made use of the Moment Approximation Method which allows calculation of a number of approximations of a function to represent the actual system. Any order of complexity is obtainable.

Most of the data reported by Flaherthy are given by a series of graphs relating a group of charactistic parameters in terms of the heat transfer units on both sides of the transfer wall. The final results indicated that the response of heat flux in the shell side to any input of tube side temperature is identical to the response of heat flux in the tube side to the same kind of input of the shell side temperature.

Another particular problem in the field, the dynamic response of heat exchangers having internal sources, which includes the heterogeneous nuclear reactor, was tackled by a team of investigators. Clark, Arpaci and Treadwell (14) studied the coolant temperature response as a function of space and time for the case in which the energy generation rate was disturbed in step-change fashion; Arpaci and Clark (1) analysed the dynamic response of the heat transfer surface temperature and the fluid-surface temperature difference to the same type of disturbance; Arpaci and Clark (2) extended the analysis to the cases in which the disturbance was a linear step change (a ramp) and an arbitrary time rate of change.

Finally Yang, Clark and Arpaci (99) investigated the behaviour of the heat exchanger having a sinusoidally time-dependent rate of internal heat generation, reporting results for both the transient and steady-periodic regime. In all four papers of this team extensive use of graphical representation of intermediate results is made, and the experimental data showed favourable agreement with the analytical predictions.

The subject of heat exchange dynamics was treated formally in text books for the first time by Campbell in his 'Process Dynamics - Dynamic Behaviour of the Production Processes' (10) in which he devoted one chapter to deal with the subject, making emphasis on different arrangements. He derived the general equations (from basic principles) for convective heat transfer, working out the response to an impulse disturbance.

Catheron, Goodhue and Hansen (11) reported their study of the control of a steam-to-water shell and tube heat exchanger. It included two parts: determination of the exchanger dynamic charactistics, and practical operation of the system under several control arrangements to keep the outlet water temperature at a set value. The usual disturbances were fluctuations in either the flow rate or the supply temperature of the water.

They developed transfer functions relating outlet water temperature to changes of steam admission, expressed as steam valve area and found that they closely predicted the experimental data. For the case when the control system was studied by frequency response of the open loop, no mathematical model was proposed.

The same year Masubuchi (64) extended the basic model originally proposed by Profos and exactly analysed the dynamic characteristics of 1,2,3 ..2n, 2n +1 pass heat exchangers. He found that the characteristic equation governing the heat exchange process in each multipass device, and therefore the corresponding transfer function involving the roots of that equation, never goes beyond third degree as long as all tube passes are identical and there is only one shell pass. If the number of tube-passes approaches infinity the flow pattern tends to the crossflow heat exchanger.

Masubuchi also modelled the multipass heat exchanger in an analog computer using the lumping techniques, by then a current procedure.

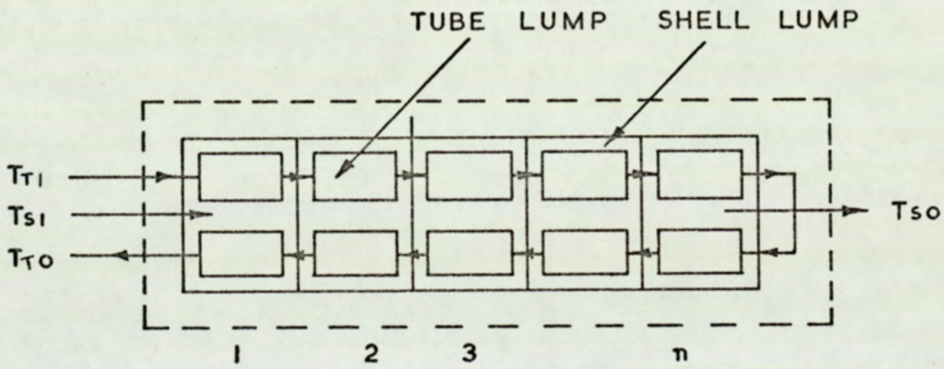

Fig.3.2 Lumped Parameter Model of a 1-2 Pass Heat Exchanger

His experimental results showed favourable agreement with the analytical predictions and remarkable similarity between the responses for shell-side disturbances and the corresponding responses for tube side disturbances.

The experimentation indicated that for purposes of feedback control the choice of flow pattern is extremely important as the parallel-counter-current flow produced very stable shell response to step changes in set point, whereas the countercurrent-parallel pattern, under the same conditions, produced unstable response.

It can be seen that four types of major disturbances are possible in an ordinary heat exchanger as variations of

(i) tube fluid temperature,

(ii) tube fluid flow rate,

(iii) shell fluid temperature, and

(iv) shell fluid flow rate.

A systematic research on the effect of those disturbances on the dynamics of heat exchangers was conducted at the University of Saint Louis: Morris (67) studied the effect of the first disturbance using two full size industrial prototypes under pulse testing. The frequency response found by Fourier analysis of the pulses was almost identical to the one predicted by the transfer function, based on two first order partial differential equations. In his results, published later, Morris (68), indicated a very significant effect of the reversal heads, and showed that a single pass model with logarithmic-mean-temperature-difference correction factor provides an excellent approximation of the more complicated multi-pass model. No resonance effects were detected in this work so supporting the belief that baffles tend to 'wash out' this phenomenon.

Hriber (45),using the same equipment as Morris studied disturbance type (iii), applying also the pulse data reduction method. His results indicated excellent agreement with those of direct frequency response testing, proving once more pulse testing to be a very reliable method. This work confirmed that simple linear approximations of the performance functions, with parameters calculated by conventional methods provide good representation of the more complex distributed heat exchanger.

Vincent (93), once more using pulse testing, examined the effect of disturbance four (variation of shell fluid flow rate) on the behaviour of the exchanger. By applying the Taylor dispersion theory he developed a mathematical description of the form

$$\frac{\partial T}{\partial t} = D \frac{\partial^2 T}{\partial X^2} - V \frac{\partial T}{\partial x} \qquad (3.12)$$

which he did not attempt to verify with experimental data. His analysis of experimental problems seems very useful to new workers.

Within the same line of thought Hearn (42) went through the analysis of a baffled shell and tube heat exchanger subject to shell flow forcing, by performing Fourier analysis on the input pulse and the pulse response. In all the works using this technique the frequency response is obtained from the performance function, defined for the experimental data as

$$PF = \frac{\sum_{i=1}^{\infty} O(i\Delta t)e^{-2j\omega i\Delta t}\Delta t}{\sum_{i=1}^{\infty} I(i\Delta t)e^{-2j\omega\Delta t}\Delta t} \qquad (3.13)$$

with $O(i\Delta t)$ and $I(i\Delta t)$ being the output and input functions read from the experimental curves at intervals Δt apart. From these data gain ratio and phase lag for the Bode plots follow directly.

Some of Hearn's data suggest resonance inflexions rather than peaks in the high frequency region, apparently overlooked by him. On the other hand he also suggests a second order non-interacting lumped parameter approximation after verifying that the pulse direction (upwards or downwards) has little effect on the experimental time constants.

Iscol (48) temperature-forced commercial heat exchangers with one shell pass and an even number of tube passes, alternately feeding cold and hot water into the tube inlet. This approach proved successful as the agreement between analytical and experimental results was excellent. The limiting factors of the upper frequency were the gain of the recorder equipment and the 60 cycle hum. Iscol suggested the use of a filter to pick the desired harmonic from the actual input and output thus reducing the amount of experimental work.

Edwards (22) made a study on a flow forced concentric tube heat exchanger, actually taking frequency response data and correlating these results with a model obtained from a linearized set of differential equations. He proposed a type of steady state harmonic analysis based upon the lumped parameter representation to approximate the describing function of the system.

Cohen and Johnson (15) used a steam-water double pipe heat exchanger and the well established method of partial differential equation linearization followed by Laplace transformation, to illustrate their theory of distributed parameter processes. For the first time, they maintained that the total response to simultaneous forcings of both vapour temperature and inlet water temperature fluctuations should be the sum of the individual transfer functions, each multiplied by the appropriate forcing. The different condition of the two individual responses is indicated by the frequency response loci shown in Fig.3.3. Although no experimental data were presented for the case of simultaneous forcings, the results reported for the individual forcings were in general in good agreement with their predictions.

Hsu (46) developed digital programs to compute the frequency response of 8 transfer function of a 1-2 heat exchanger under inlet

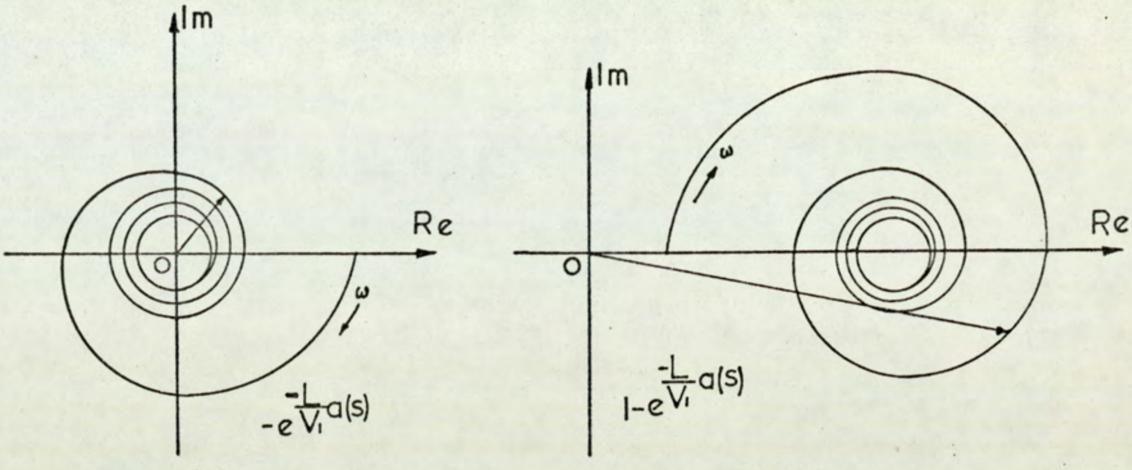

(a)

Outlet water temperature response to inlet water temperature forcing.

(b)

Outlet water temperature response to vapour temperature forcing.

Fig.3.3 Frequency Response Loci of a Steam-water Heat Exchanger

temperature forcing. He covered a frequency range from 0.03 to 0.002 cycles per second and produced sinusoidal temperature variations by a specially designed sine wave generator. His experimental data indicates that the heat capacities of tube and shell walls cannot be neglected in the analysis. The agreement with predicted results is good for the phase lag but only fair for the gain.

The following year Hsu and Gilbert (47) undertook a very useful task of collecting and systematically presenting the differential equations and the transfer functions of a wide variety of heat exchangers (lumped, distributed, composite) with the most common flow arrangements and the most usual simplifications of the system. Some models were taken from the literature and others were deduced, adopting a common nomenclature and trying to unify as much as possible the information available on the subject. Their aim was to provide other workers in the field with a 'bank' of functions obtained by rigorous mathematical analysis and valid under the assumptions underlying the differential equations of the particular system.

Vincent, Hougen and Dreifke (94) extended the study initiated by Vincent (93) on the effect of mixing in a heat exchanger. They pulse-disturbed the inlet temperature of one fluid stream while the other side of the exchanger was devoid of fluid, so that the mixing effect could be evaluated. The time data were reduced to frequency data by known procedures and compared with those predicted from the simplified mixing theory. They concluded that the parameter $\mu L/4D$ appears to characterize the mixing which occurs in both shell and tube streams.

Law (59) in an excellent paper discussed in detail condensing vapour to liquid and liquid to liquid heat exchanger dynamics; analysed the resonance effect for temperature and velocity forcings, and approximated the transfer functions by superimposing the resonance peaks on an otherwise smooth frequency response. A detailed appendix showed the actual deduction of the transfer functions for co-current and countercurrent flow arrangements.

Law's theoretical models were supported by experimental data from other workers,showing good agreement. He was able to predict the magnitude of the resonance effects based on an intermediate dimensionless group.

Following his reasoning, for the case of temperature forced and countercurrent flow, the first frequency to show a resonant peak has a period of

$$P_1 = L/V_T + L/V_s = \tau_T + \tau_s \qquad (3.14)$$

where

τ_T is tube side residence time

τ_s is shell side residence time

There will be a peak in the frequency response of the outlet temperature of the other fluid whenever the residence time is a multiple of the period of the sinewave, i.e. when

$$P_n = (\tau_T + \tau_s)/n \qquad (n = 1,2,3.....) \qquad (3.15a)$$

For the case of co-current flow, a similar argument indicates resonant peaks of periods

$$P_n = (\tau_s - \tau_n)/n \qquad (n = 1,2,3.....) \qquad (3.15b)$$

and there will be no resonance peaks in the outlet temperature of a fluid to its own inlet temperature variations.

For the case of velocity forcing, both co-and countercurrent flows will show resonance at

$$P_n = \tau_s/n \qquad (n = 1,2,3.....) \qquad (3.16a)$$

for the shell side outlet temperature under tube side forcing, and

$$P_n = \tau_T/n \qquad (n = 1,2,3.....) \qquad (3.16b)$$

for the tube side outlet temperature under tube side velocity disturbance.

Equivalent expressions were obtained by Stermole and Larson (86) in their work with a 'composite' exchanger, also approximated by ordinary differential equations.

3.1.3 The Analytical Solution

So far the equations describing the dynamics of flow forced heat exchangers had been solved only in their linearized form. Solutions obtained in this manner guarantee good accuracy only if the magnitude of the flow disturbance is small compared with the magnitude of the steady state flow rate. Koppel (55) presented the first successful analytical solution of the single equation model and compared it with the approximate linearized solution for a step change in velocity. His method makes use of the concept of the characteristic equation in which the partial differential equation that relates the temperature with time and distance is converted into two ordinary differential equations which are then solved simultaneously.

A graphical comparison of the true and approximate responses is shown in Fig. 3.4 in terms of normalized temperature times exp (P_o) vs normalized time for the particular case of $P_o(1-b)a = 1$. In this case P_o is the number of heat transfer units at the steady state conditions, b is the exponent for velocity dependence of the heat transfer coefficient and a the dimensionless magnitude of the step change in velocity.

3.1.4 Numerical Solutions

As the 60's progressed the number of works on the dynamics of heat exchangers grew even faster with gradual increase of interest in the numerical solution of the models in the time domain. The main emphasis had been the solutions in the frequency domain, due to the mathematical difficulties of solving the differential equations

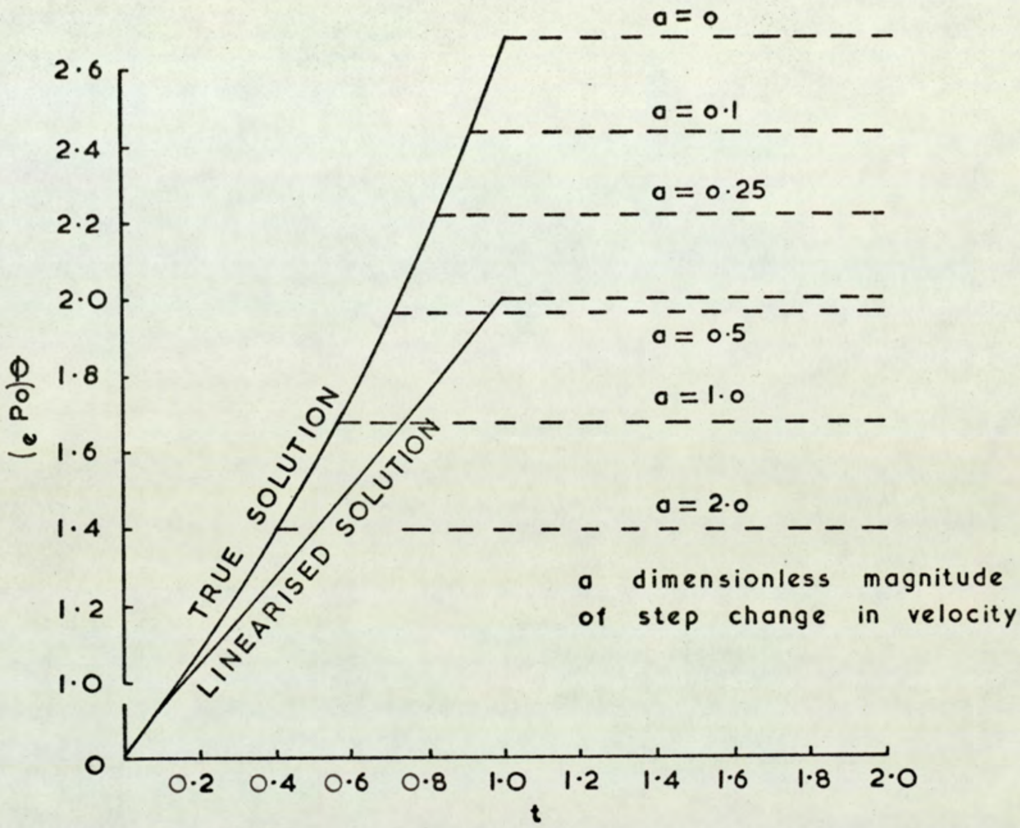

Fig. 3.4 Comparison of Exit Temperature Responses, Exact and Linearized.

describing the system, and the lack of successful numerical algorithms to solve them by computer. However as new numerical methods were developed, papers dealing with the solution of the exact models in the time domain started to appear along with papers applying the more conventional techniques. Among the former are significant the contributions of Keller (53), Herron (43), Privott (75), Rodehorst (79) and Beckman (4).

Keller presented the theoretical and experimental study of a heat exchanger having internal heat generation under flow rate transience. A numerical solution of the model formulated in the time domain was achieved by the use of finite difference equations. The experimental work included measuring the dynamic performance of the system to the following flow transients: rising step change, rising exponential, decreasing ramp, decreasing exponential and sinusoidal. The analysis of the results indicated that major consideration must be given to the manner in which the heat transfer coefficient varies under dynamic conditions. Keller made a stability analysis and a convergence analysis of his numerical technique to solve the model which included implicit and explicit relationships. It was apparent that although the implicit equations possess stability advantages, as compared with the explicit equations, for good accuracy small time and distance grid spacing is required. This spacing is approximately the stability requirement of the explicit equations.

A striking finding of this work was that for fully developed turbulent flow, the local heat transfer coefficient becomes an irregular function of distance, along the main axis of the exchanger. The prediction of temperature response for non-periodic transients by a linearized model was only approximate. For sinusoidal forcings there was some indication that the heat transfer coefficient decreases with increasing frequency and increasing Reynolds number.

It is convenient to mention at this point that Bundy (9) as quoted by Rodehorst (79) obtained some intriguing results when he tried to determine heat transfer coefficients by frequency response testing, with inlet temperature sinusoidal forcings. He constructed a mathematical model of the system and from it he formulated an analytic expression for the amplitude ratio as a function of frequency and heat transfer coefficient. He was then able to determine a value of the heat transfer coefficient at each frequency which caused the model to coincide with the data. These frequency dependent coefficients increased with frequency.

However, Bundy's model (which neglected axial dispersion) was shown to be adequate for zero frequency (steady state) and increasingly inadequate with increasing frequency. Although it was impossible to obtain the referenced work to examine the analysis in more detail, the subject seems very interesting and worthy of further research.

Herron in 1964working with a double pipe heat exchanger derived four models for the system:

(1) A constant coefficient model (constant velocities),

(2) A variable coefficient linear model (velocities functions of time only).

(3) A variable coefficient non-linear model (velocities and properties functions of time and temperature),

(4) A wall capacitance model.

Only the first model was suitable for analytical solution, and this was not simple. Herron developed a digital simulation of this model by a conventional numerical method but this was very much in error around the discontinuity of the function, when large increments of distance and time were used. He then, using the Douglas-Paceman and Rachford algorithim,(43) obtained very good results.

The digital simulation of models 2, 3 and 4 was accomplished successfully by a similar procedure though it was estimated that the non-linear model may not be so different from the linear one to warrant the increased calculation time it usually requires.

Privott (75) and Privott and Ferrell (76) with equipment similar to Herron's analysed the liquid-liquid heat exchanger forced by variations in the flow rates. They developed general and simplified mathematical models which were solved by an explicit numerical method. Using the Dittus-Boelter heat transfer correlations they could obtain excellent predictions of steady and transient state temperature distributions. The approximate linearized representation of the process predicts temperature responses generally in substantial error for even small changes in fluid velocity.

In the sinusoidal analysis the maxima and minima of the periodic responses of the general system have substantially different amplitude ratios and phase lags, bracketing the data generated by the approximated model, and the smaller the amplitudes of the sinusoidal forcing functions the nearer the responses corresponding to maxima and minima of the non-linear response.

They also solved the general model on two Pace TR-48 analog computers using six distance nodes (lumped stages). The transients of this analog simulation agreed very well with the digital simulation and the steady state values agreed with the analytical solution.

The contributions of Rodehorst (79) and Beckman (4) are especially significant because they discarded the long used assumption of negligible heat transfer by diffusion in the axial direction. Their models are then sets of second order partial differential equations of the type indicated by equation (3.12) in which the second order derivative terms account for the diffusion contribution. The dispersion effects of the Taylor, eddy and molecular type are lumped in a term such that

$$\mathfrak{D} = \mathfrak{D}_T + \mathfrak{D}_E + \mathfrak{D}_M \tag{3.17}$$

The approach of Rodehorst makes use of a two-equation model, one for the fluid and one for the wall to describe the transient behaviour of the heat exchange for the case of turbulent flow of water in an insulated pipe, including the axial dispersion. After being normalized, the equations are formulated into finite difference form using the Crank-Nicholson analogs obtained by centering the equations at the distance-grid points but at the midpoint of the time grid,

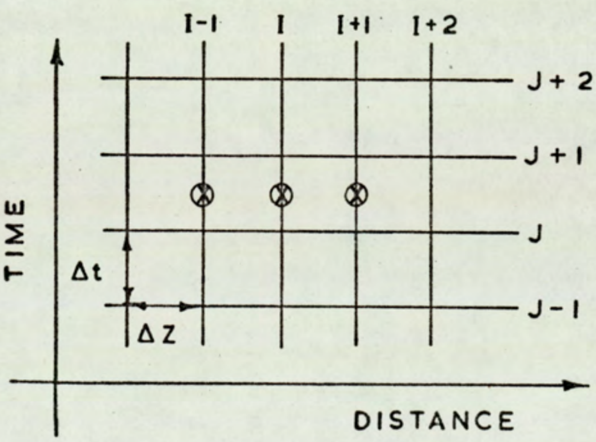

Fig.3.5 Finite Difference Grid in Rodehorst's Integration.

After the complete system of finite difference equations is written, the resulting set, in matrix notation is:

$$A\,\underset{\sim}{T}_f + B\,\underset{\sim}{T}_w = \underset{\sim}{D}_f \tag{3.18}$$

where A and B are the coefficient matrices of the simultaneous set, and $\underset{\sim}{T}_f$ and $\underset{\sim}{T}_w$ are the corresponding fluid and wall temperature vectors, and $\underset{\sim}{D}_f$ is the driving temperature vector. This bi-tri diagonal matrix is then solved by an appropriate algorithm.

The results indicated that the representation was adequate and that the axial dispersion has a very significant effect in the unsteady state turbulent pipe flow.

Rodehorst's work started to explain the findings of Bundy (9) and concluded that the heat transfer coefficient correlations usually used for the steady state regime hold for mildly transient conditions, and that the dispersion theory of Taylor (88,90) should be used for the prediction of the axial heat transfer dispersion coefficient for conditions of Reynolds number above 30000.

Beckman (4) developed a more complete model of four second order partial differential equations to describe a double pipe heat exchanger in the following two versions:

(i) A constant coefficient model (applicable to temperature disturbances only) and

(ii) A variable coefficient model with heat transfer coefficients and dispersion coefficients changing with velocity.

Because not enough boundary conditions could be drawn from the operating conditions of the system, Beckman made use of the 'extended model' concept to draw the missing information. According to this concept, assuming one 'inside extension' to one end of the physical exchanger and one 'outside extension' to the other end, allowed the first derivatives of the respective temperatures at some distance from the real exchanger, if large enough, to be considered zero.

Using the original set of equations plus those derived from energy balances around the ficticious extensions and all the initial

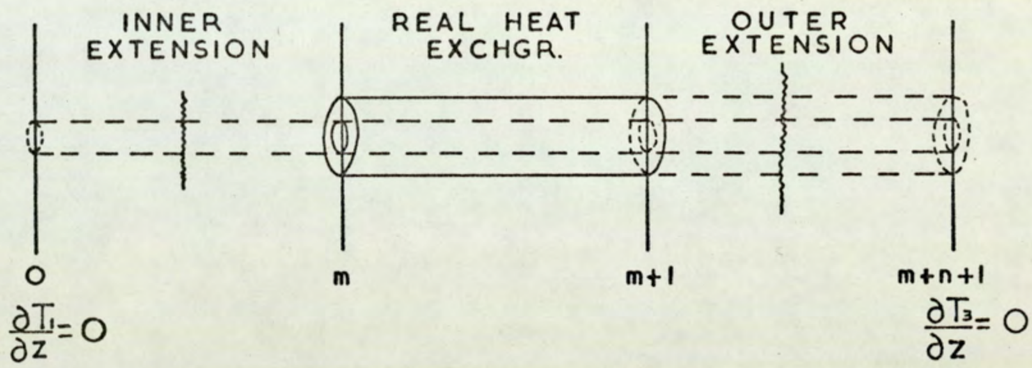

Fig.3.6 Extended Model Concept

and generated boundary conditions, Beckman had a set of equations that could be transferred to a set of simultaneous difference equations using the Price-Varga-Warren analogs in order to digitally simulate it by an implicit method.

The numerical simulation proved effective when compared with pulse testing data whereas the sinusoidal testing data exhibited erratic behaviour at high frequencies. On the other hand the dispersion coefficients obtained were one order of magnitude larger than the isothermal values reported in the literature.

Although an analog simulation by the lumped parameter approach proved good enough to accurately predict transient responses, the conventional controller tuning methods were unable to provide settings which carried out satisfactory feedback control of the system.

The inclusion of the dispersion term in Beckman's model though an improvement from the theoretical point of view was not so for the experimental results since he had to correct the predicted coefficient by factors as large as fourteen.

Parallel with the previous works directed to find the integral relationship between temperature and time, which gives an indication of the system performance directly, more studies based on the transformation technique continued, shedding more light on this complex subject.

For example, Isom (49) worked in the liquid-liquid heat exchanger under flow variations, his most significant achievements being:

(i) The dynamics of outlet temperature are the same regardless of which flow is varying, with the exception of 180^{o} difference in phase between shell flow driving and tube flow driving,

(ii) Within the range of flows studied tube outlet temperature dynamics could be correlated in terms of tube flow without regard to the level of shell flow and vice versa,

(iii) Resonance was observed in the shell side only for one shell flow, indicating that this effect is not significant for baffled shell, as Morris had found previously.

An analog model with eight sections failed to show resonance as well.

A similar investigation carried out by Stermole (85) found that the effects of wall capacitance and heat transfer coefficient variations have little effect on the frequency response predictions but the changes of the latter significantly affect the transient response. In addition, Stermole found that descriptions of partial differential equations with constant coefficients were good for frequency response over all frequencies tested but good for transient response only in the case of small variations. On the other hand descriptions of ordinary differential equations with variable coefficients represented the transient response adequately for both large and small variations but represented the frequency response adequately only at low frequencies.

Some studies on heat exchanger dynamics were made when they were used as examples to illustrate the more general theory of distributed parameter systems. They are useful since they help to understand how studies carried out specifically for heat exchangers can be extended to other important distributed systems like tubular reactors. Among them are worthy of mention the works of Mc Cann (66), Gaither, Mc Cann and Taft (33), and Friedley (32) who developed an approximate method to predict the dynamics of plug flow processes, asymptotically correct for both high and low frequencies.

The flow variations in a heat exchanger are extremely important from the control point of view since most of the time it is by flow manipulations that the automatic control is carried out. That is why much more work has been reported on the subject.

Finlay (24), Finlay and Dalgleish (26) and Finlay (25) from the National Engineering Research Laboratory reported different aspects of the behaviour of a 1-2 pass heat exchanger, that was modelled as a distributed system, as a sectionally lumped system and as a totally lumped system. Although a totally lumped model is a very crude approximation to a distributed system, since it is unable to distinguish between countercurrent and parallel flow, its predictions were in reasonably close agreement with the experimental data. The sectionally lumped model is a closer representation but the purpose of 'lumping' - to simplify calculations - is lost because the results of this model must be obtained by complex vector summations.

Axon (3) and Stainthorp and Axon (84) analysed a five-pass steam-heated exchanger to variations in steam temperature and flow rate, and process fluid inlet temperature and flow rate.

One such exchanger can be represented by the following block diagram.

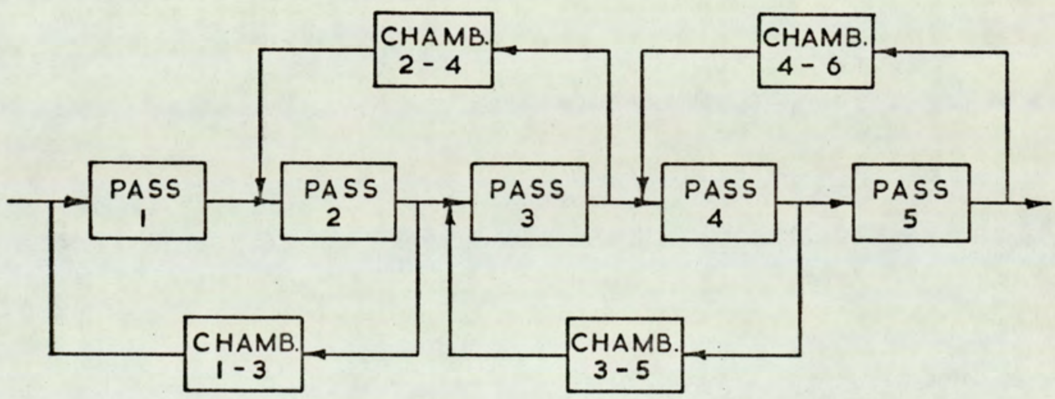

Fig.3.7 Block Diagram Representation of a Five-pass Heat Exchanger Including Reversal Chambers.

Their models started from simple concentric tubes and gradually removed simplfications to include difference in the passes and the effect of reversing chambers. The experimental data suggested that the five-pass model could be simulated by a one-pass model.

In another steam-heated exchanger, this time a double pipe one, Yang (98) tested a two-equation model, one for the tube liquid (coolant) and one for the wall, and solved it in the frequency domain and in the time domain for the cases in which the disturbances in the liquid flow rate were step changes, linear increase (ramp), exponential change and sinusoidal variations. Because the resulting solutions were involved expressions, several parameters had to be correlated in graphical form to ease the application of such solutions, in a way analogous to the works of Arpaci et al., and Yang (97).

Kamman (51), Stermole (85), and Kamman and Koppel (52) made further contributions by comparing linearized and exact models of a flow forced 'composite' heat exchanger.

Fisher (27) used four different sized heat exchangers of the concentric tube type to compare their dynamics when flow-disturbed between Reynolds numbers of 4000 to 20000 and Prandtl Numbers from 3.0 to 40.0.

This work was followed by papers by Fisher and Kadlec (28) and (29). In the first one they investigated the effect of Reynolds and Prandtl numbers on the frequency response of the exchanger, reaching the conclusion that as either of these parameters increase for both shell and tube disturbances, the attenuation and phase shift of the tube outlet temperature increase whereas the corresponding ones of shell outlet temperature decrease. They detected resonance, which proved most prominent under conditions of low velocity, low frequency, long exchangers, large equivalent diameters and low metal-to-contained fluid-heat capacity ratio.

In the second paper the same authors studied the effect of size of the exchanger on its frequency response characteristics, finding experimentally that as the flow area of dynamically similar heat exchangers decreases, the attenuation and phase shift of the outlet fluid temperature increases and is greater when the fluid is being forced. Their predictions proved good for relatively large exchangers operated at a Reynolds number above 20000 but tended to be smaller for smaller exchangers, so limiting the applicability of a generalized model.

3.1.5 Synopsis

This survey of the literature on heat exchange process dynamics is not intended to be exhaustive. The purpose has been to show the way in which the field has developed, the specific problems that investigators have tried to solve and the methods they have used to tackle them in different cases. It has been also the intention to look in perspective on the state of the art at the moment of starting the present work, which obviously must be based on the body of knowledge previously accumulated.

A lot more than mentioned in the above text has been done. The reviews of Williams and Morris (96) and Rosenbrock (80) are good sources of additional information as well as the bibliography presented by Harriott (41) and Gould (38) in their respective books, in the chapters devoted specifically to heat exchange dynamics. Two additional papers by Koppel (56) and (57) have been significant contributions to the theory of this field,as well as the attempt by Thal-Larsen (91) to generalize the description of heat exchangers response by the concept of normalized parameters.

From all the previous information it is concluded that

(1) A large amount of work has been published on many aspects of heat exchange dynamics,

(2) Several analytical techniques have been used successfully to predict the dynamics of heat exchangers in the time and in the frequency domain,

(3) Practically all work done is concerned with single-disturbed processes.

Therefore, there is a well defined need to analyse the heat exchanger as a multiple-disturbed system, in order to identify the mechanism it follows to combine disturbances from different sources, and how they affect the behaviour of the heat exchange process.

This thesis is concerned with the investigation of this problem by extending to multi-disturbances the techniques which were previously developed for single-disturbance situations.

3.2 HEAT TRANSFER COEFFICIENT CORRELATIONS

The convection heat transfer theory is based on the concept of heat transfer coefficient and whenever a calculation by this mechanism is made 'a priori', the resistance to the heat flow has to be estimated from the conditions of the process by means of semi-empirical correlations using dimensional analysis. An extensive amount of research has been done in attempts to make those correlations as general and reliable as possible amidst the huge amount of conditions that are possible when different physical properties are combined with different geometries in a wide variety of orientations. So far the success has been moderate but a fair degree of certainty has been achieved in estimating the heat coefficients of fluids moving in turbulent and viscous regimes within tubular enclosures.

In most of the heat exchange-process dynamics studies previously carried out, the experimental prototypes have been of the concentric pipe type, in which both individual heat transfer coefficients of interest can be calculated by similar expressions of the type mentioned before. Although almost any particular value from a correlation can be made to fit a particular set of conditions in steady state, by the use of correction factors, it is the real suitability of the correlation, as tested by the range of conditions covered by a transient test that makes the prediction useful.

This consideration is even more critical in the case of shell and tube exchangers, as the one used in this work, particularly for the correlation of the shell side heat transfer coefficient.

3.2.1 Tube Side Heat Transfer Coefficient

Formulae have been published for this case since the late years of the last century when Graetz, as cited by Whitaker (95) gave the solution for laminar flow in a pipe. Sieder and Tate (82) modified the expression to include the effect of temperature on the viscosity of the fluid to yield

$$Nu = 1.86 \ (Re.Pr \ D/L)^{1/3} (\mu_b/\mu_o)^{0.14} \qquad (3.19)$$

This correlation is satisfactory and widely used today for laminar flow, with physical properties of the fluid evaluated at the mean bulk temperature, except μ_o which is evaluated at the mean wall temperature.

For turbulent flow, Whitaker gives an expression of the same type and slightly different ones have been proposed by Perry (74) and Kern (54).

In the transitional zone the situation is less clear and no definite correlation has attained general acceptance.

In spite of this, it can be said that the tube side heat transfer coefficient can be correlated with relative ease since the geometry of the system is simple and the flow patterns are easy to estimate.

3.2.2 Shell Side Heat Transfer Coefficient

The serious problem arises with this correlation because of the relatively complex geometry of the space, the complex flow patterns and the uncertainties introduced by the fitting of the solid components, namely tubes, baffles and outer wall of the shell. The problem has been studied extensively, though the success has been limited. From the Co-operative Research Program on Shell and Tube Heat Exchangers at the University of Delaware three comprehensive reports, eleven published papers and twenty six theses have stemmed during the span of sixteen years - see Bell (5) - most of them devoted to the analysis of heat transfer and pressure drop across structures of the type found in a baffled tube and shell heat exchanger. Short (81), Tinker (92) and Bergelin et al.(6) in particular have made significant contributions.

Probably the best analysis of the flow pattern is that given by Tinker (92) who divided the fluid stream into four paths defined by

(i) The main path of the fluid,

(ii) baffle-tube clearance,

(iii) shell-baffle clearance and

(iv) peripheral tube bundle - outer shell space,

as indicated in the following diagram.

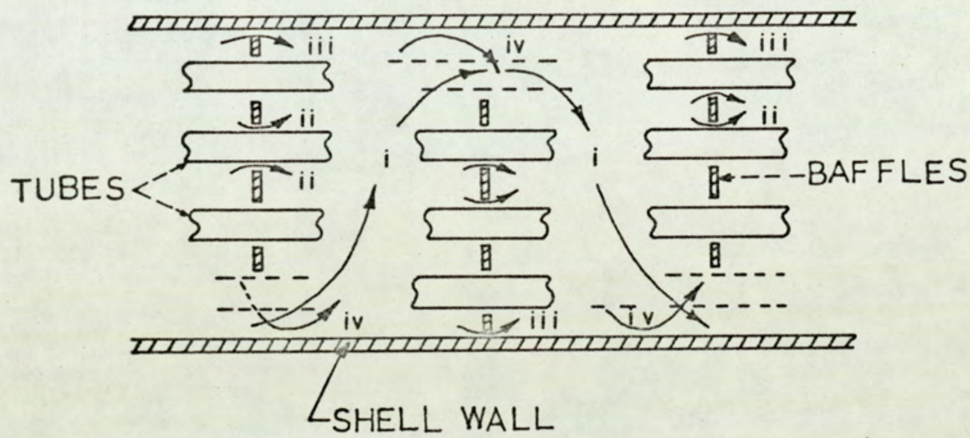

Fig.3.8 Flow Distribution in a Baffled Shell-tube Bundle Space, According to Tinker Model.

The City and Guilds College prepared for The British Shipbuilding Research Association Report No.148 (1955) a correlating equation which takes into account most of the significant geometric factors of the shell and is therefore the most comprehensive and descriptive for a quick rating of a heat exchanger, (reference 8).

It must be remarked, however, that this equation (presented and discussed in the next chapter) takes no account of the by-pass space between the bundle and the shell, the fourth flow both of Tinker's model, though Emerson (23) recommends it only second to the more involved step-by-step method given by Bell (5).

In any case, the shell results have to be viewed with great care since the model used still neglects other factors. From the analysis of local heat transfer coefficients, Narayan (70), Gay and Williams (34), Gay and Roberts (35) and others have found that the coefficient not only changes axially due to the effect of temperature on the properties of the fluid, but also changes radially due to the changes in velocity, and not in a regular shape, but rather by zones.

CHAPTER 4

THEORETICAL PRINCIPLES

4.1 THE HEAT EXCHANGER MODEL

This chapter deals with the theoretical concepts involved in the development of the mathematical model representing the system studied in this work. It covers the analysis of the heat transfer phenomenon in the liquid-liquid shell-and-tube heat exchanger, the current simplifications made to facilitate its solution and the deduction of the set of simultaneous partial differential equations that describes such a process. It also presents the principles and methods of analysis used to find the frequency response of the exchanger and the alternative approach by pulse testing followed by data reduction using the Fourier Transform technique.

4.1.1 The Heat Exchange Process

Several mathematical descriptions of the heat exchange process that takes place in a liquid-liquid concentric-tube heat exchanger have been derived in the past. The procedure followed consists of making heat balances around a differential element of the exchanger. The resulting description may consist of one to four partial differential equations depending on whether one overall heat balance or individual balances for each fluid and wall are carried out, and whether contributions of one or both walls to the overall dynamics of the exchanger are significant enough to be taken into consideration, i.e. when the thermal capacitance of the walls is large compared with the heat throughput of the exchanger.

Four mechanisms of heat transfer are possible in the process of transferring thermal energy from one fluid to another in a heat exchanger:

(i) Heat transfer by bulk flow or forced fluid convection,

(ii) Heat transfer by conduction across solid walls,

(iii) Heat transfer by radiation,

(iv) Heat transfer by dispersion or thermal diffusion, which includes conduction within the fluids.

In most cases the contribution of the first mechanism is very important by itself whereas the contributions of the last two, very difficult to evaluate individually, are combined by a semi-empirical procedure under the concept of heat convection. In this case the description of the process consists of a set of first order differential equations. Some workers (4 , 79), however, have developed models considering the contribution of dispersion separately, in which case the description of the process becomes a set of second order differential equations.

Since the main purpose of this investigation was to analyse the way in which the heat exchanger combines signals, the description leading to first order equations was adopted. It was estimated that if some allowance is made for the fact that in the baffled shell-and-tube heat exchanger, the fluid outside the tubes does not move parallel to the tube axis but along some elaborate path between parallel and pure crossflow patterns, in which the fluid moves perpendicular to the tube bank, then this exchanger could be approximated by a modified description of the concentric tube heat exchanger.

The main difference between the two types of exchangers, from the point of view of modelling, consists of the rather complex hydrodynamics of the shell side fluid flow which leads to the consideration of several factors not present in the concentric tube device. Such factors (see Fig.4.1) are:

(i) Leakage between tubes and baffles (A)

(ii) Leakage between shell and baffles (B)

(iii) Short circuiting between tube bundle and shell (C)

(iv) Baffle spacing (D)

(v) Baffle cut (E)

(vi) Tube distribution pattern in the bundle (F).

All these factors are very important because they contribute to the definition of the effective heat transfer coefficient of the shell side and therefore must appear in the correlation used to estimate this coefficient.

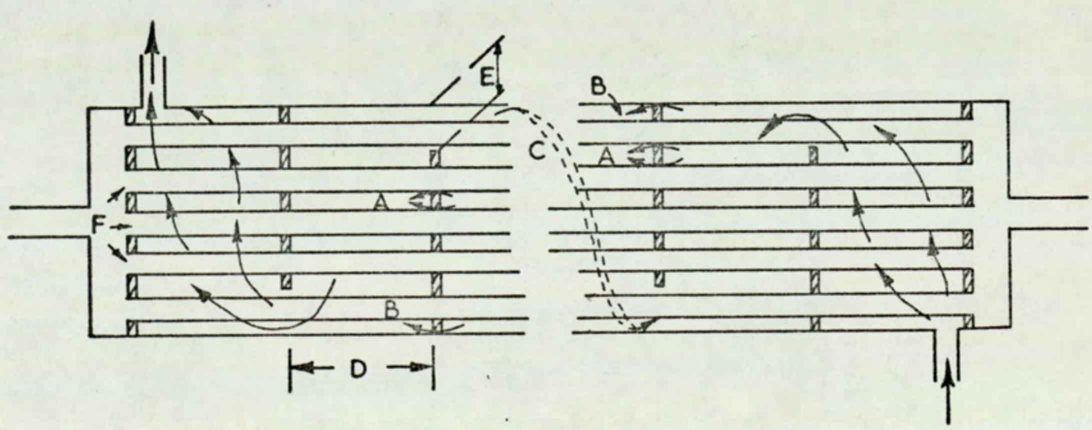

Fig.4.1 Shell Side Fluid Flow Pattern

They are included by redefining the fluid velocity in the shell side and they affect the heat transfer coefficient by correction factors that incorporate the geometric characteristics of the flow path.

4.1.2 The Heat Transfer Correlations

The correlation chosen from the literature to evaluate the shell side heat transfer coefficient was that derived by the City and Guilds College for the British Shipbuilding Research Association (7), equation (4.1), with all properties evaluated at the average bulk temperature of the stream

$$Nu_s = 1.9\, Re_s^{0.6}\, Pr_s^{0.33} \left(\frac{\mu_s}{\mu_\omega}\right)^{0.14} F_1^{0.4} . F_2^{2} . F_3 \qquad (4.1)$$

where

$$Nu_s = \frac{h_s d_o}{k}\text{, Nusselt Number} \qquad (4.2a)$$

$$Re_s = (V_s \rho_s d_o / \mu_s)\text{, Reynolds Number} \qquad (4.2b)$$

$$Pr_s = (C_s \mu_s / k_s)\text{, Prandtl Number} \qquad (4.2c)$$

(μ_s / μ_w), Viscosity ratio

$$F_1 = (d_o/D_i)\ (P - d_o)/P\text{, tube arrangement factor} \qquad (4.2d)$$

$$F_2 = A_b/(A_b + A_c)\text{, clearance ratio} \qquad (4.2e)$$

$$F_3 = \{ L_2 + (L_1 - L_2)\ [2L_3/(L_1 - L_2)]^{0.6} \} / L_1\text{, end space factor} \qquad (4.2f)$$

In this correlation the mass velocity, $V_s \rho_s$, is evaluated making use of a ficticious flow area equal to the harmonic mean of baffle window area, minimum and maximum real crossflow areas between baffles (see equation 4.16).

The corresponding correlation to evaluate the tube side heat transfer coefficient depends on the type of flow. Since no extreme conditions exist in the exchanger, the Dittus-Boelter correlation is applicable for the turbulent regime (Re>10000).

$$Nu_t = 0.023\, Re_t^{0.8}\, Pr_t^{n} \qquad (4.3)$$

Where the Nu, Re and Pr groups are defined in a similar way to those in the shell side correlation, with properties also evaluated at the bulk temperature of the tube side stream.

The exponent n is 0.4 for the heating condition or cold fluid in the tube, and 0.3 for the cooling condition, although some workers suggest a single value (0.33) for both conditions.

For the transition region ($2100 < Re < 10000$) the accepted correlation is

$$Nu_t = 0.116\,(Re^{1/3}-125).Pr^{1/3}(\mu/\mu_w)_t^{0.14}\cdot[1 + (D/L)^{2/3}] \tag{4.4}$$

And for the laminar regime ($Re < 2100$) the corresponding expression is

$$Nu_t = 1.86\,(Re.Pr.D/L)^{1/3}(\mu/\mu_w)_t^{0.14} \tag{4.5}$$

A more specific correlation for water was obtained from the data of Eagle and Ferguson (21) reported in graphical form by Kern (54) in British units, which after conversion to c.g.s. units gave

$$h = 0.0000304\,(T + 70).V^{0.804}\ \mathrm{Cal/cm^2.S.^oC} \tag{4.6}$$

with T, temperature in degrees centigrade and V, velocity (cm/s) of the water inside the tube. This heat transfer coefficient was used in this work with better results than those obtained by the use of other correlations. The use of equations(4.4) and (4.5) lead always to results lower than the experimental ones, so that the application of equation (4.6) instead of them, for the experimental conditions of this work implied a better prediction of the system behaviour.

It must be stressed at this time that equations (4.1) and (4.3) to (4.6) were originally developed for steady-state conditions, i.e. when velocities and physical properties of the fluids are time invariant. However their use has been extended in the past for moderate deviations from the steady state conditions by several workers without noticeable adverse effect on their results. Hence the previously mentioned correlations for heat transfer coefficients were adopted in this work to calculate both steady state and transient temperature profiles.

4.1.3 Process Simplifications

Before setting up the mathematical model of the process it is convenient to define the simplifications made to it in order to obtain a description suitable for analysis and solution without undue effort. These simplifications are:

(i) There is no exchange of heat between the exchanger and the surroundings. This was accomplished in practice by insulating the exchanger from the environment with asbestos lagging.

(ii) Neither heat generators nor heat sinks are present within the exchanger; that is to say viscous dissipation is negligible and the mechanical energy, mainly kinetic and potential, is also negligible, compared with thermal energy throughput.

(iii) Due to the moderate temperature gradients, axial diffusion and conduction are negligible. The theory indicates that this is the case when flow velocity is high, but becomes less so as the velocity decreases. This assumption was cautiously adopted with the intention of finding a practical limit to its application. The results are discussed in Chapter 7.

(iv) The properties of the fluids and metal walls are independent of the temperature gradients within the exchanger. This simplification can be justified because of the moderate gradients along it and because the properties of the materials can be evaluated at an overall average temperature so that the effect of the difference between the real and the used temperatures on the overall behaviour of the exchanger tends to cancel out.

(v) The radial temperature distributions are averaged so allowing the temperatures of both streams to be defined as the bulk or 'mixed cup' temperatures. The concept of flat temperature profile in tubular flow requires a high degree of turbulence and therefore its application has been restricted to Reynolds numbers larger than 10000. In the baffled shell-and-tube heat exchanger, the shell side flow is characterised by the effect of frequent changes of direction and the successive accelerations and decelerations caused by the restrictions and expansions of the flow path, resulting in a turbulent regime extended well below the limiting Reynolds Number set for similar tubular conduits. On the other hand the small diameter of the tubes in the bundle, makes the development of sharp temperature profiles more significant when the bundle instead of the tubes is considered. It is therefore true that for the same level of Reynolds Number the overall temperature profile of the bundle is much sharper than that found in an equivalent tube carrying the same mass flow as the bundle (see Fig.4.2).

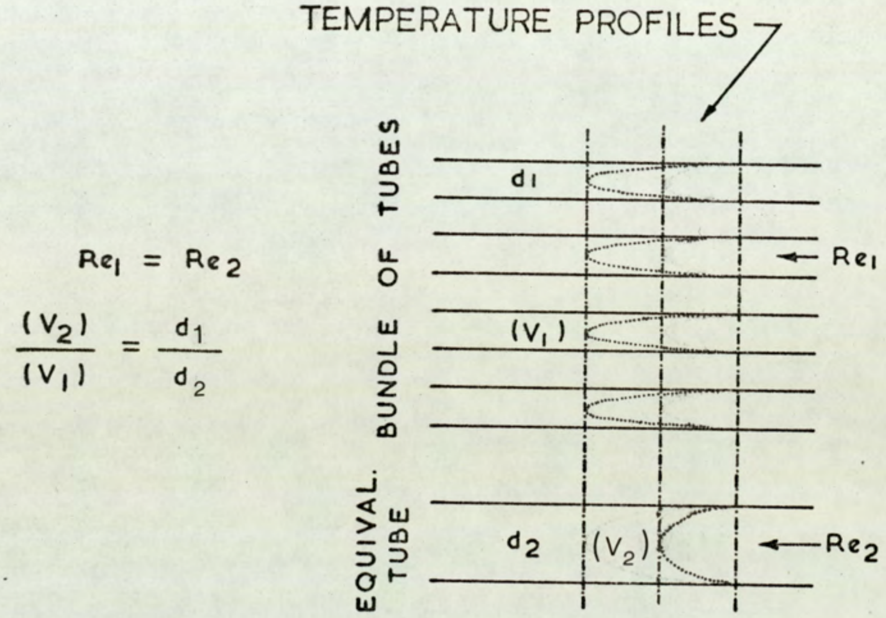

Fig.4.2 Effect of Subdividing the Flow, at Fixed Reynolds Number on the Spread of the Temperature Profile.

Each tube is then surrounded by an environment of fluid whose temperature changes gradually and uniformly in the direction of the main axis of the heat exchanger but is constant in the transverse direction. It can be noticed that besides the effects just mentioned, the shell fluid travelling in a sinusoid-like path induces an oscillating rate of heat exchange, and therefore of temperature variation, due to its partially 'folded' trajectory along the tube bundle, thus creating regions of high and low heat transfer rate within a single section between baffles. Because one region of high transfer is followed by a region of low transfer, such deviations tend to cancel out and their net effect is to produce a gradually changing 'mixed' temperature in both streams.

(vi) The effects of buoyancy are negligible in both streams and only forced convection of the fluids is considered.

(vii) The effects of radiation and radial conduction in the fluid are considered as included in the local heat transfer coefficient. This is justifiable since in the experimental origin the local coefficient is deduced with this consideration in mind.

(viii) The heat transfer coefficients are direct functions of the fluid velocities via Reynolds number and within moderate changes of velocity the functionality is linear. In practice this is so because the gradual changes of individual heat transfer coefficients with variations of fluid velocity permit one to assume a linear relationship within moderate ranges of variation. Mathematically this is achieved by a linearisation procedure explained in Section 4.1.6.

4.1.4 Mathematical Description

With the previous simplifications established, the mathematical description of the process can be carried out by simple heat balances around the differential element of heat exchanger shown in Fig.4.3.

The heat balance is carried out for both fluids and both walls, according to the general equation,

Heat Accumulation = Heat in by Bulk Flow + Heat in by Exchange
- Heat out by Bulk Flow - Heat out by Exchange (4.7)

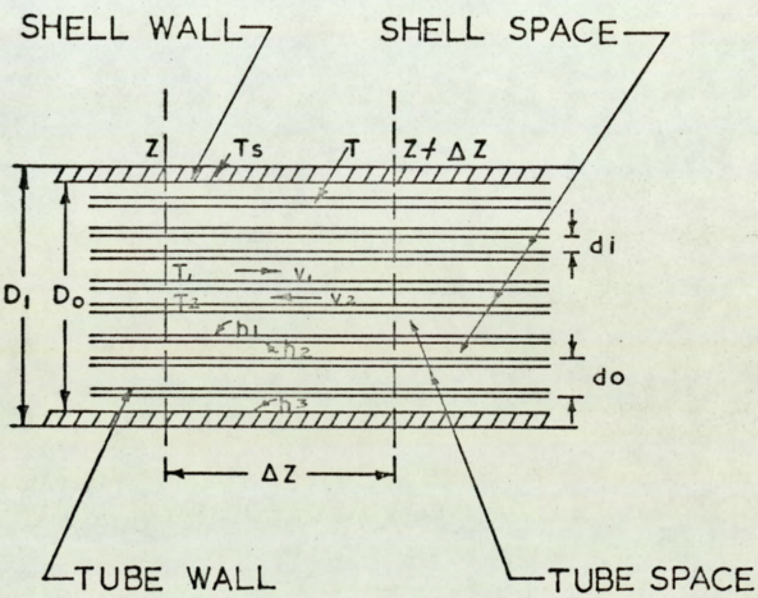

Fig.4.3 Differential Element of Heat Exchanger

Assuming countercurrent flow and the hot stream in the tubes, the individual balances, where prime (') designates dimensioned variables, become

For the tube fluid

$$N\pi R_1{}^2\Delta z'\rho_1 C_1\frac{\partial T'_1}{\partial t'} = G_1{}'C_1\left[T_1'(z',t') - T_R'\right] - G_1'C_1\left[T'_1(z',+\Delta z',t') - T_R'\right]$$

$$- 2\pi NR_1\Delta z'h_1{}'\cdot\left[T_1{}' - T_w{}'\right] \qquad (4.8)$$

The z'-co-ordinate is chosen to agree always with the tube flow direction.

For the tube wall,

$$N\pi\left[R_2{}^2 - R_1{}^2\right]\cdot\Delta z'\rho_w C_w\frac{\partial T_w{}'}{\partial t} = 2\pi NR_1\Delta z'h_1{}'\left[T_1{}' - T_w{}'\right]$$

$$- 2\pi NR_2\Delta z'h'_2\left[T_w{}' - T_2{}'\right] \quad (4.9)$$

For the shell side fluid,

$$\pi\left[D_1^{\;2}/4 - NR_2^2\right]\rho_2\, C_2\;\frac{\partial T_2{}'}{\partial t'} = G_2{}'C_2\left[T_2{}'(z'+\Delta z',t') - T_R'\right]$$

$$+\; 2\pi NR_2\Delta z'h_2{}'\cdot\left[T_w{}' - T_2{}'\right]$$

$$-\; G_2{}'C_2\;\left[T_2{}'(z',t') - T_R{}'\right]$$

$$-\; \pi D_i\Delta z'h_3{}'\;\left[T_2{}' - T_s{}'\right] \qquad (4.10)$$

And for the shell wall,

$$\frac{1}{4}\,\pi\cdot\left[D_2^{\;2} - D_1^{\;2}\right]\cdot\Delta z'\rho_t C_t\;\frac{\partial T_s{}'}{\partial t'} = \pi D_1\,\Delta z'h_3{}'\;(T_2{}'-T_s{}') \qquad (4.11)$$

By expansion of the functions of $(z' + \Delta z')$ using the Taylor Series, dividing all equations by $\Delta z'$ and then letting $\Delta z' \rightarrow 0$, the above four balances become

$$\frac{\partial T_1{}'}{\partial t'} = \frac{-G_1{}'C_1}{N\pi R_1^{\;2}\rho_1 C_1}\cdot\frac{\partial T_1{}'}{\partial z'} - \frac{2\pi NR_1 h_1{}'}{\pi NR_1^{\;2}\rho_1 C_1}\,(T_1{}'-T_w{}') \qquad (4.12)$$

$$\frac{\partial T\;'}{\partial t'} = \frac{2\pi NR_1 h_1{}'}{\pi N(R_2^{\;2}-R_1^{\;2})\rho_w C_w}\;(T_1{}'-T_w{}') - \frac{2\pi NR_2 h_2{}'}{\pi N(R_2^{\;2}-R_1^{\;2})\rho_w C_w}\,(T_w{}'-T_2{}') \qquad (4.13)$$

$$\frac{\partial T_2{}'}{\partial t'} = \frac{G_2{}'\;C_2}{\pi(\frac{1}{4}D_1^2-NR_2^2)\rho_2 C_2}\cdot\frac{\partial T_2{}'}{\partial z'} + \frac{2\pi NR_2 h_2{}'}{\pi(\frac{1}{4}D_1\,2-NR_2^2)\rho_2 C_2}\,(T_t{}'-T_2{}') +$$

$$-\;\frac{\pi D_1 h_3{}'}{\pi(\frac{1}{4}D_1^{\;2}-NR_2^{\;2})\rho_2 C_2}\,(T_2{}'-T_s{}') \qquad (4.14)$$

and

$$\frac{\partial T_s{}'}{\partial t'} = \frac{\pi D_1 h_3{}'}{\pi(D_2^2-D_1^2)\;\frac{1}{4}\rho_s C_s}(T_2{}'-T_s{}') \qquad (4.15)$$

where

$$G_1' = S_1V_1'\rho_1 \text{ and } G_2' = S_2V_2'\rho_2$$

Note that in these expressions S_1 is the total transverse flow area, i.e. total transverse section of all tubes but S_2 has a less clear meaning, depending on the way the fluid velocity is defined in the correlation used to estimate the shell side heat transfer coefficient. In this work S_2 has been made a function of the net flow area through the baffled window, A_b, the minimum crossflow area between baffles, A_p, and the maximum crossflow area between baffles, A_m, according to the expression

$$\frac{1}{S_2} = \frac{1}{3}\left(\frac{1}{A_b} + \frac{1}{A_p} + \frac{1}{A_m}\right) \tag{4.16}$$

On the other hand the coefficients of equations (4.12) to (4.15) are ratios of dimensional groups whose physical meaning is heat throughput divided by heat capacitance per unit length of the exchanger. For example the first coefficient of equation (4.12) is thermal throughput by bulk flow of the tube fluid, divided by the thermal capacitance of the same fluid contained per unit length of the exchanger. Similarly, the first coefficient of equation (4.13) is thermal throughput across the inner surface of the tube wall, divided by the thermal capacitance of the same wall, per unit length. In order to keep this relationship clear and at the same time bring into the expression the velocity of the fluids we make use of the identities

$$G_1' = S_1V_1'\rho_1 = N\pi R_1^{\,2}V_1'\rho_1 \tag{4.17a}$$

and

$$G_2' = S_2V_2'\rho_2 \tag{4.17b}$$

If now constant K_o is defined as

$$K_o = \frac{S_2}{\pi(\frac{1}{4}D_1^{\,2}-NR_2^{\,2})} \tag{4.18}$$

the total shell side mass flow becomes

$$G'_2 = K_o\pi(\frac{1}{4}D_1^{\,2}-NR_2^{\,2}) \tag{4.19}$$

Substituting the two expressions for G_1' and G_2' into equations (4.12) and (4.14) and simplifying the mathematical model of this heat transfer process becomes

$$\frac{\partial T_1'}{\partial t'} = -V_1'\frac{\partial T_1'}{\partial z'} - \frac{2h_1'}{\rho_1 C_1 R_1}(T_1' - T_w') \tag{4.20}$$

$$\frac{\partial T_w'}{\partial t'} = \frac{2R_1 h_1'}{(R_2^{\,2}-R_1^{\,2})\rho_w C_w}(T_1'-T_w') - \frac{2R_2 h_2'}{(R_2^{\,2}-R_1^{\,2})\rho_w C_w}(T_w'-T_2') \tag{4.21}$$

$$\frac{\partial T_2'}{\partial t'} = V_2'K_o\frac{\partial T_2'}{\partial z'} + \frac{2NR_2 h_2'}{(D_1^{\,2}/4-NR_2^{\,2})\rho_2 C_2}(T_w'-T_2') - \frac{D_i h_3'}{(D_1^{\,2}/4-NR_2^{\,2})\rho_2 C_2}(T_2'-T_s') \tag{4.22}$$

and

$$\frac{\partial T_s'}{\partial t'} = \frac{4D_1 h_3'}{(D_2^{\,2}-D_1^{\,2})\rho_s C_s}(T_2' - T_s') \tag{4.23}$$

This description is equally valid for the parallel fluid in which case the sign V_2' in equation (4.22) is negative.

The model just defined involves a set of four simultaneous partial differential equations with two partial derivatives of temperature with respect to axial distance and four partial derivatives of temperature with respect to time. In order to render the system soluble each distance-derivative requires one time-independent condition to be known for a given point in the heat exchanger, and the four time-derivatives require as many different temperature-distance relationships for a given time. The first two conditions correspond to the fluids inlet temperature, i.e. the boundary conditions of the fluid temperature in the limits of the exchanger. For the counter current case they are

$$T_1'(0,t') = T'_1(t') \tag{4.24a}$$

$$T_2'(L,t') = T_2'(t') \tag{4.24b}$$

For the parallel flow case the second condition changes to

$$T_2'(0,t') = T_2'(t') \tag{4.24c}$$

In this study the above three conditions are further restricted to be constant.

The four temperature-distance relationships are the temperature profiles of the exchanger when operating in the steady state condition

$$T_1'(z',0) = T_1'(z') \tag{4.25a}$$

$$T_W'(z',0) = T_W'(z') \tag{4.25b}$$

$$T_2'(z',1) = T_2'(z') \tag{4.25c}$$

$$T_s'(z',0) = T_s'(z') \tag{4.25d}$$

It should be mentioned that the four previous profiles, which are valid for either countercurrent or parallel flow are determined using conditions defined by equations (4.24a) and (4.24b) as split boundary conditions or (4.24a) and (4.24c) as initial steady state conditions.

4.1.5 Normalization of Variables

In order to ease the analysis procedure and at the same time reach more general conclusions about the system operation it is convenient to express the variables as dimensionless groups by means of the following relationships:

$$T_i = \frac{T_i' - T_2'(L)}{T_1'(O)-T_2'(L)} \tag{4.26a}$$

with i = 1,2,w,s

$$Z = Z'/L \tag{4.26b}$$

$$t = t'/(L/V_{10}') \tag{4.26c}$$

$$V_i = V_i'/V_{io}') \tag{4.26d}$$

with i = 1,2

$$v = V_{20}'/V_{10}' \tag{4.26e}$$

$$H_i = h_i'/h_{io}' \tag{4.26f}$$

with i = 1,2,3

When these relationships are substituted into the real variable equations the following equations in terms of the normalized variables are obtained after some simplification.

$$\frac{\partial T_1}{\partial t} + V_1 \frac{\partial T_1}{\partial Z} = \frac{2H_1 h_{10}'(L/V_{10}')}{\rho_1 C_1 R_1} (T_W - T_1) \tag{4.27}$$

$$\frac{\partial T_w}{\partial t} = \frac{2R_1 H_1 h_{10}'(L/V_{10}')}{(R_2^2-R_1^2)\ \rho_w C_w}(T_1 - T_w) + \frac{2R_2 H_2 h_{20}'(L/V_{10}')}{(R_2^2-R_1^2)\ \rho_w\ C_w} (T_2 - T_w) \tag{4.28}$$

$$\frac{\partial T_2}{\partial t} - v\ V_2\ K_o\ \frac{\partial T_2}{\partial Z} = \frac{2NR_2 H_2 h_{20}'(L/V_{10})}{(D_1^2/4-NR_2^2)\rho_2 C_2}(T_w - T_2) + \frac{D_1 H_3 h_{30}'(L/V_{10}')}{(D_1^2/4-NR_2^2)\rho_2 C_2}(T_s - T_2) \tag{4.29}$$

$$\frac{\partial T_s}{\partial t} = \frac{4D_1H_3h_{30}'(L/V_{10}')}{(D_2^{\ 2} - D_1^{\ 2})\rho_s C_s}(T_2 - T_s) \tag{4.30}$$

The corresponding boundary conditions become

$$T_1(0,t) = T_1(t) = 1 \tag{4.31a}$$

and $$T_2(L,t) = T_2(t) = 0 \tag{4.31b}$$

for counter-current flow; or

$$T_2(0,t) = T_2(t) = 0 \tag{4.31c}$$

for parallel flow.

The steady state profiles or initial conditions for the solution of the unsteady regime are, then

$$T_1(Z,0) = T_1(Z) \tag{4.32a}$$

$$T_w(Z,0) = T_w(Z) \tag{4.32b}$$

$$T_2(Z,0) = T_2(Z) \tag{4.32c}$$

$$T_s(Z,0) = T_s(Z) \tag{4.32d}$$

Furthermore, each variable coefficient of equations (4.27) to (4.30) can be decomposed into two factors: The one includes all constant parameters and the other, including the variation caused when the flow velocity changes, is the normalized heat transfer coefficient itself. Denoting the constant factor by P_i (i = 1, ...6)

$$P_1 = \frac{2h_{10}'(L/V_{10}')}{\rho_1 C_1 R_1} \tag{4.33a}$$

$$P_2 = \frac{2R_1 h_{10}'(L/V_{10}')}{(R_2^{\ 2} - R_1^{\ 2})\rho_w C_w} \tag{4.33b}$$

$$P_3 = \frac{2R_2 h_{20}'(L/V_{10}')}{(R_2^{\ 2} - R_1^{\ 2})\rho_w C_w} \tag{4.33c}$$

$$P_4 = \frac{2NR_2h_{20}'(L/V_{10}')}{(D_1^2/4-NR_2^2)\rho_2C_2} \tag{4.33d}$$

$$P_5 = \frac{D_1h_{30}'(L/V_{10})}{(D_1^2/4 - NR_2^2)\rho_2C_2} \tag{4.33e}$$

$$P_6 = \frac{4D_1h_{30}'(L/V_{10}')}{(D_2^2-D_1^2)\rho_sC_s} \tag{4.33f}$$

Hence the general normalized equations of the model become:

$$\frac{\partial T_1}{\partial t} + V_1\frac{\partial T_1}{\partial z} = P_1H_1(T_w-T_1) \tag{4.34}$$

$$\frac{\partial T_w}{\partial t} = P_2H_1(T_1-T_w) + P_3H_2(T_2-T_w) \tag{4.35}$$

$$\frac{\partial T_2}{\partial t} - v\ V_2K_o\ \frac{\partial T_2}{\partial Z} = P_4H_2(T_w-T_2) + P_5H_3(T_s-T_2) \tag{4.36}$$

$$\frac{\partial T_s}{\partial t} = P_6H_3(T_2-T_s) \tag{4.37}$$

4.1.6 Linearisation Procedure

With regard to the type of disturbance applied to the system this general model may be linear if only the input temperature vector changes or non-linear if the disturbances are applied to the input flow vector. The first type of disturbance does not affect the heat transfer coefficient, provided the effect of temperature changes on the properties of the materials can be neglected, and therefore the equations of the model are of the constant coefficient class.

The non-linearity in the case of flow forcing is due to the fact that the heat transfer coefficients are related to fluid velocities by the fractional power defined in the correlations of equations (4.1) for shell side and (4.3) to (4.6) for the tube side, depending on the value of Reynolds Number. That relationship is of the general form

$$h' = \alpha V'^{n} \tag{4.38}$$

for real variables or

$$H = V^{n} \tag{4.39}$$

for normalized variables.

However, by making use of the Perturbation Theory, the general equation can be linearised for the case of flow forcing, if the magnitude of the velocity deviation allows. This is done by expressing all variables in the equations representing the transient conditions as the sum of a steady state component plus a deviation component. For example, in normalized variables,

$$T = T_{ss} + T_{D} \tag{4.40a}$$

$$V = V_{ss} + V_{D} \tag{4.40b}$$

$$H = H_{ss} + H_{D} \tag{4.40c}$$

When these last two expressions are substituted into the heat transfer correlation it is easily seen that

$$H = (V_{ss} + V_{D})^{n} = (1 + V_{D})^{n} \tag{4.41}$$

Making use of the binomial expansion valid for all $V_D < 1$ and neglecting powers of V_D, the following linear relationship is obtained

$$H = 1 + n\,V_{D} \tag{4.42}$$

This linearised expression is substituted into the model equations, all the products of deviations are neglected and then the corresponding equations representing the steady state condition are subtracted from those representing the transient conditions. After further re-arrangement and simplification the linearised model is

$$\frac{\partial T_{1D}}{\partial t} + \frac{\partial T_{1D}}{\partial Z} + V_{1D}\frac{\partial T_{10}}{\partial Z} = P_1(T_{wD}-T_{1D}) + V_{1D}P_1(T_{wo}-T_{10})\,n_1 \qquad (4.43)$$

$$\frac{\partial T_{wD}}{\partial t} = P_2(T_{1D}-T_{wD}) + n_1V_{1D}P_1(T_{10}-T_{wo}) + P_3(T_{2D}-T_{wD}) + n_2V_{2D}P_3(T_{20}-T_{wo}) \qquad (4.44)$$

$$\frac{\partial T_{2D}}{\partial t}\ v\ K_o\ \frac{\partial T_{2D}}{\partial Z} - vK_oV_{2D}\ \frac{\partial T_o}{\partial Z} = P_4(T_{wD}-T_{2D}) + n_2V_{2D}P_4(T_{wo}-T_{20}) + P_5(T_{sD}-T_{2D}) + n_3V_{2D}P_5(T_{so}-T_{20}) \qquad (4.45)$$

$$\frac{\partial T_{sD}}{\partial t} = P_6(T_{2D}-T_{sD}) + n_3V_{2D}P_6(T_{20}-T_{so}) \qquad (4.46)$$

The details of this deduction for a concentric tube heat exchanger model, have been presented in ref. (75). The linearised model is presented here for completeness since the analysis in this work was devoted to the general case, described by equations (4.34) to (4.37), with boundary conditions of equations (4.32a to d). The numerical solution, presented in Chapter Five, made possible the continuous updating of the coefficients as the flow rates changed. The correction for temperature variation was approximated by evaluating the properties of the fluids at the mean point of the exchanger.

4.2 FREQUENCY RESPONSE ANALYSIS

The analysis of a system by its quasi-steady state response to sinusoidal disturbances of different frequencies, generally called 'frequency response analysis' has proved very useful in describing the general dynamic behaviour of the system. The conceptual simplicity of the method and its relatively unsophisticated experimental implementation have made it a widely used method in many areas of control engineering.

It has, however, a significant drawback: strictly speaking it can only be applied to invariant parameter linear systems, i.e. those which can be described by linear differential equations with constant coefficients, because only they can be directly Laplace transformed. The operation of Laplace transformation on a mathematical description in terms of deviation real variables, T(t) and V(t), changes the domain of the description, usually time as shown, to the domain of the complex variable s of the transform. If the mathematical description is of the form

$$a_o T(t) + a_1 T'(t) + a_2 T''(t) + \dots + a_n T^{(n)}(t) = V(t) \qquad (4.47)$$

where T and V are the state function and forcing function respectively, the operation of Laplace transformation on both sides of the equation gives

$$(a_o + a_1 s + a_2 s^2 + \dots + a_n s^n)\, T(s) = V(s) \qquad (4.48)$$

From the previous equation the advantage of using deviation variables in the mathematical description of the system is evident; the resulting differential equation in time, equation (4.47) after being transformed becomes immediately an algebraic equation in s without regard for the initial steady state of the system, since all initial conditions are zero and the coefficients, $a_o \dots a_n$, are constant.

By definition (17) the cause-and-effect relationship in the complex domain, characteristic of the system, is given by the ratio of the Laplace transform of the output to the Laplace transform of the input and is called the transfer function of the system.

From equation (4.48) it is found to be

$$\frac{T(s)}{V(s)} = \left[\frac{1}{a_o + a_1 s + a_2 s^2 + \ldots + a_n s^n}\right] = G(s) \tag{4.49}$$

For the particular case in which

$$V(t) = A \sin \omega t \tag{4.50}$$

and consequently

$$V(s) = \frac{A\omega}{\omega^2 + s^2} \tag{4.51}$$

It is shown in several texts (17, 41) that the frequency response of the system is obtained simply by replacing the operator s by the complex angular frequency $j\omega$ in the transfer function,

$$\text{i.e.} \quad \frac{T(j\omega)}{V(j\omega)} = G(j\omega) = \frac{1}{a_o + a_1(j\omega) + a_2(j\omega)^2 + \ldots + a_n(j\omega)^n)} \tag{4.52}$$

Since $G(j\omega)$ is a complex quantity its conversion to polar form results in the definition of Magnitude and Angle

$$\text{Magnitude} = \left|\frac{1}{a_o + a_1(j\omega) + a_2(j\omega)^2 + \ldots + a_n(j\omega)^n}\right| = \left|G(j\omega)\right| \tag{4.53}$$

$$\text{Angle} = \angle \frac{1}{a_o + a_1(j\omega) + a_2(j\omega)^2 + \ldots + a_n(j\omega)^n} = \angle G(j\omega) \tag{4.54}$$

These quantities correspond precisely to the Amplitude Ratio and Phase Angle that as functions of frequency describe the dynamic behaviour of the system. All that is needed for the method to be applicable is that each of the roots of the characteristic equation of (4.47) has a negative real part. That makes the complementary solution of the differential equation vanish exponentially in time and ensures stability of the system.

As mentioned before, frequency response analysis cannot be applied directly to non-linear mathematical models because no transfer function exists for them. However an indirect application can be made if the models are linearized. Since linearization is an approximation technique, usually valid for small deviations from a given steady state, the results so obtained must be evaluated keeping in mind those restrictions.

In the case of the analysis of the shell-and-tube heat exchanger under flow disturbances it becomes a time variable parameter system. In order to make its model Laplace transformable and at the same time keep as much resemblance as possible to the general model of equations (4.34) to (4.37), the dependence of heat transfer coefficients on their respective velocities was linearised according to equations (4.40b) to (4.42), and the complete set of equations was linearised using the principles of perturbation theory.

4.3 PULSE TESTING AND FOURIER ANALYSIS

The theoretical fundamentals of frequency response are very sound and elegant but although the experimental technique is easy in principle, it has the disadvantage of requiring a very long time to collect adequate information for a significant frequency range. This is a serious drawback when analysing large and complex systems whose operating conditions are very critical and expensive, or when the testing period is bound to generate out-of-specification products. In these cases evident economic considerations make the use of sinusoidal testing questionable.

Fortunately the development of the pulse testing technique (19, 44) has greatly reduced the previously mentioned experimental limitations and makes it possible to obtain frequency response data with shift of part of the experimental effort to computer calculations.

Pulse testing theory is based on Fourier Analysis. When the fundamental period (2P) of the Fourier expansion of a time function T(t) is increased, the discrete amplitude and phase spectra, which indicate the harmonic content of the expansion, tend to become in the limit continuous spectra. Under that condition the Finite Fourier Expansion becomes the Continuous Fourier Integral of T(t).

$$T(t) = \int_{-\infty}^{\infty}\left[\int_{-\infty}^{\infty} T(t)\, e^{-j2\pi ft}dt\right] \cdot e^{j2\pi ft}df \qquad (4.55)$$

for which the conditions of validity (Dirichlet's conditions) are

(i) $\int_{-\infty}^{\infty} |T(t)|dt$ must be finite,

(ii) T(t) must have a finite number of discontinuities,

(iii) T(t) must have a finite number of maxima and minima.

Defining the expression within brackets in the previous equation as θ (f),

i.e., $$\theta(f) = \int_{-\infty}^{\infty} T(t)\, e^{-j2\pi ft}dt \qquad (4.56)$$

it is seen that the time function T(t) can be considered as the sum of an infinite number of frequency components, each of an infinitesimal amplitude θ(f)df . θ(f) is the frequency spectrum of T(t), generally complex and therefore containing both amplitude and phase.

$T(t)$ and $\theta(f)$ are called a Fourier transform pair which can be related in symbolic notation as

$$\theta(f) = F[T(t)] \tag{4.57}$$

and

$$T(t) = F^{-1}\,[\theta(f)] \tag{4.58}$$

The Fourier integral thus indicates a way of obtaining the frequency spectrum of a time function and vice versa.

If a stable system is disturbed by a transient function $v(t)$ a pulse for example, the response of the system is bound to be transient as well. The input function and the output function can be Fourier transformed to find their frequency content and a further relating of the two frequency functions ought to give the characteristic frequency response of the system.

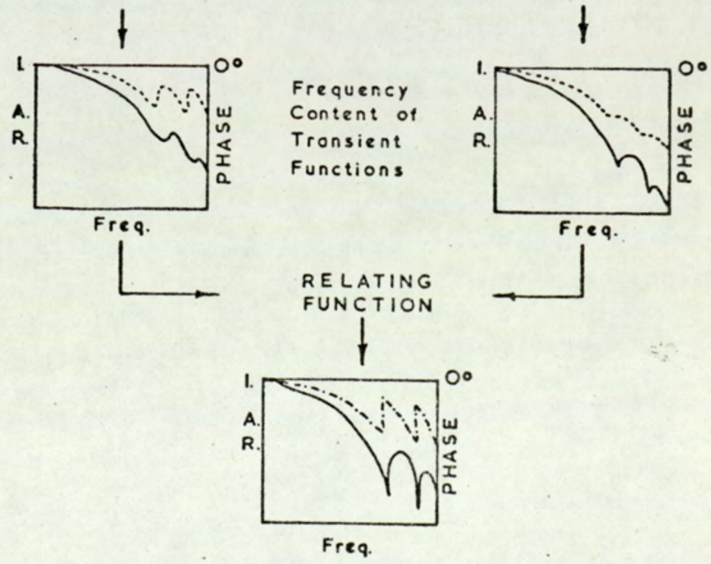

Fig.4.4 Schematic Diagram to Find the Frequency Response of a System by Transient Pulse Analysis.

This last information is obtained from the Relating Function, defined as

$$\text{Relating Function} = \frac{F[T(t)]}{F[v(t)]} = \frac{\int_{-\infty}^{\infty} T(t)e^{-j2\pi ft}dt}{\int_{-\infty}^{\infty} v(t)e^{-j2\pi ft}dt} \qquad (4.59)$$

The two Fourier transforms are continuous functions of frequency expressed in complex form and therefore their ratio must also be a continuous function of frequency equally expressed in complex form, from which the frequency response of the system can be deduced. The method is described graphically in Fig.4.4.

Since in practice, both forcing and response functions are made available as graphical records rather than analytical functions, the corresponding Fourier transforms have to be approximated by summations of segmental Finite Fourier Transforms, defined by the functional curves, along the time axis. Under these conditions the functions are Fourier transformable where in addition to being continuous, they go to zero for sufficiently positive or negative values, of the independent variable.

The summation can be carried out by several methods, the most accurate being, perhaps, by the trapezoidal approximation of the curve. By this method the area under the curve is divided into trapezoidal segments of the same width as for graphical integration, and the Fourier transform of each segment is found. The Fourier transform of a complete transient function is then approximately equal to the summation of the Fourier transforms of all segments under the curve.

The fact that each trapezoidal segment can be replaced by two overlapping isosceles triangular pulses, as shown in Fig.4.5 makes the approximation easy to obtain since the Fourier transform of any isosceles triangular pulse, in non-dimensional form, is

$$FTP = \int_{(k-1)\Delta t}^{(k+1)\Delta t} I(k\Delta t)e^{-j2\pi ft}dt \tag{4.60}$$

$$= \int_{(k-1)\Delta t}^{(k+1)\Delta t} \left[\frac{\mathrm{Sin}\pi f\Delta t}{\pi f\Delta t}\right]^2 T(k\Delta t)e^{-j2\pi ft}dt \tag{4.61}$$

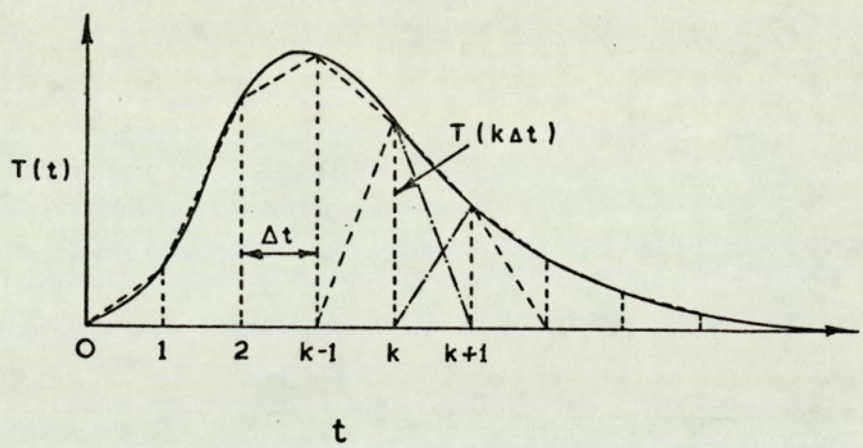

Fig.4.5 Trapezoidal Approximation of a Transient Function.

In the last two equations $I(k\Delta t)$ is defined as the isosceles triangular pulse function, existing within the limits of the integral with height $T(k\Delta t)$, while $\left[\frac{\mathrm{Sin}\pi f\Delta t}{\pi f\Delta t}\right]^2$ is the Fourier transform of the unit isosceles triangular pulse function.

Using the previous results the approximation of the transient function becomes

$$F[T(t)] = \int_{-\infty}^{\infty} T(t)e^{-j2\pi ft}dt \simeq \left[\frac{\mathrm{Sin}\pi f\Delta t}{\pi f\Delta t}\right]^2 \cdot \sum_{k=1}^{\infty} T(k\Delta t)e^{-j2\pi fk\Delta t}\Delta t \tag{4.62}$$

Note that when Δt tends to zero the factor in brackets tends to unity and therefore the summation tends to the integral. As a consequence the relating function of equation (4.59) can be approximated by the ratio of the two summation Fourier transforms

$$\mathrm{R.F.} = \frac{\left[\frac{\sin\pi f(\Delta t)_1}{\pi f(\Delta t)_1}\right]^2 \cdot \sum_{k=1}^{\infty} T(k(\Delta t)_1)e^{-j2\pi fk(\Delta t)_1}(\Delta t)_1}{\left[\frac{\sin\pi f(\Delta t)_2}{\pi f(\Delta t)_2}\right]^2 \cdot \sum_{l=1}^{\infty} v(l(\Delta t)_2)e^{-j2\pi fl(\Delta t)_2}(\Delta t)_2} \qquad (4.63)$$

and by taking time increments of the same size for both summations the expression is simplified to

$$\mathrm{R.F.} = \frac{\sum_{k=1}^{\infty} T(k\Delta t)\, e^{-j2\pi fk\Delta t}}{\sum_{k=1}^{\infty} v(k\Delta t)e^{-j2\pi fk\Delta t}} \qquad (4.64)$$

This complex expression, then provides values of Gain and Phase Angle Φ for each value of $\omega = 2\pi f$, according to the well known expressions.

$$\mathrm{Gain} = \left[(\mathrm{R.F})^2_{\mathrm{Im}} + (\mathrm{R.F})^2_{\mathrm{Re}}\right]^{0.5} \qquad (4.65)$$

and

$$\Phi = \tan^{-1}\left[(\mathrm{RF})_{\mathrm{Im}}/(\mathrm{RF})_{\mathrm{Re}}\right] \qquad (4.66)$$

where subscripts Im and Re stand for imaginary and real parts respectively.

The results so obtained are by no means free from further evaluation. Since the method is an approximation it is necessary to find some criterion of certainty to judge whether the frequency response obtained characterises the system closely enough. Several sources of inaccuracy introduce errors that are in general more significant at higher frequencies.

The maximum frequency for which valid results may be expected depends mainly on the characteristics of the Fourier transformation of the input and the relative magnitude of the noise affecting the output signal.

The magnitude of a pulse is defined as the area it encloses with the time axis and therefore depends on pulse duration and pulse amplitude. Theoretically only an impulse-pulse of infinitesimal time duration and infinite amplitude - has a uniform harmonic content that can excite the system with all its frequencies of constant amplitude. In all practical pulses, however, the amplitudes of the exciting frequencies diminish with the wavelength in a way that depends on the shape of the pulse as seen in Fig.4.6. For pulses of the same shape the usual frequency content is higher as they diminish in duration. It is worthy of note that pulses free from drastic changes of direction have the highest harmonic content.

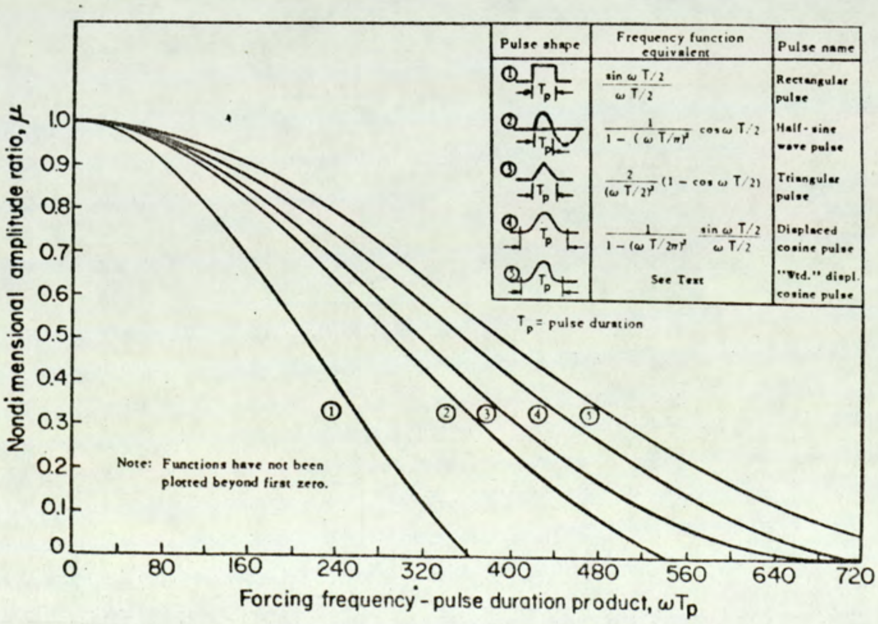

Fig.4.6 Comparison of the Harmonic Content of Several Practical Pulses (Taken from Reference 44).

The pulse function used in this work to collect experimental data was the Displaced Cosine Pulse Function (DCPF), number 4 in Fig.4.6, which besides being of high harmonic content can be easily produced by manual operation of a sinusoidal Function Generator

No rules can be formulated about which must be the characteristics of a pulse function for analysing a given system, because many factors must be taken into account. The direct experimentation with the system under study and the careful analysis of the results are the best guide.

In general the experimental effort must be directed to

(i) Use of input pulses of short duration compared to the response pulse duration.

(ii) The magnitude of the pulses must be enough to produce an acceptable signal to noise ratio in the response.

(iii) If the input pulse induces a change in the parameters of the system, the effect of its magnitude on the output pulse must be investigated.

CHAPTER 5

METHODS OF SOLUTION

The basic idea in developing a mathematical model of a physical system is the representation of its operating variables by numerical relations that enable the analyst to study the effect of different conditions and parameters on the performance of the system without it being actually operated.

In order to reach this stage, the differential equations that represent the mathematical model must be solved, i.e. integrated to yield an adequate form for the 'numerical operation' of the described system.

The general model derived in the previous chapter can be solved in two ways, and each way by several techniques

(i) Solutions in the time domain

(ii) Solutions in the frequency domain

The two types of solution provide complementary information. Thus the one yielded by the frequency analysis, though very important for purposes of design and control, cannot replace the information provided by the time domain solution, since it is this fundamental time domain information in terms of the system real variables that gives the actual performance of the operating process.

5.1 TIME DOMAIN SOLUTIONS

There are three normal time domain solutions:

(i) Pure Mathematical Analytical Solution, sometimes with computer evaluation

(ii) Analog Solution, implemented in passive or active analog computers

(iii) Numerical solution, usually implemented in a digital computer.

These three methods of solution find the relationship between the actual dependent variables of the system in terms of the independent variables, in this case temperatures of the fluids and walls of the heat exchanger in terms of axial distance and real time. Although, from the theoretical point of view the three methods should give the same results when applied to a given model, they are usually somewhat different due to limitations like the accuracy or sensitivity of the analog computers and the deviations introduced by the numerical technique.

5.1.1 Analytical Solution

The mathematical or analytical solutions are based on ordinary mathematical procedures, whose complexity depends on the type of equations to be solved. For the steady state, when distance is the only independent variable, the model becomes a system of ordinary differential equations with constant coefficients, which is relatively easy to solve. Under the restriction of steady state, valid for any time less than zero, equations (4.34) to (4.37) become

$$\frac{dT_1}{dz} = P_1(T_w - T_1) \tag{5.1}$$

$$0 = P_2(T_1 - T_w) + P_3(T_2 - T_w) \tag{5.2}$$

$$- vK_o \frac{dT_2}{dz} = P_4(T_w - T_2) + P_5(T_s - T_2) \tag{5.3}$$

$$0 = P_6(T_2 - T_s) \tag{5.4}$$

since the derivatives with regard to time are zero and the normalised v's and H's are unity.

From equations (5.4) and (5.2) it is evident that

$$T_s = T_2 \tag{5.5}$$

and

$$T_w = \frac{P_2}{P_2+P_3} T_1 + \frac{P_3}{P_2+P_3} T_2 \tag{5.6}$$

This last equation indicates that the tube wall temperature is the weighted average of the temperature of the two fluids on either side of the wall.

On substituting equations (5.5) and (5.6) into the differential equations (5.1) and (5.3) these become

$$\frac{dT_1}{dz} = \frac{P_1 P_3}{P_2+P_3}(T_2-T_1) \tag{5.7}$$

and

$$\frac{dT_2}{dz} = \frac{P_2 P_4}{vK_o(P_2+P_3)}(T_2 - T_1) \tag{5.8}$$

The solution of this set of simultaneous ordinary differential equations, according to the conventional calculus is of the form

$$T_1 = A_1 e^{r_1 z} + A_2 e^{r_2 z} \tag{5.9}$$

$$T_2 = B_1 e^{r_1 z} + B_2 e^{r_2 z} \tag{5.10}$$

where the A's and B's are constants defined by the boundary conditions and the r's are the roots of the characteristic determinant of the system.

After some algebraic manipulations it is found that

$$r_1 = 0 \tag{5.11}$$

$$r_2 = \frac{P_2 P_4}{vK_o(P_2+P_3)} - \frac{P_1\ P_3}{P_2+P_3} \tag{5.12}$$

This deduction was based on the original countercurrent flow element of the exchanger. When a similar procedure was followed for the parallel flow element only the sign of the shell velocity is changed and for this case the second root is

$$r_2 = -\frac{P_1P_3}{P_2+P_3} - \frac{P_2P_4}{vK_o(P_2+P_3} \qquad (5.13)$$

Considering both heating and cooling processes in co-current and countercurrent flow, the four sets of boundary conditions give rise to four different sets of solutions. They are presented in Table 5.1 in which

$$f = \frac{P_2+P_3}{P_1P_2} r_2 + 1 \qquad (5.14)$$

and the T's and z are normalised variables according to Section 4.1.5.

STEADY STATE SOLUTIONS				
PROCESS	HEATING	COOLING	HEATING	COOLING
Boundary Conditions	$T_1(0) = 0$ $T_2(1) = 1$	$T_1(0) = 1$ $T_2(1) = 0$	$T_1(0) = 0$ $T_2(0) = 1$	$T_1(0) = 1$ $T_2(0) = 0$
Profile of $T_1(z) =$	$\frac{e^{r_2z} - 1}{fe^{r_2} - 1}$	$\frac{fe^{r_2} - e^{r_2z}}{fe^{r_2} - 1}$	$\frac{e^{r_2z} - 1}{f-1}$	$\frac{f - e^{r_2z}}{f-1}$
Profile of $T_2(z) =$	$\frac{fe^{r_2z} - 1}{fe^{r_2} - 1}$	$\frac{f(e^{r_2} - e^{r_2z})}{fe^{r_2} - 1}$	$\frac{fe^{r_2z} - 1}{f-1}$	$f(1-e^{r_2z})$
Equations	(5.15a, b)	(5.16a,b)	(5.17a,b)	(5.18a,b)

TABLE 5.1 STEADY STATE SOLUTIONS FOR DIFFERENT BOUNDARY CONDITIONS

It is important to note that for the particular case in which $r_2 = 0$, which is only possible in countercurrent flow,

$$P_1P_3 = \frac{P_2P_4}{vK_o} = a \tag{5.19}$$

the corresponding solutions become indeterminate. In this case equations (5.7) and (5.8) take the form

$$\frac{dT_1}{dz} = a\ (T_2-T_1) \tag{5.20}$$

and

$$\frac{dT_2}{dz} = a(T_2-T_1) \tag{5.21}$$

'a' being constant. Straightforward analysis indicates that the temperature profiles of the two fluids are then parallel lines of constant slope

$$T_1 = 1 - \frac{a}{1+a} z \tag{5.22a}$$

$$T_2 = \frac{a}{1+a} (1-z) \tag{5.22b}$$

for the cooling process.

Similarly for the heating process, the corresponding profiles are

$$T_1 = \frac{a}{1+a} z \tag{5.23a}$$

$$T_2 = \frac{1}{1+a} (1+az) \tag{5.23b}$$

This particular condition in which $r_2 = 0$ is important because it actually corresponds to the case in which the thermal capacitance of both streams are equal, i.e.,

$$C_1\rho_1V_1S_1 = C_2\rho_2V_2S_2 \tag{5.24}$$

S_1 and S_2 being the net (or equivalent) flow transverse area on the two sides of the exchanger. If the same fluid is used in both streams, then the above situation arises simply when both mass flows are equal.

The equations of Table 5.1 together with equations (5.22) and (5.23) give the normalised temperature profiles of the fluids along the heat exchanger for all possible combinations of operating conditions. Used together with equations (5.5) and (5.6), they completely describe the temperature distributions in the fluids and metallic walls of the heat exchanger in the steady state. These distributions are all that is needed to start the solution of the appropriate transient regime cases.

The solution of the mathematical model for this regime by analytical procedures is, however, far more difficult and was not attempted in this work. It was thought that it would be preferable to obtain a numerical solution using proven techniques than to try to get an analytical solution that itself might have to resort to a computer.

The procedure followed was to find the four analytical temperature profiles of the steady state and to use them to start the transient solution stepwise by applying an explicit numerical algorithm. This is discussed later in this chapter, in section 5.1.3.1, and the digital computer program developed out of it is presented in Appendix B.

5.1.2 Analog Solutions

Once more, in solving mathematical models by analog computers, it is the constant coefficient steady state models which are more easily solved and with less hardware. Besides that, the steady state description, as presented in equations (5.1) to (5.4), is directly programable. The procedure requires that the temperature functions be integrated along the axial distance, and since the operating variable of the computer is real time, time has to be used to represent axial distance of the exchanger. The integration is allowed to proceed until it reaches a scaled point in time equivalent to the total length of the exchanger.

The use of nonlinear components, like multipliers, dividers and function generators, extends the capability of the analog computer to deal with variable coefficient models, still of the single independent variable type, at the expense of reduced accuracy, since in general these nonlinear components work based on approximation principles. The transient regime solution of a model with two independent variables is made possible by the 'lumping' technique. In this case it implies that the heat exchanger is divided into a series of several modules in which one of the independent variables is assumed constant within the limits of each module at given stepped values. That is equivalent to replacement of the distributed parameter system by a series of lumped parameter 'sub-systems' which will be close enough to the original if the number of 'lumps' is high enough. In spite of some conflicting reports in the literature it is estimated that an acceptable degree of representation is achieved with six or more modules. That, however, greatly increases the number of components needed for a given patching, with the result that rather large computational facilities are required to solve even simple models. In the absence of sufficient hardware the use of the analog computer was restricted to the steady state solution based on the normalised equations (5.1) to (5.4). The block diagram for this case is presented in Fig.5.1 which as indicated by the equations, consists in the solution of two simultaneous ordinary differential equations with constant coefficients.

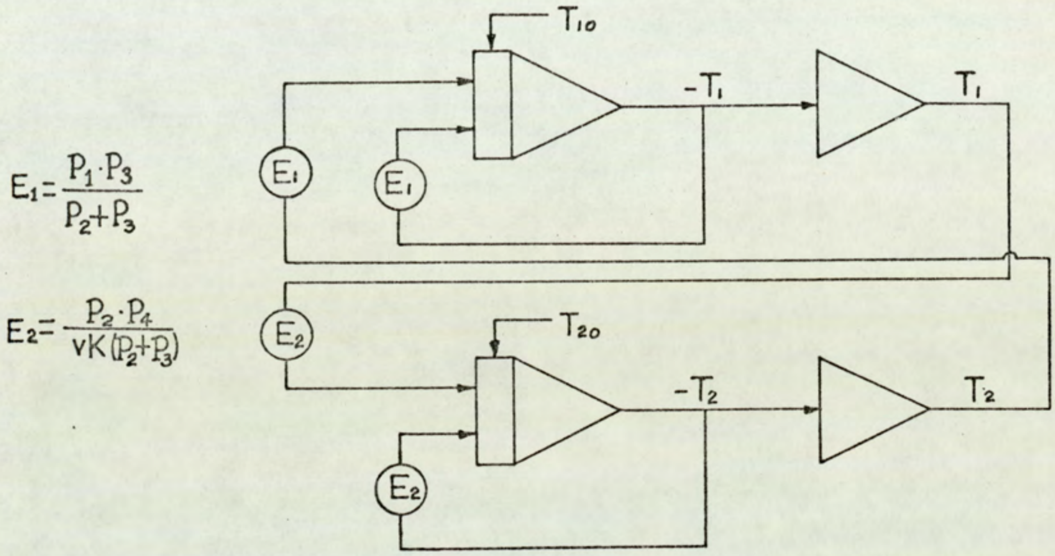

Fig.5.1 Analog Computer Block Diagram of the Heat Exchanger Steady State Solution.

5.1.3 Numerical Solution

Since no analytical solution is available in the time domain for the heat exchange system discussed in this work, the numerical solution, which has proved to be the most successful for distributed parameter systems, is used here. This method is essentially based on the 'discretization' technique that consists in replacing the derivatives of the equations in the model by the ratios of finite differences of the corresponding variables so converting the continuous differential equations into an approximate set of finite difference equations. The large amount of arithmetical operations generated by this conversion is very aptly handled by the use of sequential electronic calculators.

In physical terms the 'discretization' is equivalent to the division of the two-dimensional space defined by the two independent variables, time and axial distance, into discrete sections within which the functional variables are kept constant. With regard to the whole domain of the independent variables, the functional variables then change by steps produced in the limits of the 'discretized' sections.

The approximation of partial differential equations by finite difference equations is discussed in detail in several texts; thus Lapidus (58) and Smith et al (83) among others have presented the deduction of the most common forms of approximation, namely the forward, central and backward differences for first order derivatives and the central difference for second order derivatives. The method is based on the expansion of the functional variables by Taylor Series and subsequent truncation of the higher terms with the corresponding generation of truncation error.

The central differences are more accurate than either the backward or the forward differences because the terms neglected are of higher order, i.e. the truncation error is smaller, all other conditions being equal. For this reason the central differences are preferred whenever possible.

It is possible to use central differences in the distance direction since for each constant time a complete temperature profile along the exchanger can be estimated. It is not possible, however, to use central differences in the time direction because any time-point calculation must be based on previous time calculations. For convenience then, a backward finite difference is adopted for the time derivative approximation.

The approximations in the two directions are

$$\frac{\partial T(z,t)}{\partial z} = \frac{T(z+\Delta z,t) - T(z-\Delta z,t)}{2\Delta z} + O(\Delta z)^3 \qquad (5.25)$$

and

$$\frac{\partial T(z,t)}{\partial t} = \frac{T(z,t) - T(z,t-\Delta t)}{\Delta t} + O(\Delta t)^2 \tag{5.26}$$

where it can be noted that the truncation errors are third and second order respectively.

If the plane z-t is divided into a mesh whose intersection points each define a value of temperature, the co-ordinate of any point in the plane can be expressed in terms of the steps Δz and Δt and the integer subscripts i and j.

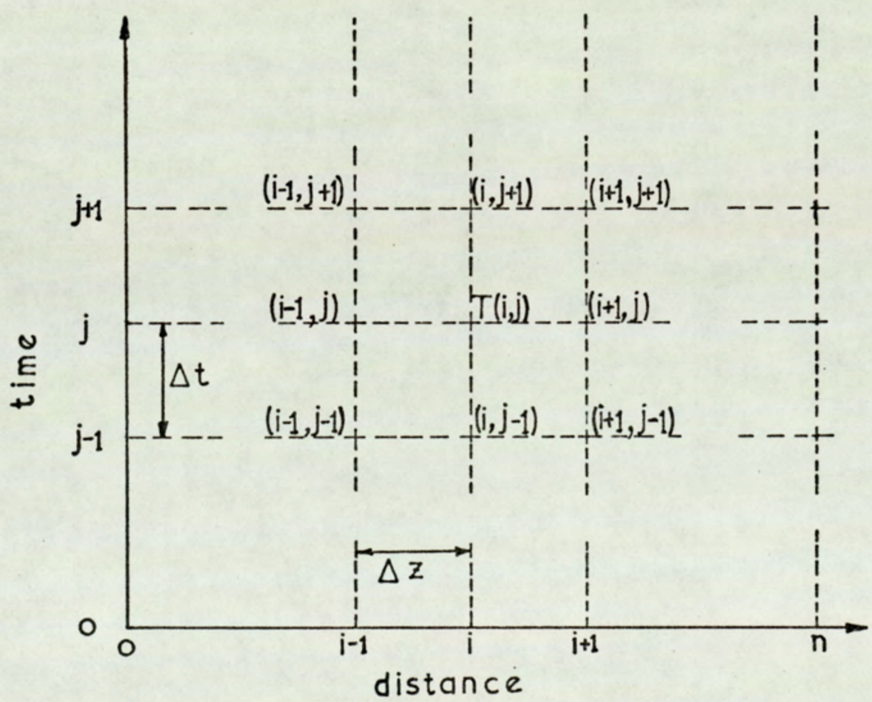

Fig.5.2 The Distance-time Plane.

By further dropping the steps from the notation and omitting the truncation error terms, equations (5.25) and (5.26) can be rewritten as

$$\frac{\partial T(i,j)}{\partial z} = \frac{T(i+1,j) - T(i-1,j)}{2\Delta z} \tag{5.27}$$

and

$$\frac{\partial T\ (i,j)}{\partial t} = \frac{T(i,j) - T(i,j-1)}{\Delta t} \tag{5.28}$$

Since any temperature evaluation can be done using values previously found, it is convenient to retract the distance derivative approximation one step in the time direction so that instead of $\frac{\partial T(i,j)}{\partial z}$, the quantity used is

$$\frac{\partial T(i,j-1)}{\partial z} = \frac{T(i+1,j-1)-T(i-1,j-1)}{2\Delta z} \tag{5.29}$$

This allows the development of one explicit algorithm since each new point value can be obtained from previous evaluations.

When equations (5.18) and (5.19) are substituted into the general normalized model, equations (4.34) to (4.37) become

$$\frac{T_1(i,j)-T_1(i,j-1)}{\Delta t} + V_1(j-1)\ \frac{T_1(i+1,j-1)-T_1(i-1,j-1)}{2\Delta z} = P_1H_1(j-1)(T_w(i,j-1)-T_1(i,j-1)) \tag{5.30}$$

$$\frac{T_w(i,j)-T_w(i,j-1)}{\Delta t} = P_2H_1(j-1)\cdot[T_1(i,j-1)-T_w(i,j-1)] + P_3H_2(j-1)\cdot[T_2(i,j-1)-T_w(i,j-1)] \tag{5.31}$$

$$\frac{T_2(i,j)-T_2(i,j-1)}{\Delta t} - K_o vV_2(j-1)\ \frac{T_2(i+1,j-1)-T_2(i-1,j-1)}{2\Delta z} = P_4H_2(j-1)\cdot[T_w(i,j-1)-T_2(i,j-1)] \quad P_5H_3(j-1)\cdot[T_s(i,j-1) - T_2(i,j-1)] \tag{5.32}$$

$$\frac{T_s(i,j)-T_s(i,j-1)}{\Delta t} = P_6H_3(j-1)\cdot[T_2(i,j-1)-T_s(i,j-1)] \tag{5.33}$$

It is obvious from them that the four distance-time temperatures can be expressed as

$$T_1(i,j) = T_1(i,j-1)+\Delta t\cdot\Big[-V_1(j-1)\frac{T_1(i+1,j-1)-T_1(i-1,j-1)}{2\Delta z} +$$

$$P_1H_1(j-1)\ (T_w(i_1j-1)-T_1(i,j-1)\ )\Big] \qquad (5.34)$$

$$T_w(i,j) = T_w(i,j-1)+\Delta t\cdot\big[P_2H_1(j-1)(T_1(i,j-1)-T_w(i,j-1)\ ) +$$

$$P_3H_2(j-1)(T_2(i,j-1)-T_w(i,j-1))\big] \qquad (5.35)$$

$$T_2(i,j) = T_2(i,j-1)+\Delta t\Big[K_o vV_2(j-1)\ \frac{T_2(i+1,j-1-T_2(i-1,j-1)}{2\Delta z} +$$

$$P_4H_2(j-1)(T_w(i,j-1)-T_2(i,j-1))+ P_5H_3(j-1)(T_s(i,j-1)-T_2(i,j-1))\Big]$$

$$(5.36)$$

$$T_s(i,j) = T_s(i,j-1)+\Delta t\ .\ P_6H_3(j-1)\cdot[(T_2(i,j-1)-T_s(i,j-1))]$$

$$(5.37)$$

These last four equations together with the initial conditions from the steady state analytical solution, equations (5.10) and (5.11) or equations (5.13) and (5.14) together with equations (5.2) and (5.4) comprise the numerical scheme used to solve the mathematical model. Since the steady state solution provides the four initial temperature profiles and the scheme is explicit in the time and distance directions, the transient solution can be started with the information available and proceeds thereafter in sustained stepwise form.

5.1.3.1 The Digital Computer Algorithm

The digital computer program developed to solve the liquid-liquid 1-1 shell and tube heat exchanger model by finite differences approximation was written in Fortran IV and run in the computers ICL 1905E of Aston University and ICL 1906-A of the Manchester University Regional Computer Center (UMRCC) with only minute changes. This algorithm considers all possible combinations of the following conditions:

(i) Fluid flow pattern: co-current and countercurrent,

(ii) Heat flow pattern: cooling and heating,

(iii) Origin of disturbances: tube flow, shell flow and both,

(iv) Type of disturbance: step change and sinusoidal change.

In addition, the results can be obtained in terms of real variables or normalised variables.

The disturbances mentioned are only those investigated in the experimental work since any type of analytical time-dependent function can be simulated with the subroutine that enters the perturbation into the simulated system.

Because of the wide range of operating conditions that can be simulated, the model can be regarded as a generalized representation of the heat exchanger under flow disturbances.

The main idea for the development of the algorithm corresponds to the one presented in the previous section, i.e. the steady state analytical solution is found to set the initial temperature profiles and from them the successive temperature profiles at each time step are constructed using the relationships given by the finite difference approximations.

The physical properties of the materials, water and copper, were taken from the current literature. Although to some extent all properties are a function of temperature, that functionality is only significant in the case of the viscosity of water, and to a lesser degree its thermal conductivity. The following correlation of water viscosity in terms of temperature was taken from Perry (74).

$$\mu = 1/\{2.1482(T'-8.435) + \left[8078.4 + (T'-8.435)^2\right]^{\frac{1}{2}} - 120\} \quad (5.38)$$

The corresponding correlation for conductivity was deduced from data from different sources for the range of interest (0-100^{o}C),

$$k = 0.001419 + 2.216 \times 10^{-6}\ T' \quad (5.39)$$

To find the stream average temperatures to evaluate the properties, the equation presented by Mc Adams (65) was used,

$$T'_h(\mathrm{OUT}) = \frac{T'_h(\mathrm{IN}) + (a_s - 1)T'_c(\mathrm{IN})}{a_5 - z} \quad (5.40)$$

where

$$a_5 = \mathrm{EXP}\left[U\ A\ (1 - z)/W_h C_h\right] \quad (5.41)$$

and $$z = W_h C_h / W_c C_c \quad (5.42)$$

In these last three equations subscripts h and c stand for hot and cold streams respectively.

The corresponding value of T_c(OUT) was found by heat balance. For the particular case in which $W_h C_h = W_c C_c$, z = 1), the previous prediction becomes

$$T_h(\mathrm{OUT}) = \frac{T_h(\mathrm{IN}) + a_6 T_c(\mathrm{IN})}{1 + a_6} \quad (5.43)$$

with

$$a_6 = U\ A/W_h C_h \quad (5.44)$$

All the different possible conditions were encoded with numbers that are defined at the beginning of the program, so allowing easy selection of the appropriate path for each solution.

In the case of step perturbation, with no control valve effects, fluid velocities, heat transfer coefficient and the partial equation coefficients were modified only once, according to the linearised relationship defined by equation (4.42), but in the case of sinusoidal perturbation, those parameters were updated each time a temperature profile was completed, using the subroutine DISTURB. When the dynamics of the control valves was taken into consideration the updating was done until the effect of the transient response of the valves was negligible. Because the distance derivative is approximated by central differences, the nodes placed at the extreme ends of the heat exchanger make it necessary to evaluate one temperature value beyond the physical limits of the system for each evaluation of T_1 and T_2, as seen in Fig. 5.3.

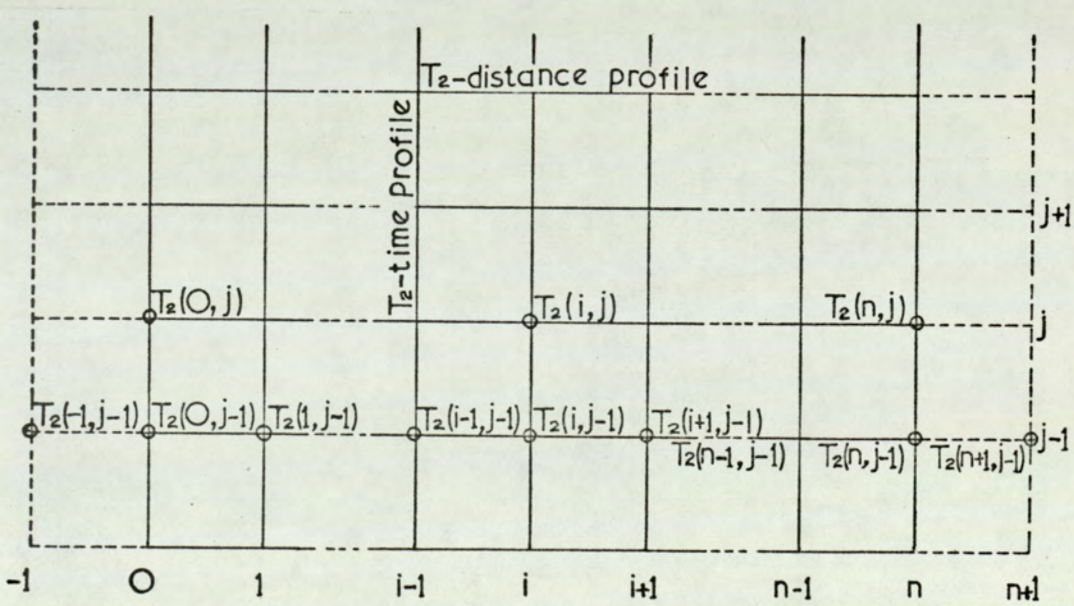

Fig.5.3 Integration Mesh for T_2, Showing Extrapolation Beyond the Physical Limits of the System.

The procedure requires then, the extrapolation of the temperature profiles to levels (-1) and (n+1) in each time step, to make possible the evaluation of the following profile. In the program this is done by simple linear extrapolation, extending the curves one step on both ends of the heat exchanger

$$T_{-1} = 2T_o - T_1 \tag{5.45a}$$

$$T_{n+1} = 2T_n - T_{n-1} \tag{5.45b}$$

The listing of the program is presented in Appendix B and the block diagram is included in the following three pages.

The behaviour of the model itself was evaluated by analysing its response for several types of disturbances and conditions of either one and of both flow rates. The results are shown in Figs. 7.1 to 7.11. They indicate that the model responded in a logical form to all types of disturbances and conditions used for testing, and was able to cope with the particular situations that required a different approach, as found by the analysis for the steady state condition (section 5.1.1).

The quality of the model, expressed as the accuracy with which it represents the physical system behaviour, is discussed in section 7.5.

5.1.3.2 Convergence and Stability

The criteria of convergence and stability are fundamental for any numerical algorithm. The first criterion implies that the numerical method approaches the exact solution of the differential equations as the size of the independent variable steps approach zero. The second one means that the errors introduced by the approximation do not increase as the calculations progress. For an explicit method the stability is very critical since errors tend to be carried forward from one calculation to the next so making the solution diverge as well as unstable if the

Figure 5.4 -Flow diagram of the time domain computer algorithm.

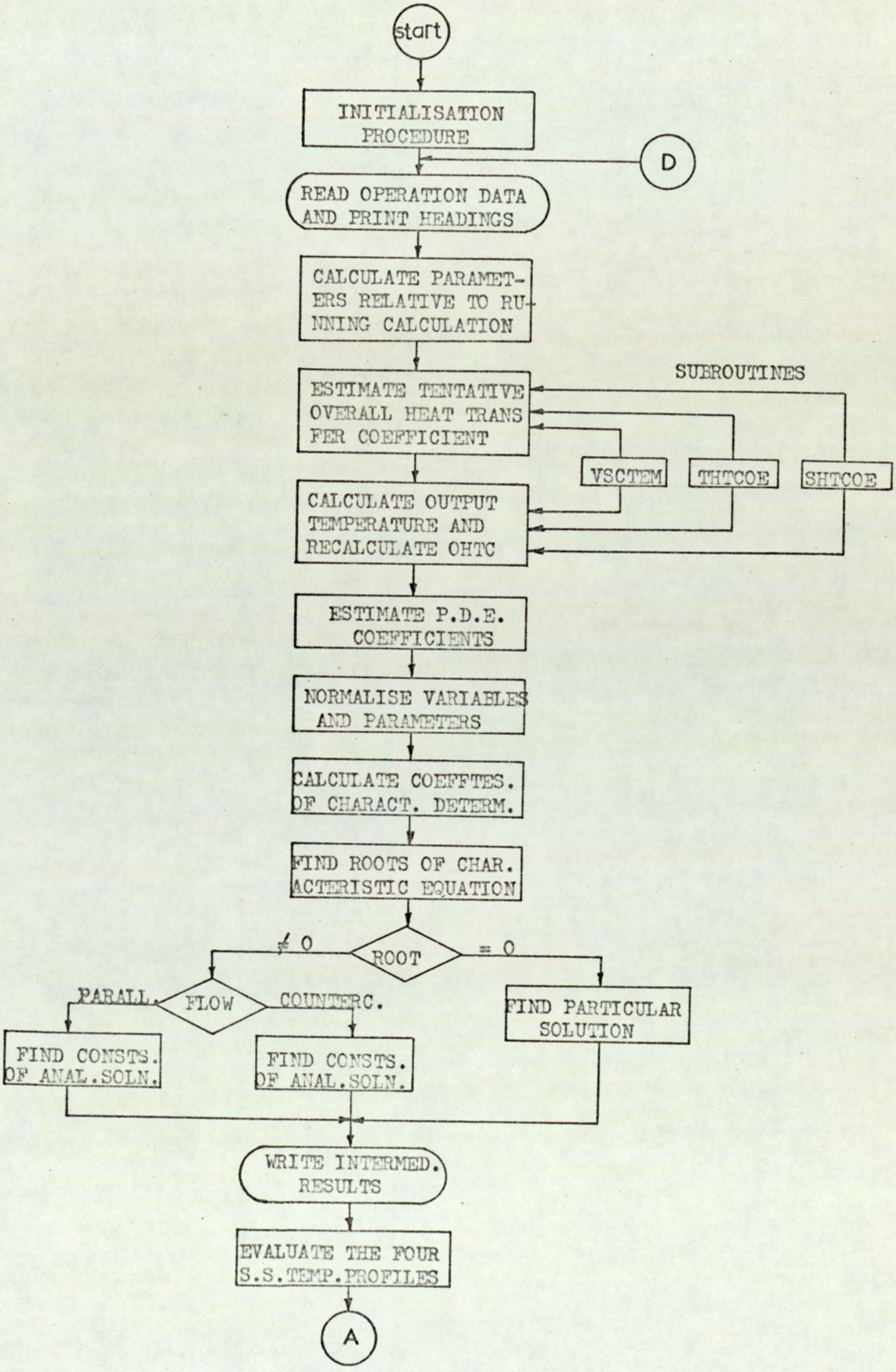

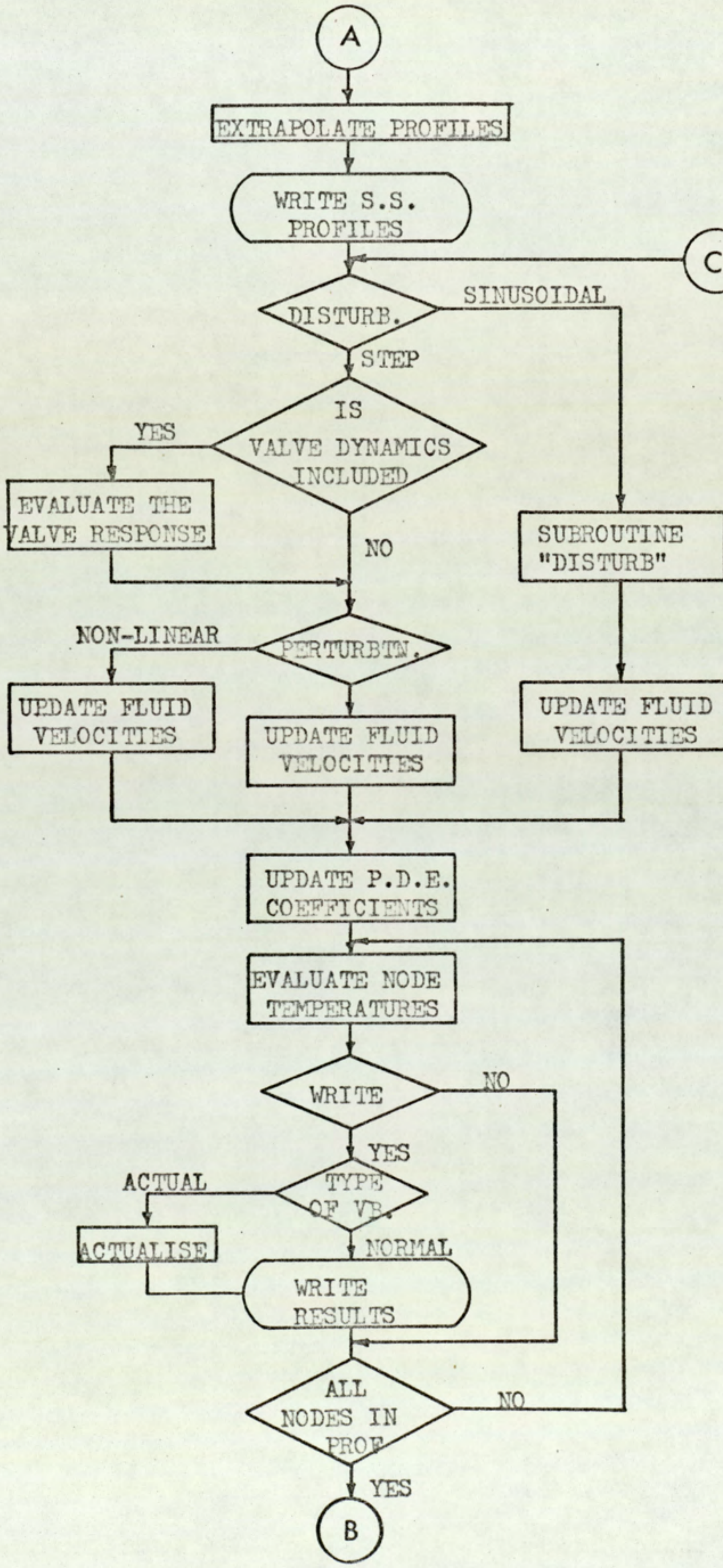

Figure 5.4 -(Continued)

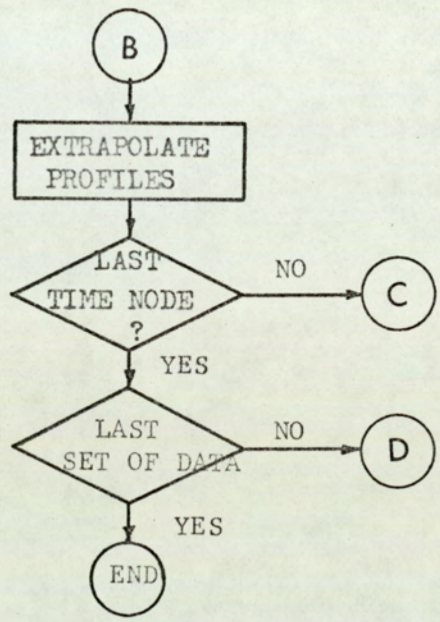

Figure 5.4 -(Continued)

step size is not kept small enough.

Unfortunately, there is not a fully analytical method to set criteria of convergence and stability for the solution of differential equations with coefficients that are functions of the independent variables as treated here. The most used approach is direct trial and error, using the computer. Obviously, for reasons of economy in computer time, the main objective of the analysis is to use the largest possible steps in the integration that can guarantee a convergent and stable solution.

Several trials, done in this work with different step sizes, clearly indicated that the time step is the most critical for the solution. The values finally chosen were

$$\Delta t = 0.0833, \quad (1/12) \quad \text{and}$$

$$\Delta z = 0.005, \quad (1/200)$$

of normalised units. These values were satisfactory for all perturbations and operating conditions reported, which included runs as long as 180 seconds of real time.

5.2 FREQUENCY DOMAIN SOLUTION

The solution of the model in the frequency domain complements the analysis in the time domain. In spite of the methods available for obtaining frequency response from transient pulse (section 4.3) and from step response (71), the most widely used method follows the principles presented in section 4.2, which when applied to a nonlinear mathematical description, as the one obtained in this work, requires the linearisation approach (section 4.1.6) before performing the Laplace transforation on it.

The single-flow-disturbed heat transfer process was analysed by Law (59) and the algorithm developed here for the two-flow -disturbed process follows basically his approach. However, in programming four of his transfer functions (those corresponding to the parallel flow in the previous reference) no satisfactory results were achieved. Subsequent deduction gave somewhat different expressions which yielded satisfactory computer results.

The lengthy algebraic manipulations are omitted in this thesis, but the final transfer functions can be obtained from the corresponding computer program included in Appendix B, which was written keeping Law's nomenclature, whenever possible to facilitate comparison.

The basic idea in obtaining the transfer function of the simultaneously flow-disturbed process was to consider it as the superposition of the individual transfer functions of each single-disturbed case.

The resulting digital algorithm was applicable to any region of Reynolds number, for the countercurrent and parallel flow, and for the single and double disturbed processes.

The behaviour of the frequency domain model was also evaluated for several sets of conditions presented in Figs.7.12 to 7.19, and analysed in Section 7.2.2. The experimental results and the predictions of the model were compared in Figs.7.40 to 7.63 and discussed in Section 7.6.

CHAPTER 6

EXPERIMENTAL WORK

The experimental work of this research was conducted at the Department of Chemical Engineering of the University of Aston. A tube-and-shell heat exchanger was designed for that purpose and with it an operating system was assembled to collect the data to test the mathematical model. The experimental procedure consisted in generating predetermined flow disturbances in either or both streams of the exchanger, previously running at steady state, and recording the responses of the outlet temperatures of the fluids. The data so obtained for several sets of operating conditions was compared with the equivalent solutions generated by the computer programs implementing the mathematical model of the process.

6.1 EXPERIMENTAL SYSTEM

The general layout of the experimental system used in this work appears in Fig.6.1, and a listing of its components appears in Table 6.1. The main items of the rig are discussed in the following sections. Reference (39) presents a detailed description of the pneumatic function generator used.

6.1.1 The Heat Exchanger

The central piece of equipment was the heat exchanger, see Fig. 6.2, made in two sections of 60 cm length, joined together by eight symmetrically distributed screws around a flanged joint. Each section consisted of a copper shell of 10.24 cm I.D. and 10.62 cm O.D. The tube bundle had 37 copper tubes 0.79 I.D. and 0.95 cm O.D. arranged in triangular pitch, with eight baffles spaced regularly at 7.5 cm intervals

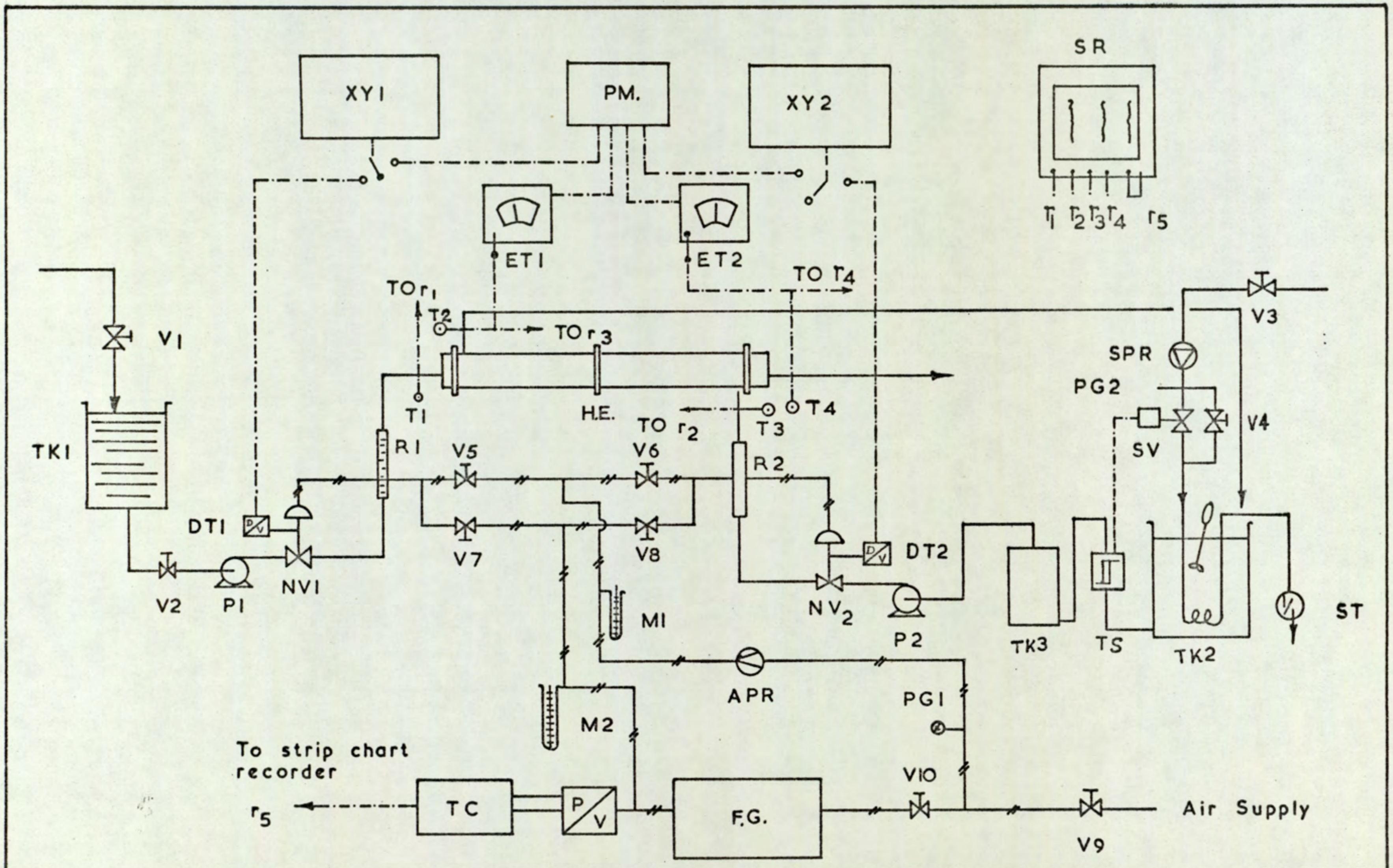

FIG. 6-1 GENERAL LAYOUT OF EXPERIMENTAL SYSTEM

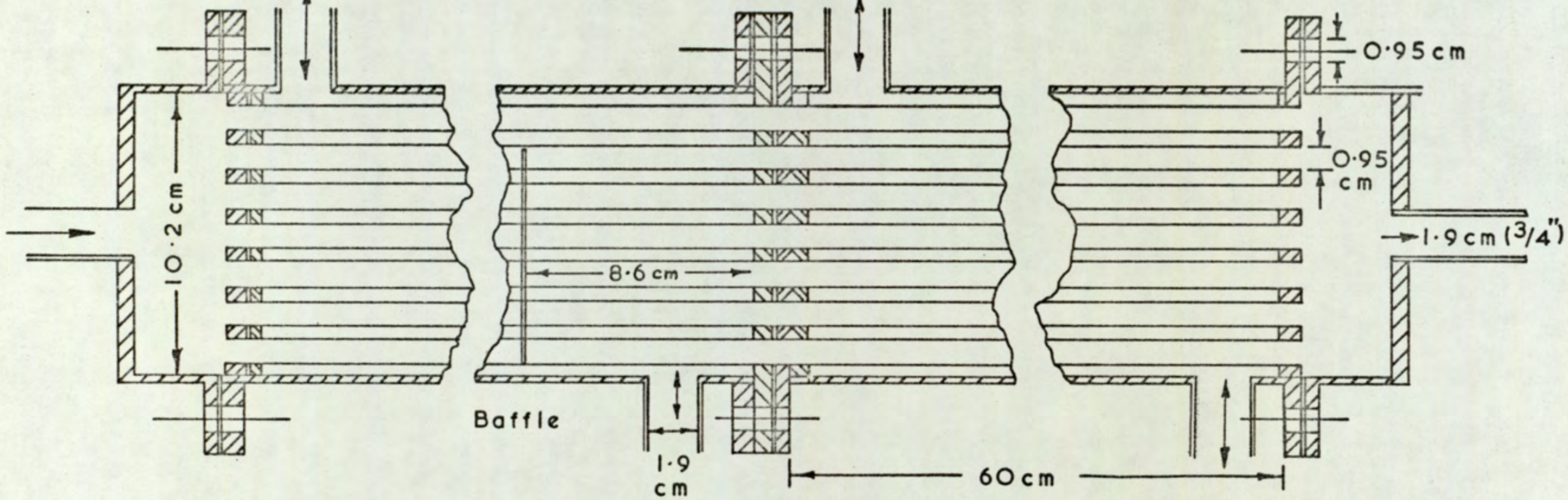

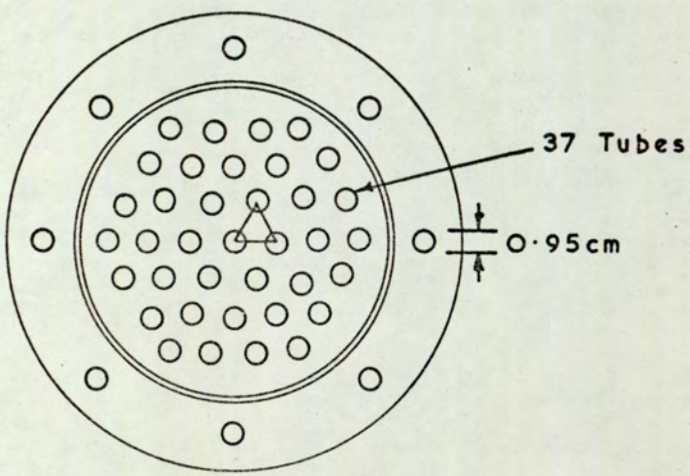

MATERIAL OF TUBES AND SHELL : COPPER	
Bundle tubes:	D. I. = 0·79 cm
	D.O. = 0·95 cm
	PITCH = 1·42 cm (Triangular)
Baffles:	Cut to 18·8% (1·9 cm)
	SPACING = 8·6 cm
Shell:	D. I. = 10·24 cm
	D.O. = 10·62 cm

FIG. 6 – 2 DETAILS OF THE HEAT EXCHANGER

and cut segmentally at 18.8% (segment cut of 1.9 cm height). The total heat transfer area of the exchanger was 11019 cm^2, based on the tubes I.D. At a later stage in the experimentation 30 tubes were blocked to analyse the effect of a change in the total heat transfer area, down to 2085 cm^2, on the process response. With this modification was also intended to have a substantial increase of the tube flow velocity so to transfer the operation of this side of the exchanger into the higher part of the transition region, without significant change of the total mass flow.

To ensure a tight seal between the two sections and between shell space and tube space, rubber packings were used. The one used between the two sections, however, under the pressure of the tying screws, tended to creep into the tube bore and had to be rectified twice during the experimentation. The reason for having the exchanger built in two sections instead of one was the intended accurate fitting between the tube bundle and the shell to reduce short circuiting in the shell side flow pattern. This close fitting is obviously better achieved with smaller pieces of equipment.

The cylindrical mixing chambers at both ends of the tube bundle had a volume of 275 cm^3 that accounted for most of the time lag in the measuring of the tube side temperature.

The whole exchanger was insulated with 1/8" asbestos tape. The hot stream was water circulated in a closed circuit. It was heated in a 0.25 m^3 tank by an immersed coil through which saturated steam at 18 psig was passed. The tank was agitated by two 1/25 H.P, 2200 r.p.m. stirrers in order to obtain uniform heating and good heat transfer from the coil to the water. The temperature of the tank was regulated by a mercury thermostatic switch which operated a solenoid valve in the steam line. Because the action of this two-position controller caused a cycling usually of about 0.3°C peak-to-peak amplitude in the temperature of the hot water, an additional glass vessel of about 0.02 m^3 was added after the measuring point, TK3 in Fig.6.1, to smooth out such cycling. The result was a reduction in the amplitude to about 0.1°C.

After going through the heat exchanger this stream returned to the heating tank.

The cold water was taken from the mains at ambient temperature into two interconnected tanks of 0.175 m^3 each used as reservoir. After passage through the exchanger this water went to drain.

Each fluid stream was driven by a 1.0 H.P. 2850 r.p.m. Stuart Turner centrifugal pump, regulated by a Cressall-Torovolt auto transformer. The flows delivered by the pumps were regulated by two direct action Introl, type 10-334 pneumatic valves of ½" plug. Because the plugs specified as 'linear' by the manufacturers gave an unsatisfactory characteristic curve, brass plugs were tailor-made in the departmental workshop to obtain a more nearly linear flow-displacement relationship.

To reduce corrosion of the mild steel components of the system, borax was added to the hot tank at a concentration of about 400 ppm. It effectively reduced corrosion and prevented scale deposition.

6.1.2 Measuring Equipment

The temperatures of the streams were measured by thermopiles made of five chromel-alumel thermocouples, provided with a cold function of melting ice in a thermos flask. The five elements of the thermopile were placed, using a 'T' junction, parallel to the stream direction and

TABLE 6.1

COMPONENTS OF THE EXPERIMENTAL SYSTEM

CV1, CV2	Flow rate control valves	'Introl' ½", Type 10-334 - Pneumatic Action, 3-15 psig. Air to open. Full lift 2.8 cm.
DT1, DT2	Displacement Transducers	10K Ω coil circular rheostats, excitation of 2V DC.
ET1, ET2	DC Preamplifiers	'Comark Electronic Thermometers', Type 1601/1 Ni Cr/Ni Al. Output 0-1 Volt.
FG	Function Generator	Mechanical to Pneumatic Type, 0-40 cpm. P-to-P. Amplitude, Frequency and mean value continuously variable.
HE	Heat exchanger	See section 6.1.1.
M1, M2	Mercury Manometers	U type, 100 cm.
P1, P2	Cold and Hot water pumps	'Stuart Turner', 1 H.P., 2850 r.p.m. 2000/850 gph at 15/45 ft.hd.
PG1	Air Pressure Gauge	0-200 psig, Bourdon type
PG2	Steam Pressure Gauge	0-50 psig, Bourdon type
PM	Suppression Potentiom.	'Croydon Precision Instr.', 'Cropico Galvanometer.
PR1	Air Pressure Regulator	'Negretti-Zambra' - 12/65 psi.
PR2	Steam Press-Regulator	'Spirax Sarco', Type BRV, 20-60 psi.
PV	Pressure Transducers	'S.E. Laboratories', Pressure to Voltage Inductive cell. Type D5749-20 and
R1, R2	Cold and Hot water Rotameters	'Rotameter Mfg.Co.', Type C135S, s.s.float, 5-50 L·/min.
SR	Strip Chart Recorder	'Kent Mark 3 Electronic', Range 0-3 mv, Sixteen Measuring Stations.
ST	Steam Trap	Spirax FT 155.
SV	Steam Solenoid Valve	'Dewrance' ASCO 3/8", 0-35 psi.

TABLE 6.1 Cont....

T1, T2, T3, T4	Mercury thermometers	'Gallenkamp', -5 - 105°C, 0.1°C div.
TC	Transducer Converter	'S.E. Laboratories' T/C SE 905/1.
TK1	Cold water tank	Two compartment, 350 lt. capacity.
TK2	Hot water tank	250 lt, heated by a 300 cm coil of 3/8" copper tube.
TK3	Postmixer hot water tank	20 lts glass aspirator.
V1	Cold water valve	½" 'Prestex' stopcock BS59.
V2	Cold water valve	'Hattersley' 1", Gate type, 250 psi.
V3	Steam valve	'Hattersley' ½", Globe type, 200 psi.
V4	By pass steam valve	'Prestex' stopcock BS59, ½".
V5, V6, V7, V8	Air regulation valves	'Simplifix' gas taps D505 x /16/16.
V9	Air supply valve	½" Saunders valve
V10	Air valve to FG	¼" Saunders valve
XY1	X-Y Plotter	ICL Variplotter 1110, 8 ranges from 5mv/cm to 10v/cm
XY2	X-Y Plotter	Jay-Jay Instruments, Type PL100. Five ranges from 50μv/cm to 500 mv/cm.

around a mercury thermometer immersed in it. This arrangement indicated in Fig.6.3 ensured a good representation of the bulk temperature of the stream.

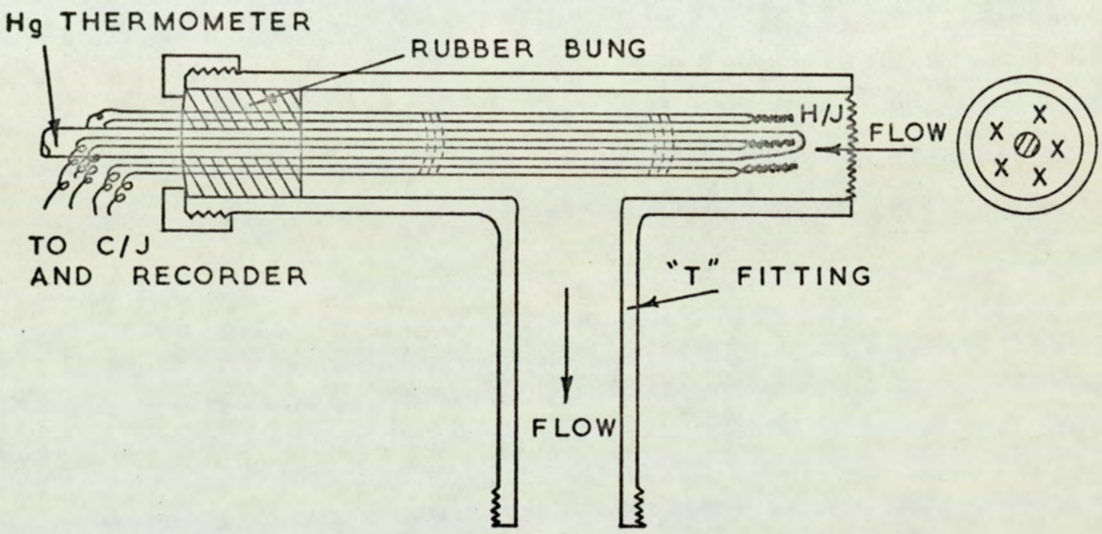

Fig.6.3 Location of the Measuring Thermopile in the Fluid Streams.

The signals from the thermocouple were further amplified using a Comark, type 1601 electronic thermometer which works as a DC amplifier with gains of 24, 77 and 244.

The signals from the amplifier were sent either to a recorder EA1 Variplotter 1110 or a J-J X-Y plotter type 100, each with several ranges of speed and sensitivity to suit the experimental conditions.

In order to monitor all the temperatures of the heat exchanger, single thermocouples were placed in all input and output points and each connected to two measuring stations of a 16 station Kent strip chart recorder which could scan one temperature every five seconds. At the same time the transduced pressure of the function generator was also connected to eight measuring stations of the same strip chart recorder so this instrument could show at a glance the general behaviour of the system.

Since the object of the experimental work was to study the response of the exchanger output temperatures to changes in the fluid flow rates, and these could be directly related to the opening of the control valves, the valve stems were connected to resistive type displacement transducers. The signals so generated were used to give the corresponding record of the flow variations, assuming no time lag between stem position and flow through the valve.

6.2 EXPERIMENTAL PROCEDURES

The data collected during the experimentation was of three types.

(i) Steady state data.

(ii) Actual sinusoidal data.

(iii) Pulse testing data.

6.2.1 Steady State Data

The first type includes the data taken to evaluate the steady state regime of the heat transfer process. It always preceded any other type of data collection and was performed by setting the temperature of the hot water tank to a given value, setting the pneumatic valves to a given position by regulating the pressure on their diaphragms, and allowing the system to run unchanged until all the temperatures and flows were constant. The information collected was the flows and temperatures of both streams with the corresponding scheme of flow, thus giving enough data to calculate the heat balance in the exchanger and its overall heat transfer coefficient.

6.2.2 Sinusoidal Data

The actual sinusoidal operation started from the steady state condition of a value manually preset near the mean value of the sinusoidal oscillation in the flow rate to be used. One frequency was set in the function generator while in 'standby' mode, as well as a peak-to-peak amplitude, and the required mean value. An appropriate combination of values V5 to V8 allowed the oscillating signal to be applied to either one or both pneumatic valves.

In the cases in which the sinusoidal signals were used to obtain temperature-time information, time was measured with a stopwatch from the moment the Function Generator was changed to operating mode and the recorders were started immediately until several cycles indicated quasi steady state operation at the preset frequency.

When the purpose was to obtain frequency response data, the system was allowed to run until all transients disappeared, which usually took a number of cycles varying with the frequency used. When the system was undergoing sustained oscillations, both signals, the transduced stem displacement and the output fluid flow temperature of either stream were recorded.

Two methods were tried to record this data: since no double-pen recorder was available to record input and output signals simultaneously against time, the Lissajous curves were tried initially. This method is very useful because it allows recording of the two time-varying signals in one single curve independent of time and the attainment of the quasi-steady state condition is easily estimated by the superposition of consecutive cycles. During the recording one signal is connected to one axis (input to the X-axis, for example) and the second signal to the other axis. As time progresses the change of the two periodic variables describes a curve which is closed when the transients have died out. For sinusoid-like signals the curve is an ellipsoid. From the closed curve the values of gain and phase angle can be obtained easily. Fig.6.4 indicates the equivalent information provided by Lissajous curves and sinusoidal time-dependent curves.

Although this method is faster than the conventional time-dependent records and easier to apply, it is very sensitive to corruptions of the signals, especially noise and drift, which were notorious, especially at high frequencies. Only a restricted amount of useful data was obtained by this method. The recording of time varying input and output signals had to be done successively insteady of simultaneously. This was possible because the stability of the signal from the Function Generator was remarkably good and permitted the use of the cross-over point with the mean value, read in a mercury manometer, as the reference to synchronise the recording of all the signals. A typical experimental record by this method is shown in Fig.6.5. Once the record for one set of conditions was made, a new set was chosen and the complete procedure repeated.

6.2.3 Pulse Testing Data

Finally, the pulse data was collected starting also from a steady state regime. To produce the pulse the same Function Generator was used under manual operation. It was put in standby mode when at the lowest (or highest) point of the sinusoidal signal, by approaching such point under operation at very low frequency and careful observation of several cycles. With the control valve (S) set at this pressure the required frequency was chosen in the Function Generator but kept in standby. The

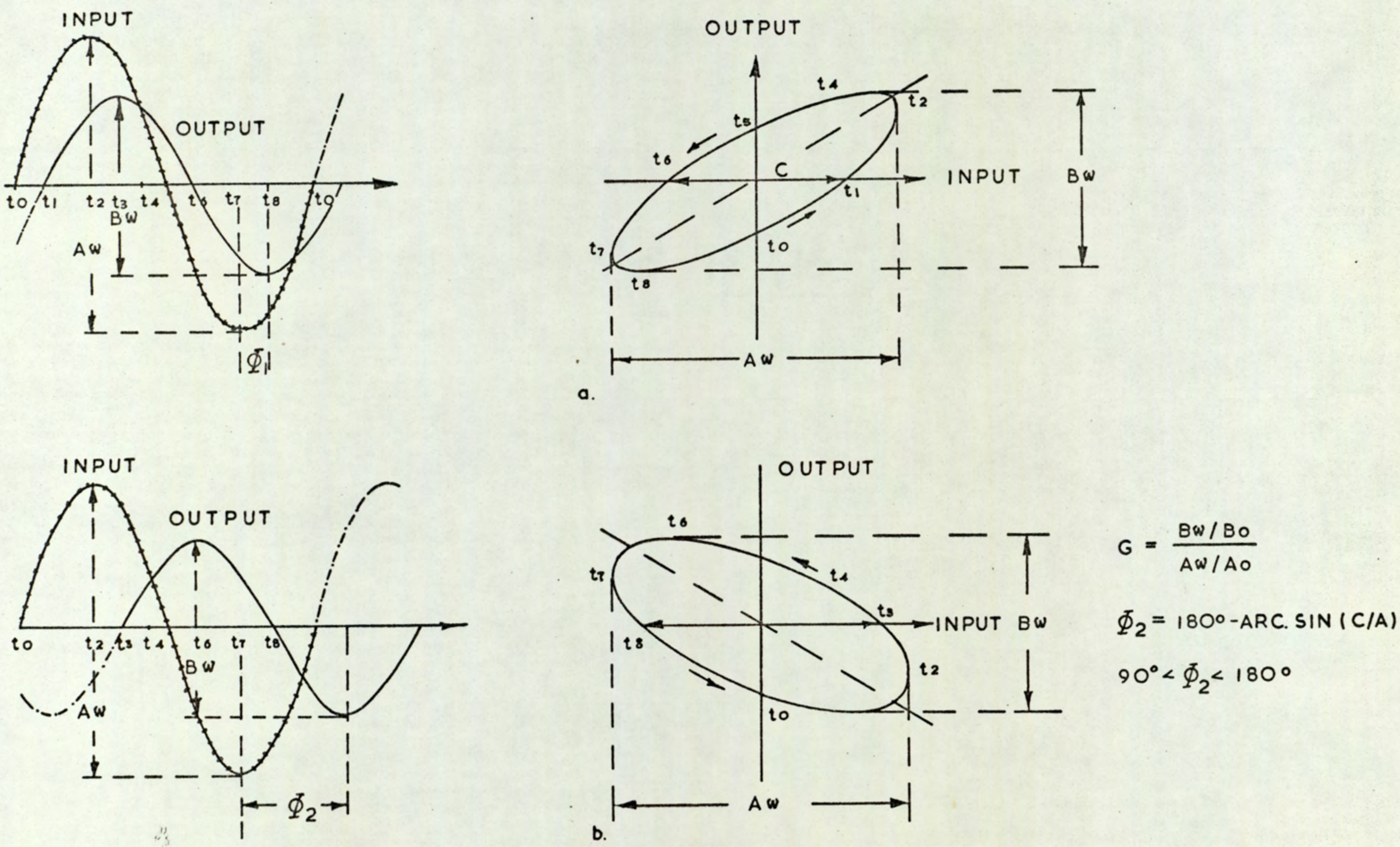

Fig.6.4 Equivalence of the Information Provided by Lissajous Curves and the Simultaneous Time-varying sinusoidal signals.

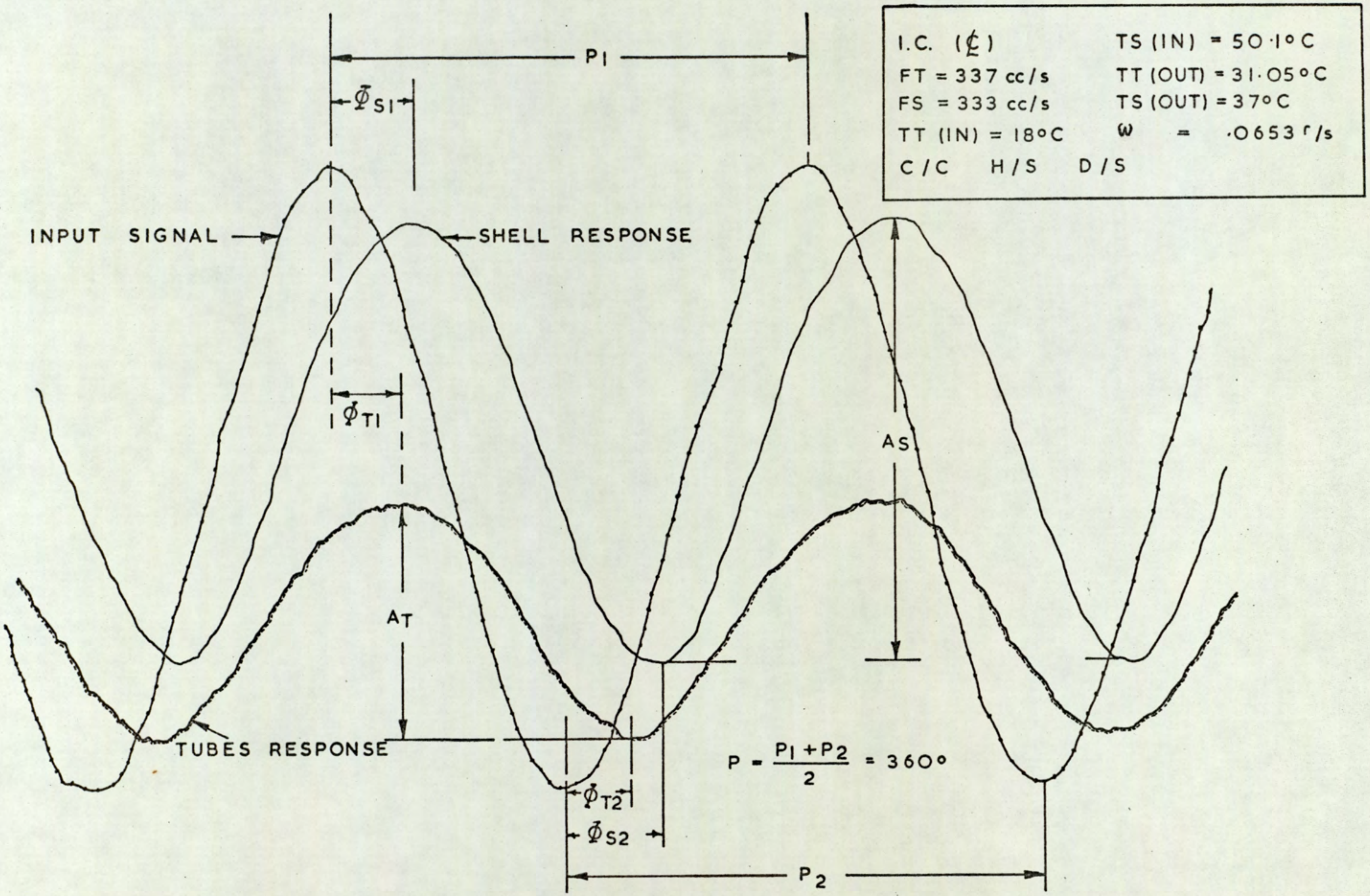

Fig.6.5 Typical Experimental Recording of the Cyclical Variables in Quasi-steady State.

system was allowed to run until steady state condition was reached and then the Function Generator changed to run-mode for one full cycle, after which it was returned to standby. This type of operation produced a displaced cosine pulse function (DCPF) negative or positive, depending upon whether the steady state condition was reached at the highest or lowest point of the sinusoidal cycle. Simultaneously with the input, throughput was also recorded in a different X-Y plotter, previously synchronised to the same velocity as the one recording the input, so that the two curves could be analysed on the same time basis.

The procedure was repeated for several amplitudes and durations of the pulse for a given set of conditions in the rig, until results were considered satisfactory.

6.3 EXPERIMENTAL PROBLEMS

Several problems not fully overcome affected the collection of experimental data, the most significant of all being noise. Both electric noise and thermal noise were present in the system under analysis, and each caused noticeable contamination of the data.

In all previous work where the heat exchanger was disturbed in a single variable manner, the static gain of the system was large enough to produce output signals whose noise to signal ratio was within satisfactory levels. When the frequency of the perturbation became very large, the attenuation produced by the process response on the output signals, reduced the ratio to levels at which distorted data was produced. The same was experienced in this work for those runs in which only one of the fluids was disturbed, but for the case of simultaneous disturbances the counterbalancing effect of both changes greatly reduced the static gain of the system, as can be seen by comparing Figs. 7.21/22 with Fig.7.23, making it much less sensitive to the level of fluid flow rate variations. As a result, the recording instruments had to be set at very large gains even for the low frequencies, leaving all unsuppressed noise in the system more disturbing.

Two general types of noise are usually found during the transmission of information within a dynamic system: normal-mode noise which is unwanted signals generated simultaneously with the desired signal, and is usually reduced by filtering the signal after the generation stage; and common mode noise which is a spurious signal generated by sources independent of the wanted signal. This type of noise can be reduced by several methods determined by the source of the spurious signal. In this work an example of the first type was the random variations in electromotive force shown by the temperature recordings, caused by random temperature gradients within the fluid streams as a result of imperfect mixing. An example of the second type was the 'spikes' produced on the same recordings by the action of the sinusoid valve and other relays of the equipment.

During the data collection the e.m.f. of the thermopiles was pre-amplified using an electronic thermometer provided with 3 scales corresponding to static gains of 24, 77 and 244. This pre-amplification combined with the gain of the recorders and the multiplication of the thermopile was able to produce signals up to the order of 38.5 cm per degree centrigrade, equivalent to 0.19 cm per microvolt generated in an individual thermocouple. Obviously at such large gains the effect of electric and magnetic fields created by electric equipment and any deficiency in mixing of the fluid streams and polarization of the thermocouples produced relatively large amplitude interference.

The heat exchanger is by many reasons a thermal noise generator: changes in the local heat transfer coefficients due to different local velocities and differential fouling of the metallic surface create temperature gradients on both sides of the tube wall that are easily picked up by fast and punctual measuring devices like the thermocouples. To reduce this noise the mixing chambers and the section of tubing immediately after the exchanger outlets were packed with a rolled metallic mesh to promote temperature homogenization of the fluid before reaching the thermopile, this was also placed in the stream so as to promote mixing (see Fig.6.3). Under all conditions the smoothest signal was the one of the shell side, perhaps because the outside geometry of the bundle promoted a much better mixing of the fluid and consequently a less noisy signal.

To reduce the electric noise, besides grounding and shielding of the most critical pieces of the equipment, twisting of all two-lead connections and RC filtering were also used; although the effect was reduced, they did not suppress it completely.

A method of filtering suggested by Chao (12) using an analog computer integrator suppressed the random noise, but did not smooth out the 50 cycle hum.

Another factor that might have affected the data is related to the stirring of the hot water tank that tends to suspend in the stream tiny bubbles of air, later on released in the process. Although the equipment was flushed at high flows before a run was started, vents on both mixing chambers were frequently purged, and the second mixing tank (TK3 in Fig.6.1) worked as an air trap, there is still a possibility that small bubbles could have developed on the inner surface of the tube bundle taking advantage of the low horizontal velocity of the streams, and so creating an additional resistance to the heat flow.

Finally, the parallax error in reading the mercury thermometers adds a source of inaccuracy to the data. In spite of the systematization and care of reading temperatures, it was realised that a typical temperature reading could carry an error of $\pm 0.1^{o}C$.

6.4 RANGE AND SCOPE OF THE EXPERIMENTAL WORK

Since the number of arrangements under which this process can be run is quite large when multivariable operation and more than one perturbation are considered, it was thought more important to investigate the behaviour under such different arrangements than to work over a wide span of a few sets of conditions. The outcome was frequency response experimental results for each case corresponding to types of flow (2), types of process (2) and types of disturbances (3), for velocities in the range of 17.3 to 21.2, i.e. Reynolds number from 1595 to 2905.

The time response data could not be as systematic because frequency and amplitude of the perturbation introduced additional variety, making total data collection an overwhelming job.

The range of conditions reported are shown in the following table.

Table 6.2 Range and Scope of Experimental Work

Conditions	Range			
	V_1,cm/s	V_3,cm/s	RN1	RN3
S.S. C/C & P/F	5 - 36	8.3 - 32.4	560 - 4750	940 - 4080
Transient S. (Step Dist.) D/T & D/B	7.1 - 62.2	5. - 20.4	588 - 8346	560 - 3281
Transient (Sinusoidal Dist.) D/S & D/B	16.9 - 22.6	16.3 - 23.6	2104- 2996	1251 - 2207

CHAPTER 7

ANALYSIS OF RESULTS

7.1 INTRODUCTION

In this chapter a discussion of the results obtained in the present work is presented. The discussion includes the analysis of each of the two models developed to represent the process, per se; the analysis of the steady state data, the dynamics of the control valves, the analysis of the data collected to verify the model of the transient response and finally the analysis of the data obtained for the verification of the frequency response model.

Before starting the discussion it is advisable to summarise the ideas so far presented. It was proposed to investigate the behaviour of a tube and shell 1-1 liquid-liquid heat exchanger under simultaneous disturbances of its two fluid flow rates and, accordingly, to extend the theory and methods of analysis of single-variable disturbed heat exchanger processes to the case of similar multi-variable processes. An important consequence of the conditions of the experimental verification has been the collection of data in the region of transitional and laminar Reynolds number enabling analysis of the dynamics of this heat exchange process for the first time in these regions. It must be stressed that though the approach used has been based on techniques of analysis applicable for conditions of fully turbulent flow, with flat temperature and velocity profiles (an idealised situation), it is recognised that in going from the turbulent to the laminar regime the process undergoes changes in the magnitude of hydrodynamic and thermal effects rather than in the character of them, as is indicated by the conventional heat transfer theory which lumps all possible differences into the semi-empirical concept of convective heat transfer coefficient for the three regions in which the Reynolds number domain is divided.

One mathematical model to represent the system in the time domain and another to represent it in the frequency domain were developed with provisions to consider a wide variety of operating conditions, including velocities in the turbulent, transitional and laminar regions. The transient response model can accept, with minor changes, any type of analytical disturbances and can incorporate the transient response of the valves used to regulate the fluid flow rates. The two models can be used to describe a single variable process or a double variable process by applying the linear superposition of signals. Also in the numerical solution of the transient model the flow disturbances to the system can be applied as the exact nonlinear effect produced by the relationship between fluid velocity and heat transfer coefficient, or the more common linearised effect, very useful during the mathematical analysis of the process.

A varied amount of experimental data have been collected to test those models. Thus in addition to the direct sinusoidal data taken to test the frequency response model, some data have been taken using the pulse testing method, followed by reduction into the frequency domain by use of the Fourier Transform technique. The experimental transient data has been collected for sinusoidal and step changes only whereas the model was also tested with a ramp disturbance.

7.2 THE MATHEMATICAL MODELS

7.2.1 Time Domain Model

The modelling of the process in the time domain resulted in a package that when run in the computer ICL-1906-A of the University of Manchester took a compilation time of slightly more than one second, and the execution time was roughly one second for each 130 to 150 seconds of simulated time.

The tests carried out on the model, using step changes (linearised velocity-heat transfer coefficient relationship) and sinusoidal disturbances indicated that its general behaviour was as expected for all conditions intend

All the tests using step function disturbances indicated clearly that the initial contour of the temperature responses follow the sluggish s-shaped curve characteristic of systems whose order is greater than one.

Figs.7.1 to 7.8* show how the amplitude of the disturbance affected the response of the system for both cases of single and double disturbed process. One feature found by inspection is that the temperature response of the fluid on which the perturbation is produced is faster and larger than the response on the other side, for similar levels of flow rates. This is in agreement with the signal flow concept by which the transmission of the perturbation from one stream to the other undergoes effects of attenuation and transportation lag due to the resistance and capacitance of the flow path. When the disturbances were simultaneous, the shell side

---

* In order to simplify the identification of the test conditions, the following nomenclature was adopted for the figures.

P/F = Parallel flow

C/C = Countercurrent flow

H/T, H/S 3 Hot stream in tubes,in shell

D/T, D/S, D/B = Disturbance in tubes, in shell, in both streams.

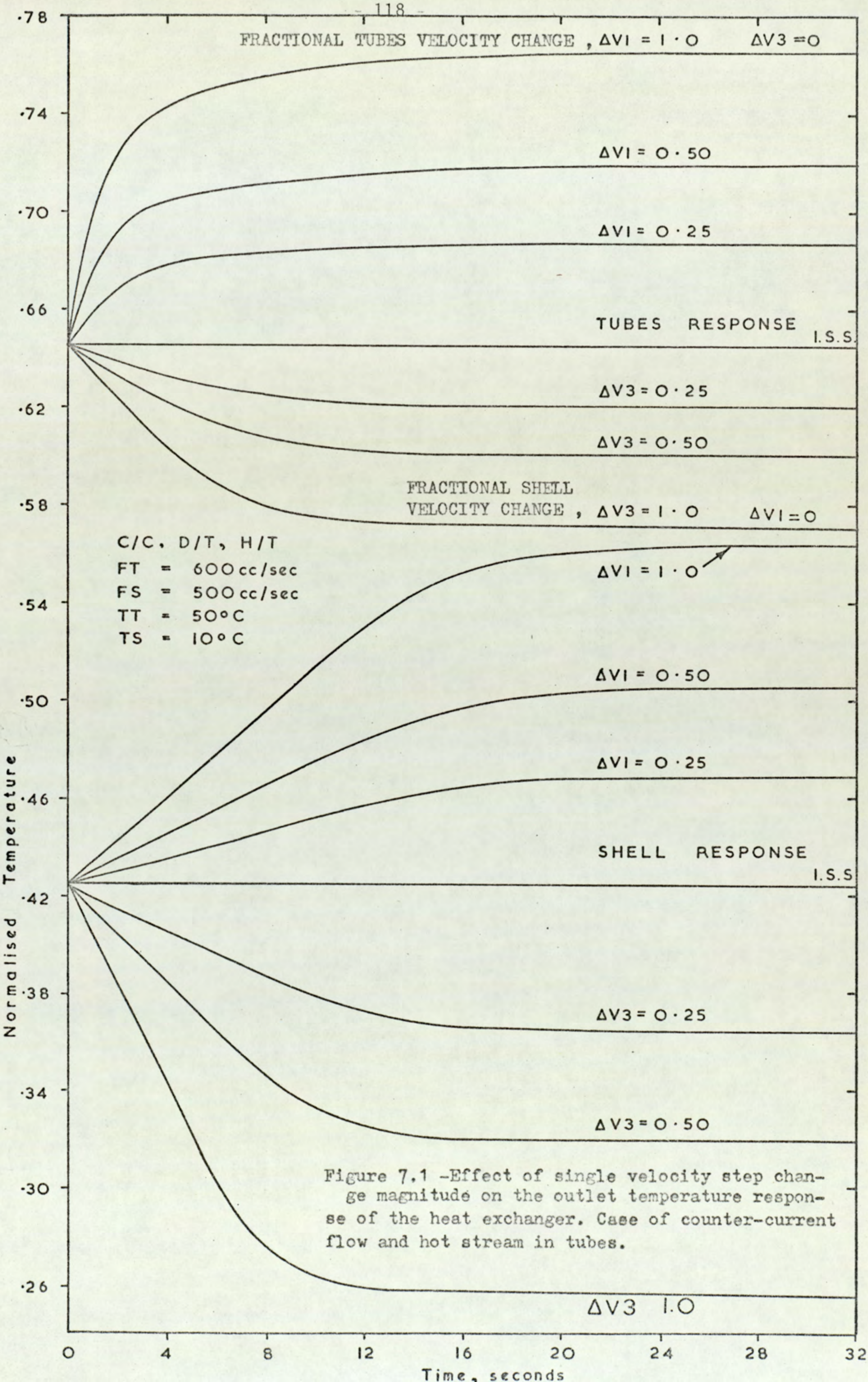

Figure 7.1 -Effect of single velocity step change magnitude on the outlet temperature response of the heat exchanger. Case of counter-current flow and hot stream in tubes.

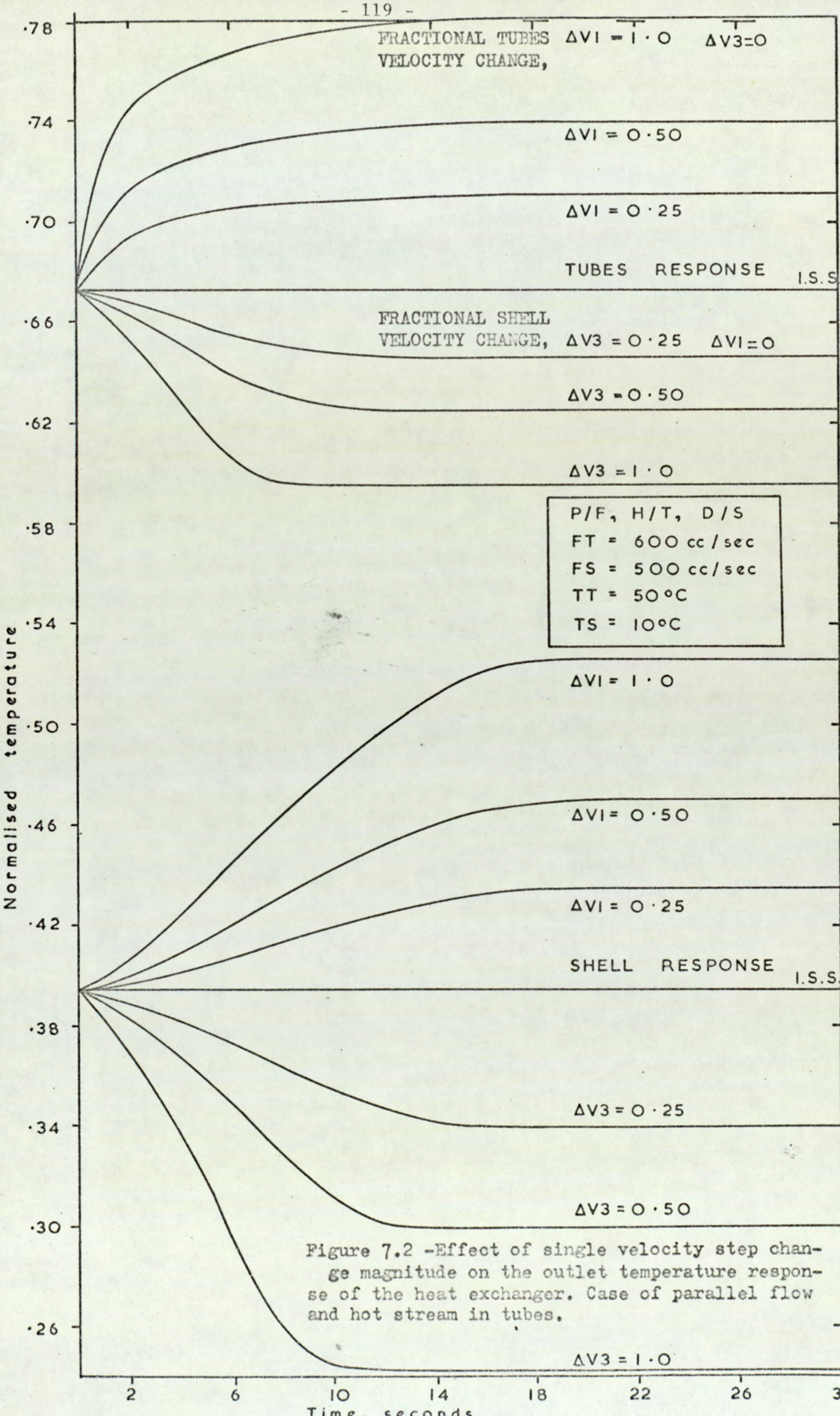

Figure 7.2 -Effect of single velocity step change magnitude on the outlet temperature response of the heat exchanger. Case of parallel flow and hot stream in tubes.

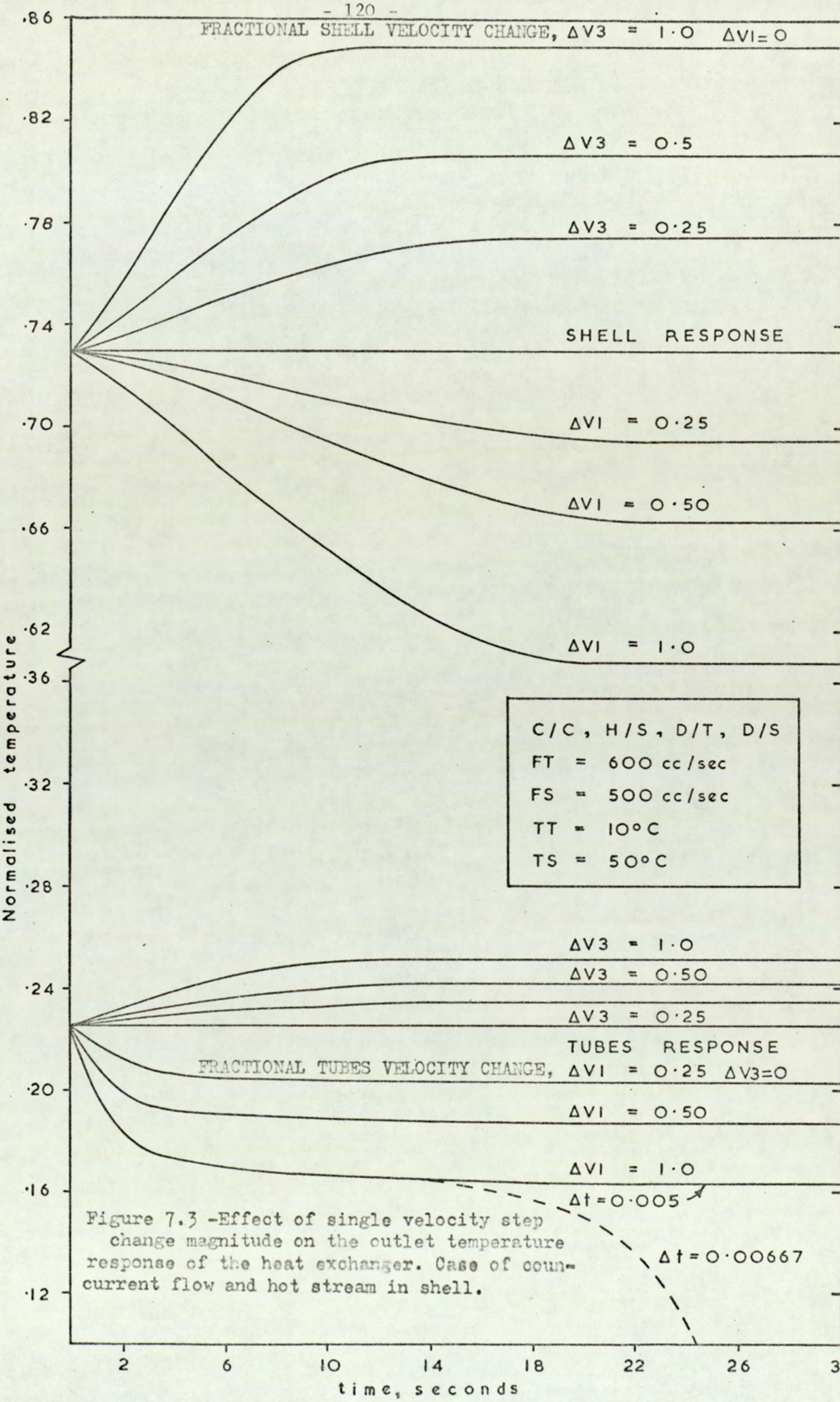

Figure 7.3 -Effect of single velocity step change magnitude on the outlet temperature response of the heat exchanger. Case of concurrent flow and hot stream in shell.

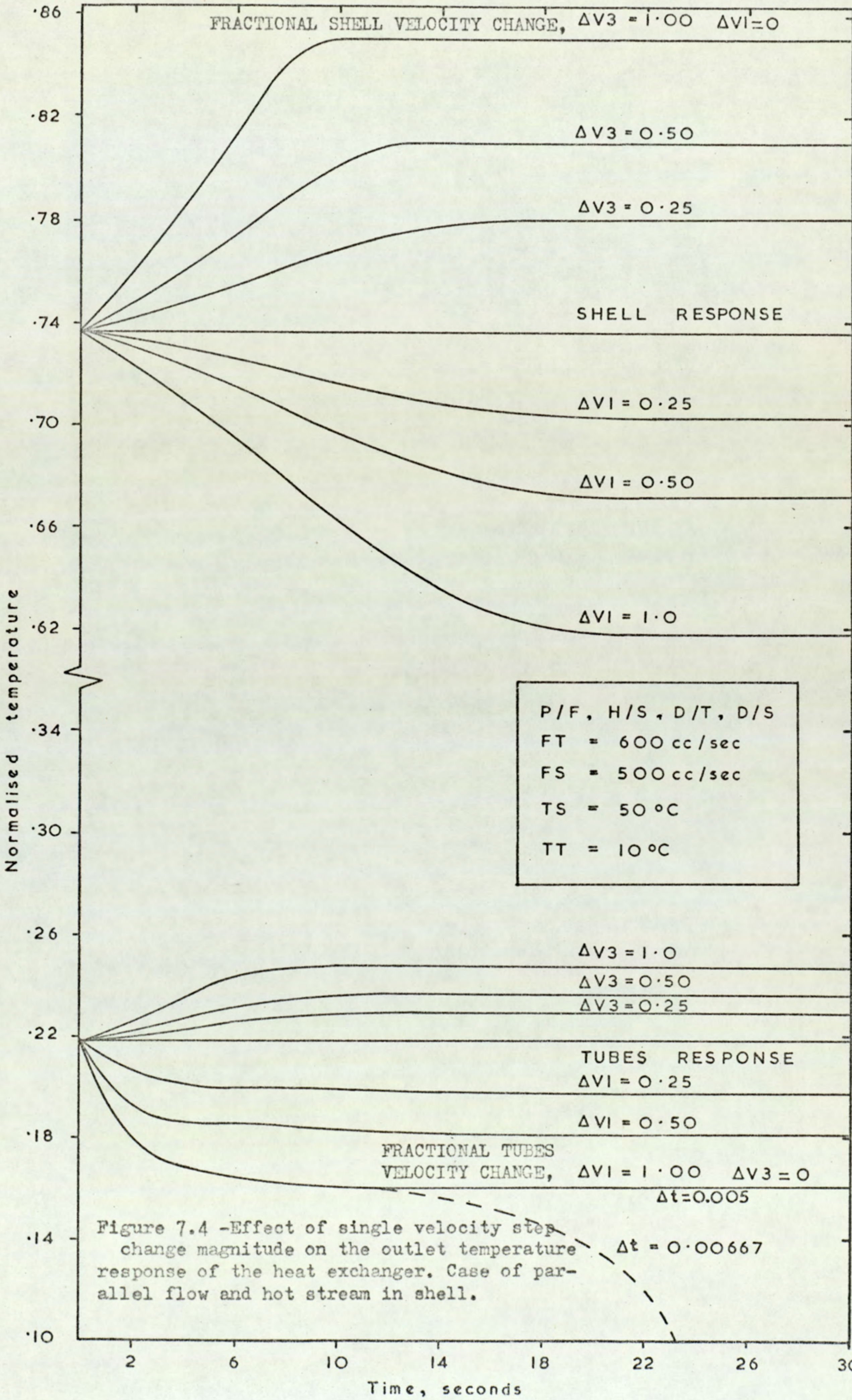

Figure 7.4 -Effect of single velocity step change magnitude on the outlet temperature response of the heat exchanger. Case of parallel flow and hot stream in shell.

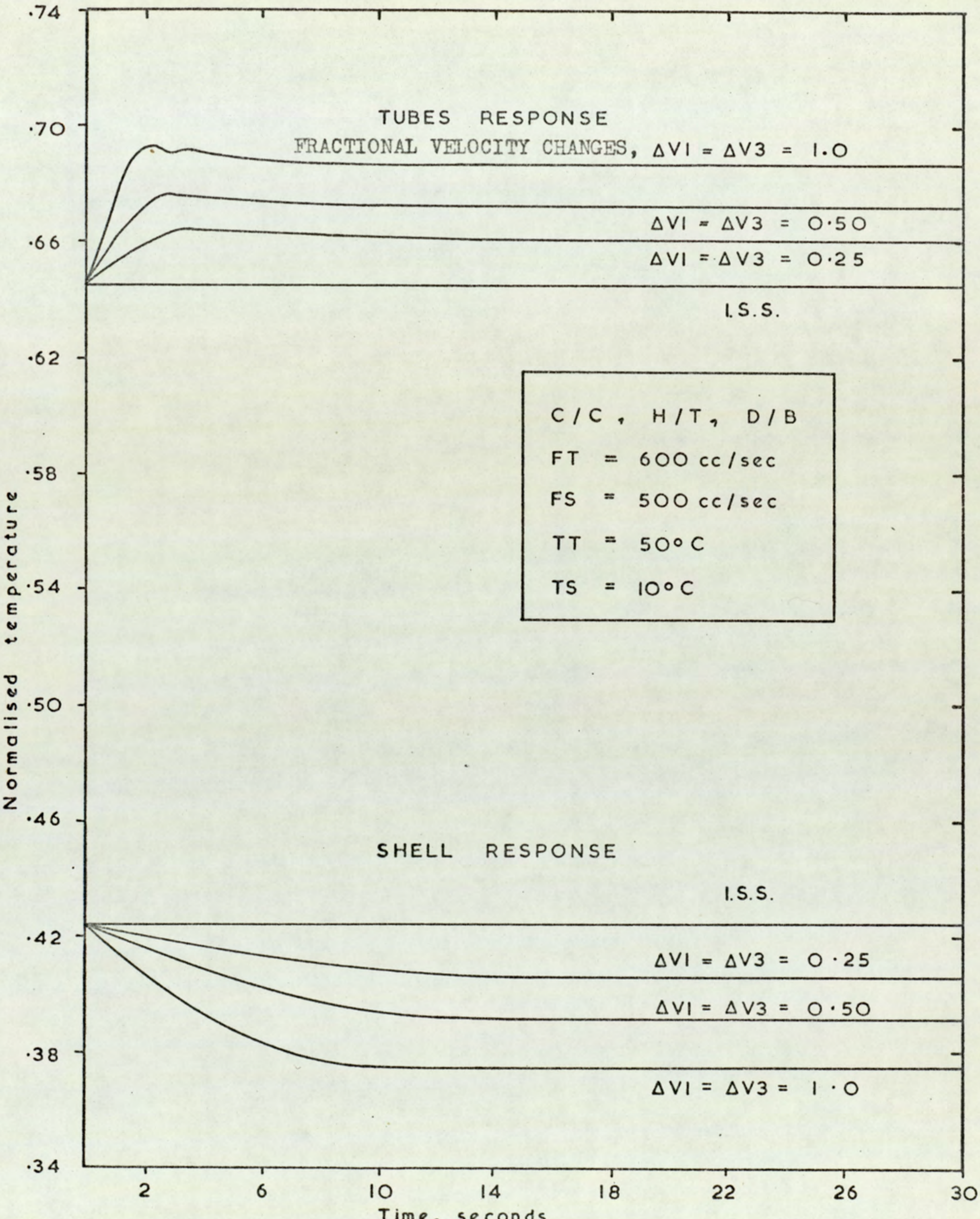

Figure 7.5 -Effect of the magnitude of simultaneous velocity step changes on the outlet temperature response. Case of countercurrent flow and hot stream in tubes.

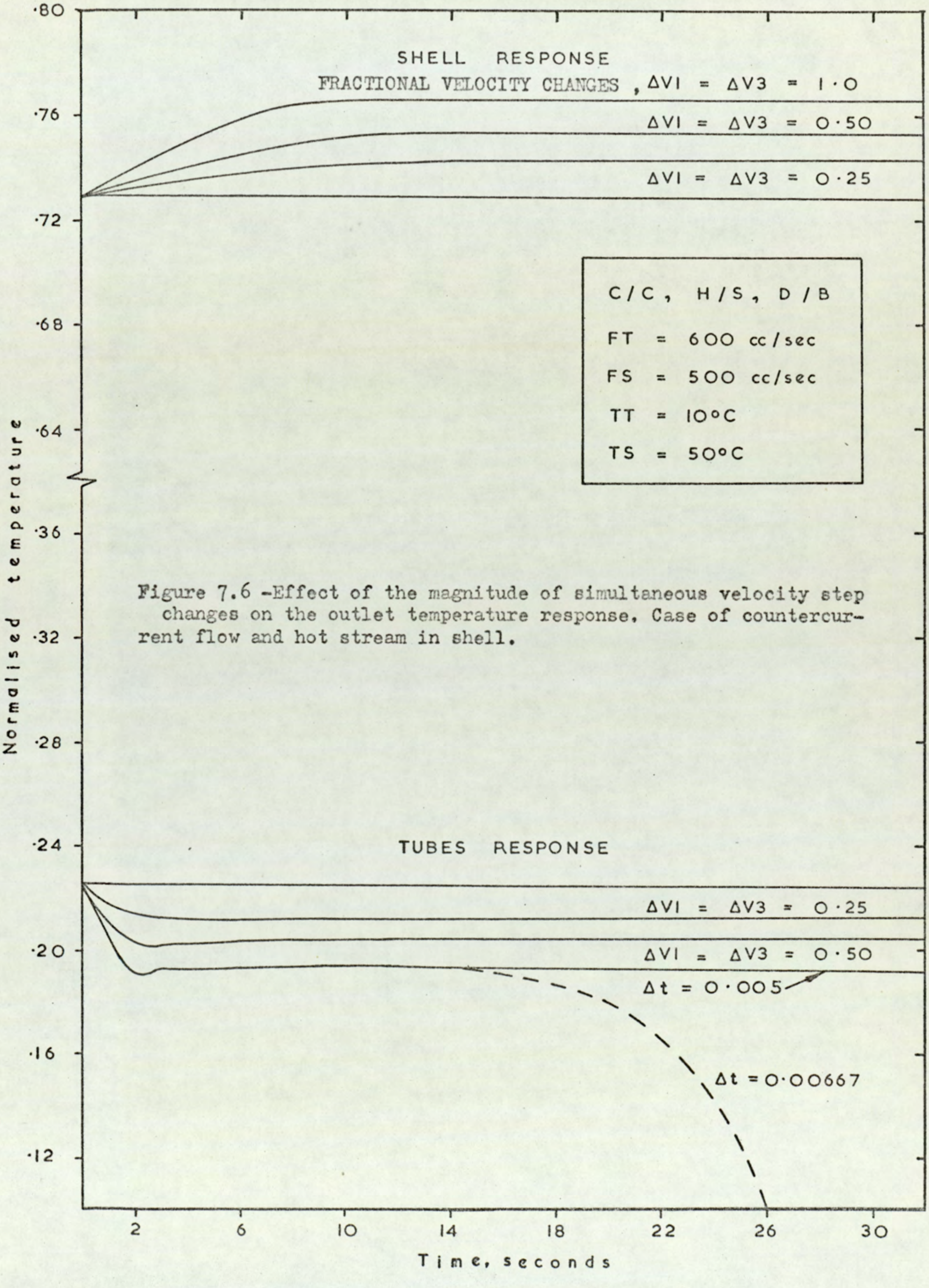

Figure 7.6 -Effect of the magnitude of simultaneous velocity step changes on the outlet temperature response. Case of countercurrent flow and hot stream in shell.

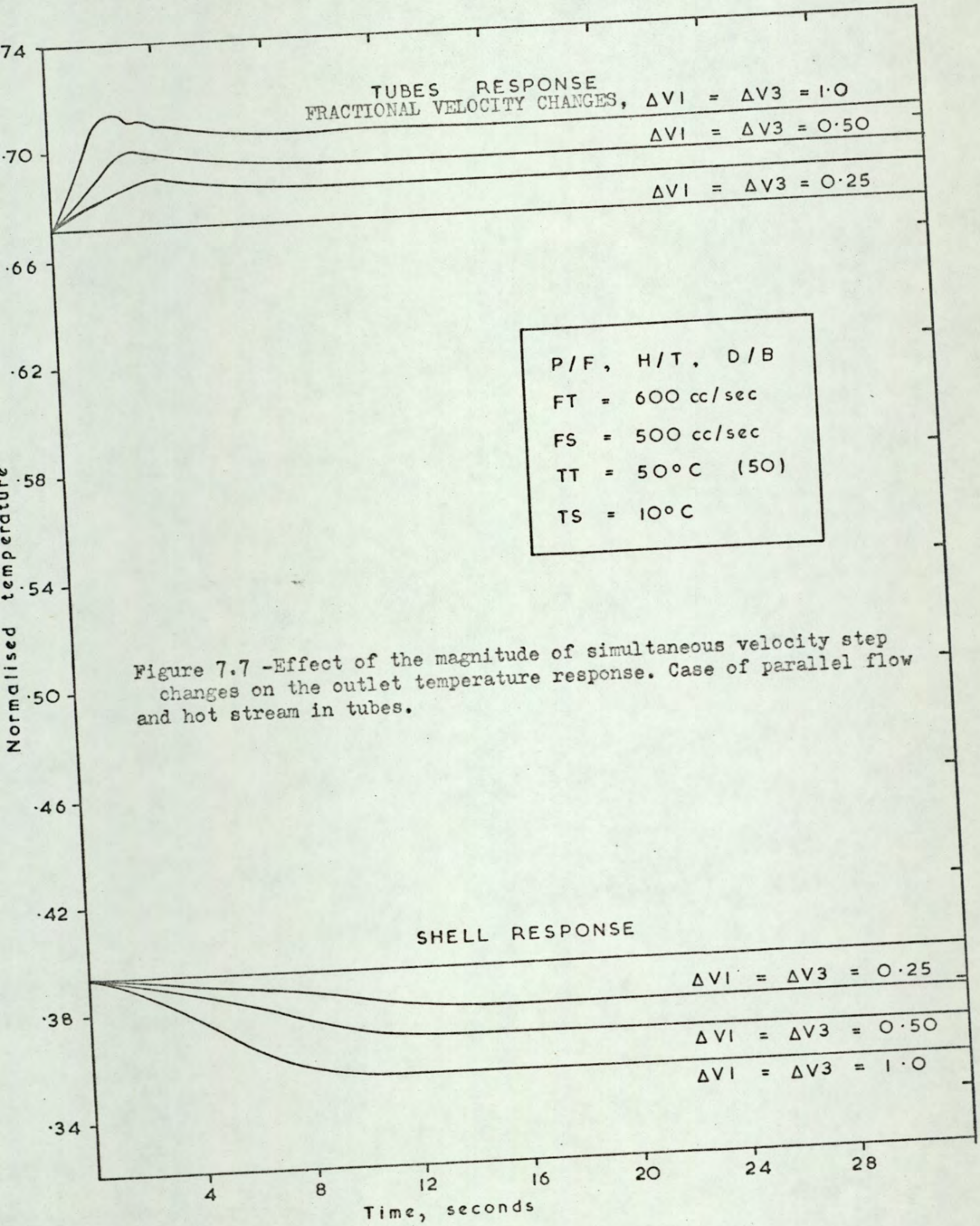

Figure 7.7 -Effect of the magnitude of simultaneous velocity step changes on the outlet temperature response. Case of parallel flow and hot stream in tubes.

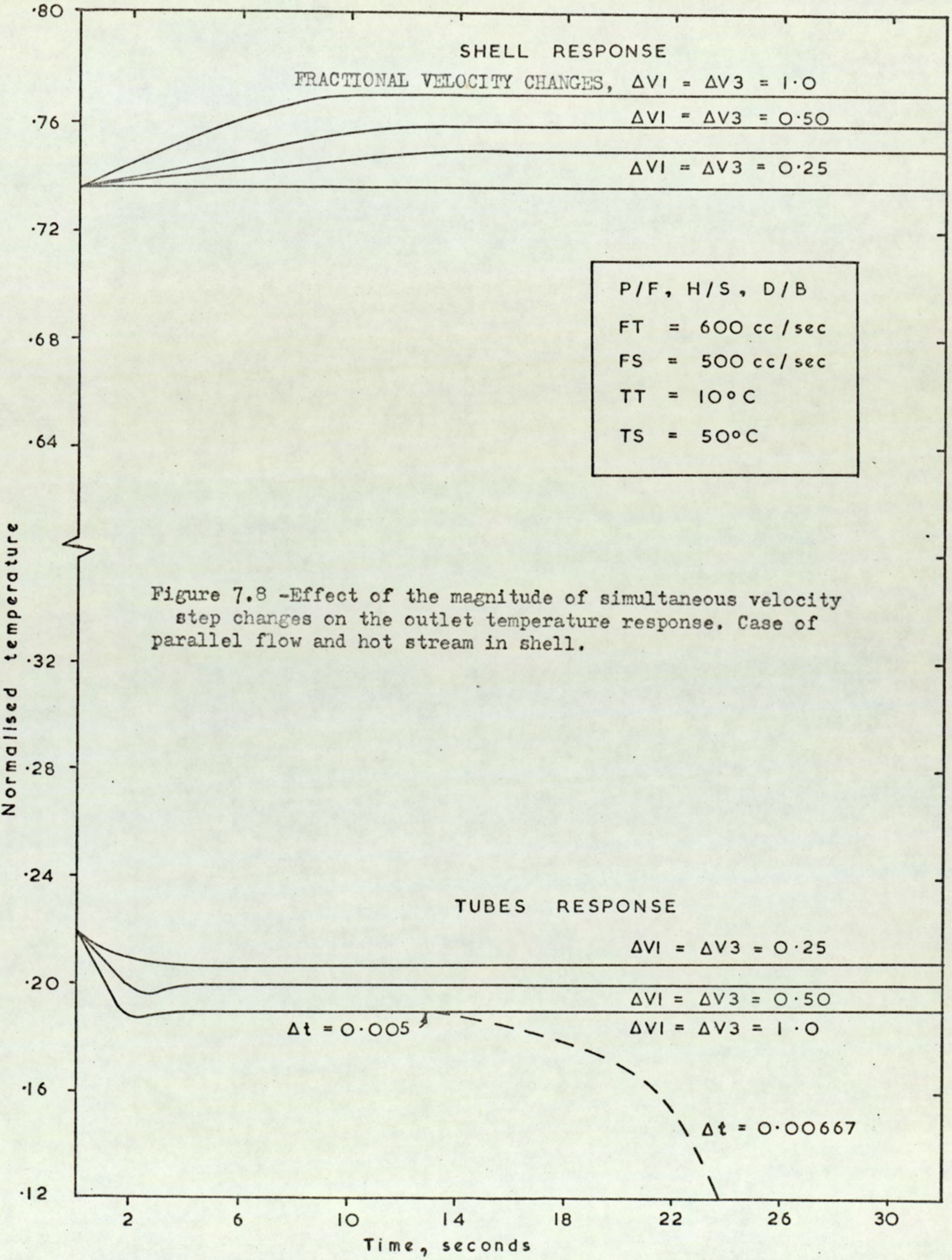

Figure 7.8 -Effect of the magnitude of simultaneous velocity step changes on the outlet temperature response. Case of parallel flow and hot stream in shell.

showed always the most sluggish response, explained by the larger fluid thermal capacitance.

A test carried out with a positive ramp signal in the shell side fluid indicates that as the flow rate grows continuously, the outlet temperatures after going through a constant rate of growth for some time, start to show signs of saturation by gradual levelling off as shown in Fig.7.9. This behaviour reflects the actual conditions, because the variations of the outlet temperatures as functions of the flow rate are always bound by the corresponding input temperatures which are approached asymptotically when either one of the flow rates increases without limit.

The 180° phase lag between the tube temperature response and the shell temperature response are evident in all the cases analysed. Other features of the model indicated by the curves are

(i) When the hot stream is in the tube, rather than in the shell, the corresponding temperature deviations are larger than in the opposite case due to the fact that the tube heat transfer coefficient is the limiting factor in the heat transfer process of this exchanger, and it is substantially increased when the average temperature of the stream is high, by the effect of viscosity on the Reynolds number.

(ii) The countercurrent flow always shows larger deviations than the corresponding parallel flow because the former is a more efficient scheme.

(iii) The two previous considerations are equally valid for the situations of only one velocity disturbed or for that of simultaneous disturbances, but the amplitudes of the second case are considerably

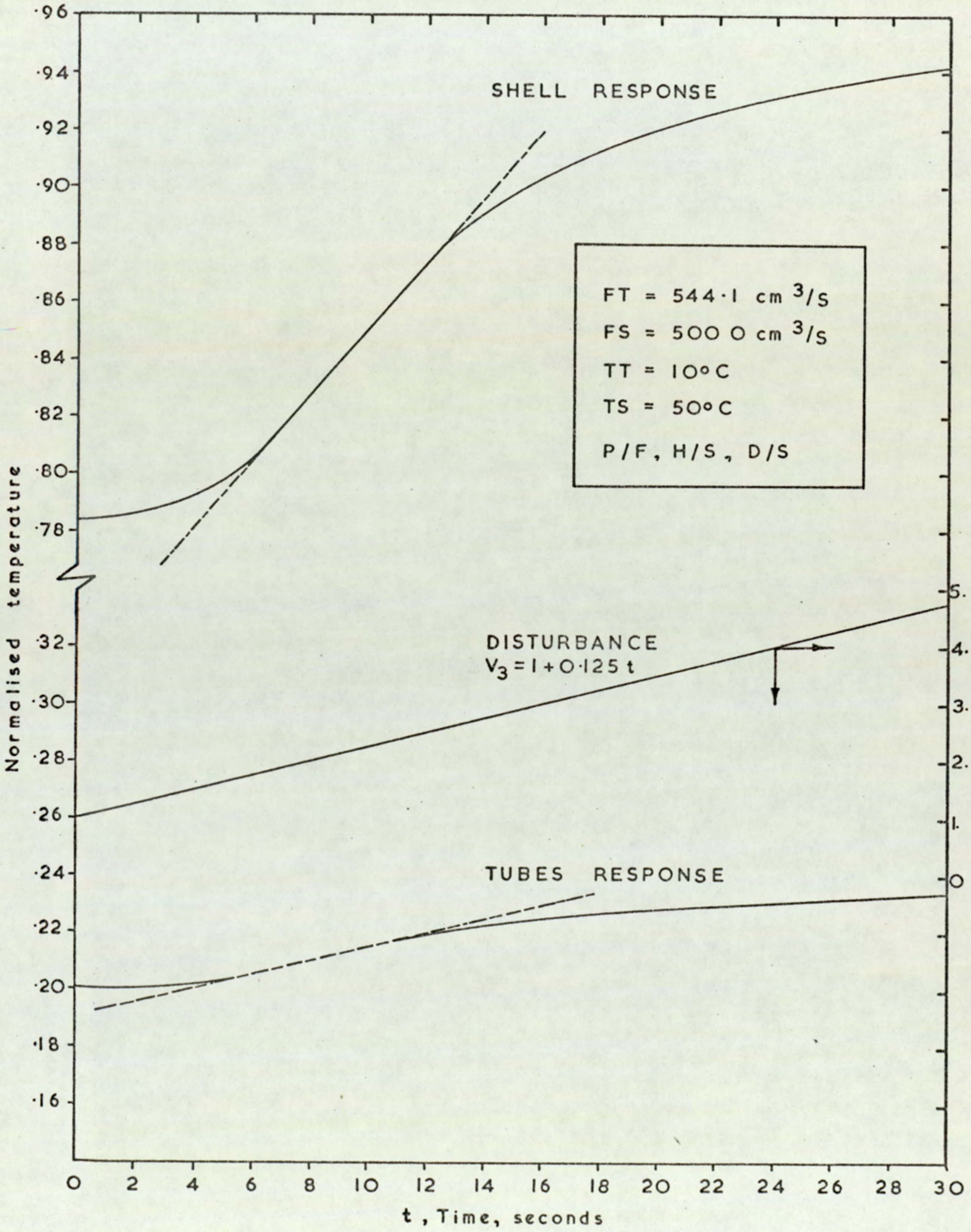

Figure 7.9 -Model response to a positive ramp disturbance. Note the saturation effect in both temperature responses.

smaller than those of the first. This decrease in the static gain of the process was already explained as the resultant of two gains of opposed sign and different magnitude in the exchanger. The experimental verification of this model effect is presented for comparison in Figs.7.21, 7.22 and 7.23. It must be noticed that since in the real system the two flow rates do not change exactly in the same way, the plots of one temperature against either flow rate do not exactly match, as seen in Fig.7.23.

The overshooting presented in Figs.7.5 to 7.8 by the tube temperature response is explained by the difference of speed in the shell and tube responses when subject to single disturbances. Since the tube temperature responds faster, it reaches a high deviation before the opposed effect of the shell temperature is large enough to produce a significant attenuation of the overall response. By analogous reasoning, in the same figures, the shell response looks extremely slow at the beginning.

(iv) A remarkable and apparently contradictory effect is shown by the model, for any set of conditions, under simultaneous disturbance operation: for any positive change in the fluid velocities the output temperature of the hot fluid becomes higher and that of the cold fluid becomes lower. This, however conforms to the conventional heat transfer theory as demonstrated in Appendix D .

Table 7.1 illustrates the previously mentioned characteristics for the case of perturbation amplitude equal to 1.0. The responses are given in normalised units of temperature

TABLE 7.1 EFFECT OF SIMULTANEOUS STEP CHANGES OF THE FLOW RATES (AMPLITUDE 100%) ON THE TEMPERATURE RESPONSES

FLOW	CONDITION	TUBE T. DEV.	SHL T. DEV.
C/C	H/T	0.042	- 0.050
	H/S	-0.033	0.039
P/F	H/T	0.033	- 0.040
	H/S	-0.029	0.035

In the response to sinusoidal disturbances, Figs.7.10 and 7.11 it is very clear how the amplitude and phase lag are functions of the frequency of the disturbance. They can be used to obtain the frequency response of the system by plotting each sinusoidal disturbance along with the corresponding time response and then measuring from the plots the respective gain and phase lag. Applying the same procedure for enough frequencies it is possible then to obtain the Bode plots for the temperature responses using only the time domain model, but at considerable cost of computer time.

The simulations indicated that the response to sinusoidal disturbances reached the quasi-steady state smoothly and without much deviation, due to the absence of drastic changes of direction in the disturbance, that makes the simulation easy to build up and free from the overshooting caused by sudden 'jumps' in the driving function.

It was noticed that when the amplitude of the upsets is large enough, the responses show some distortion which is explained by the saturation

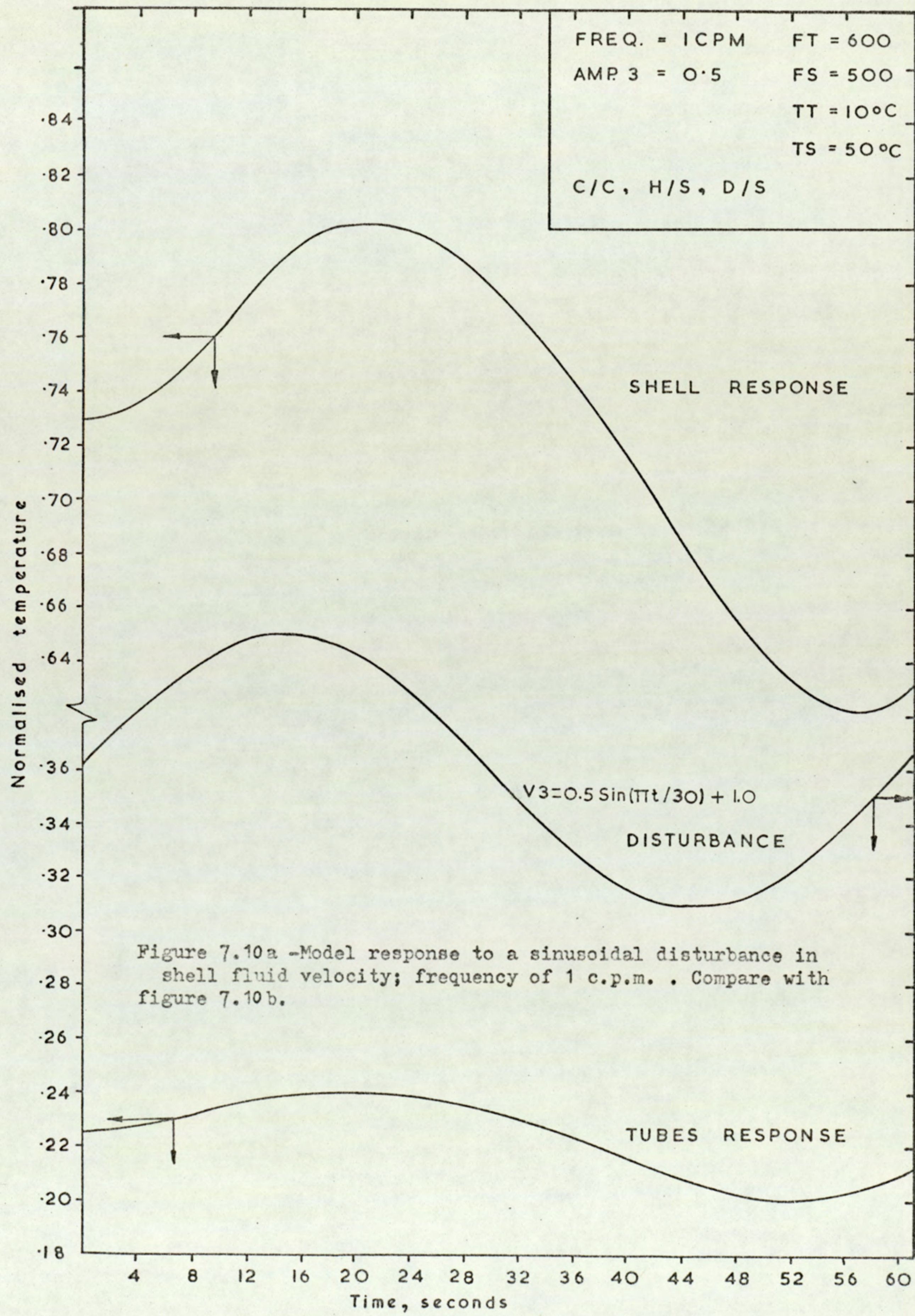

Figure 7.10 a -Model response to a sinusoidal disturbance in shell fluid velocity; frequency of 1 c.p.m. . Compare with figure 7.10 b.

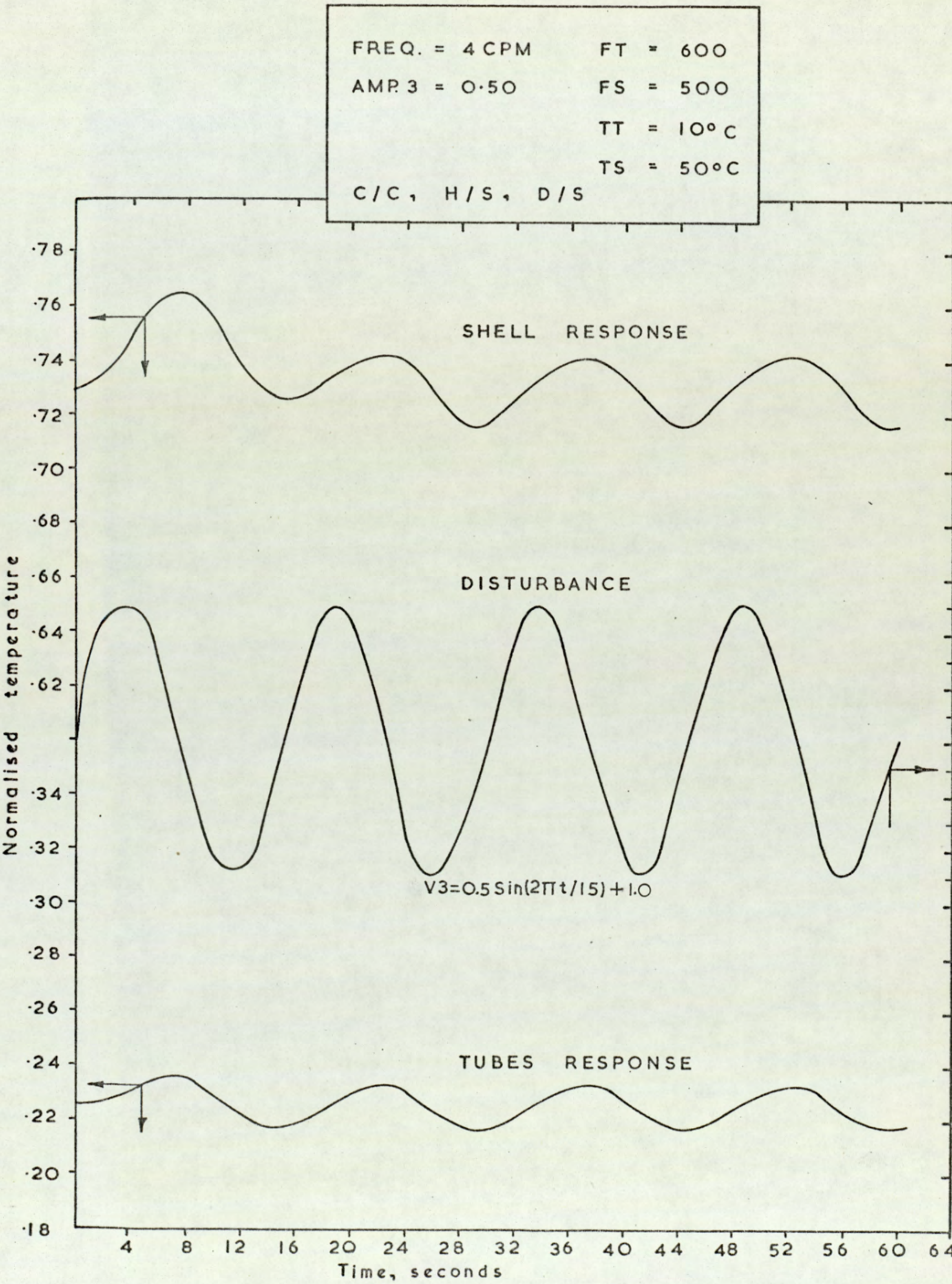

FIG. 7-10b MODEL RESPONSE TO SINUSOIDAL DISTURBANCE. FREQUENCY OF 4cpm. COMPARE WITH FIGURE 7-10a

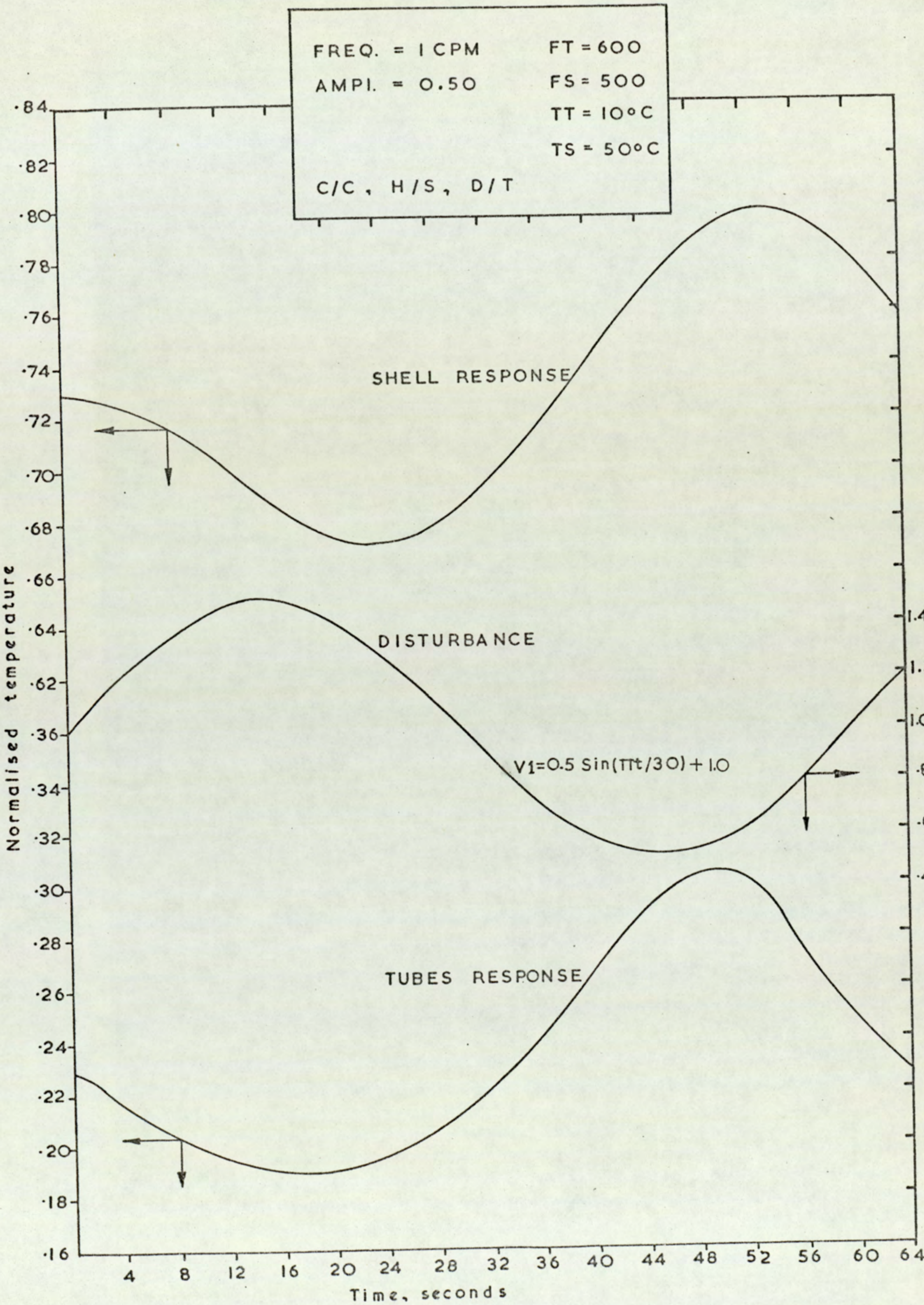

Figure 7.11a -Model response to a sinusoidal disturbance; frequency of 1 c.p.m. . Compare with figure 7.11b.

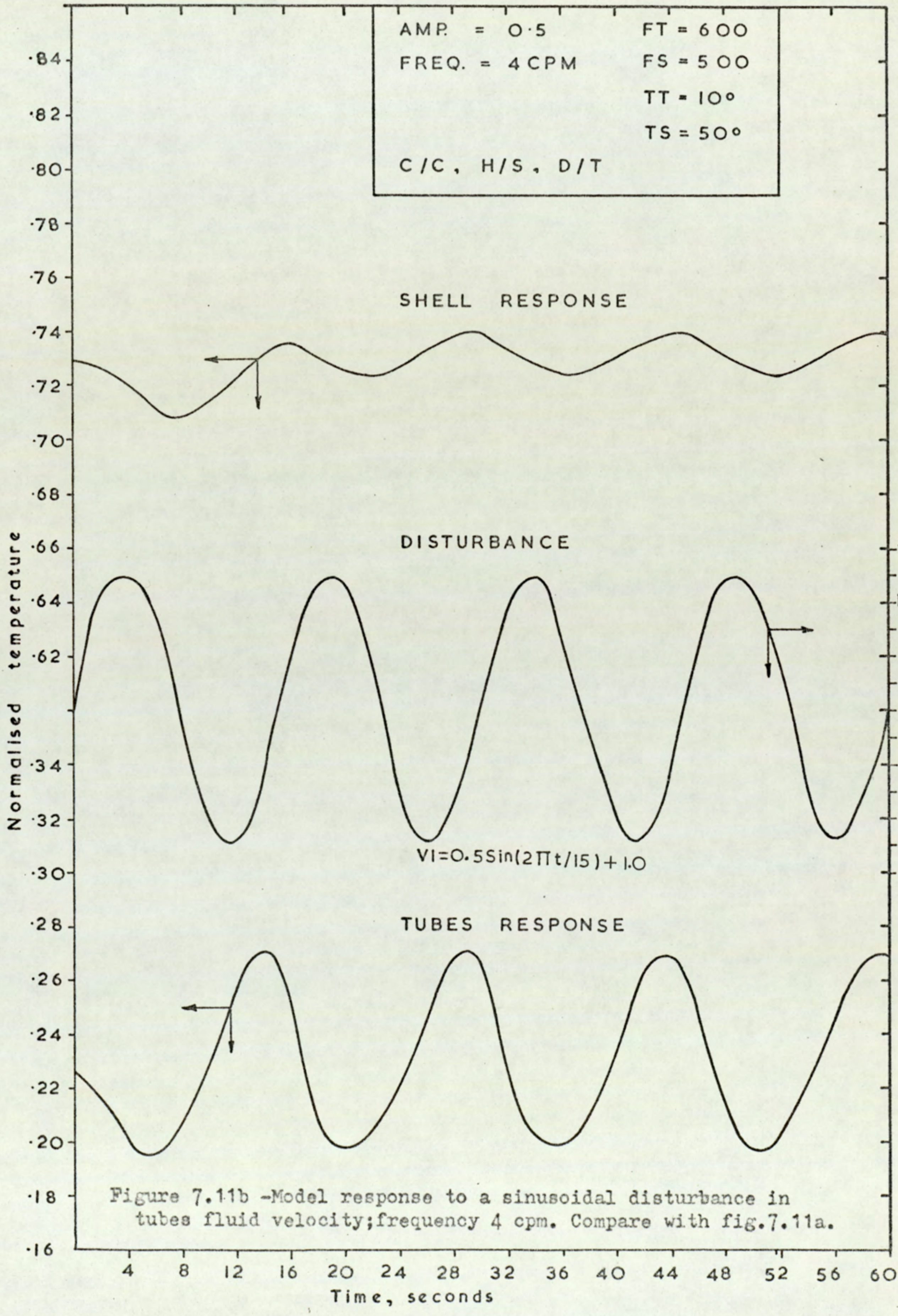

Figure 7.11b -Model response to a sinusoidal disturbance in tubes fluid velocity; frequency 4 cpm. Compare with fig.7.11a.

effect discussed before. This effect was equally observed during the collection of experimental data.

7.2.2 The Frequency Response Model

The package developed to represent the system in the frequency domain, when run in the same ICL-1906-A computer required 7 seconds of compilation time - mainly complex arithmetic - and required 0.036 seconds of execution to process a set of data through five decades of frequency with ten equally spaced points per decade.

The tests on this model indicated that the frequency response of the output temperatures to flow disturbances present resonance points, under all conditions, for each frequency whose period is a sub-multiple of the residence time of the fluid in the heat exchanger. This means that as the fluid rate is increased for successive Bode plot evaluations, the resonace peaks are gradually shifted to the region of higher frequencies as indicated in Figs.7.12 and 7.13.

One interesting feature of the simulated responses is that there is no significant difference in the gain plots when the temperature of the streams are interchanged, in spite of the notorious effect of the average stream temperature on viscosity, and therefore on the heat transfer coefficients, Fig.7.14. Figs.7.15 to 7.18, on the other hand, show that the Bode plots greatly depend on the relative values of both flow rates.

When the frequency response of either one of the outlet temperatures was analysed for the effect of the origin of the disturbances, it was found that though at very low frequencies there was no difference, the curves started diverging as they moved towards the higher frequency region

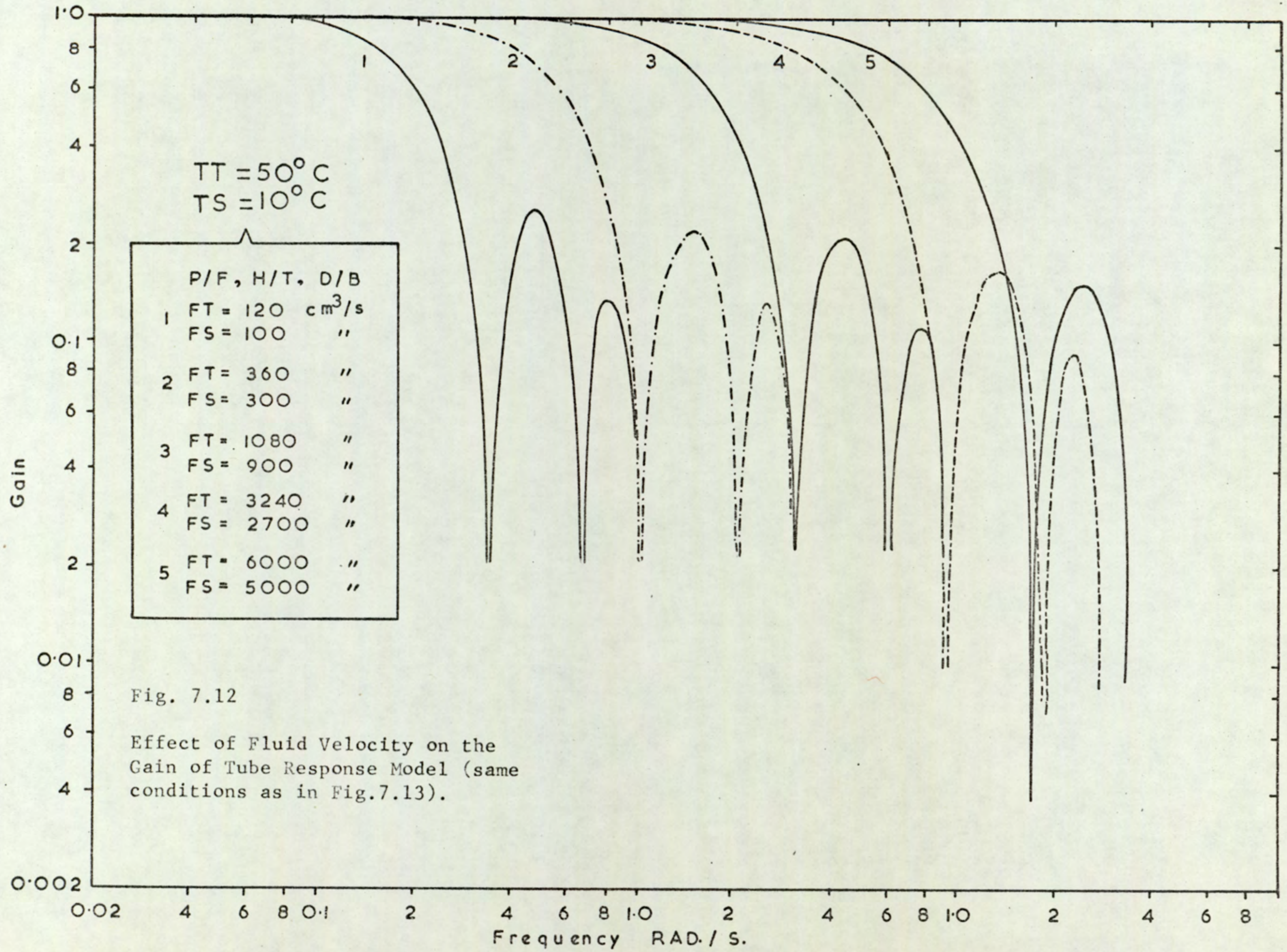

Fig. 7.12

Effect of Fluid Velocity on the Gain of Tube Response Model (same conditions as in Fig.7.13).

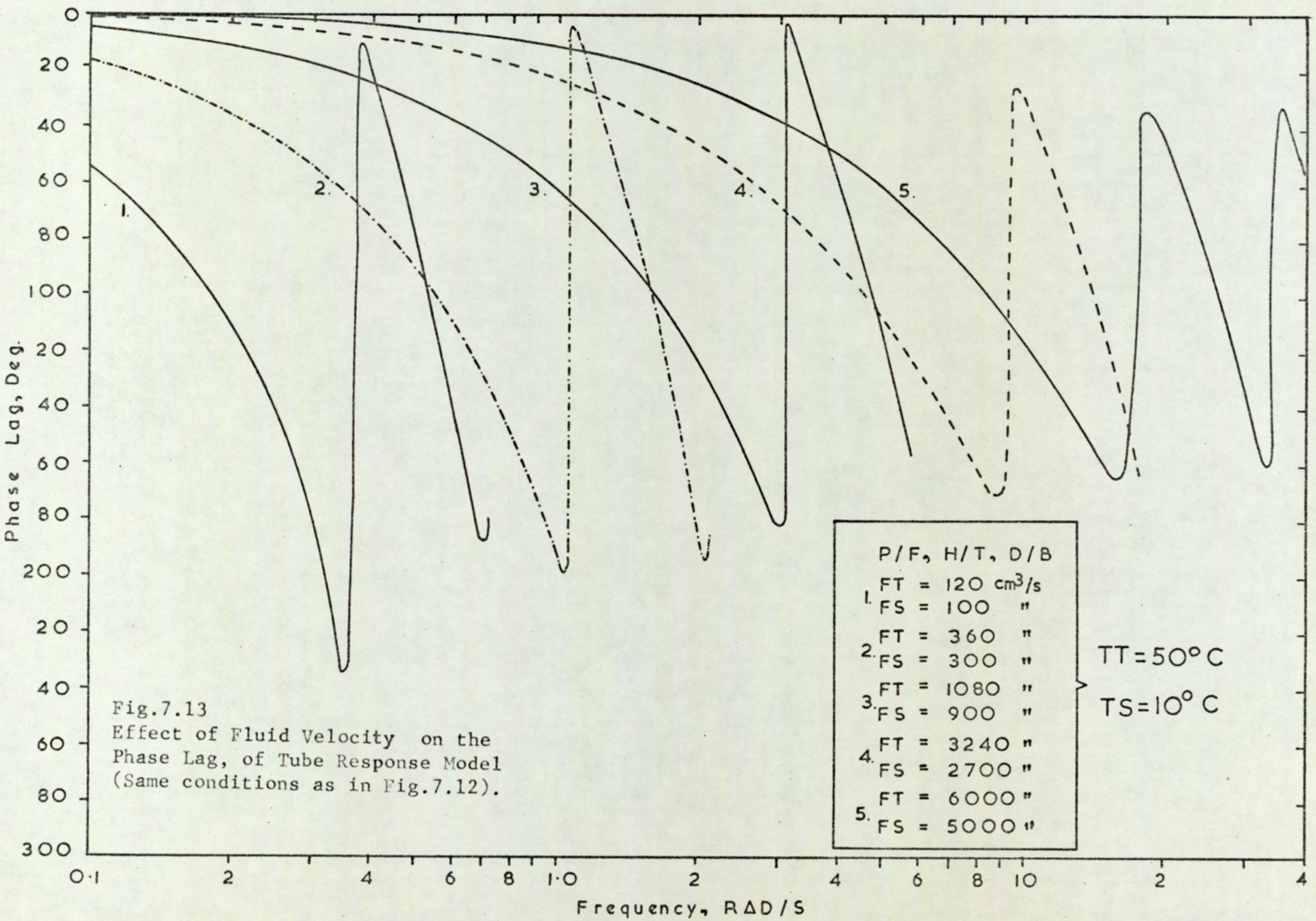

Fig.7.13
Effect of Fluid Velocity on the Phase Lag, of Tube Response Model (Same conditions as in Fig.7.12).

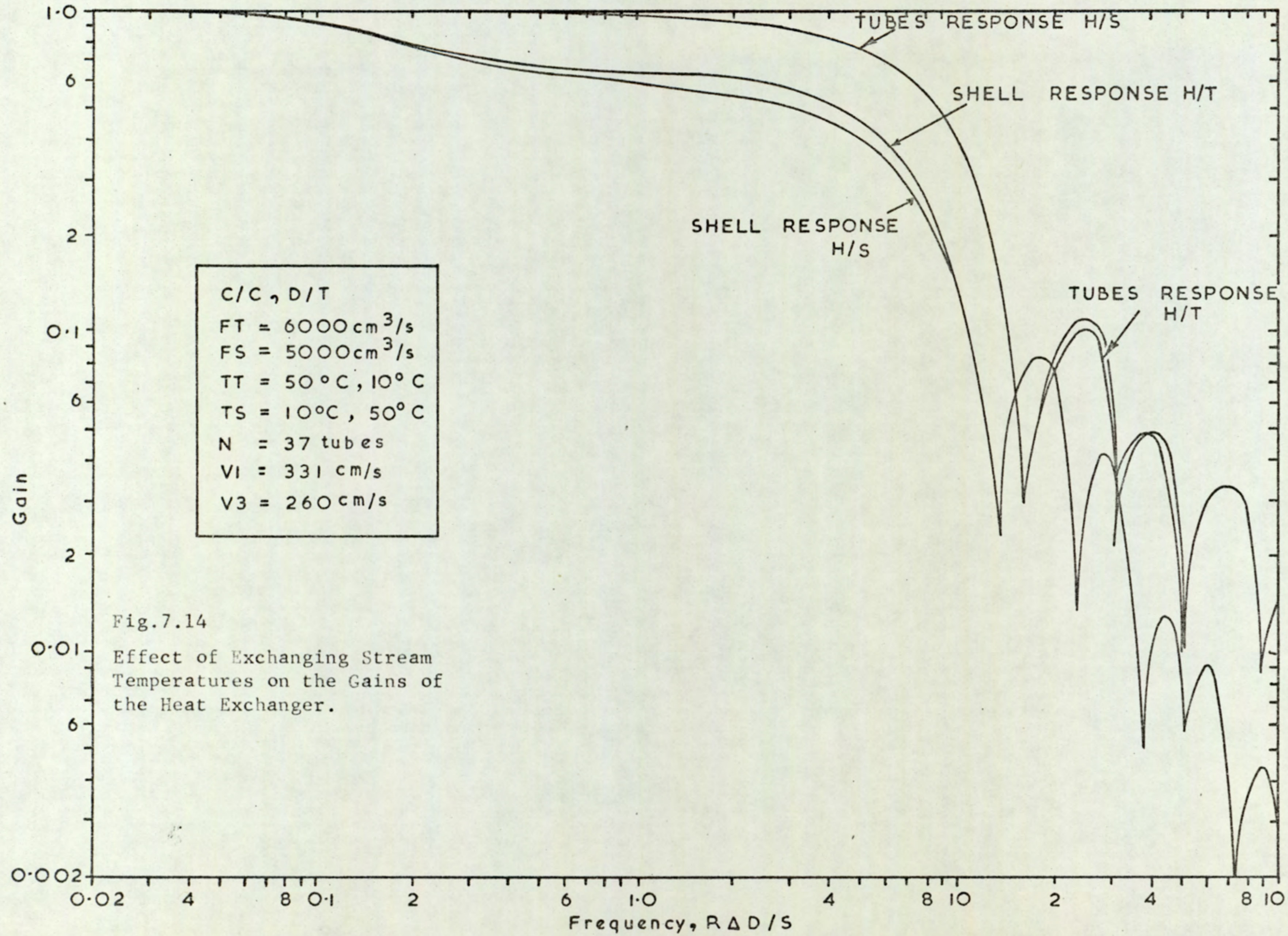

Fig.7.14

Effect of Exchanging Stream Temperatures on the Gains of the Heat Exchanger.

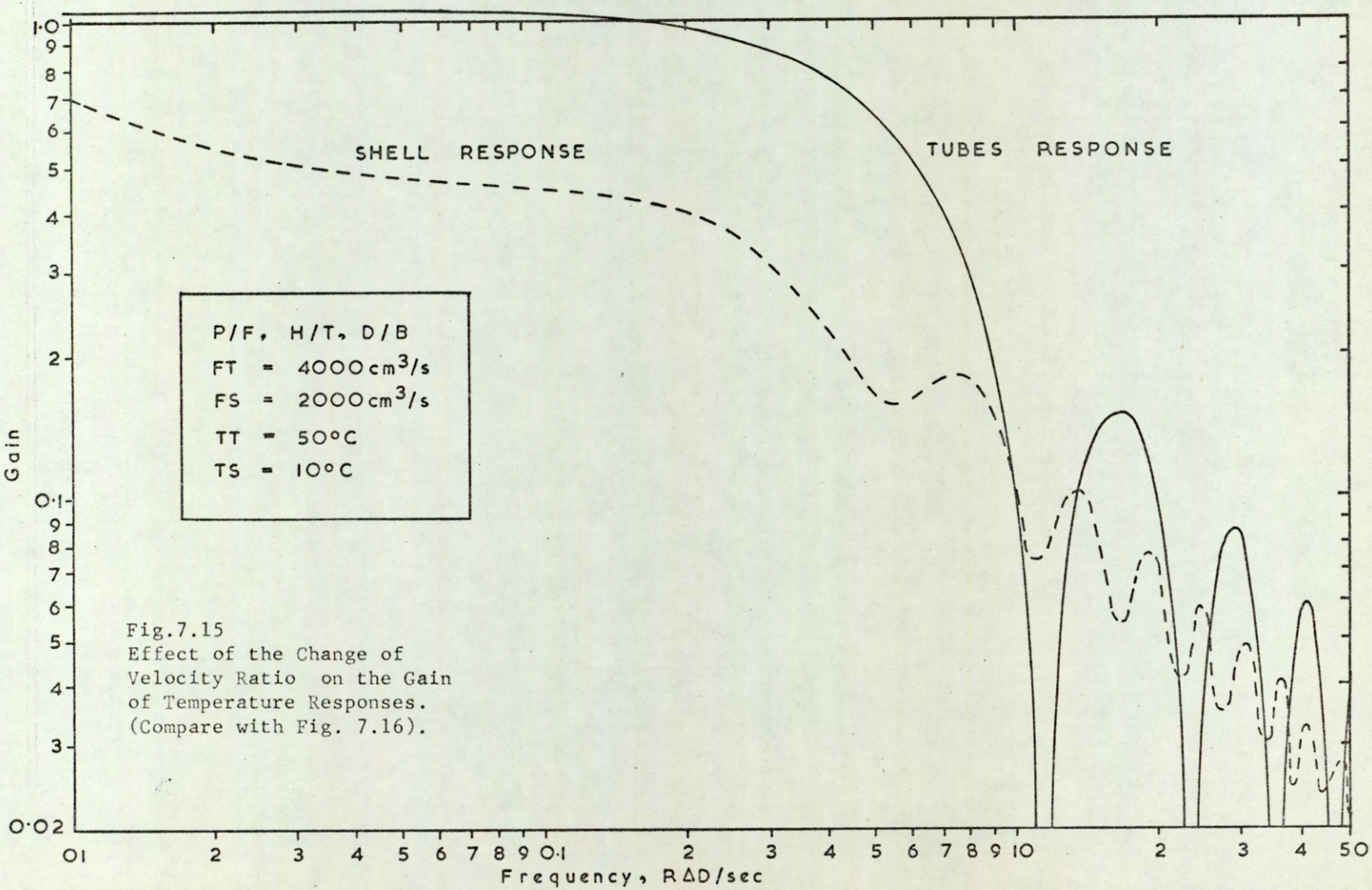

Fig.7.15
Effect of the Change of
Velocity Ratio on the Gain
of Temperature Responses.
(Compare with Fig. 7.16).

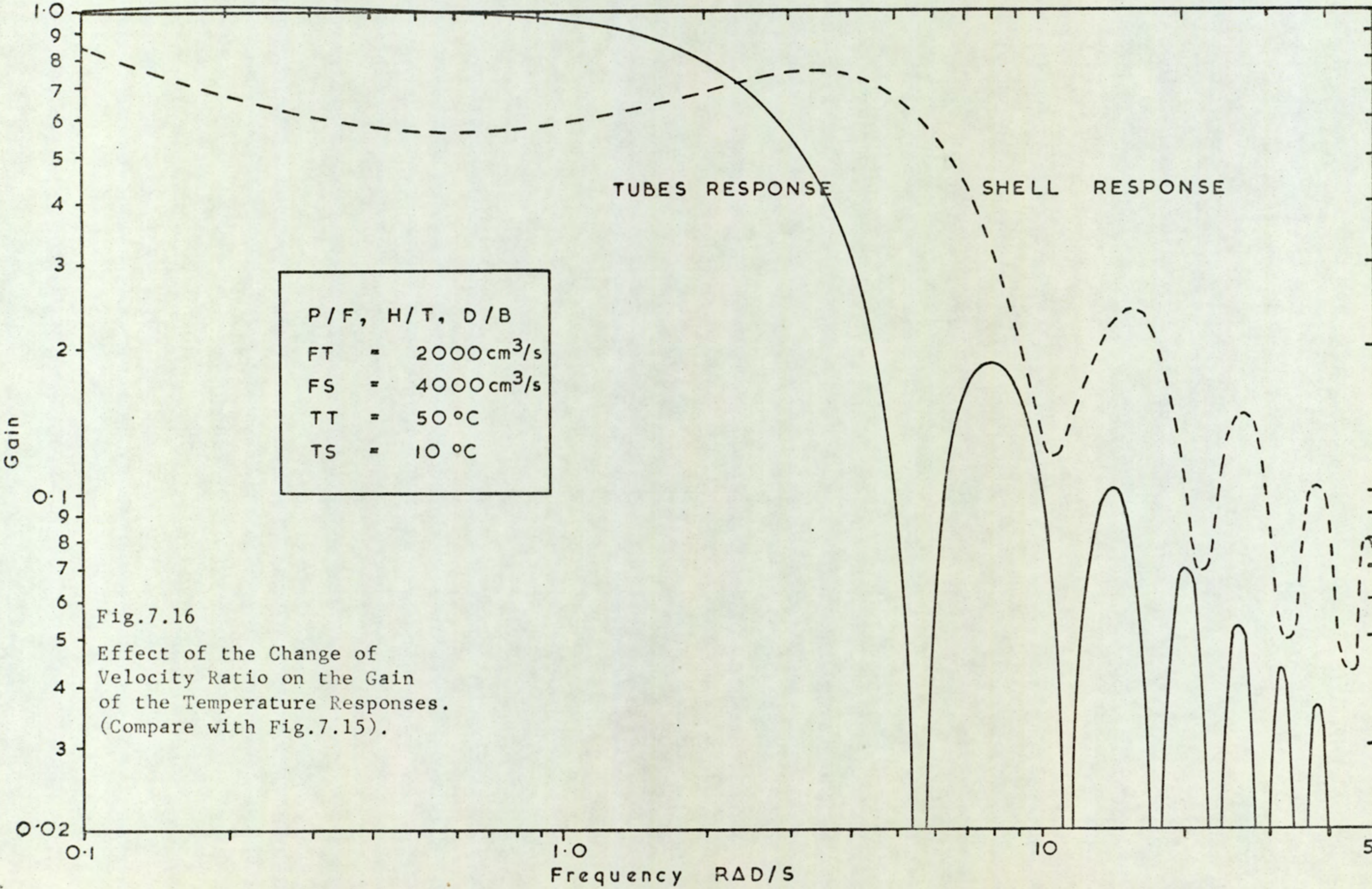

Fig.7.16

Effect of the Change of Velocity Ratio on the Gain of the Temperature Responses. (Compare with Fig.7.15).

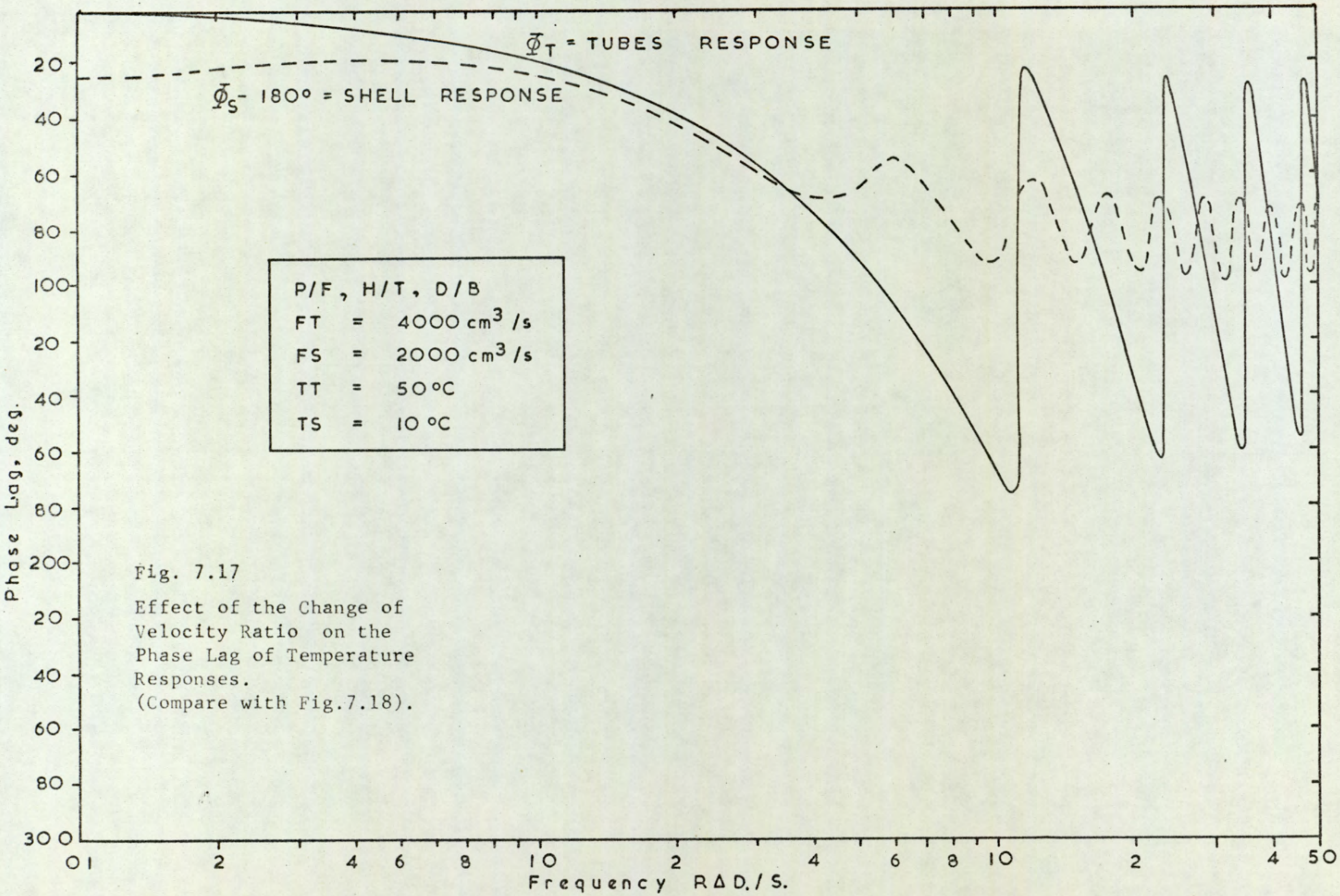

Fig. 7.17

Effect of the Change of Velocity Ratio on the Phase Lag of Temperature Responses. (Compare with Fig.7.18).

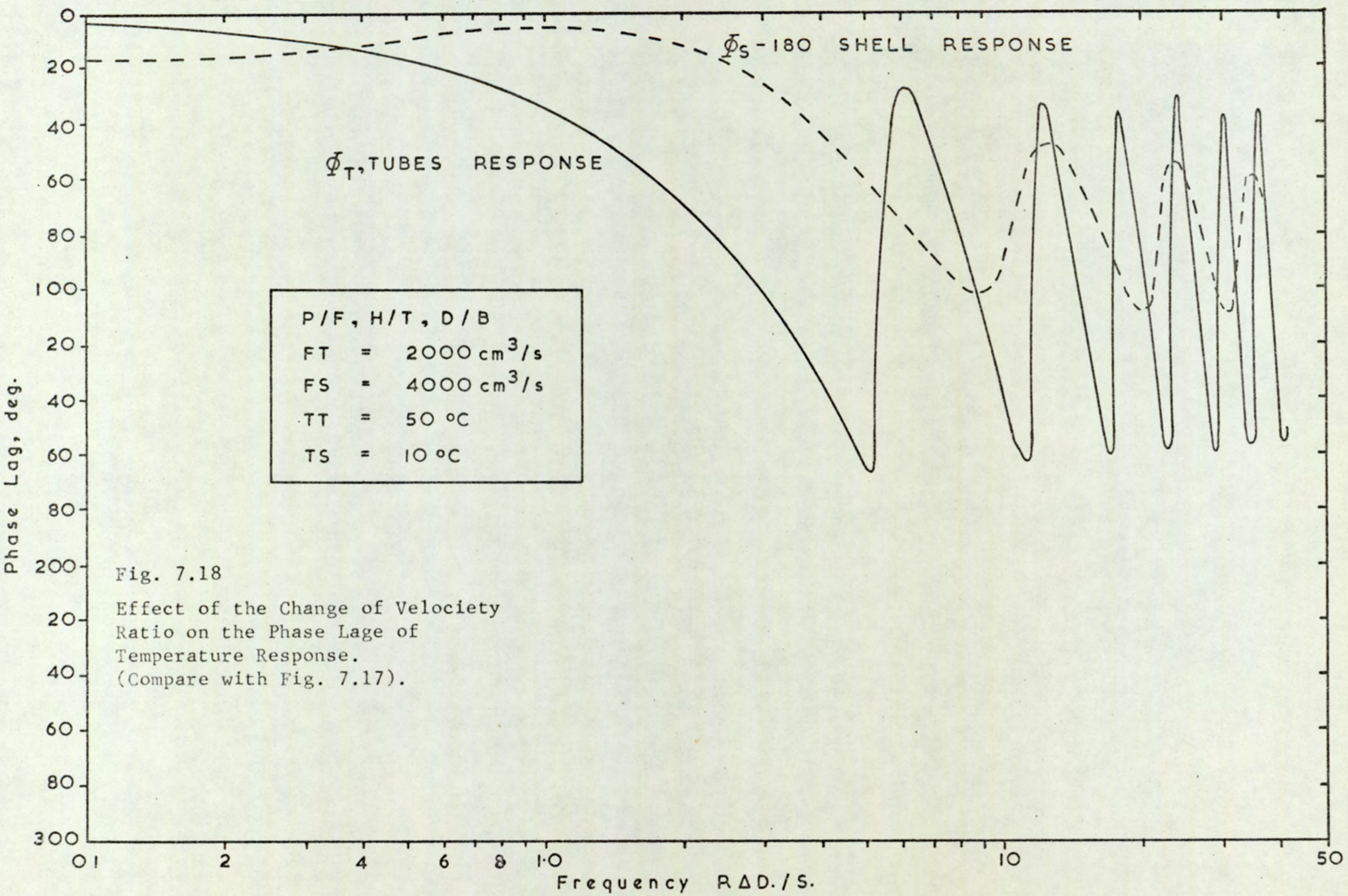

Fig. 7.18

Effect of the Change of Velociety Ratio on the Phase Lage of Temperature Response. (Compare with Fig. 7.17).

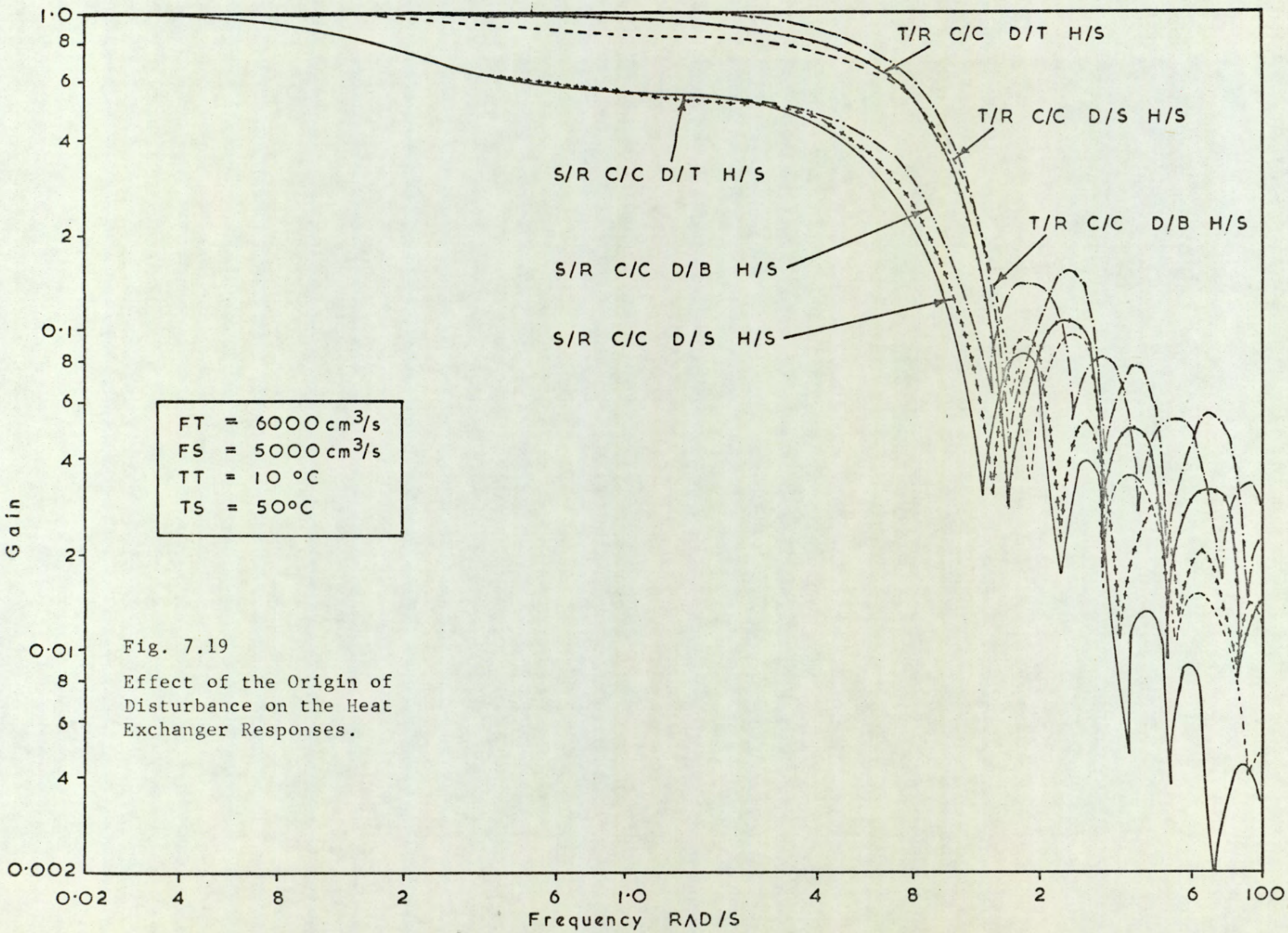

Fig. 7.19

Effect of the Origin of Disturbance on the Heat Exchanger Responses.

and were definitely apart after the first resonance peak, as shown in Fig.7.19 for the countercurrent flow case. In it the shell and tube responses are vertically spread out with the highest peaks corresponding to the responses to simultaneous perturbations. However, the lowest gains for tube response and shell response correspond to the respective disturbances in tube and in shell flow rates.

7.3 CONTROL VALVE RESPONSE

In order to make a more realistic approach to the problem, closer to the normal operating conditions of the practical system it was decided to study the effect of the control valves, used to regulate the flow rate disturbances, on the transient response of the system, instead of trying to produce nearly ideal disturbances to match the analytical functions. This meant that the 'corrupting' effect produced by the inherent transient response of the control valves on the signals produced by the function generator was included in the model. It was then possible to compare the simulation of the process subject to the real 'distorted' signals with the simulation using the ideal perturbations as generated by the analytical function. In order to do this the analytical representation of the valves was obtained by studying the experimental data of step change responses applied to the valves. It was found that both valves can be represented by a critically damped second order differential equation whose characteristic time depends on the amplitude of the step and the direction of the change. Since trying to incorporate all detailed information for each set of data only would result in marginal improvement in the fit, it was decided to adopt an average value, typical of the range of work, for the characteristic time and to use only one equation to

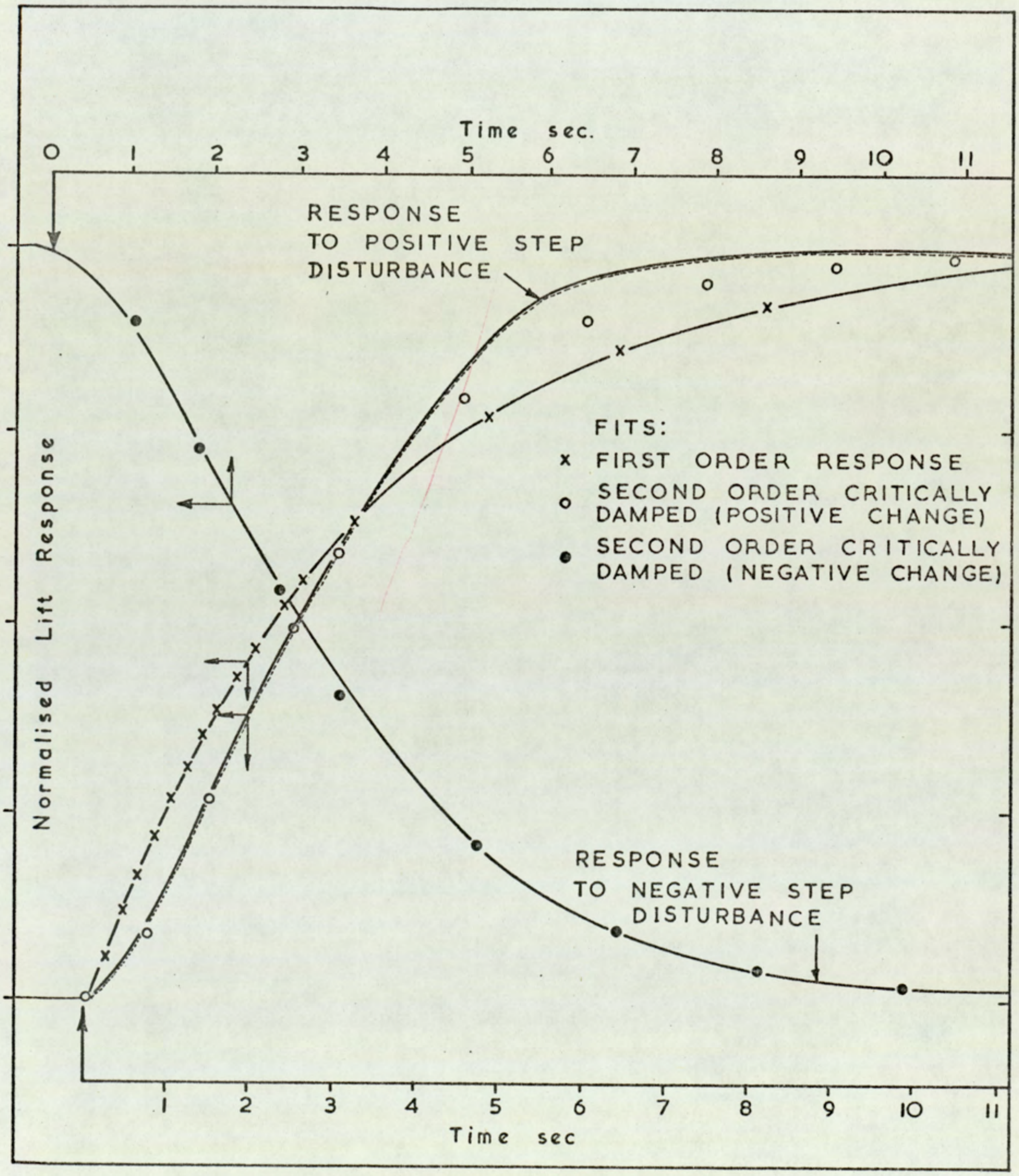

Fig. 7.20 Mathematical Fitting of the Control Valve Transient Response.

describe the transient response of both valves to changes in either direction, see Fig.7.20. In the adopted description of the pneumatic control valves (see reference 16),

$$Y = 1-(1 + t/\tau)e^{-t/\tau} \tag{7.1}$$

Y is the valve response (stem displacement) to a step change in the air pressure on the diaphragm, t, real time and τ the characteristic time, estimated as 1.3 seconds. Y is normalised.

Several runs carried out for step change disturbances were simulated with and without the inclusion of the valve's transient response. They are discussed in the section on time domain response, and in addition the frequency response of the valves is discussed in the context of the heat exchanger frequency response.

7.4 EXPERIMENTAL STEADY STATE DATA

Tables 7.2 to 7.5 present samples of the steady state data necessary to calculate the heat balance and the overall heat transfer coefficient for the conditions of parallel and countercurrent flows under heating and cooling operation. Because of the numerous calculated parameters included for each run, the data are presented in a double line for each run with the figures toward the upper left of each column one to six, corresponding to the tube side conditions and those toward the lower right corresponding to the shell side conditions. Column seven presents the calculated overall heat transfer coefficient, estimated from the individual heat transfer coefficients and based on the inside tube area, according to the expression

$$\frac{1}{U_c} = \frac{1}{h_t} + \frac{r_1}{h_s r_2} + \frac{\ln(r_2/r_1)}{k(r_2-r_1)} \tag{7.2}$$

TABLE 7.2 STEADY STATE DATA - COUNTERCURRENT FLOW H/T*

FLOW cc/sec	TEMP(IN) °C	TEMP(OUT) °C	VELOCITY cm/sec	REYNOLDS NUMBER	HEAT TRANS. COEFF.	O.H. T C CAL. & EXP.	U-DEV. % Q.DEV. %
369.8	50.0	33.4	20.4	2534	0.0310	0.0228	-5.42
372.5	10.1	26.8	19.4	1763	0.0721	0.024	-1.34
369.8	50.1	32.3	20.4	2511	0.0309	0.0235	-5.32
461.9	10.0	24.2	24.0	2113	0.0818	0.0248	0.34
369.8	50.0	31.4	20.4	2488	0.0308	0.0240	-5.91
555.4	10.0	22.3	28.9	2480	0.0911	0.0255	0.68
369.8	50.0	31.2	20.4	2383	0.0307	0.0241	-5.53
588.6	10.0	21.7	30.6	2608	0.0943	0.0255	0.94
587.1	50.1	34.7	32.4	4076	0.0453	0.0324	-1.77
588.6	9.9	25.2	30.6	2724	0.0951	0.0330	0.39
369.8	50.0	34.35	20.4	2556	0.0312	0.0222	-5.16
312.8	10.0	28.95	16.3	1519	0.0650	0.0235	-2.42
369.8	50.1	36.0	20.4	2598	0.0314	0.0212	-4.50
235.8	10.0	32.6	12.3	1197	0.0551	0.0223	-2.20
369.8	50.0	38.6	20.4	2657	0.0318	0.0198	-3.33
158.7	10.2	37.9	8.3	859	0.0437	0.0205	-4.20
158.7	50.25	37.1	8.8	1127	0.0160	0.0122	-1.23
158.7	21.5	34.9	8.3	943	0.0436	0.0124	-2.26
480.6	50.3	38.5	26.5	3459	0.0392	0.0283	-3.8
476.3	21.0	32.85	24.8	2750	0.0846	0.0294	0.48

* To identify data, see page 145, Section 7.4.

TABLE 7.3 STEADY STATE DATA - COUNTERCURRENT FLOW H/S *

FLOW cc/sec	TEMP(IN) °C	TEMP(OUT) °C	VELOCITY cm/sec	REYNOLDS NUMBER	HEAT TRANS. COEFF.	O.H. T C CAL. & EXP.	U.DEV % Q.DEV %
515.4 450.6	21.85 50.2	32.25 38.45	28.4 23.4	2630 3674	0.0352 0.0746	0.0252 0.0280	-9.85 1.84
495.0 442.0	21.85 50.2	32.4 38.5	27.3 23.0	2531 3606	0.0341 0.0738	0.0341 0.0274	-10.2 0.96
467.1 430.8	21.8 50.2	32.6 38.65	25.8 22.4	2392 3519	0.0326 0.0727	0.0237 0.0264	-10.2 1.37
435.0 408.4	21.8 50.2	32.7 38.65	24.0 21.2	2230 3336	0.0308 0.0704	0.0225 0.0250	-9.8 0.52
409.0 384.9	21.75 50.1	32.85 38.6	22.6 20.0	2099 3140	0.0293 0.0680	0.0215 0.0239	-9.72 2.53
369.8 352.0	21.75 50.2	33.0 38.55	20.4 18.3	1901 2873	0.0271 0.0644	0.0200 0.0221	-9.19 1.42
320.9 315.5	21.7 50.2	33.1 38.65	17.7 16.4	1650 2577	0.02415 0.0602	0.0181 0.0222	-7.03 0.38
254.3 278.1	21.65 50.2	33.5 39.4	14.0 14.5	1313 2287	0.0201 0.0560	0.0154 0.0159	-2.62 0.32
217.5 246.4	21.6 50.	33.7 39.6	12.0 12.8	1125 2028	0.0177 0.0521	0.0138 0.0138	0.10 1.7
173.0 176.9	21.65 50.1	34.0 38.1	9.5 9.2	898 1436	0.0148 0.0428	0.0115 0.0119	-3.54 0.64

* To identify data, see page 145, Section 7.4.

TABLE 7.4 STEADY STATE DATA - PARALLEL FLOW H/T*

FLOW cc/sec.	TEMP(IN) ^oC	TEMP (OUT) ^oC	VELOCITY cm/sec.	REYNOLDS NUMBER	HEAT TRANS. COEFF.	O.H. T C CAL. & EXP.	U-DEV. % Q.DEV. %
387.6	50.2	35.8	21.4	2721	0.0326	0.0237	-2.84
372.5	11.1	26.3	19.4	1774	0.0725	0.0244	-1.43
467.7	50.3	37.15	25.8	3325	0.0382	0.0265	-1.87
372.5	11.4	27.9	19.4	1816	0.0728	0.0270	0.05
555.4	50.2	38.2	30.6	3983	0.0440	0.0298	0.35
373.9	11.0	28.9	19.4	1836	0.0731	0.0292	-0.42
655.4	50.2	39.4	36.1	4751	0.0506	0.0321	1.25
375.3	11.2	30.4	19.5	1881	0.0735	0.0317	-1.77
653.8	50.0	36.7	36.1	4618	0.0498	0.0347	-0.39
594.1	10.5	25.2	30.9	2770	0.0961	0.0349	-0.43
393.2	50.2	35.6	21.7	2754	0.03306	0.0239	-3.66
372.5	10.6	26.1	19.4	1759	0.0725	0.0248	-0.59
311.5	50.2	33.9	17.2	2149	0.0271	0.0206	-5.44
372.5	10.6	24.3	19.4	1719	0.0722	0.0218	-0.51
231.9	50.2	32.0	12.8	1572	0.0212	0.0170	-5.18
372.5	10.6	22.05	19.4	1671	0.0718	0.0179	-1.06
162.6	50.2	30.3	9.0	1085	0.0158	0.01345	-1.38
372.5	10.6	19.6	19.4	1619	0.0715	0.0135	-3.54
88.5	50.3	25.0	4.9	562	0.00947	0.0085	-18.14
372.5	10.5	16.8	19.4	1557	0.0706	0.0104	-4.66

* To identify data, see page 145, Section 7.4.

TABLE 7.5 STEADY STATE DATA - PARALLEL FLOW H/S *

FLOW cc/sec	TEMP(IN) °C	TEMP(OUT) °C	VELOCITY cm/sec.	REYNOLDS NUMBER	HEAT TRANS. COEFF.	O.H. T C CAL.& EXP.	U.DEV. % Q.DEV. %
527.2 419.5	9.2 50.0	21.7 34.5	29.1 21.8	2038 3295	0.0316 0.0663	0.0226 0.0246	-8.19 1.31
527.2 346.6	9.2 50.0	20.65 32.65	29.1 18.0	2010 2676	0.0314 0.0589	0.0217 0.0232	-6.54 0.38
525.7 197.8	9.2 50.1	17.75 26.8	29.0 10.3	1928 1447	0.0308 0.0416	0.019 0.0196	-2.7 -2.52
524.2 132.7	9.2 50.0	15.9 22.85	28.9 6.9	1875 933	0.0304 0.0326	0.0171 0.0169	1.17 -2.55
124.9 131.4	9.8 50.0	27.0 34.5	6.9 6.8	521 1032	0.0103 0.0337	0.0818 0.0098	-16.1 5.33
368.4 387.6	10.8 50.1	24.6 37.3	20.3 20.2	1509 3125	0.0243 0.0642	0.0185 0.0194	-4.66 2.43
368.4 482.0	10.7 50.1	25.6 39.0	20.3 25.1	1526 3946	0.0244 0.0734	0.0191 0.0204	-6.38 2.56
500.8 484.9	10.5 50.0	23.8 36.6	27.6 25.2	2022 3881	0.0309 0.0732	0.0228 0.0252	-9.39 2.48
487.8 383.5	10.45 50.0	22.6 34.5	26.9 19.9	1939 3012	0.0300 0.0633	0.0215 0.0234	-8.1 -0.31
483.4 199.1	10.3 50.0	19.2 28.0	26.7 10.4	1835 1472	0.0292 0.0422	0.0185 0.0192	-3.64 -1.8

* To identify data, see page 145, Section 7.4.

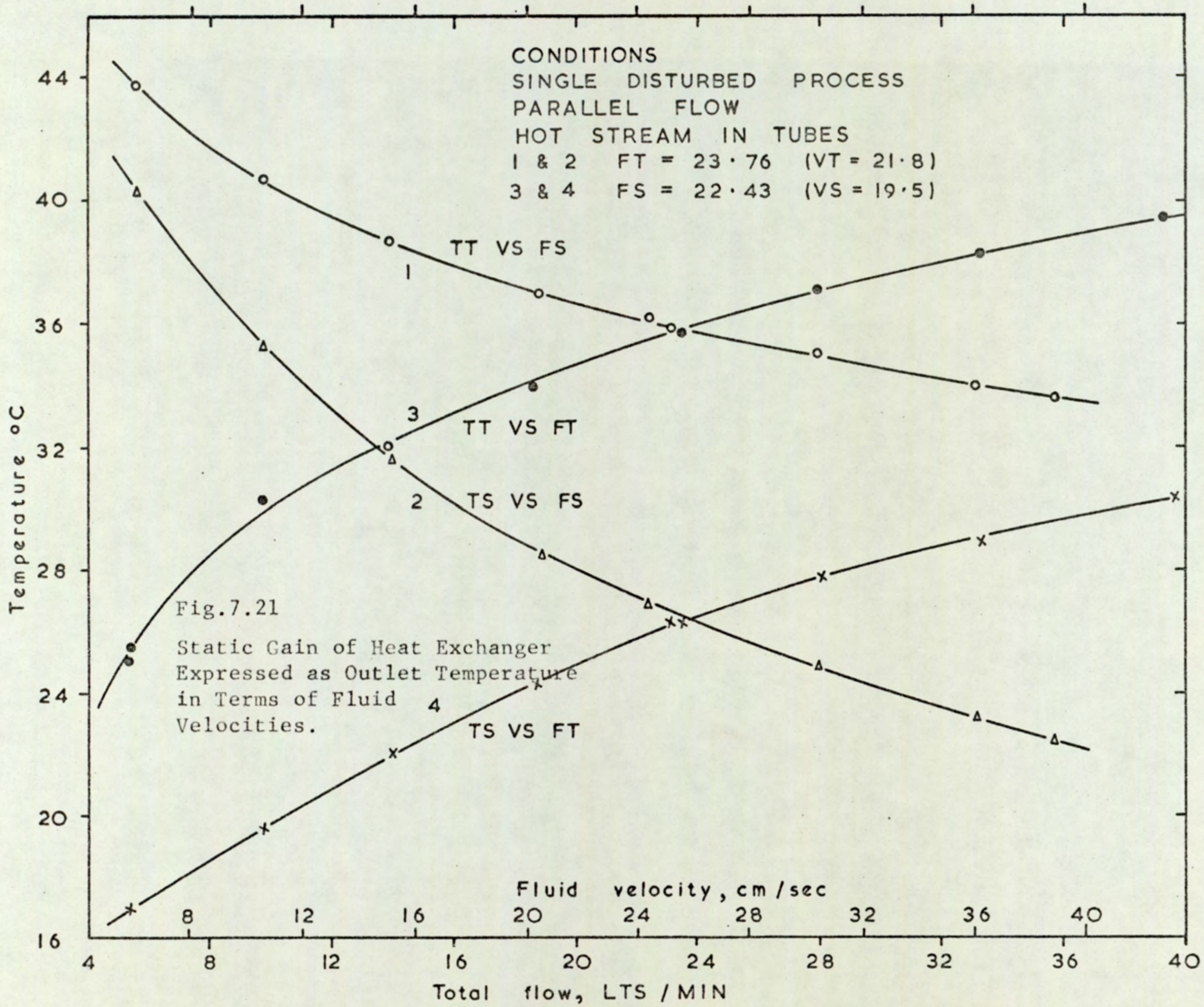

Fig.7.21

Static Gain of Heat Exchanger Expressed as Outlet Temperature in Terms of Fluid Velocities.

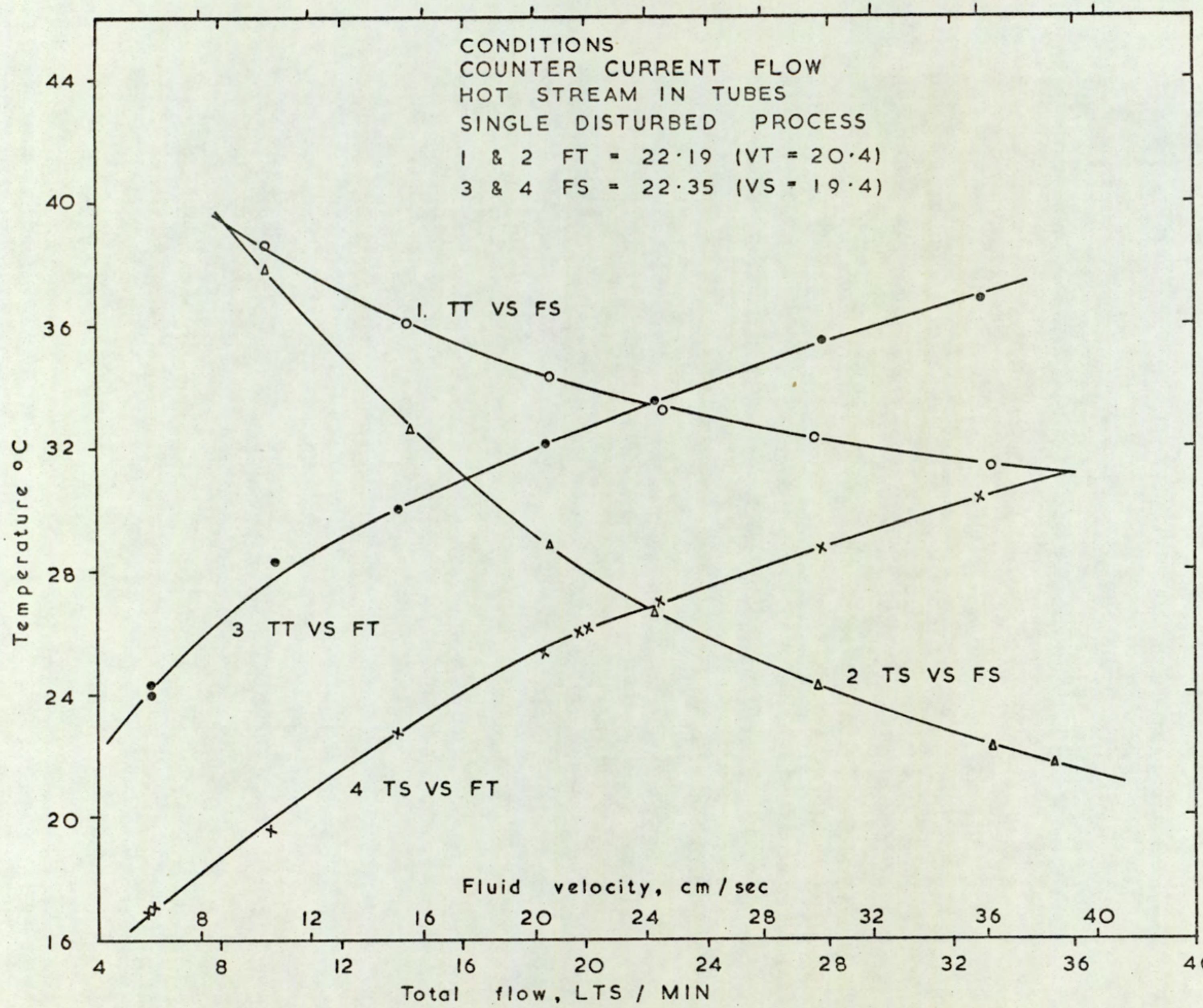

Fig.7.22 Static Gain of Heat Exchanger Expressed as Outlet Temperature in Terms of Fluid Velocities.

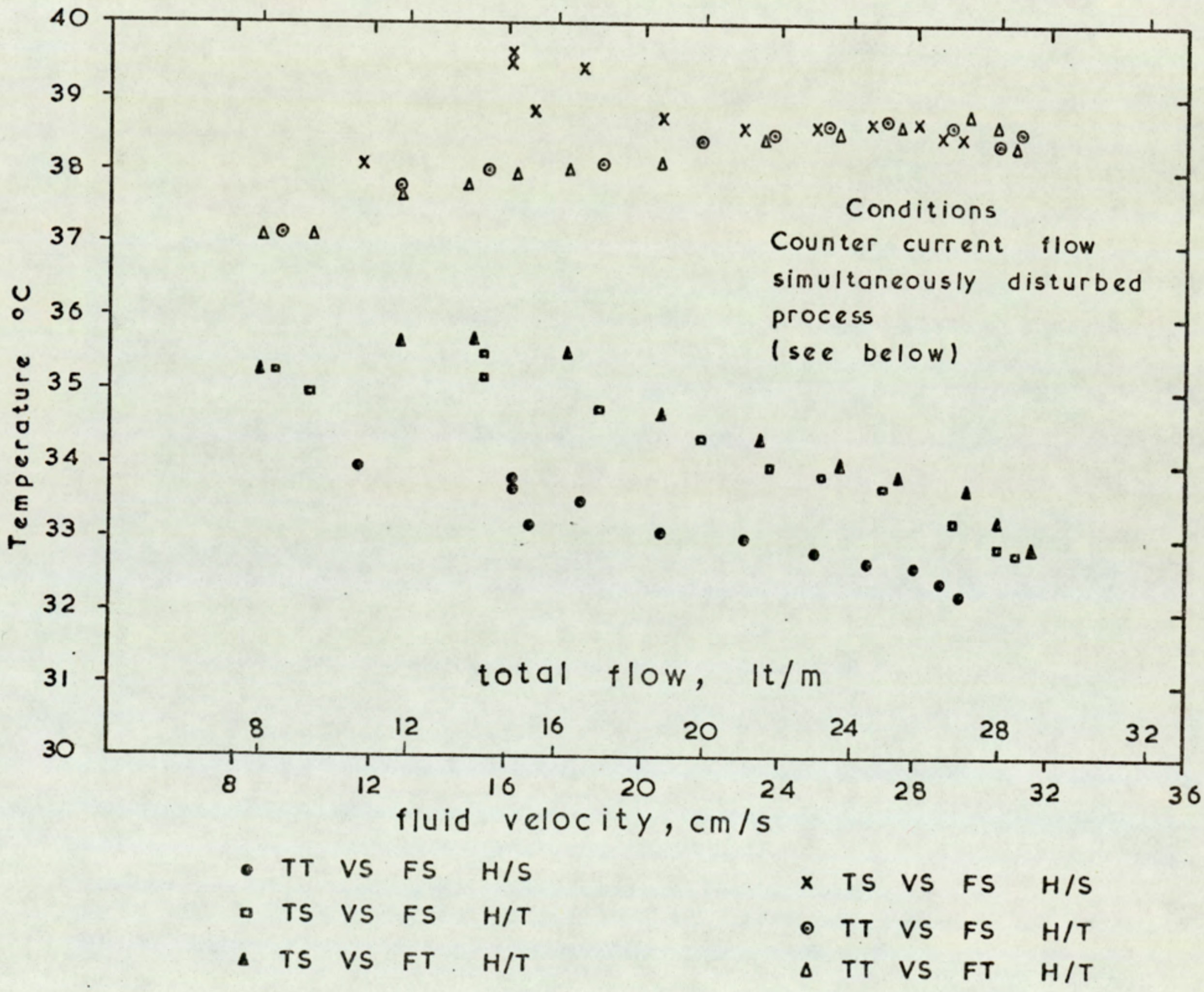

Fig.7.23 Static Gain of the Heat Exchanger in Countercurrent Flow, Expressed as outlet temperatures in Terms of Fluid Velocity, cm/s and total flow, lt/min.

In the data presented h_t was calculated by the Eagle and Ferguson Correlation (equation 4.6) and h_s was calculated by the B.S.R.A. Correlation (equation 4.1).

In the same column, seven, the overall heat transfer coefficient obtained from the heat balance, was presented as U_e, the experimental coëfficient defined by the equation

$$U_e = \frac{Q.A}{\Delta T_{ln}} \qquad (7.3)$$

where ΔT_{ln} is the logarithmic mean temperature difference. The last column of the tables includes the percentage deviation of the calculated overall heat transfer coefficient with respect to the experimental one, and the percentage deviation of the heat throughput expressed as the difference between heat input and heat output of the exchanger with respect to the average of these two values. This last figure is an indication of how adiabatic the process is, since in general such deviation accounts for the heat lost to the environment by convection and conduction, in spite of the insulation used. By inspection of the data it is clear that the runs corresponding to the lowest flow rates show the largest deviations from truly adiabatic operation, because under such conditions any heat lost becomes more significant due to the smaller heat throughput.

It is also noticeable that the countercurrent flow shows smaller deviations than the parallel flow because the logarithmic temperature difference tends to be higher for countercurrent than for parallel flow, other conditions being equal.

The fact that the calculated overall heat transfer coefficient is always smaller than the experimental one, despite no allowance having been made for fouling factors is explained by the boundary layer theory. This states that when a fluid enters a tubular duct, a boundary layer starts to build up around the cylindrical wall as the fluid moves along the pipe until the flow regime, be it laminar or turbulent, is fully developed. Within the length required to attain this regime, called the entry length, the local heat transfer coefficient can be considered proportional to the distance travelled by the fluid from the entry point, l, raised to a negative constant, a, (reference 62).

$$h_e = C.l^{-a} \tag{7.4}$$

This implies that at the entry point h_e has the largest possible value within the heat exchanger and then decreases continuously until the entry length is complete. After this point the value of h_e is constant, as defined by the current correlation. From the expressions given by Foust et al.(31) to evaluate the entry length in the laminar regime,

$$L_e = 0.0575.d_i.N_{Re} \tag{7.5}$$

and in the turbulent regime,

$$L_e = 0.693.d_i(N_{Re})^{0.25} \tag{7.6}$$

it is seen that this parameter has a very wide range of variation for the particular exchanger and conditions used in this work. Furthermore, there is an important gap of information corresponding to the transition region for which no correlation is available. See data given in Table 7.6

The previous considerations lead to the conclusion that the predicted tube heat transfer coefficient is always lower than the actual one because of the contribution of the larger local coefficients in the area within the entry length. Since no prediction could be done for the transition region and considering that the tube coefficient was the determining factor of the value of U_c, it was decided to correct h_t using as criterion the match between U_c and U_e. The coefficient so corrected was used in the dynamic calculations.

N_{Re}	Regime	L_e, cm
120	Laminar	2.5
2100	Lam/Trans.	95.4
10000	Trans./Turb.	5.5
100000	Turbulent	9.7

Table 7.6 Typical Values of Entry Length as a Function of Reynolds Number as Applicable to a Tube of the Heat Exchanger used (d_i = 0.79 cm).

7.5 EXPERIMENTAL TRANSIENT RESPONSE DATA

Figures 7.24 to 7.39, except 7.32, include some of the experimental results for different sets of operating conditions of the heat exchanger described in Section 6.1.1, together with the representation achieved by the model introduced in Section 5.2.3.1.

The data include eight examples of response to step changes (Figs. 7.24 to 7.31) and eight examples of response to sinusoidal changes (Figs.7.33 to 7.39). They further include nine cases of single variable operation (Figs.7.24 to 7.26 and 7.33 to 7.37), and seven cases of double variable operation (Figs. 7.27 to 7.31 and 7.38 to 7.39). Four runs were made with the reduced surface of the heat exchanger as explained during the description of the equipment.

In order to help in the explanation of the real system behaviour, it is useful to resort to Appendix "C" which shows the error introduced in the model when the effect of fluid velocity on the individual heat transfer coefficient is linearised by the binomial expansion (see equations 4.41 and 4.42). As is clear from the graph in the Appendix, the error is a function not only of the magnitude of the velocity deviation but also of the constant n affecting the Reynolds Number in the heat transfer correlation. On the other hand the errors are always positive regardless of the sign of the deviation and the curves are very asymetric with respect to the zero deviation point, so that the progressive negative deviations produce errors growing with increasing speed, and as the deviation tends to -1.0 the error tends to infinity. The positive deviations, however, produce a moderate, almost constant increase in the error for deviations even larger than 1.0, though the mathematical foundation of the expansion restricts the deviation magnitude to less than 1.0 in order to warrant convergence.

The effect of these errors on the overall performance of the heat exchanger has to be sought in the overall heat transfer coefficient (equation 7.2), the more significant effect on this being from the changes in the limiting individual heat transfer coefficient.

Besides the error introduced by the linearisation of the disturbance effect on the heat transfer coefficients, the model includes other errors such as the one introduced by assuming the viscosity of the fluid constant at the mean point temperature of each side in the initial steady state condition, and the obvious one produced by neglecting the diffusion term. The experimental profile, on the other hand, carried all the significant errors from the sources mentioned in chapter six, so that in some of the runs presented there is considerable divergence between the predicted and the actual results (Figs.7.24, 7.27, and 7.39). This fitting refers mainly to the levels of the initial and final steady states.

For the transient section of the response the quality of the fitting depends on the accuracy with which the ancilliary elements of the system are represented. The only one introduced into the model was, as mentioned before, the control valve represented by a critically damped system as shown before in Fig.7.20, with a characteristic time of 1.3 seconds. In consequence most of the step change examples present four different predictions identified by L, according to the following definitions:

L = 0, linearised disturbance and no valve effects

L = 1, exact disturbance and no valve effects

L = 2, linearised disturbance plus valve dynamics

L = 3, exact disturbance plus valve dynamics.

From the results it is clear that the introduction of the valve dynamics improved the quality of the prediction in the transient region of the response as shown in the step change tests for both single variable and double variable conditions. It also indicates that different characteristic times instead of the unique value used for all the cases in which the valve dynamics was included might have improved the representation.

A close inspection of the response when the temperature started to move away from the steady state suggests that some 'channelling' of the fluid in the mixing chambers of the exchanger took place, since when the time lag was subtracted from the tube response, this curve partially overlapped the predictions which included the valve response. This effect was more significant in the experiments with the reduced surface of the heat exchanger where the 'active' tubes were placed at the center of the bundle and therefore the conditions for channelling were more appropriate (Figs.7.29 to 7.31). In the case of the shell responses the time lag was so small that its contribution to the measured response was ignored. It must be noticed at this stage that the transportation lag changes for the side in which the flowrate perturbation is produced, at a rate that is inversely proportional to the change of velocity and therefore the flowrate used to calculate the transportation lag must be that corresponding to the final steady state.

Not all the responses agree with the predictions in the initial point. This is because, as seen in Fig.7.32, the initial point of the transient response corresponds to the last point of the initial steady state profile, predicted in the algorithm by the analytical solution of the model. Any deviation produced in this calculation is carried forward during the successive calculations (profiles 1 to 7 in the previous figure) in the transient state, until the final steady state is reached.

It is noteworthy that most of the tests with sinusoidal disturbances gave a closer fit than those with step changes, except the one of Fig.7.39, which shows a very large deviation in amplitude, attributable to the very large amplitude of the disturbance. The peak-to-peak amplitude of the sinusoidal perturbations in this case were 82.86% and 84.7% for the tube

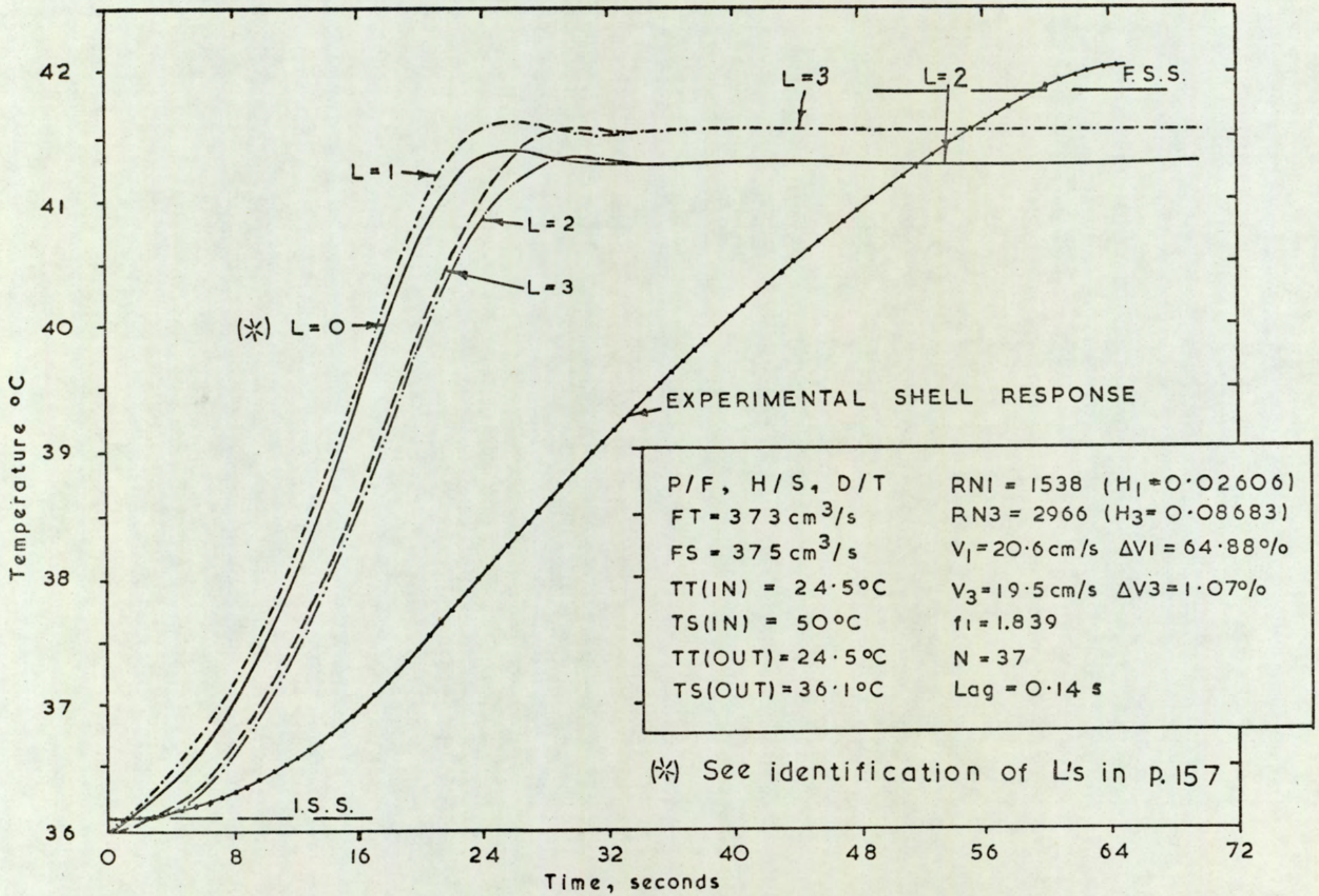

Fig.7.24 Effect of the Velocity - h.t.c. Relationship and the Control Valve Dynamics on the Shell Outlet Temperature Response, Case of P/F, H/S, D/T.

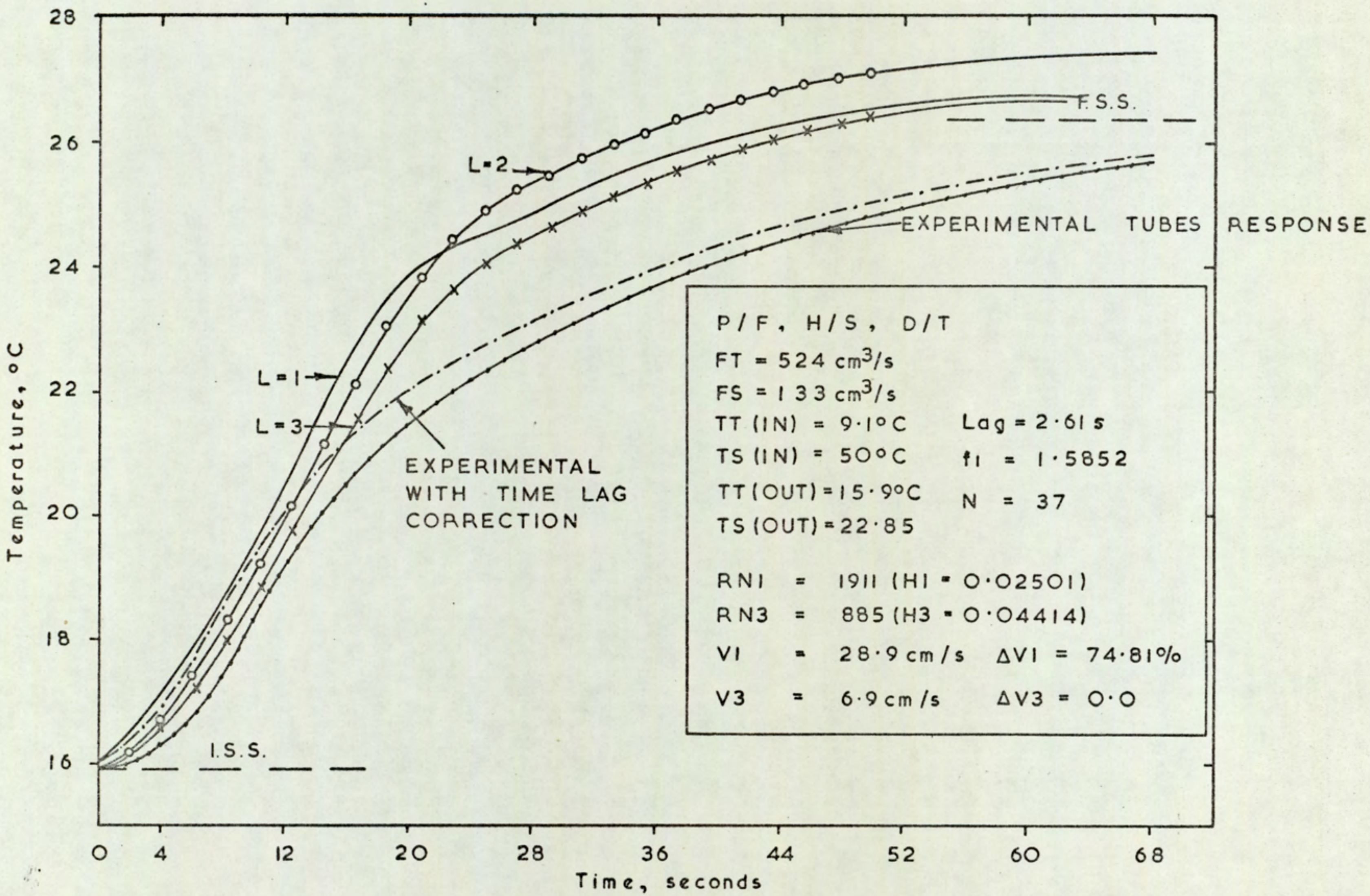

Fig.7.25 Effect of the Velocity - h.t.c. Relationship and the Dynamics of the Control Valve on the Tube Outlet Temperature Response, case of P/F, H/S, D/T.

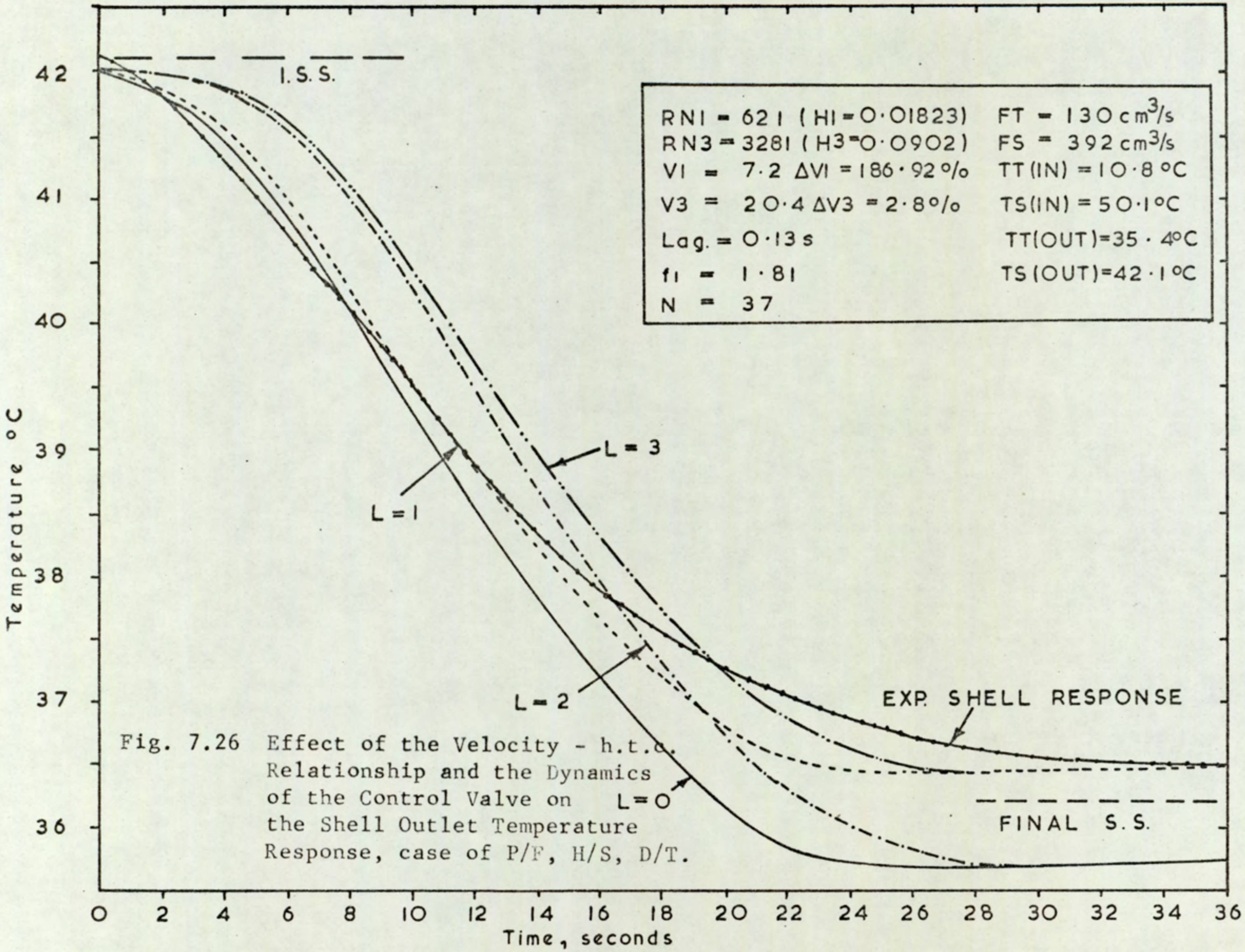

Fig. 7.26 Effect of the Velocity - h.t.c. Relationship and the Dynamics of the Control Valve on the Shell Outlet Temperature Response, case of P/F, H/S, D/T.

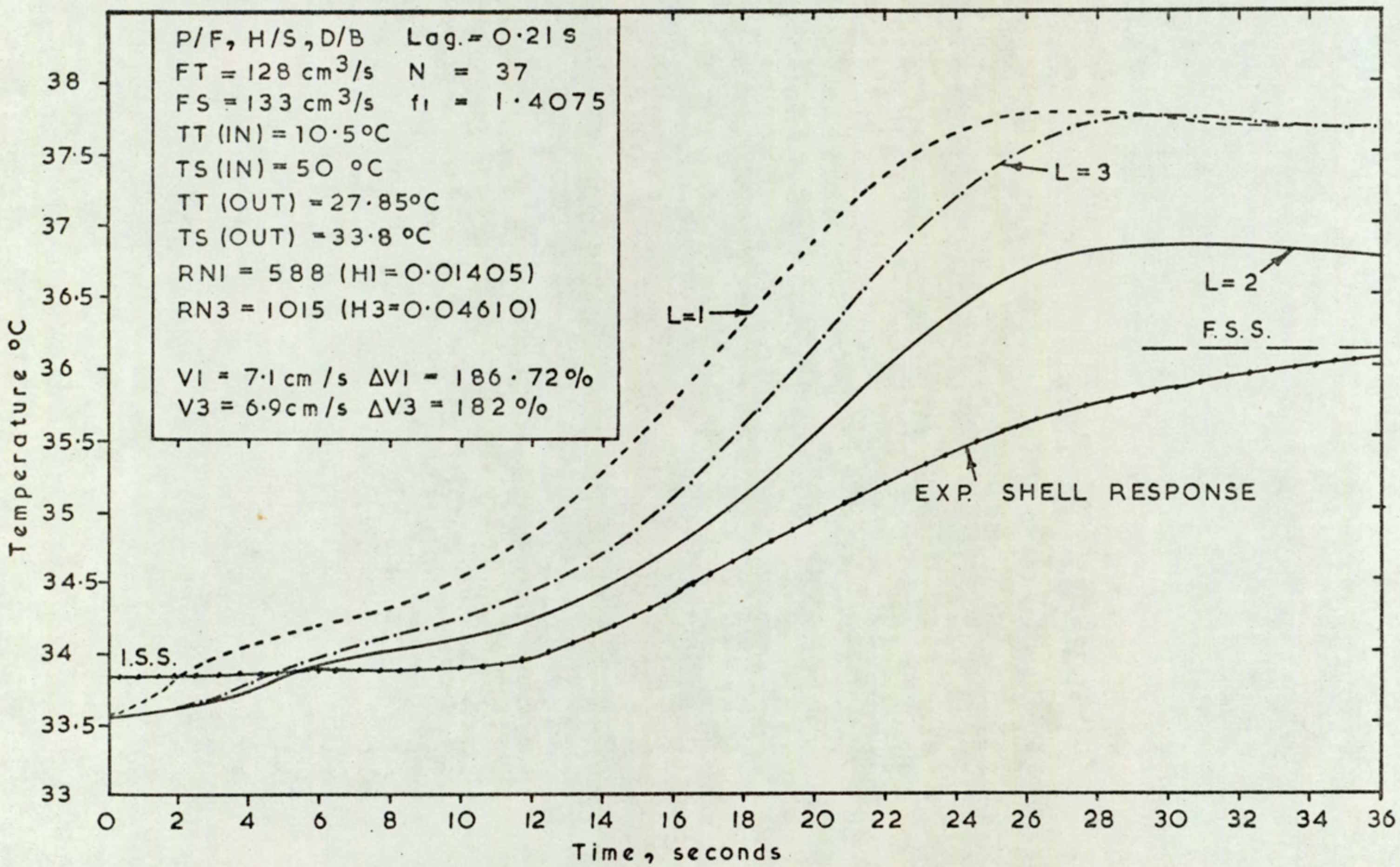

Fig. 7.27 Effect of the Velocity - h.t.c. Relationship and the Dynamics of the Control Valves on the Shell Outlet Temperature Response, Case of P/F, H/S, D/B.

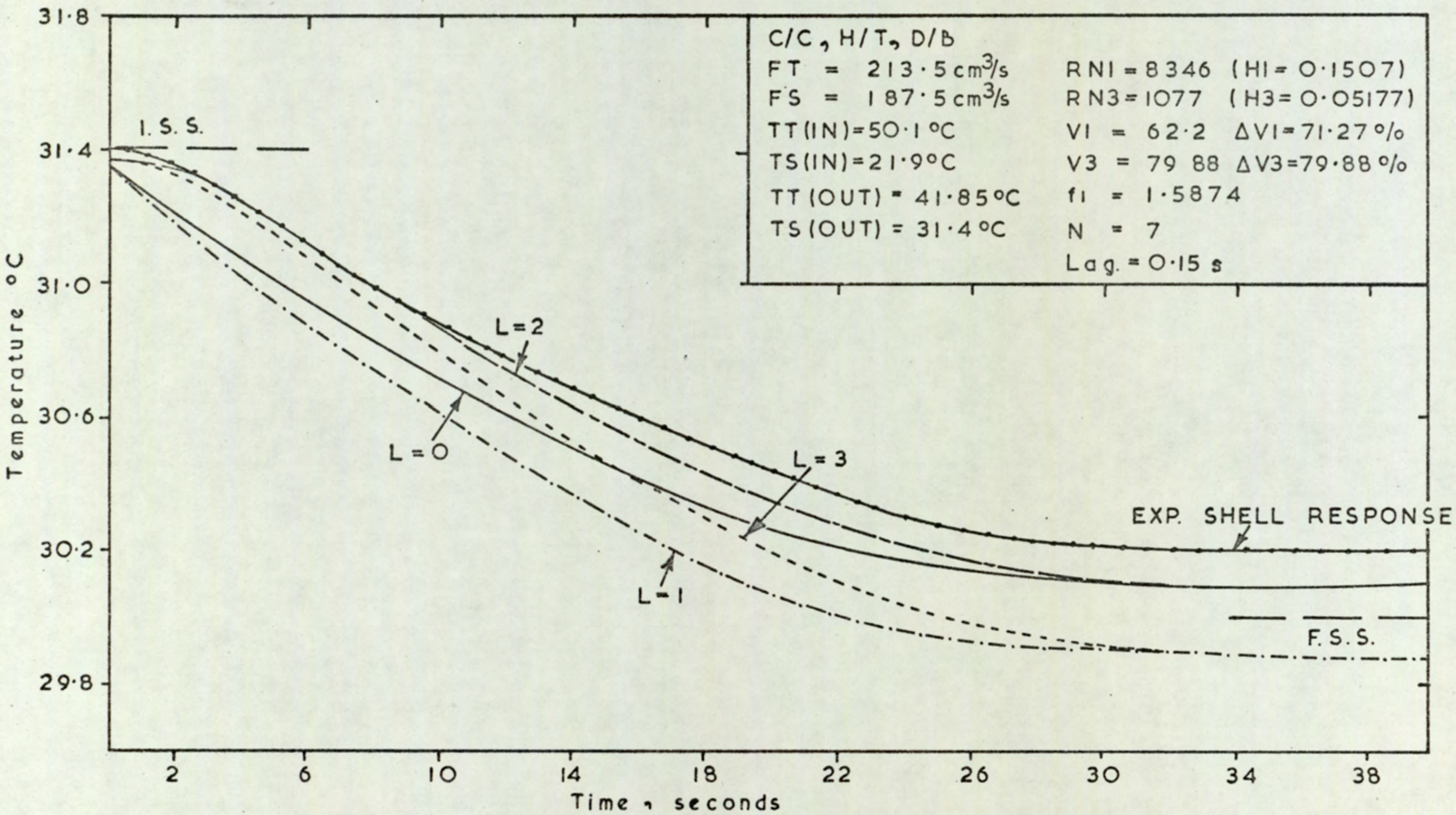

7.28 Effect of the Velocity - h.t.c. Relationship and the Dynamics of Control Valve on the Shell Outlet Temperature Response, Case of C/C, H/T, D/B.

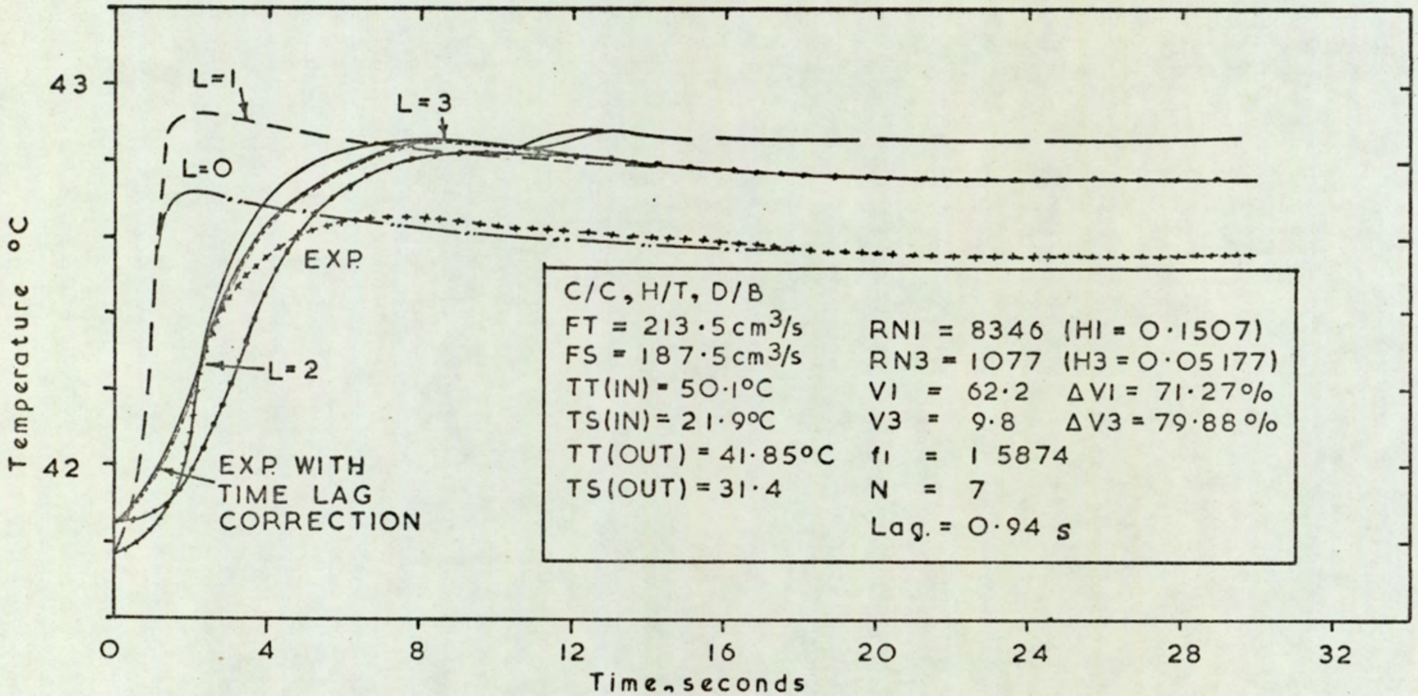

Fig.7.29 Effect of the Velocity - h.t.c. Relationship and the Control Valve Dynamics on the Tubes Outlet Temperature Response, case of C/C, H/T, D/B.

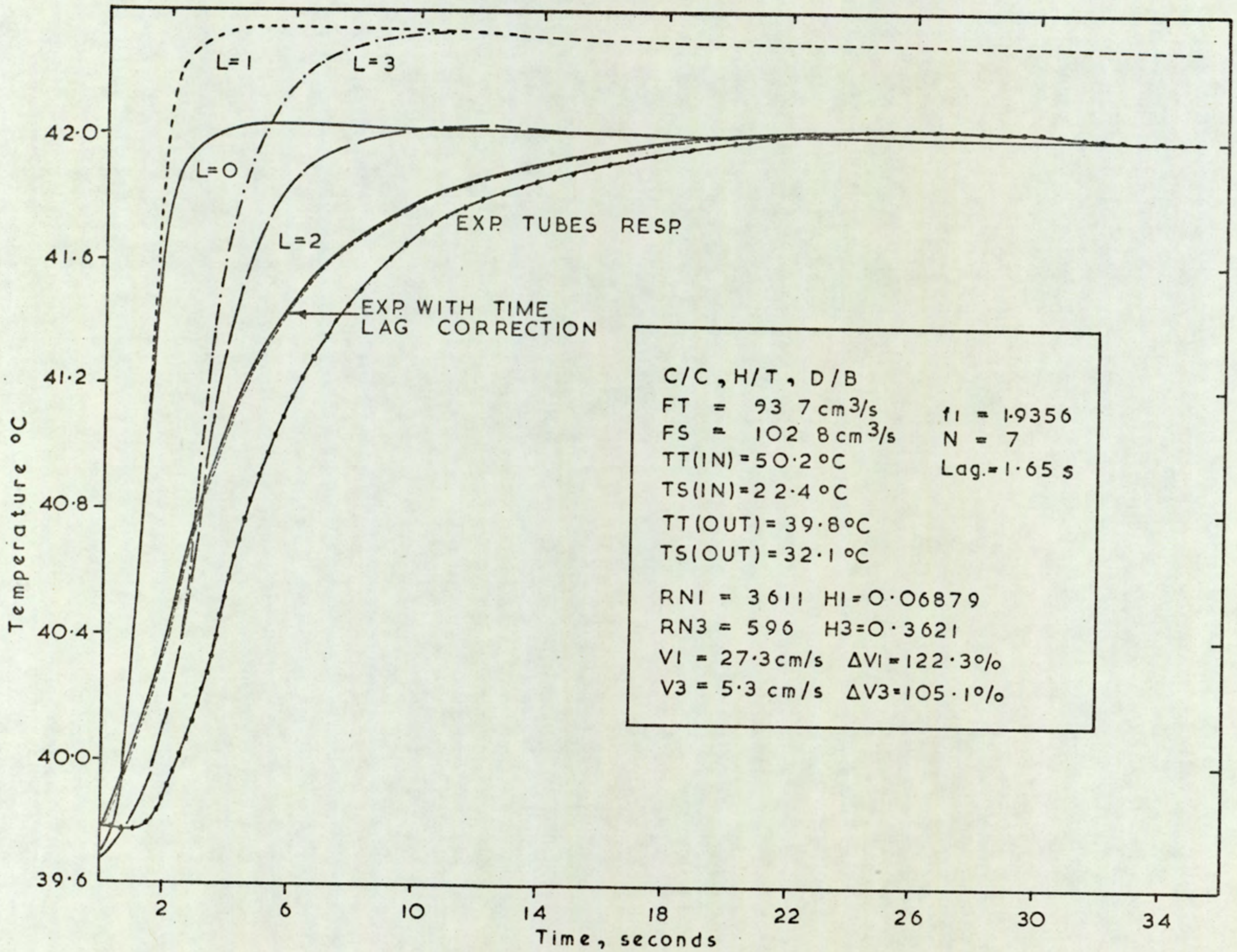

Fig.7.30 Effect of Velocity - h.t.c. Relationship and Control Valve Dynamics on the Tubes Outlet Temperature Response, case of C/C, H/T, D/B.

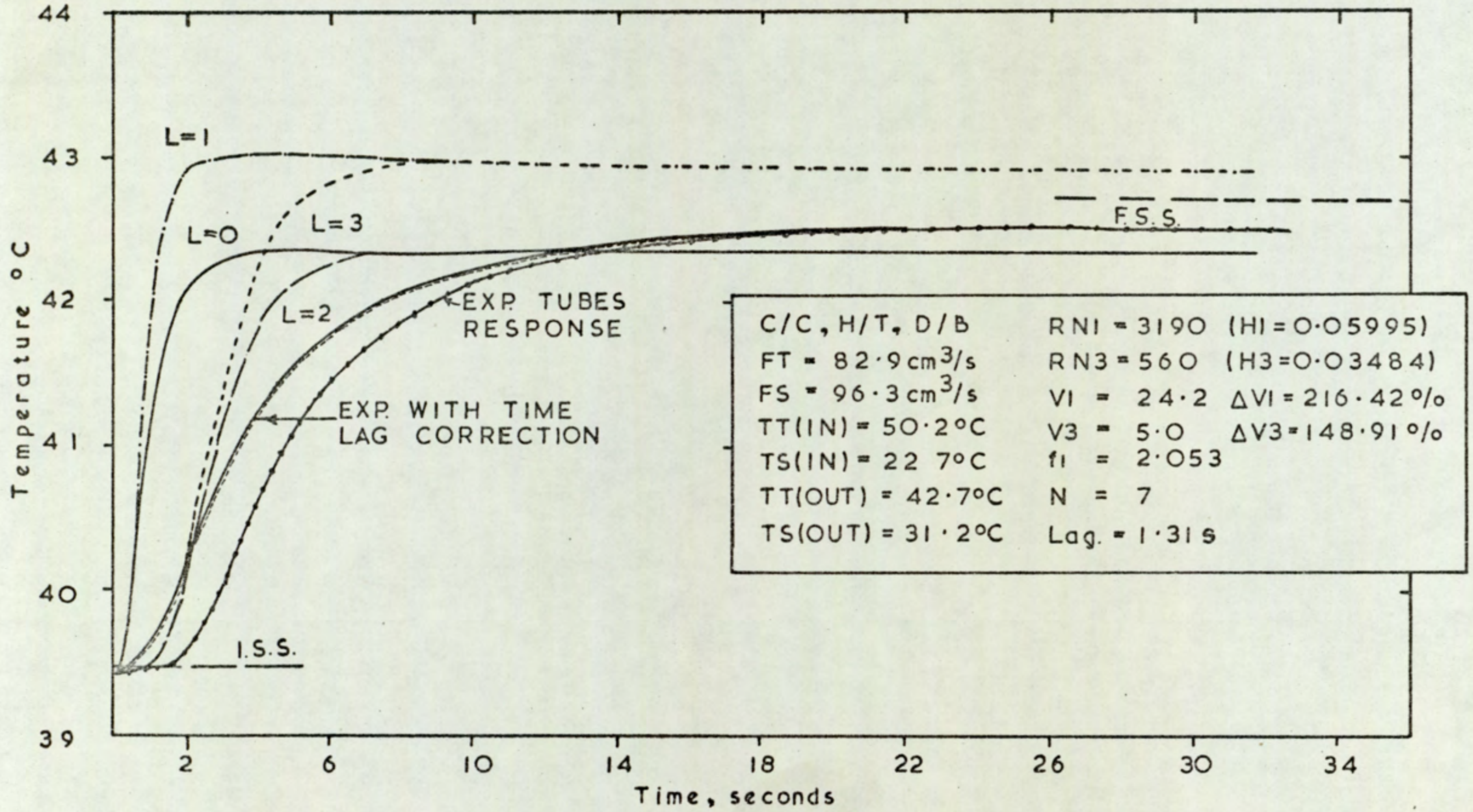

Fig. 7.31 Effect of Velocity - h.t.c. Relationship and Control Valve Dynamics on the Tubes Outlet Temperature Response, Case of C/C, H/T, D/B.

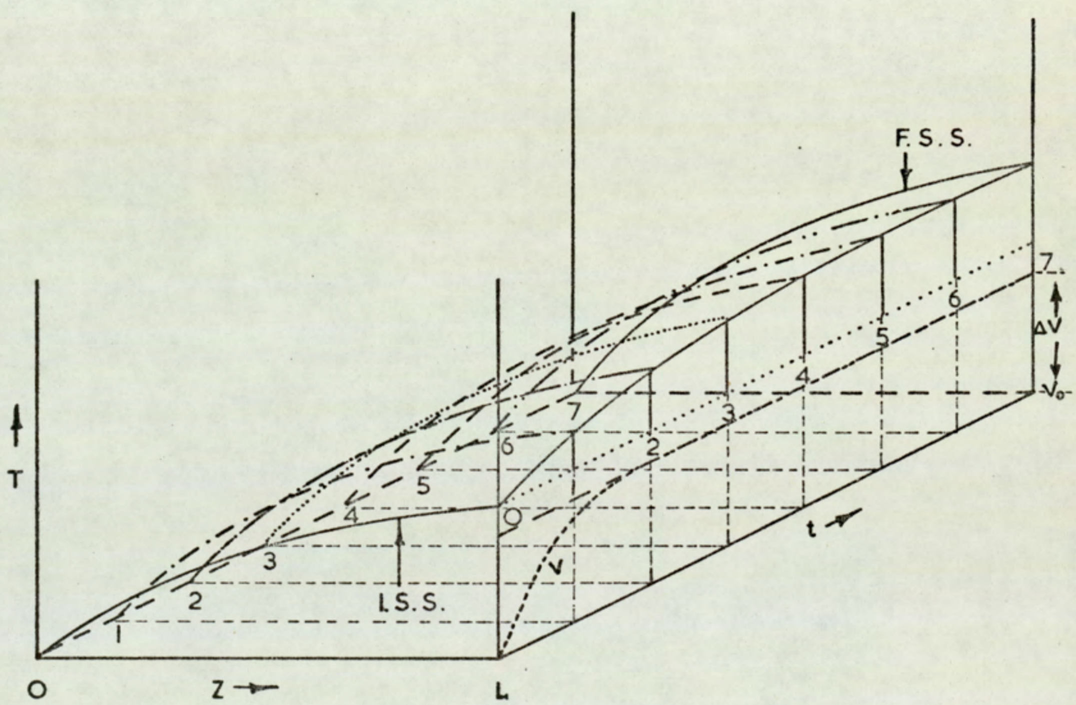

Fig. 7.32 Scheme Showing Several Temperature Profiles in the Temperature-Distance-Time-Space During the Transient Response of the Heat Exchanger to a Step Change Disturbance of one Fluid Velocity.

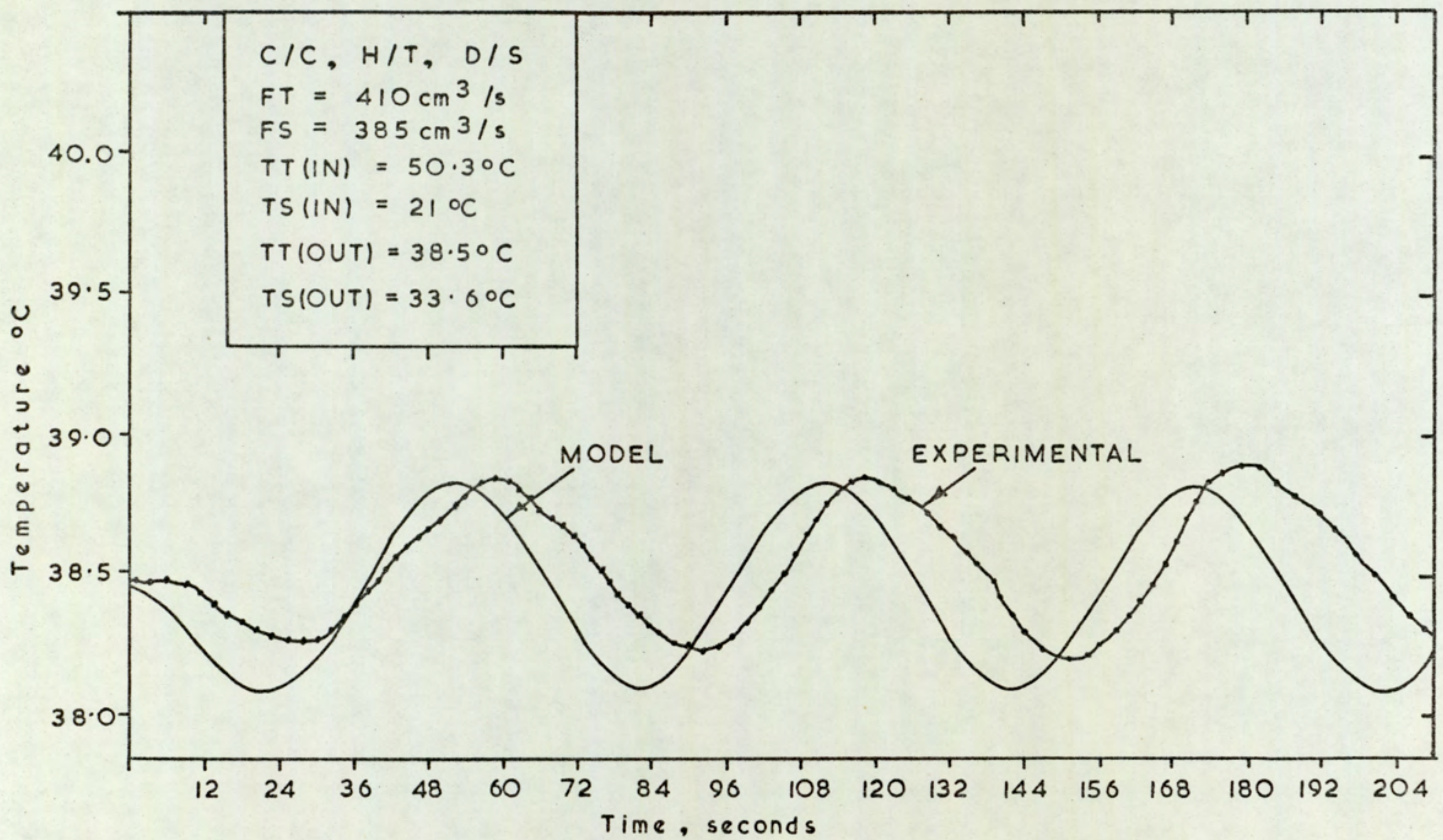

Fig. 7.33 Tubes Temperature Response to Sinusoidal Disturbance in Shell Flow Velocity (Freq. = 1.0 cpm).

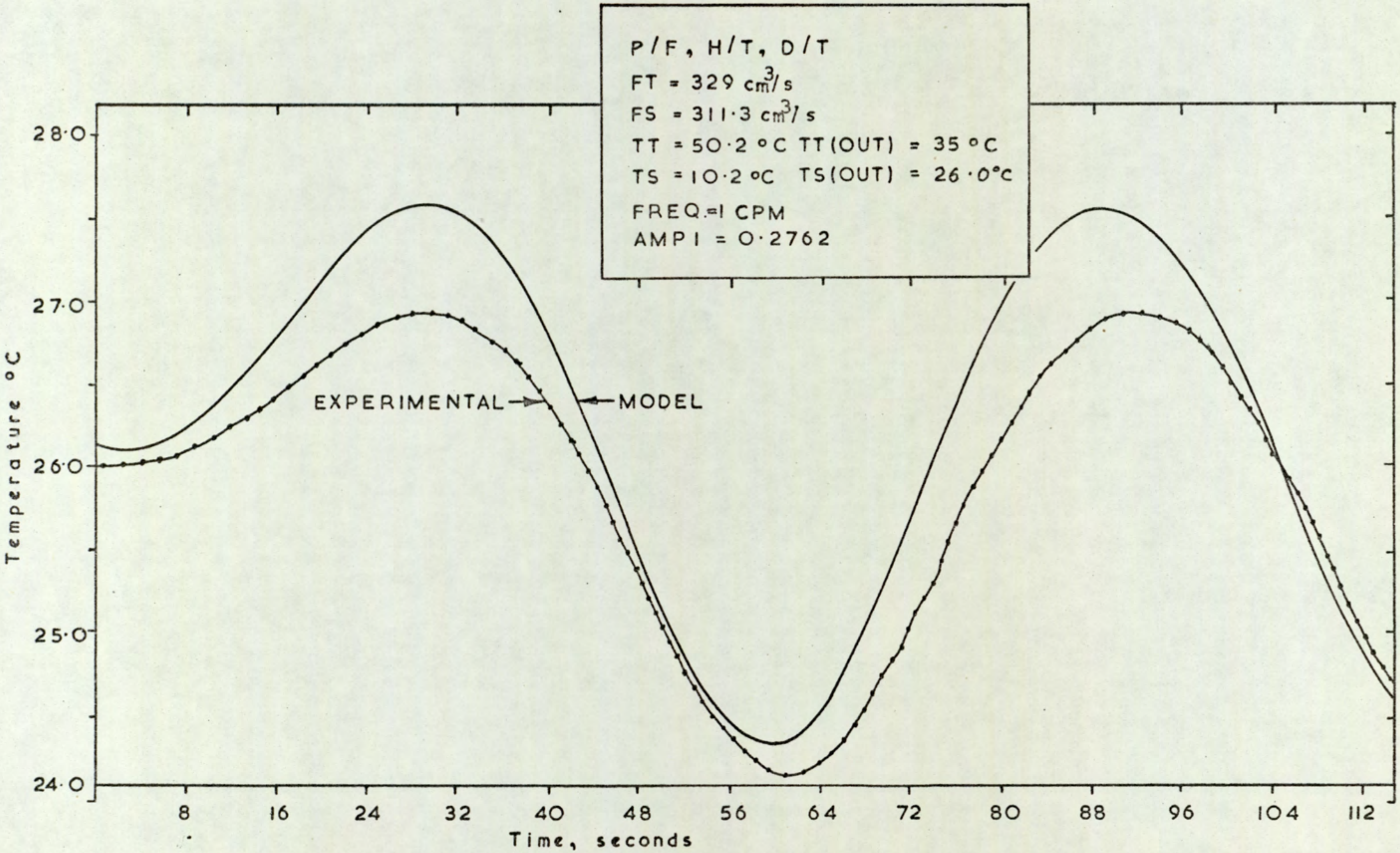

Fig.7.34 Output Shell Temperature Response to a Sinusoidal Disturbance in Tubes Flow Velocity (freq.= 1cpm).

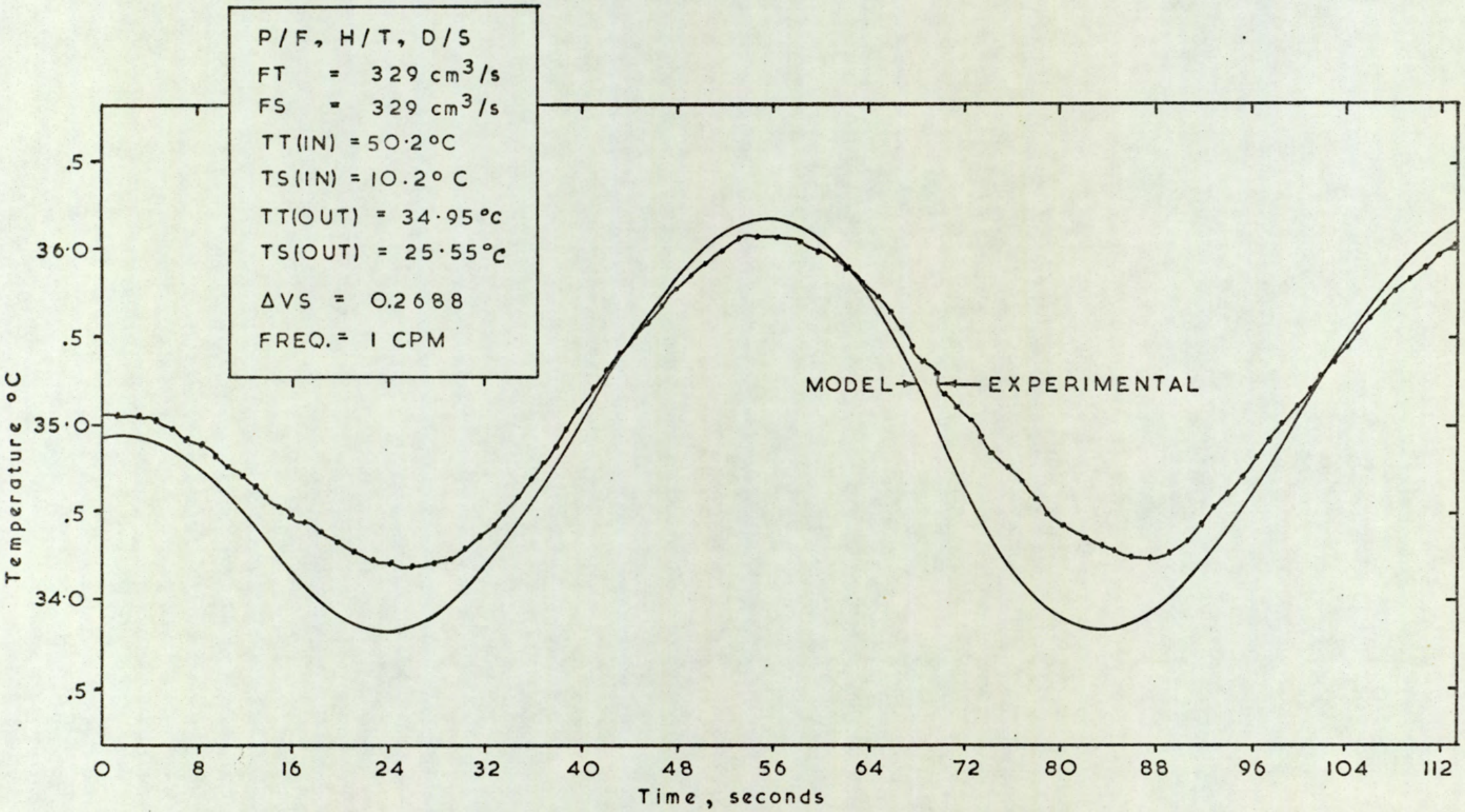

Fig.7.35 Tubes Temperature Response to a Sinusoidal Disturbance in Shell Flow Velocity (Freq. = 1 cpm).

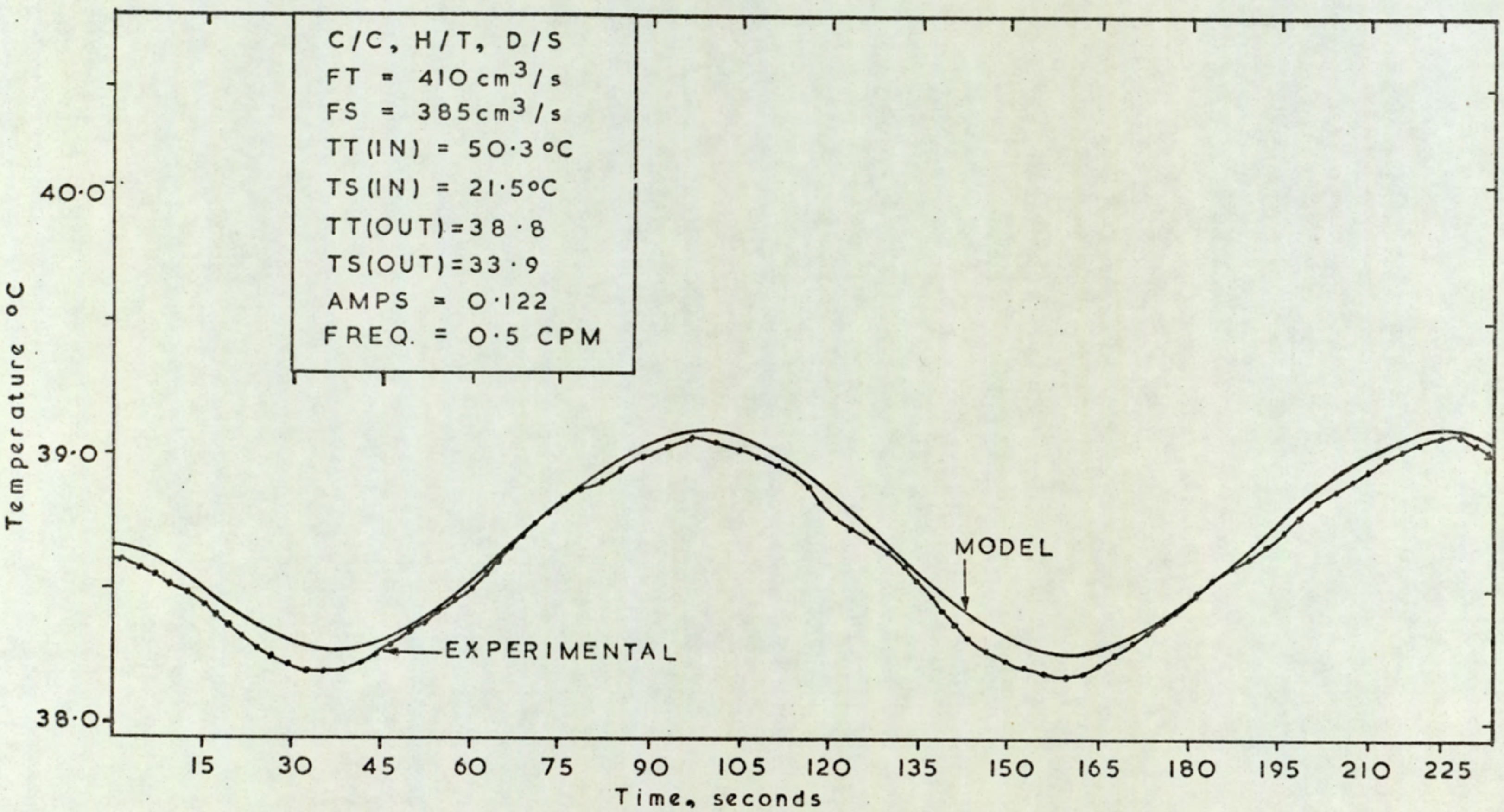

Fig. 7.36b Tube Temperature Response to a Sinusoidal Disturbance in Shell Flow Velocity (Freq.= 0.5 cpm).

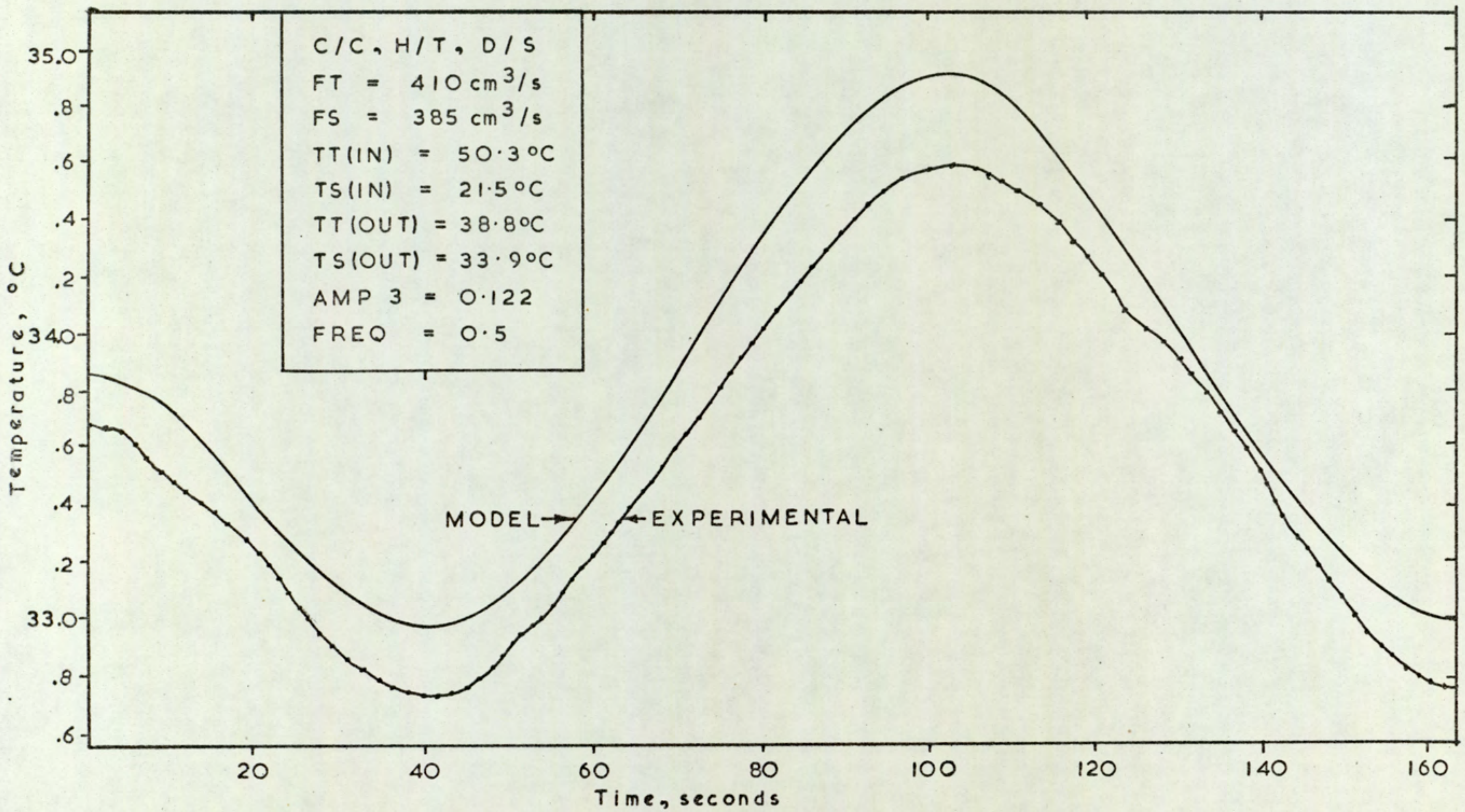

7.36b Shell Temperature Response to a Sinusoidal Disturbance in Shell Flow Velocity (Freq. = 0.5 cpm).

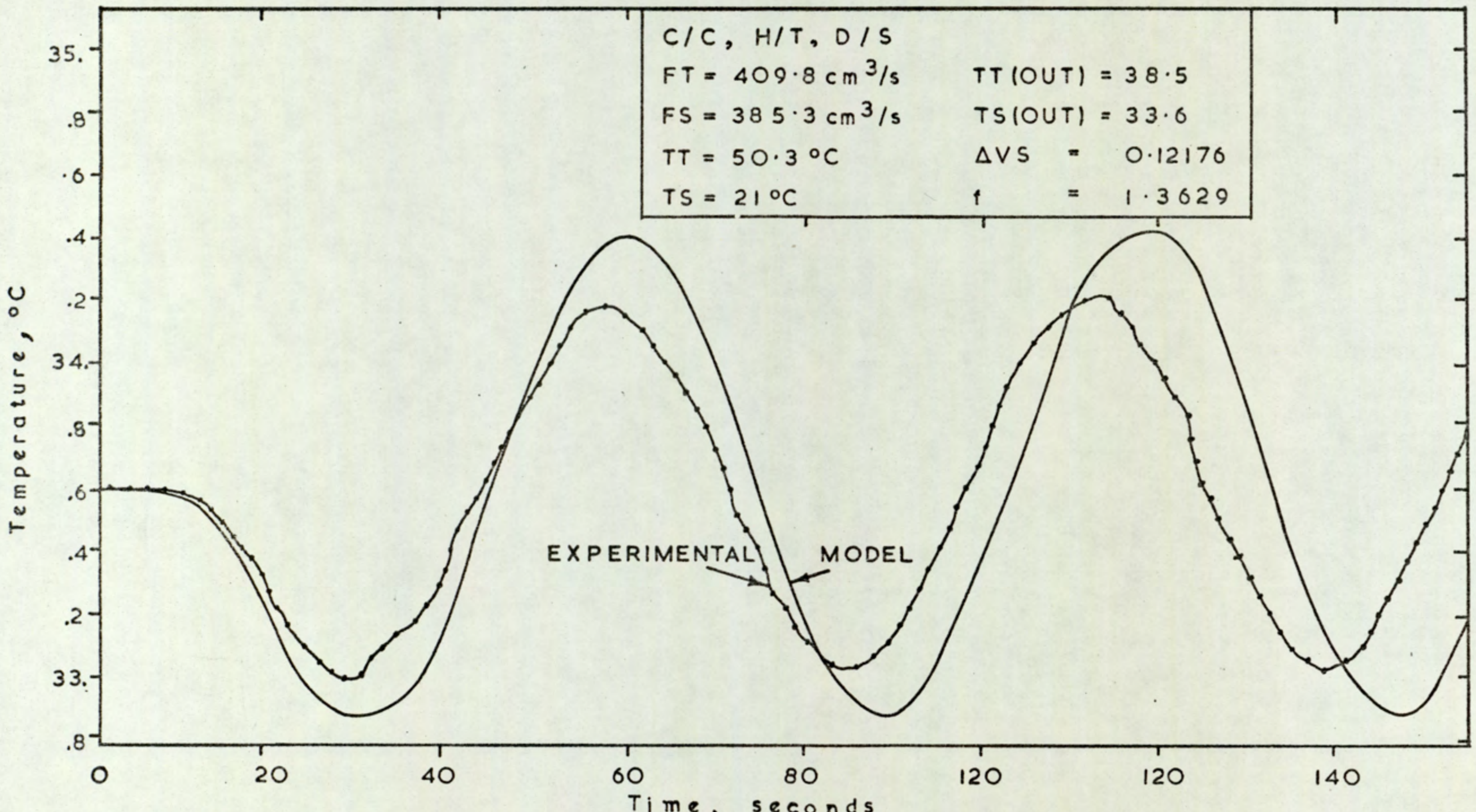

Fig.7.37 Shell Temperature Response to a Sinusoidal Disturbance in Shell Fluid Velocity (Freq. = 1 cpm).

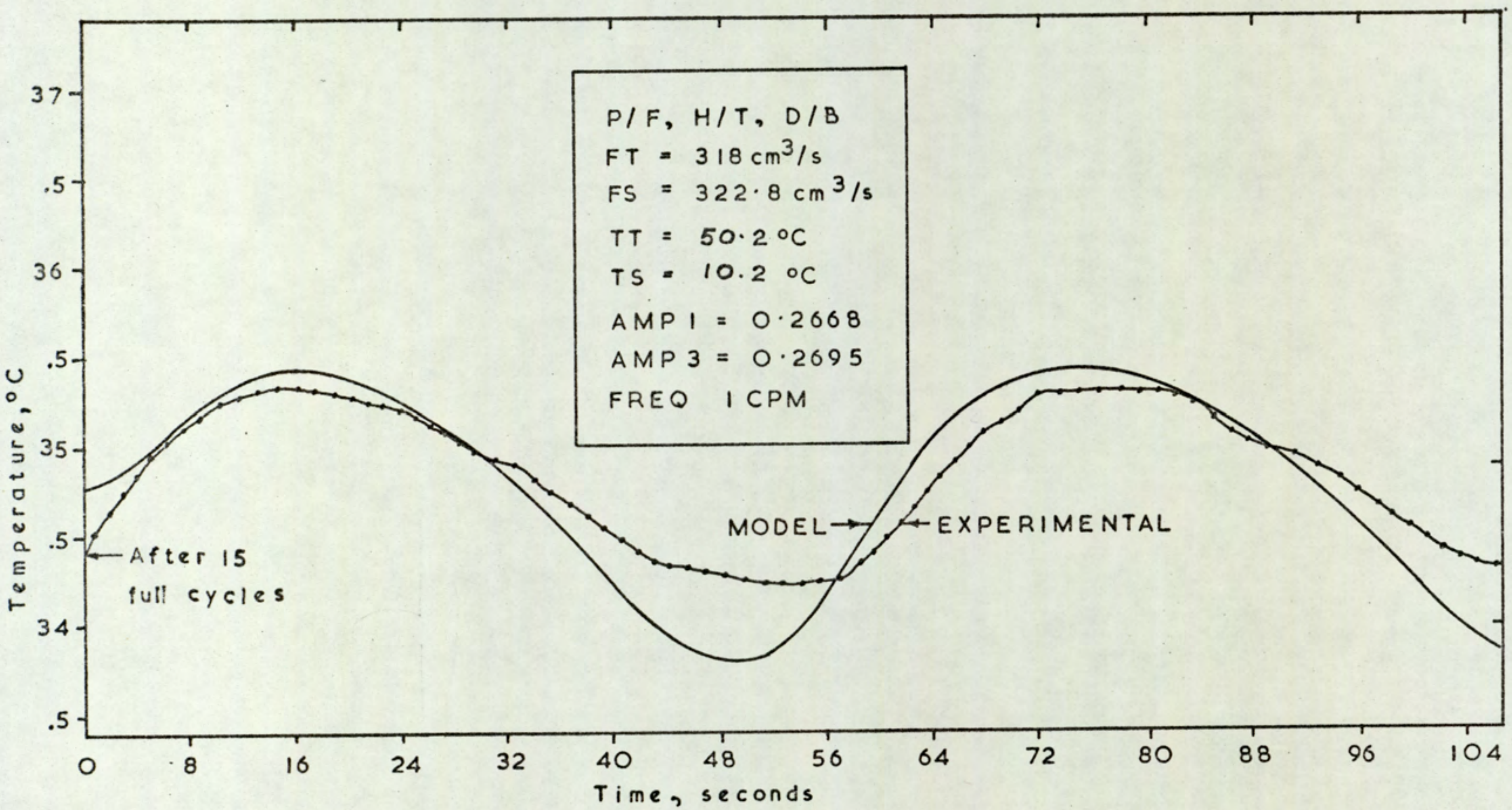

Fig. 7.38 Tubes Temperature Response to Sinusoidal Disturbances in Both Velocities (Freq. = 1 cpm). Notice in the first 15 seconds how the predicted transients differ from the experimental quasi steady state.

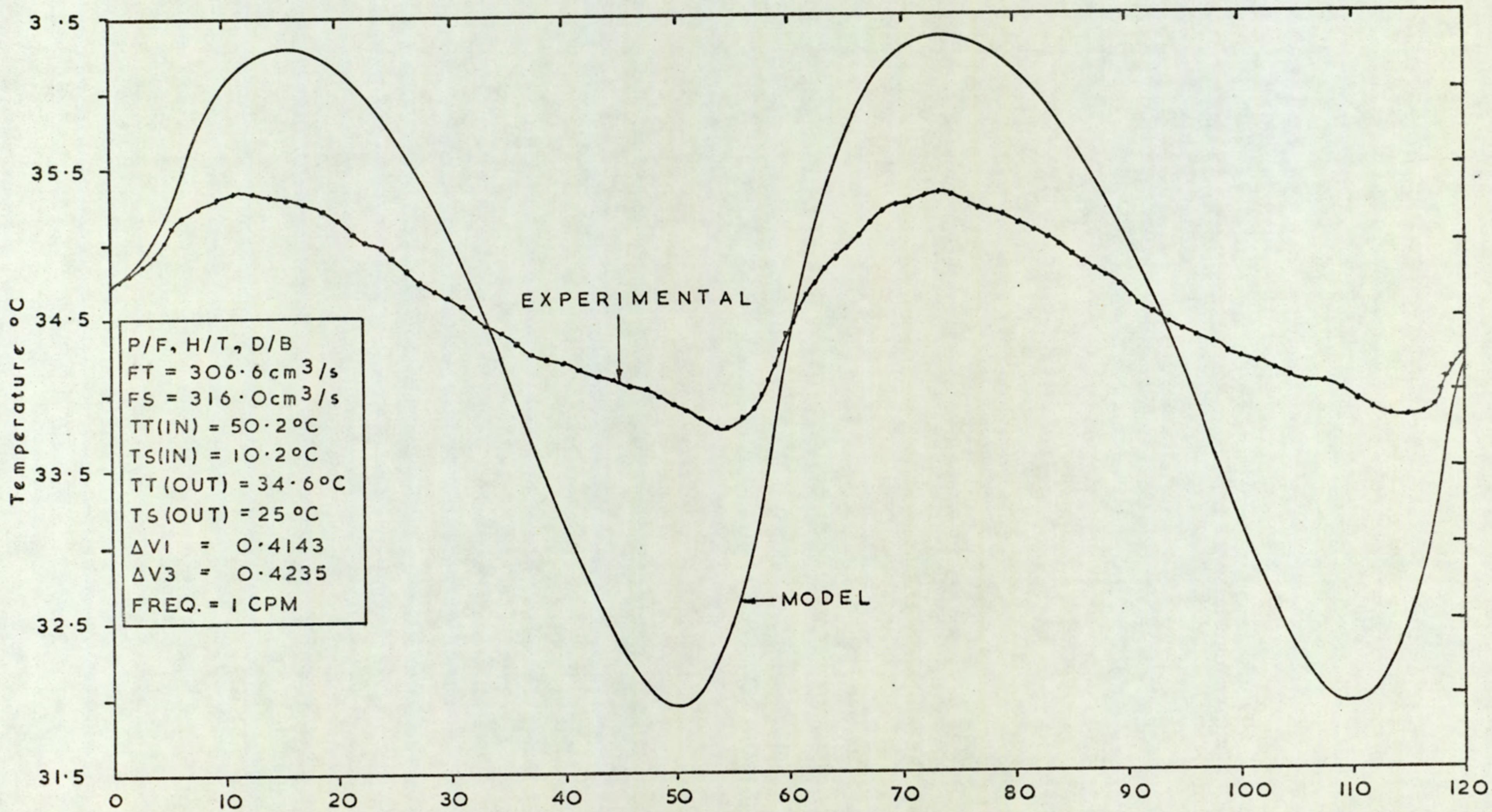

Fig.7.39 Tubes Temperature Response to Simultaneous Sinusoidal Disturbances in Both Fluid Velocities (Freq.= 1 cpm).

and shell flow rates, respectively.

In all other cases the fit was the better the lower the frequency of the oscillations because of the relatively smaller effect of the transportation lag on the response. On that basis the time lag was not subtracted from either of the cyclic responses.

There is, however, in some runs (Figs.7.33 and 7.37) a gradual drift of the prediction from the experimental results, along the time axis. The analysis led to the conclusion that either the frequency of the input signal, from the function generator, or the speed of the recorder were slightly different from the value used in the calculations and therefore the prediction and the experimental curves tended to diverge as time went on.

7.6 EXPERIMENTAL FREQUENCY RESPONSE DATA

The output temperatures from frequency response data are presented in Figs.7.40 to 7.63. It is basically composed of Bode diagrams-normalised gain plot (even numbered figures) and phase angle plots (odd numbers) - for the twelve possible sets of conditions found by combination of the two flow orientations (parallel and countercurrent) with the two process schemes (heating, H/S or cooling, H/T) and the three origins of the disturbances (in the tube flow, D/T, in the shell flow, D/S, or simultaneously in both flows, D/B). Most of the data were taken by conventional sinusoidal perturbation of the system followed by consecutive recording of the output temperatures, once the transient response had died out. The reference amplitude used to normalise the gain data was the one corresponding to the longest period in each test, usually at about 0.01 radians per second. In some tests this normalisation proved to be practically equal to the normalisation with amplitudes of lower frequency and therefore comparable with the model which was normalised with amplitudes of 0.001 radian per second.

In a very few instances the measured input signal was the air pressure on the diaphragm of the control valves. For these cases the frequency response of the control valves was subtracted from the data collected; in the rest of the cases the lift of the valve stem was measured as the input signal so that no subtraction was necessary. In all the data reported, however, the phase delay produced by the transportation lag of the signal between the point where the liquid leaves the tube bundle and the point where it reaches the thermopile was subtracted from the measured phase lag. This subtraction was substantially larger for the tube side than for the shell side because of the contribution of the mixing chambers at the ends of the tube bundle.

The total liquid hold up accounting for transportation lag in the tube side was 344 cm^3 and in the shell side was only 52 cm^3. Based on the previous considerations, the data reported represents solely the heat exchanger behaviour. To facilitate comparison, the data was organised in a way that results corresponding to a test for simultaneous disturbances are placed between the results corresponding to test for single tube flows and single shell flow disturbance. Though conditions are not exactly the same, they are comparable.

The first comment to be made on the data as a whole is that the fit between experimental results and the predictions of the model are only fair in some cases and poor in others. This fact does not preclude further analysis of the results in an effort to understand something more of the dynamics of the heat transfer process in the low Reynolds number region.

From the close study of the data, it is evident that the experimental information consistently showed the same trends and relationships for both types of processes, and so did the model representation.

While all predictions indicated resonance regions, very strong for both gain and phase angle of the tube response, and rather small and smooth for the shell response, the experimental data did not, partially because the frequency at which the first resonance dip appeared in the model, around one radian per second, was near to the upper limit of the experimental range. Beyond that the resolution of the recorders was obscured by noise and drift, enhanced by the increased gain of the instruments so that no reliable data could be obtained. In the tests in which the experimental results went beyond the frequency of the first predicted resonance dip, no significant deflection attributable to resonance was fully evident, though some indication of that effect seems to be shown in Figs.7.44, 7.54 and 7.58.

This is not surprising, however, because several workers have reported before that heat exchangers with multi-tube bundles tend to wash out the resonance effect(25, 42). A plausible explanation of it is that since each tube has within the shell a position which is almost unique, except by conditions of axial symmetry, during the operation the temperature and velocity profiles of each tube vary from being slightly different, to being very different from each other, with the result that after the mixing chamber the signal measured is free from the extreme values which can otherwise develop in individual tubes.

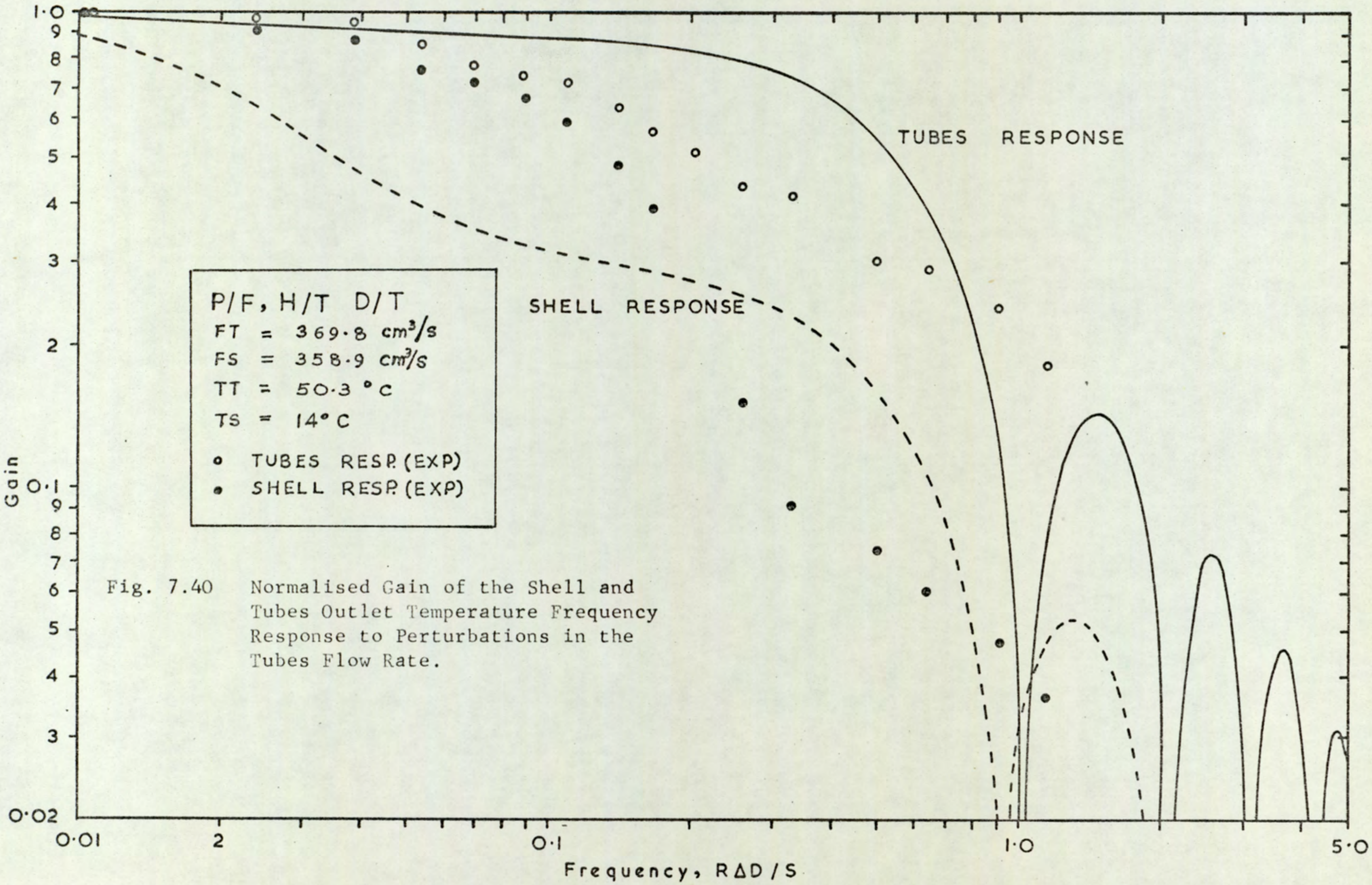

Fig. 7.40 Normalised Gain of the Shell and Tubes Outlet Temperature Frequency Response to Perturbations in the Tubes Flow Rate.

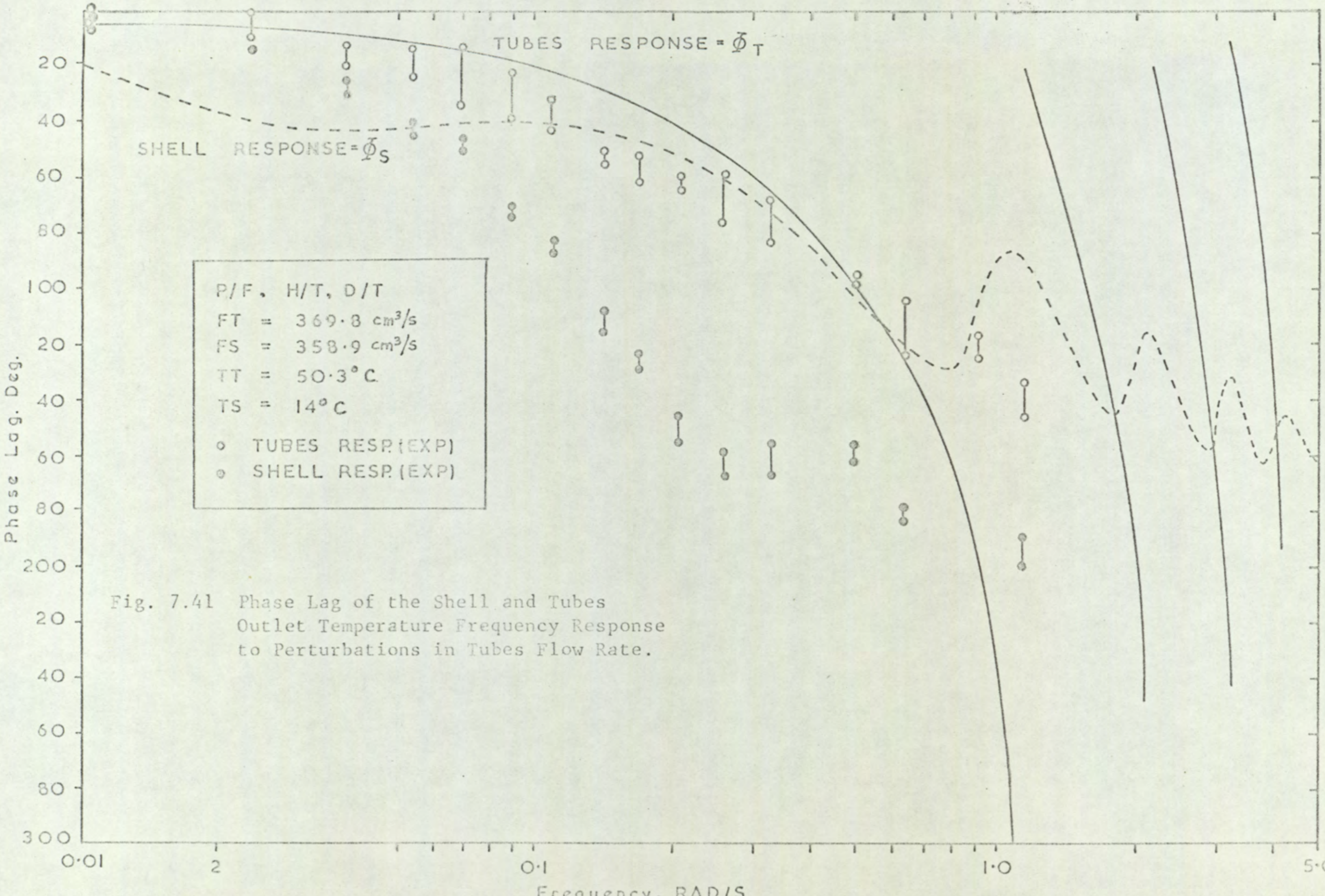

Fig. 7.41 Phase Lag of the Shell and Tubes Outlet Temperature Frequency Response to Perturbations in Tubes Flow Rate.

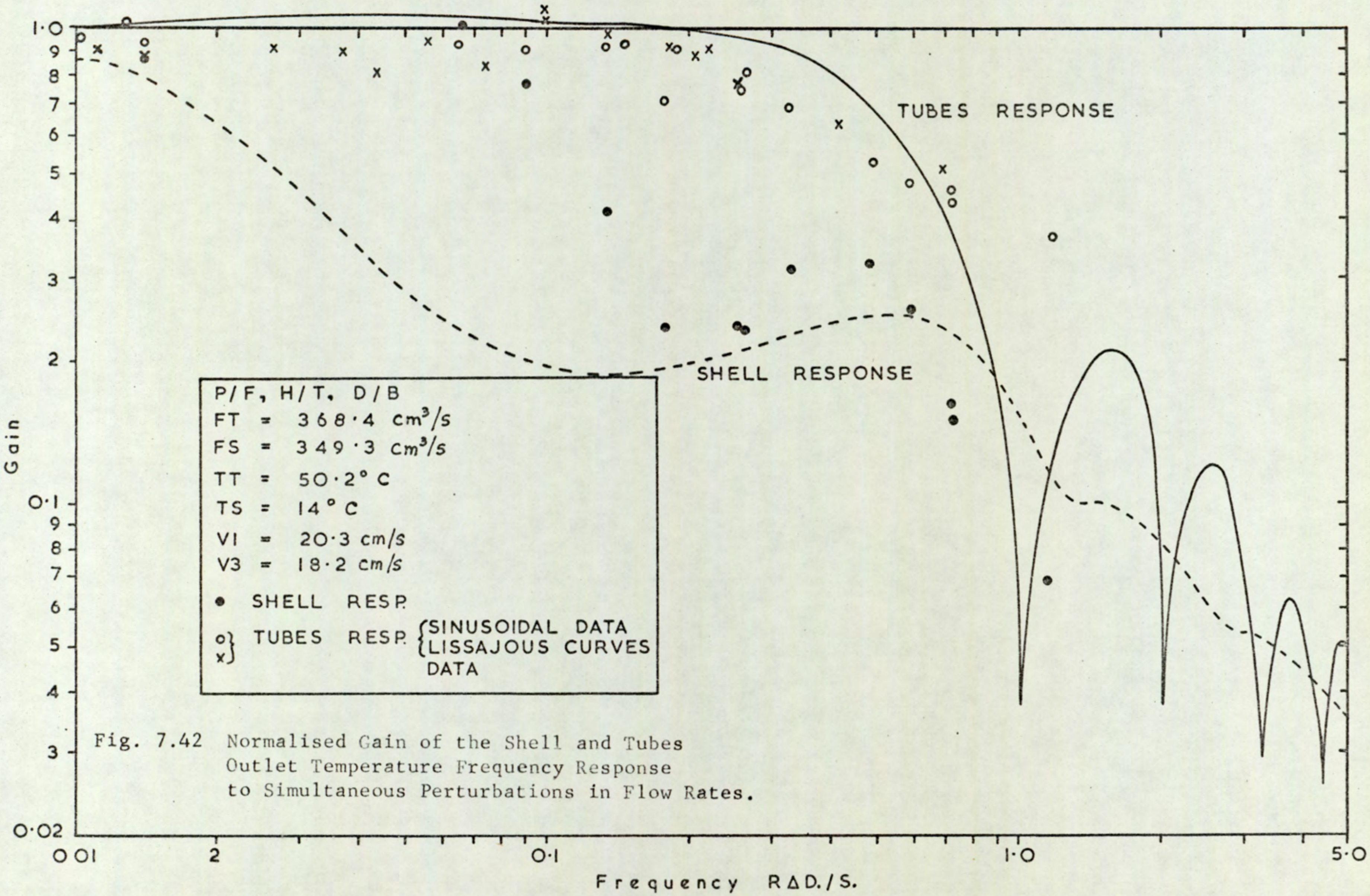

Fig. 7.42 Normalised Gain of the Shell and Tubes Outlet Temperature Frequency Response to Simultaneous Perturbations in Flow Rates.

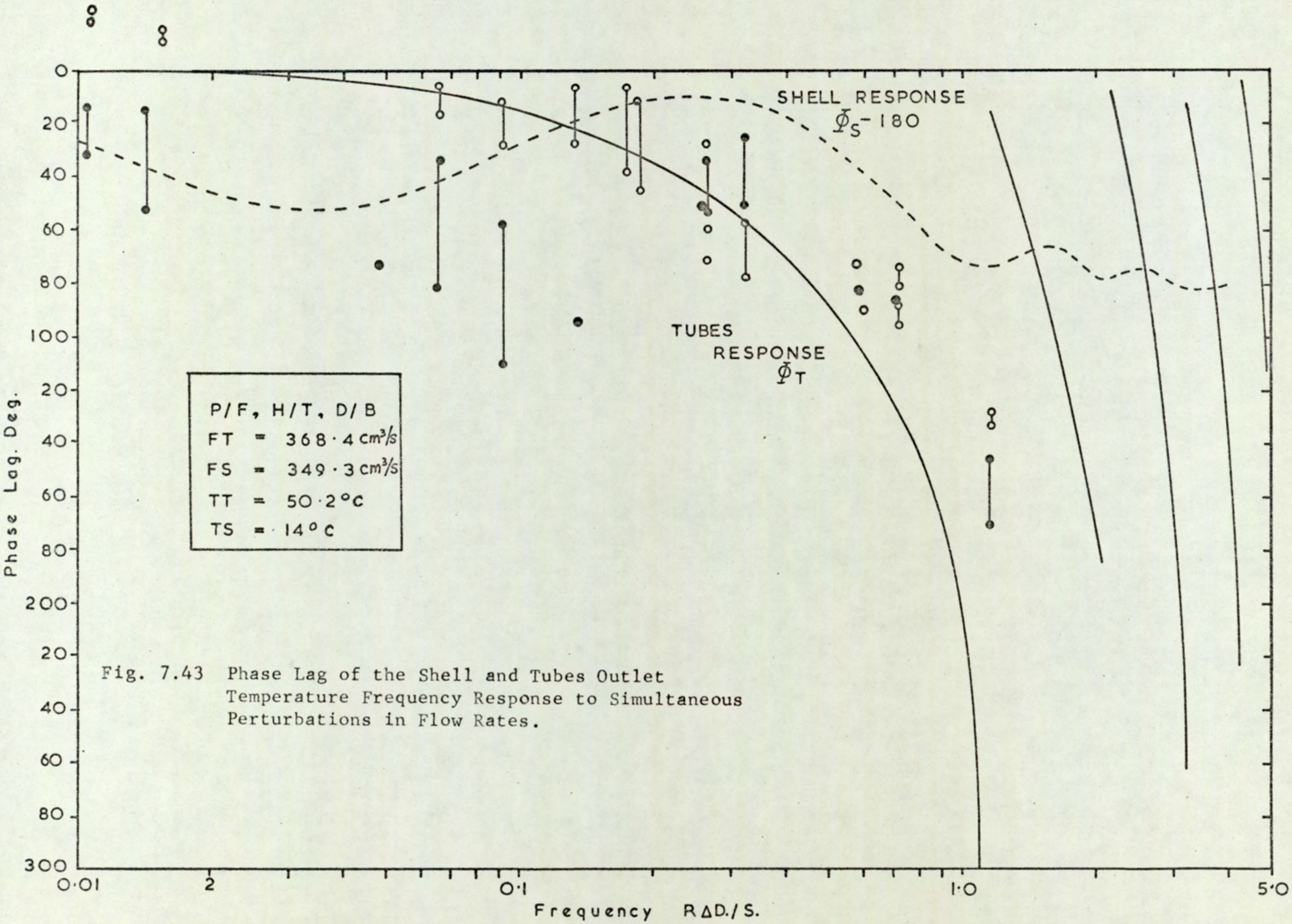

Fig. 7.43 Phase Lag of the Shell and Tubes Outlet Temperature Frequency Response to Simultaneous Perturbations in Flow Rates.

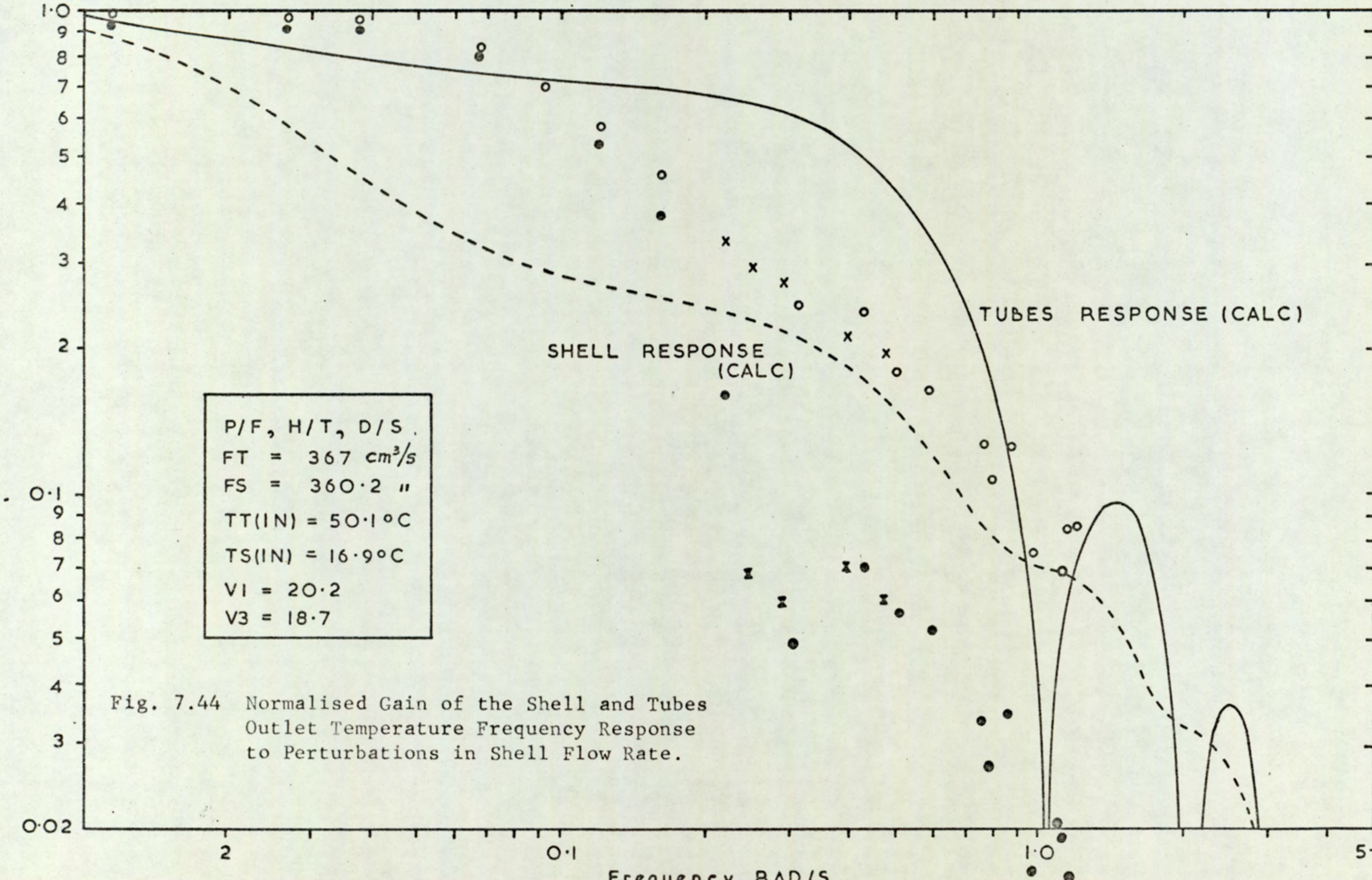

Fig. 7.44 Normalised Gain of the Shell and Tubes Outlet Temperature Frequency Response to Perturbations in Shell Flow Rate.

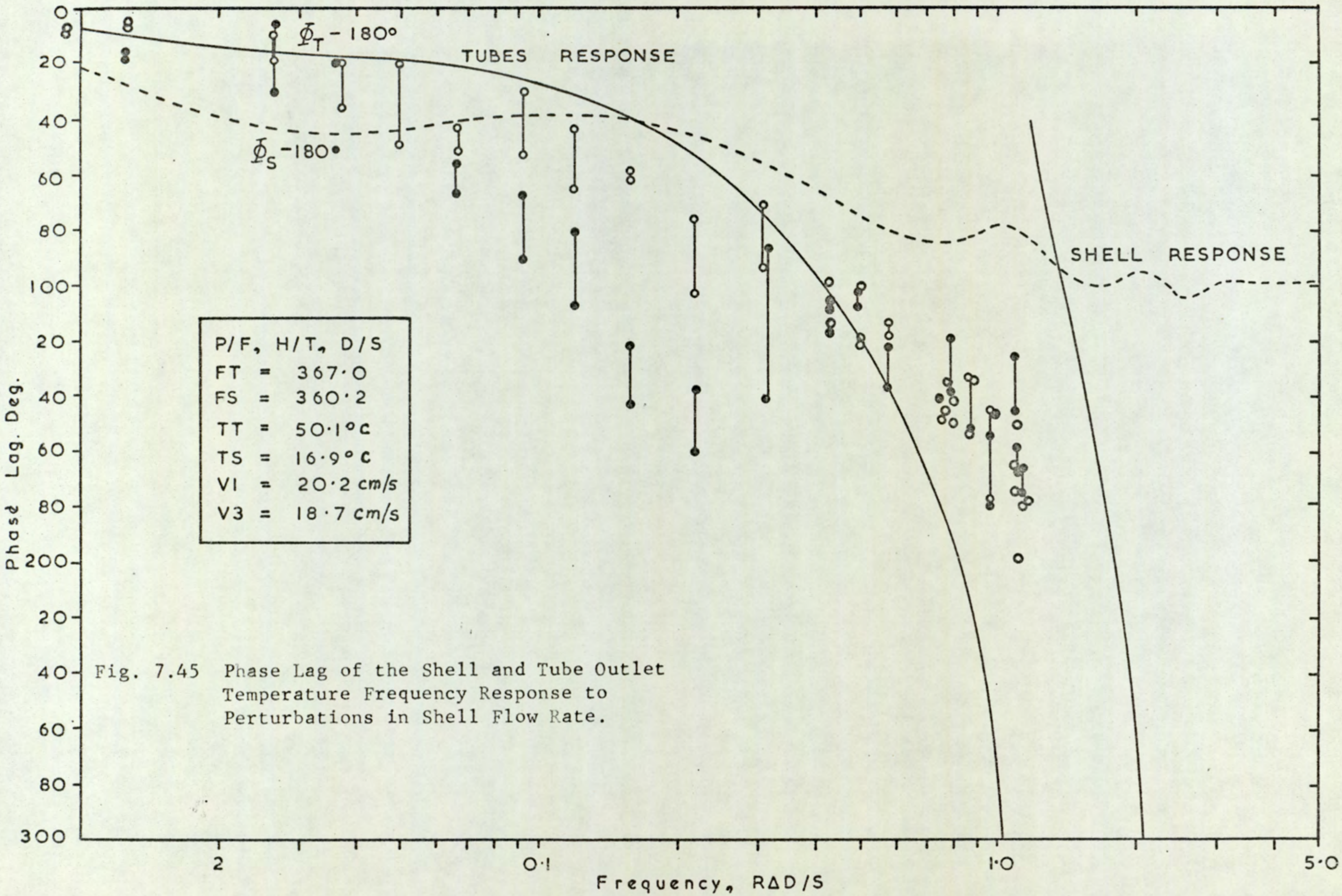

Fig. 7.45 Phase Lag of the Shell and Tube Outlet Temperature Frequency Response to Perturbations in Shell Flow Rate.

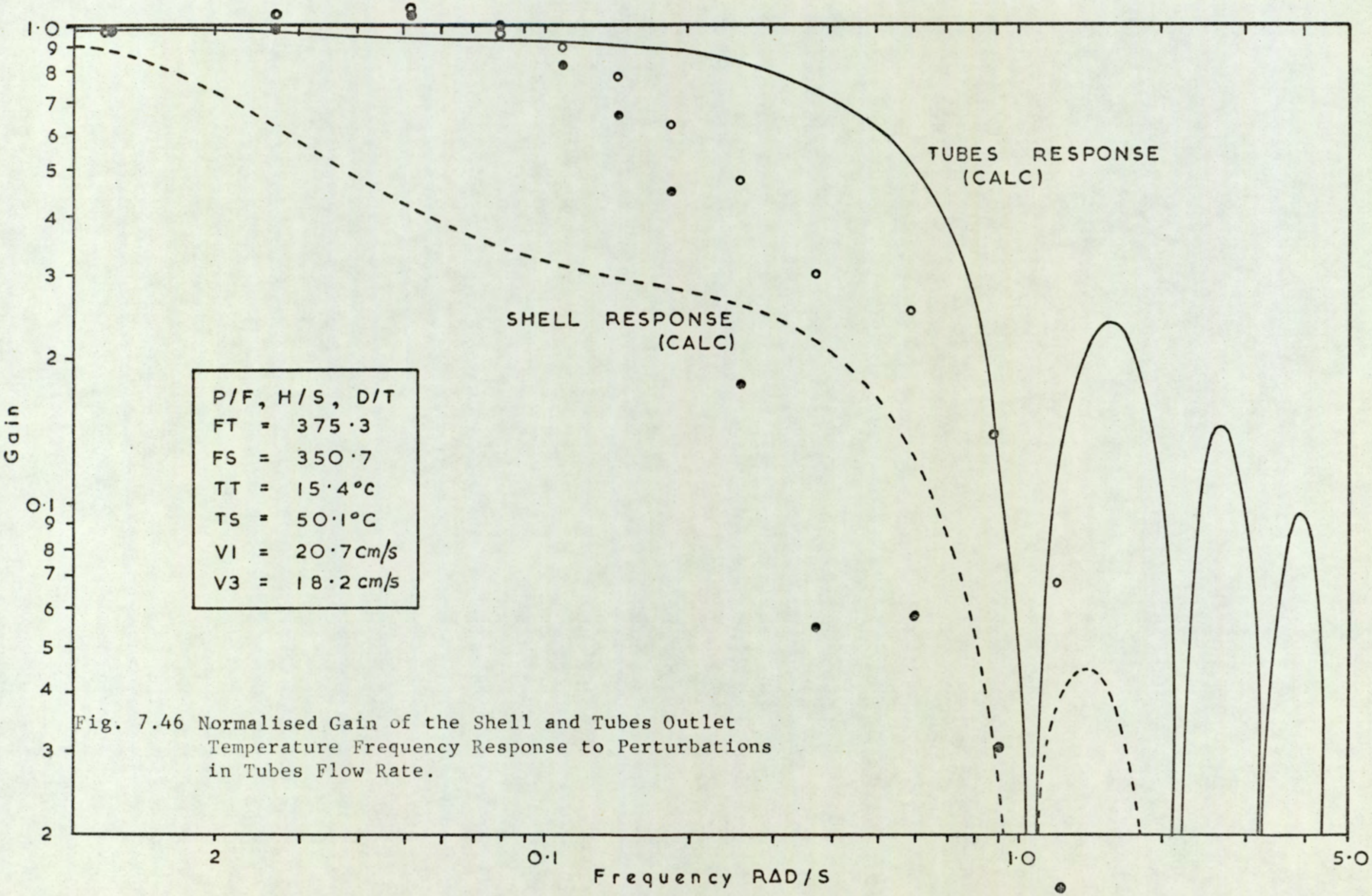

Fig. 7.46 Normalised Gain of the Shell and Tubes Outlet Temperature Frequency Response to Perturbations in Tubes Flow Rate.

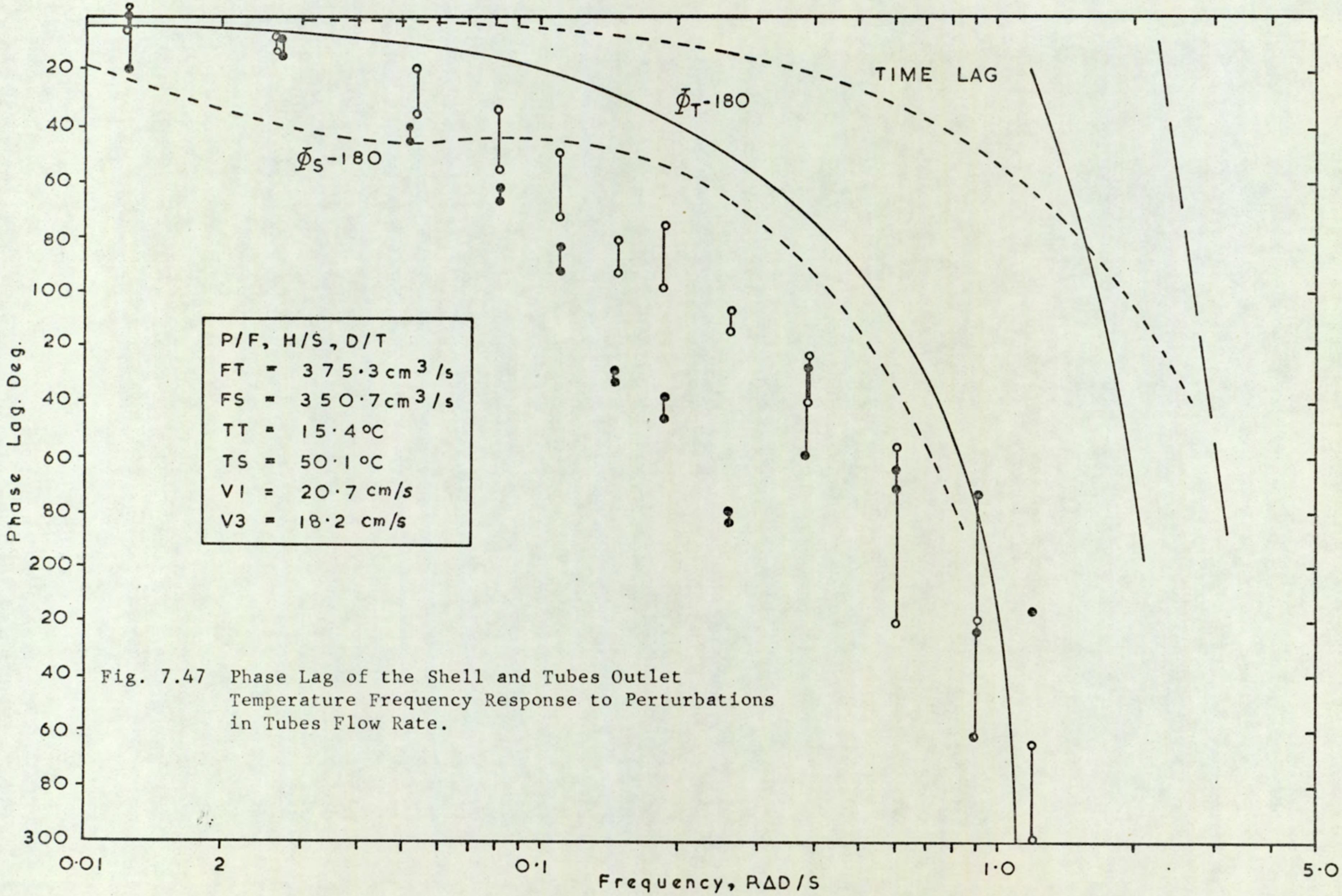

Fig. 7.47 Phase Lag of the Shell and Tubes Outlet Temperature Frequency Response to Perturbations in Tubes Flow Rate.

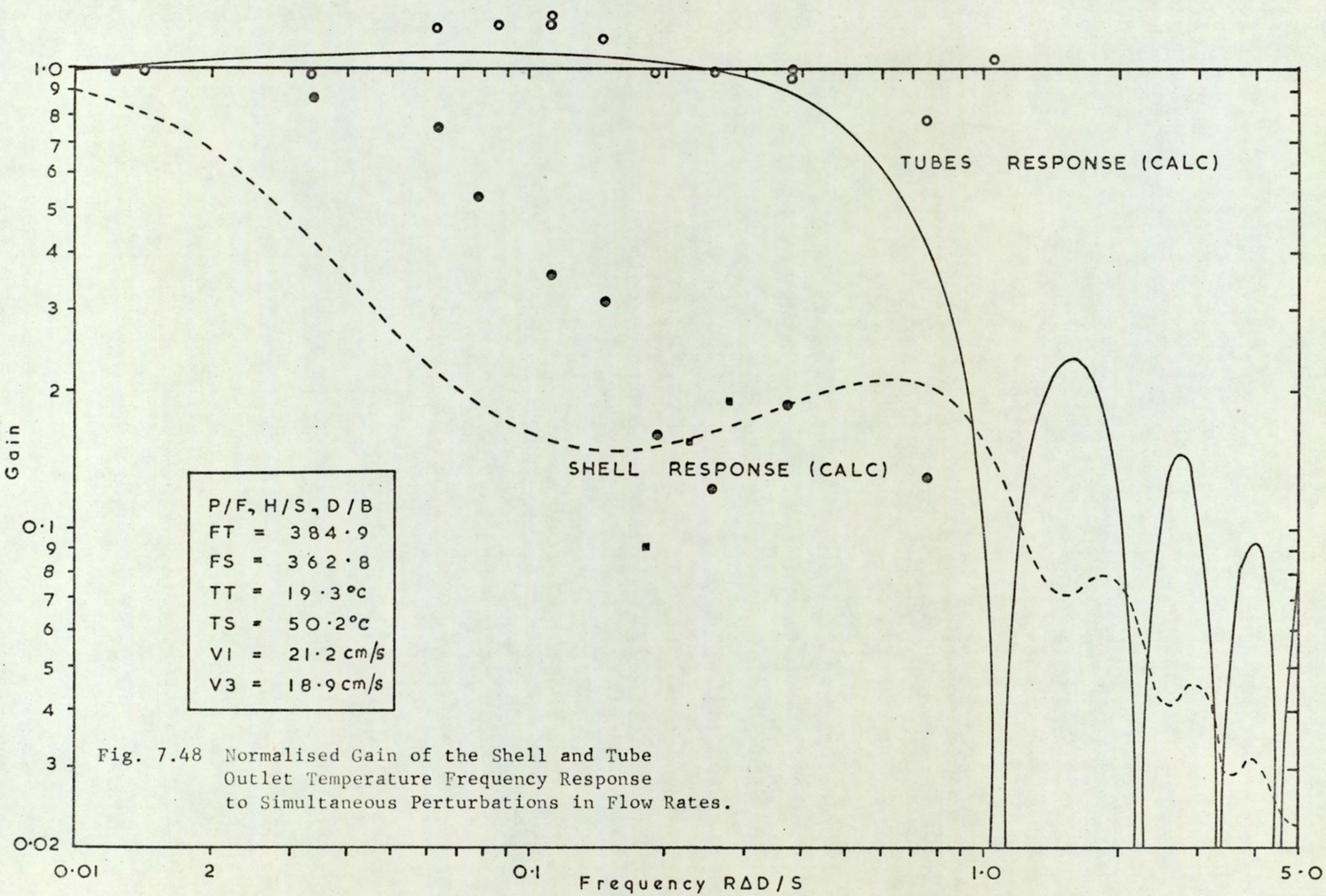

Fig. 7.48 Normalised Gain of the Shell and Tube Outlet Temperature Frequency Response to Simultaneous Perturbations in Flow Rates.

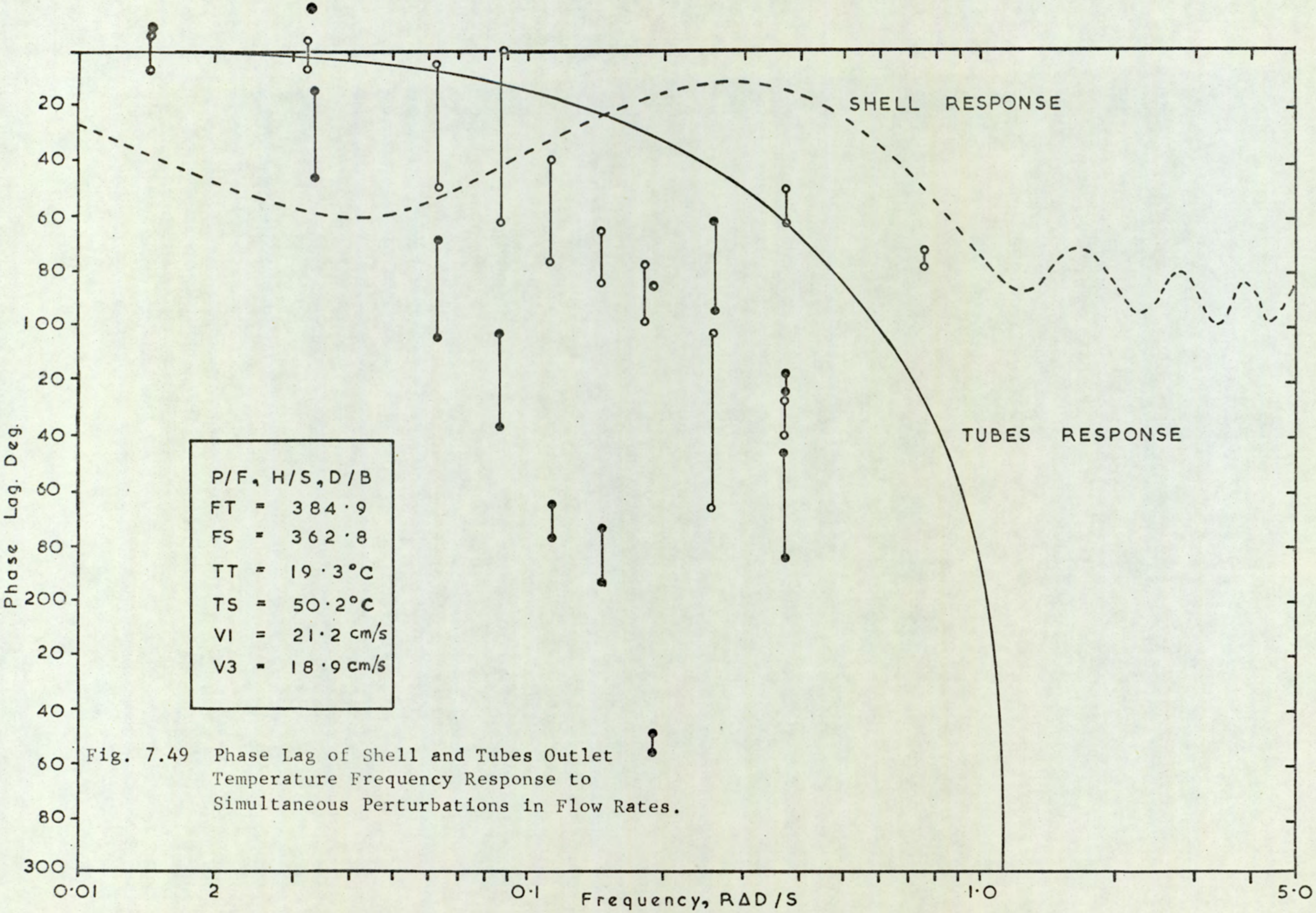

Fig. 7.49 Phase Lag of Shell and Tubes Outlet Temperature Frequency Response to Simultaneous Perturbations in Flow Rates.

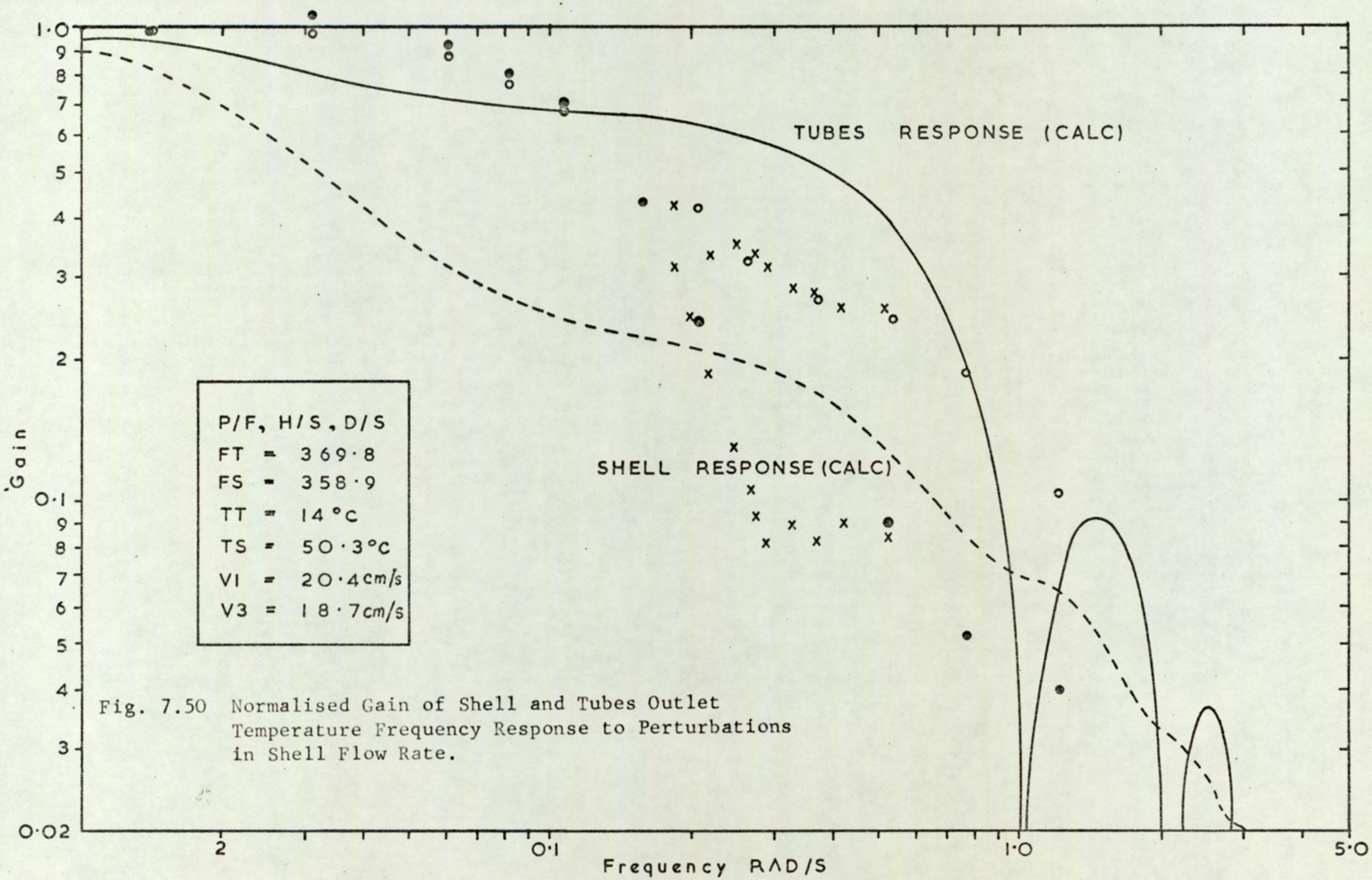

Fig. 7.50 Normalised Gain of Shell and Tubes Outlet Temperature Frequency Response to Perturbations in Shell Flow Rate.

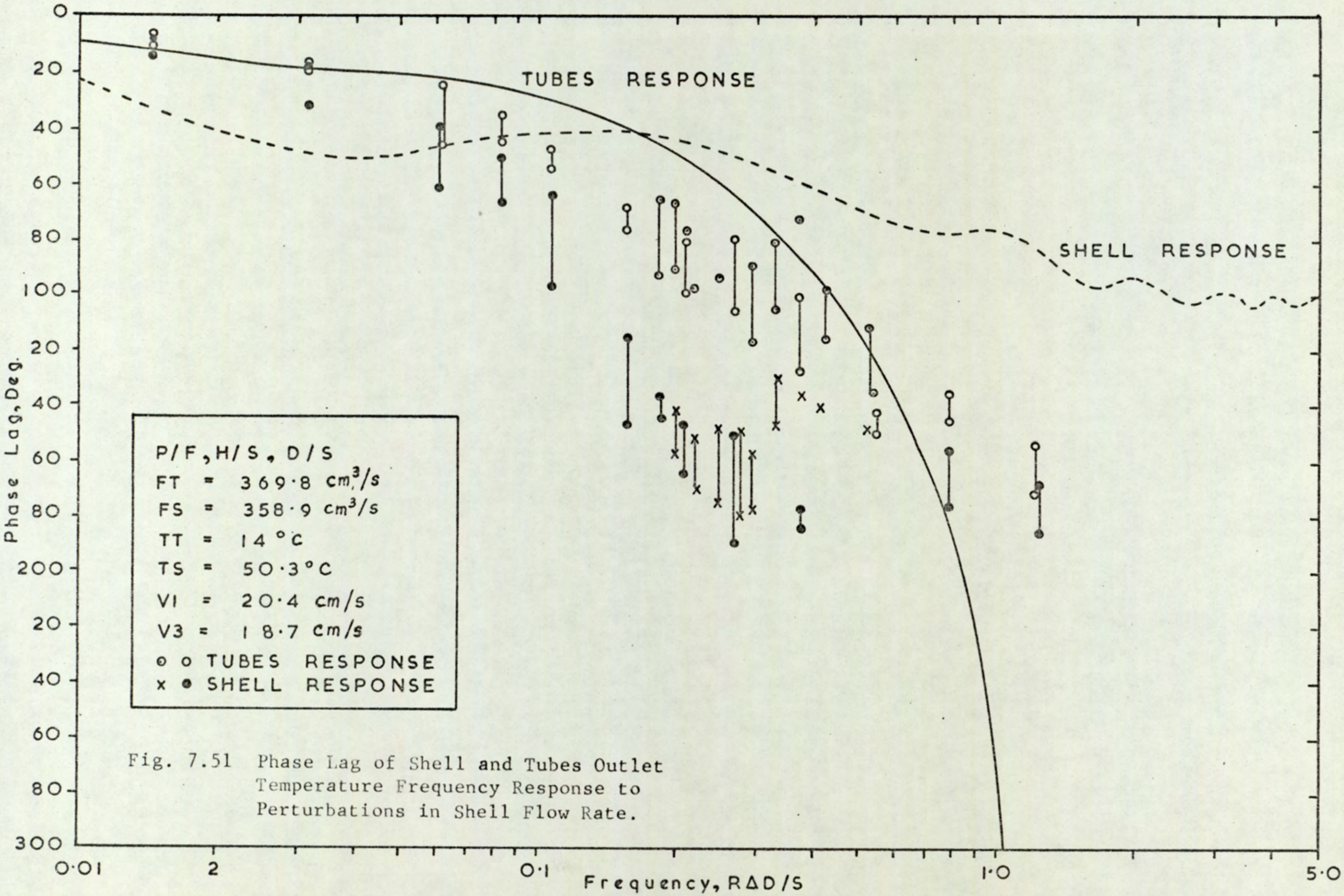

Fig. 7.51 Phase Lag of Shell and Tubes Outlet Temperature Frequency Response to Perturbations in Shell Flow Rate.

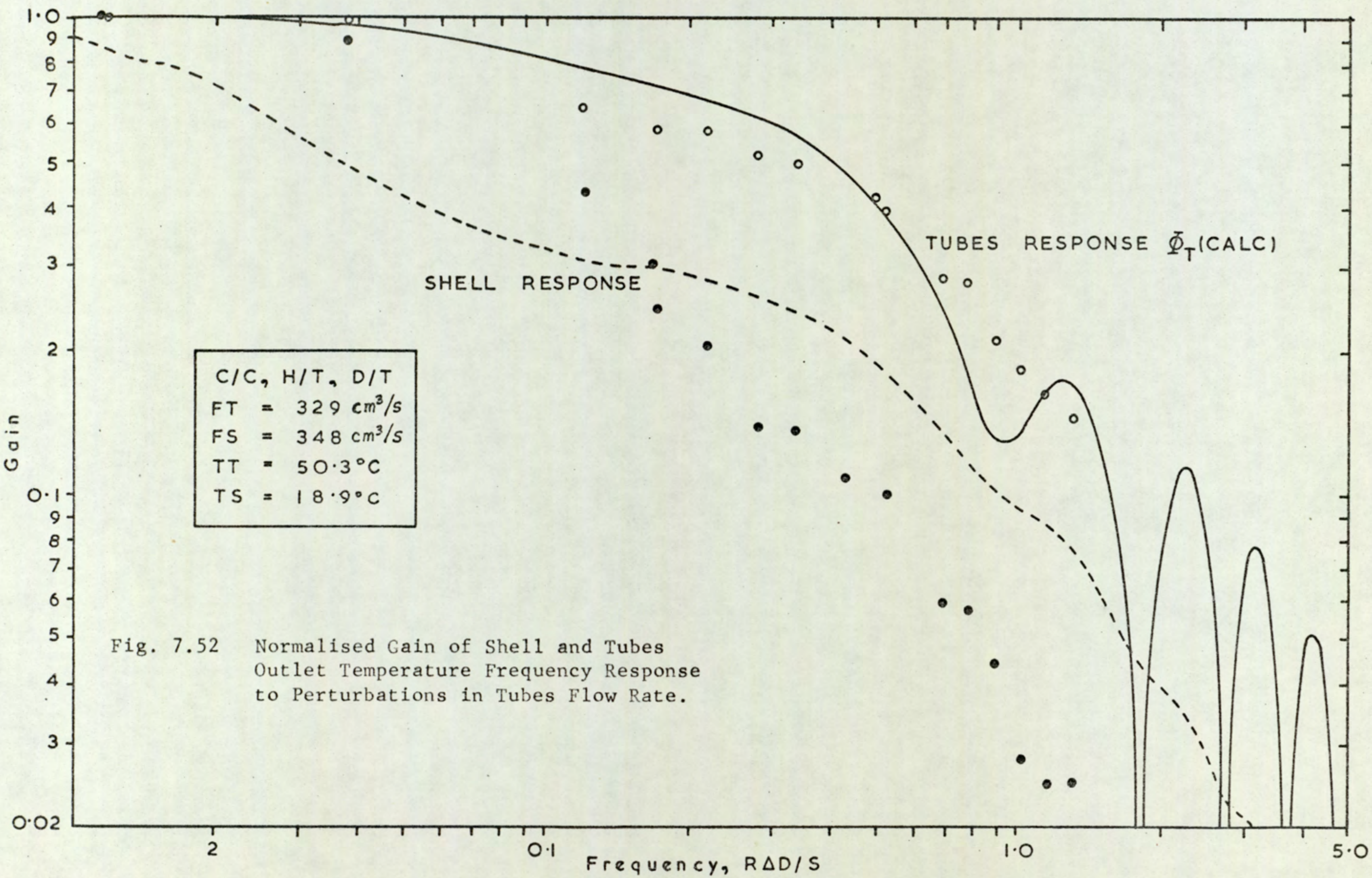

Fig. 7.52 Normalised Gain of Shell and Tubes Outlet Temperature Frequency Response to Perturbations in Tubes Flow Rate.

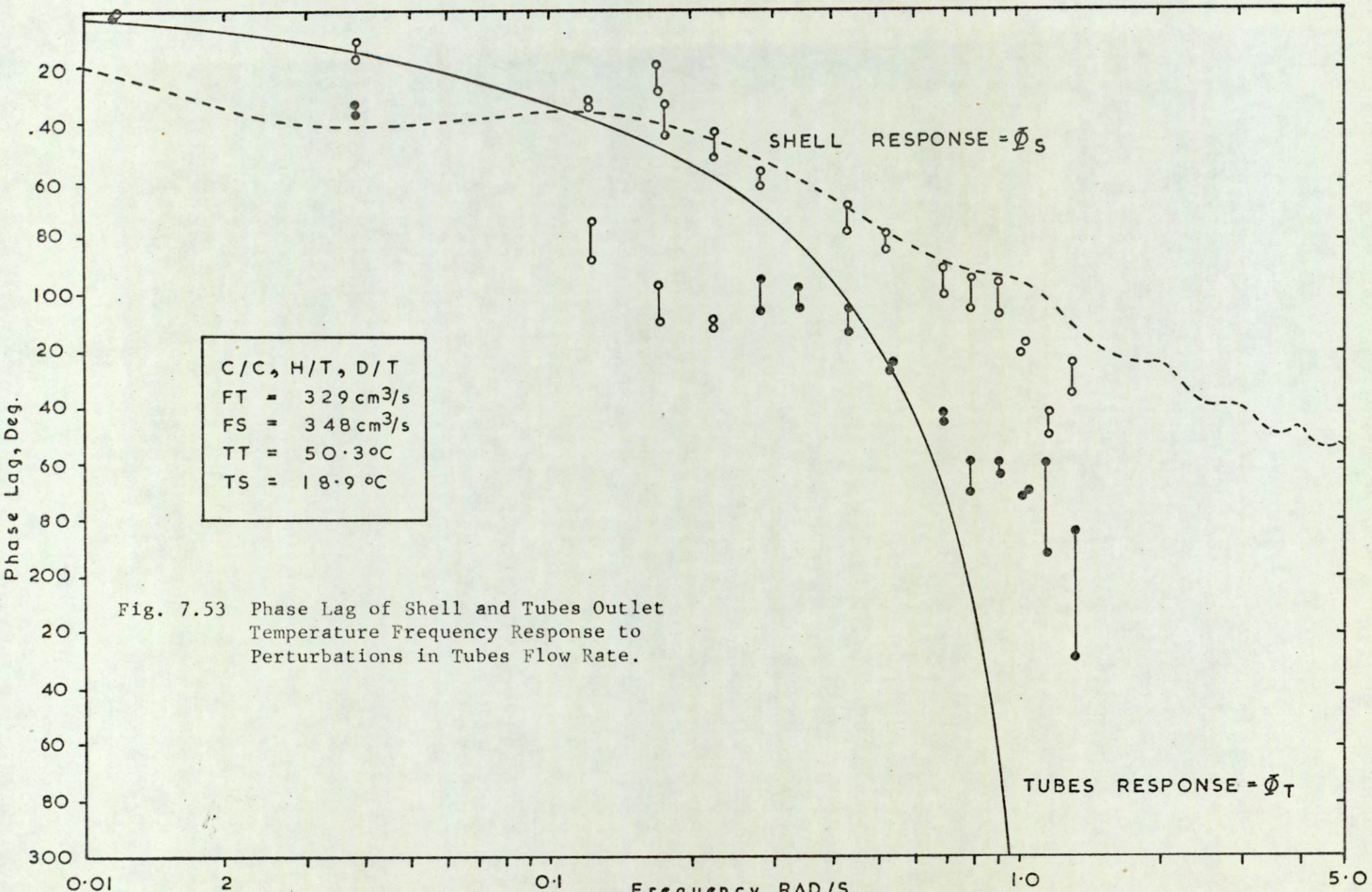

Fig. 7.53 Phase Lag of Shell and Tubes Outlet Temperature Frequency Response to Perturbations in Tubes Flow Rate.

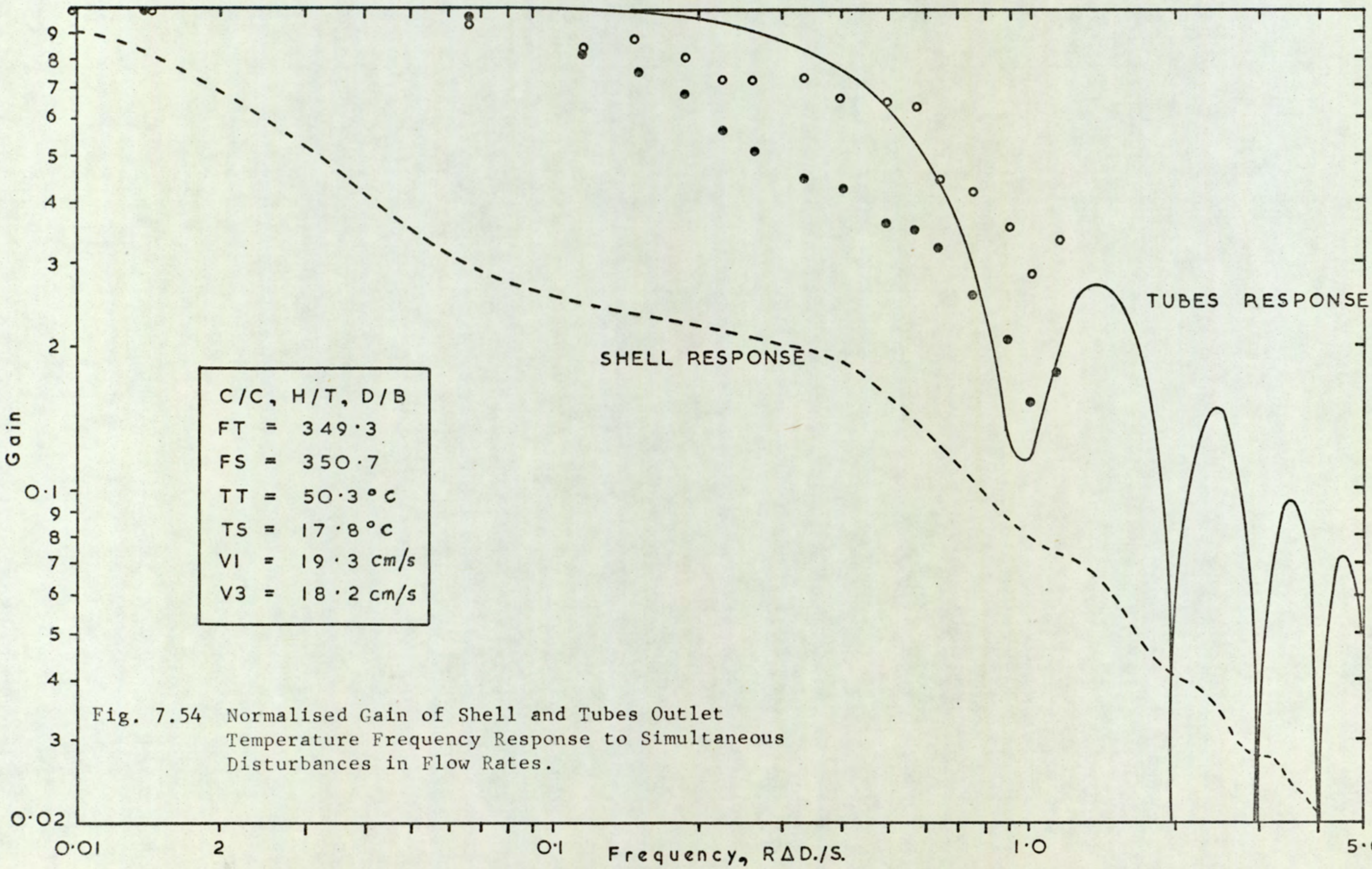

Fig. 7.54 Normalised Gain of Shell and Tubes Outlet Temperature Frequency Response to Simultaneous Disturbances in Flow Rates.

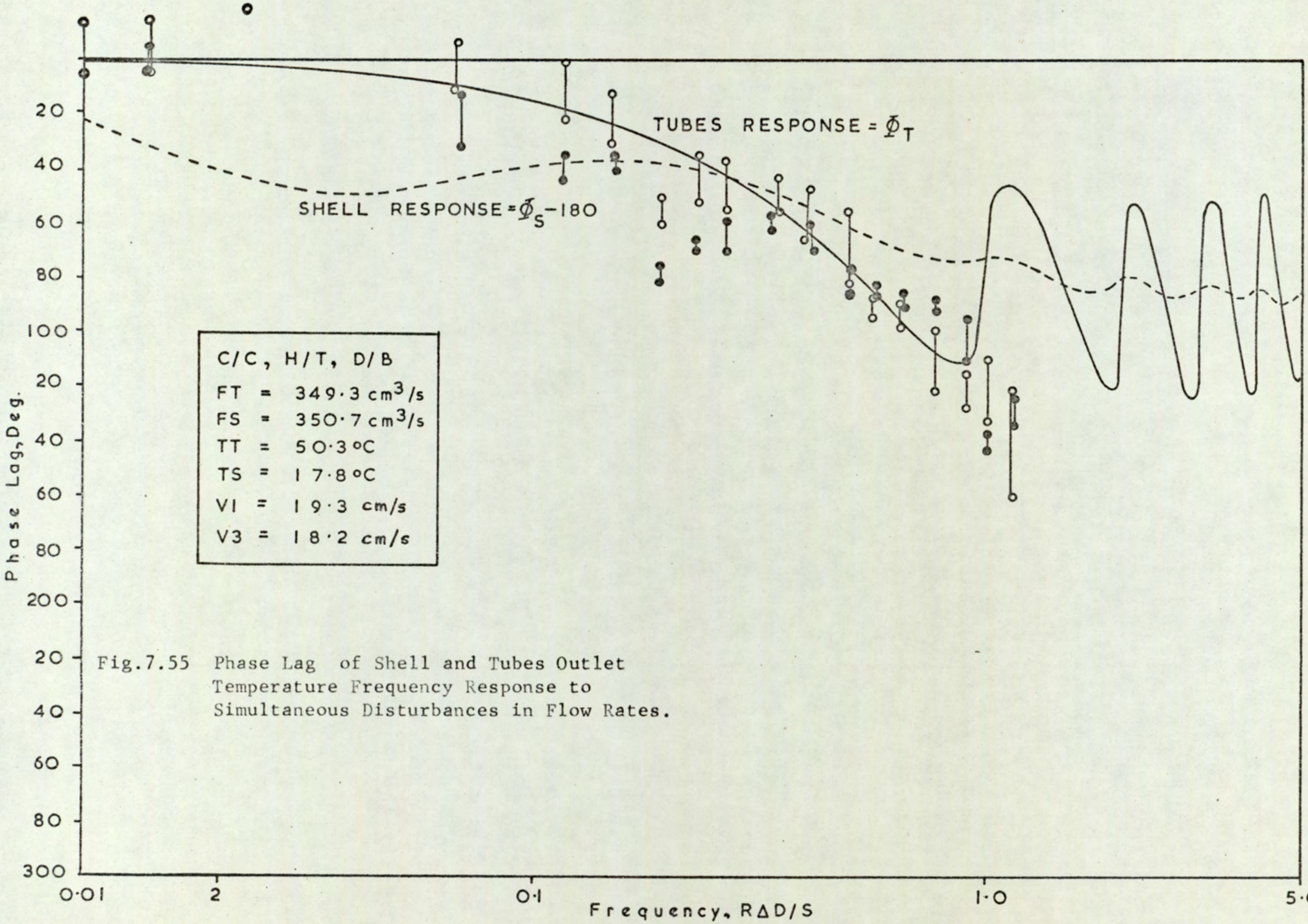

Fig.7.55 Phase Lag of Shell and Tubes Outlet Temperature Frequency Response to Simultaneous Disturbances in Flow Rates.

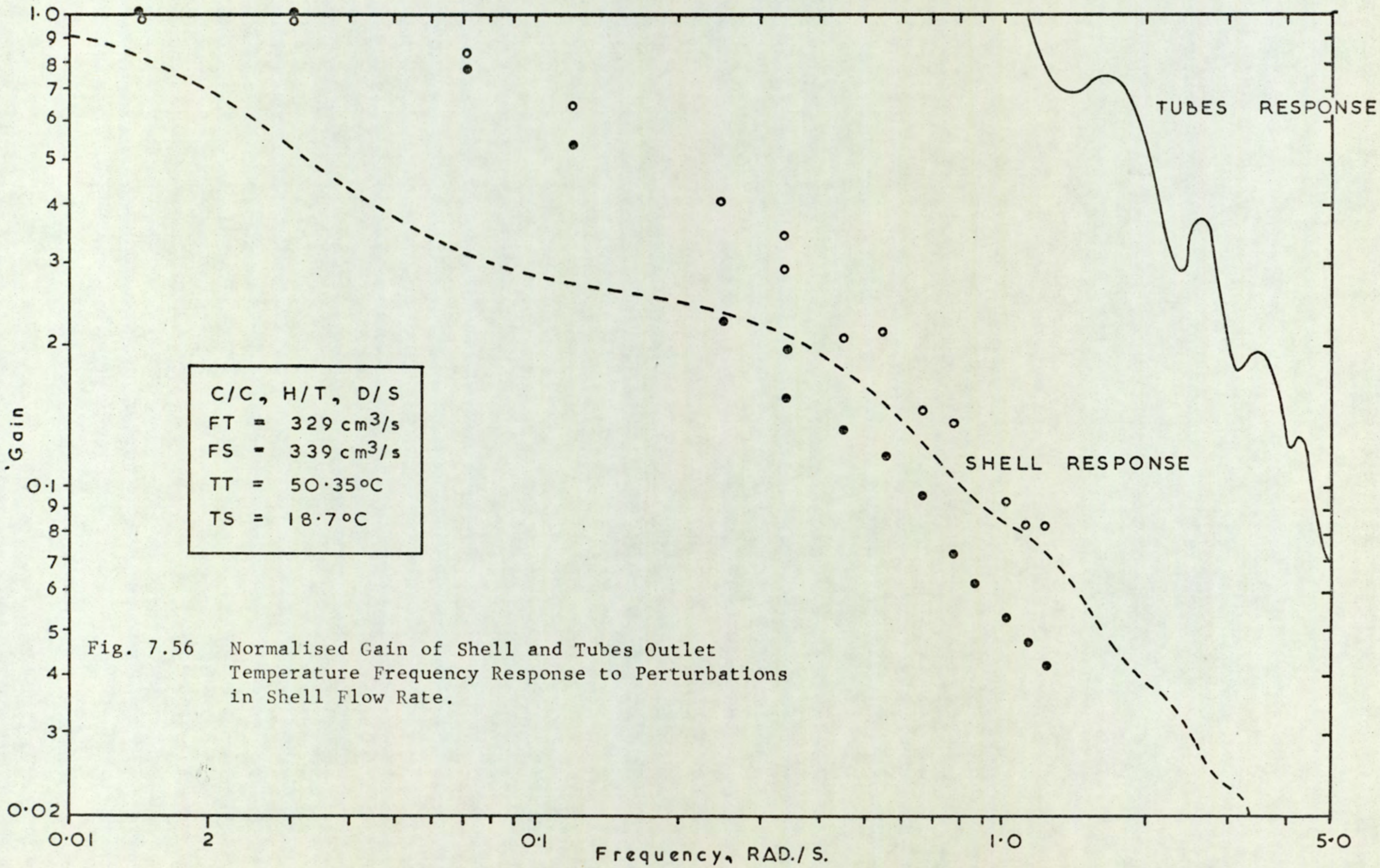

Fig. 7.56 Normalised Gain of Shell and Tubes Outlet Temperature Frequency Response to Perturbations in Shell Flow Rate.

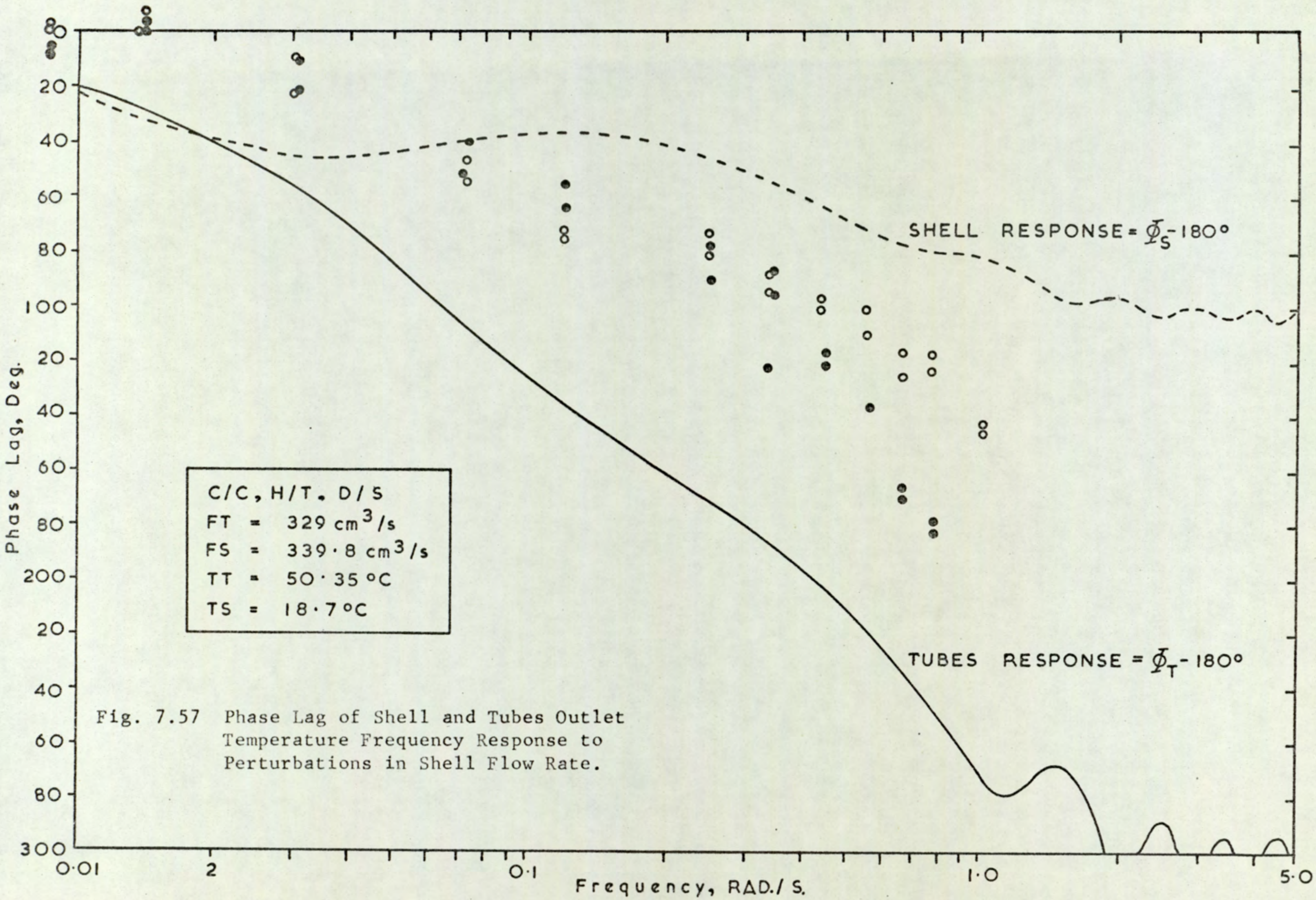

Fig. 7.57 Phase Lag of Shell and Tubes Outlet Temperature Frequency Response to Perturbations in Shell Flow Rate.

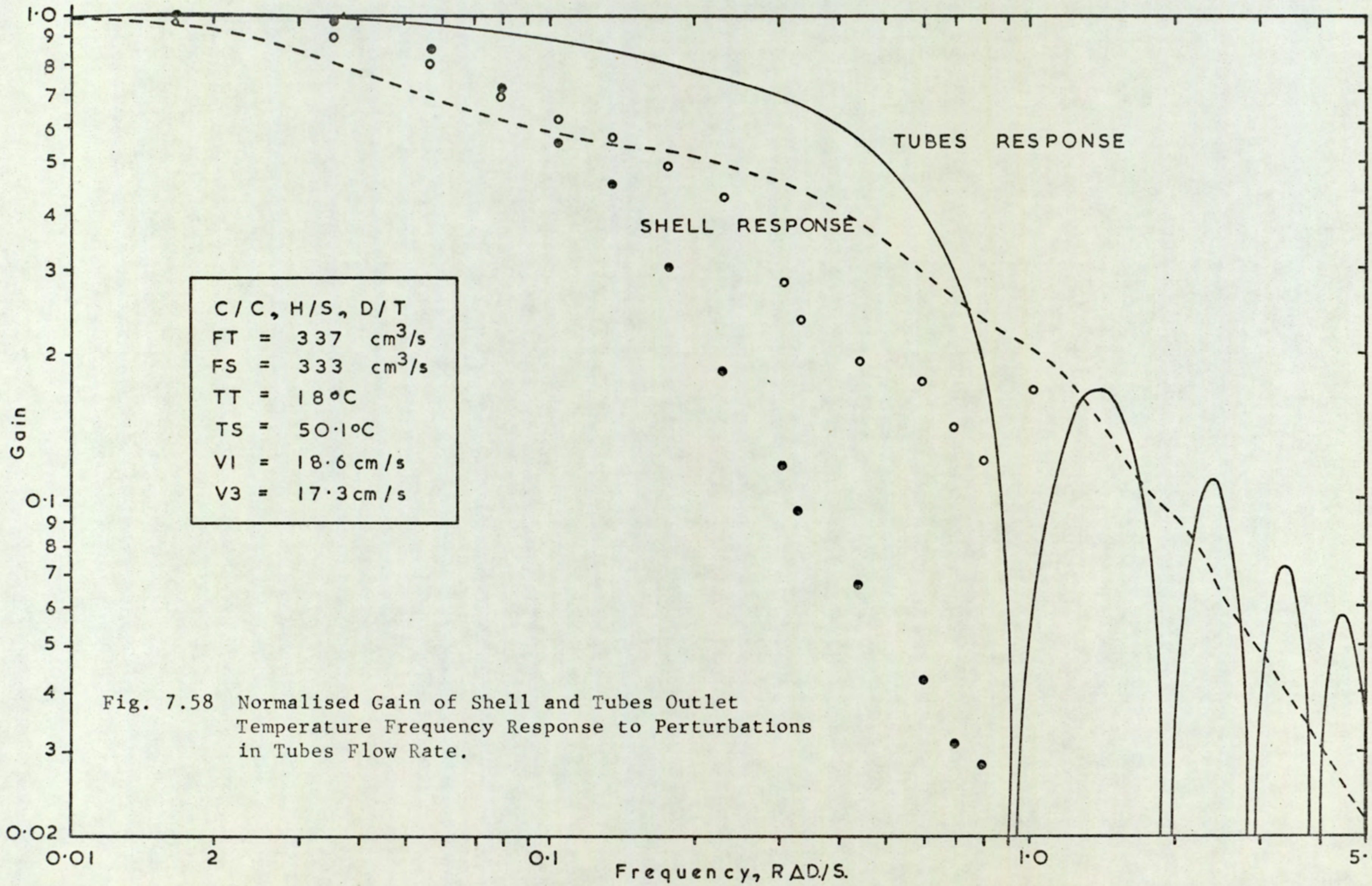

Fig. 7.58 Normalised Gain of Shell and Tubes Outlet Temperature Frequency Response to Perturbations in Tubes Flow Rate.

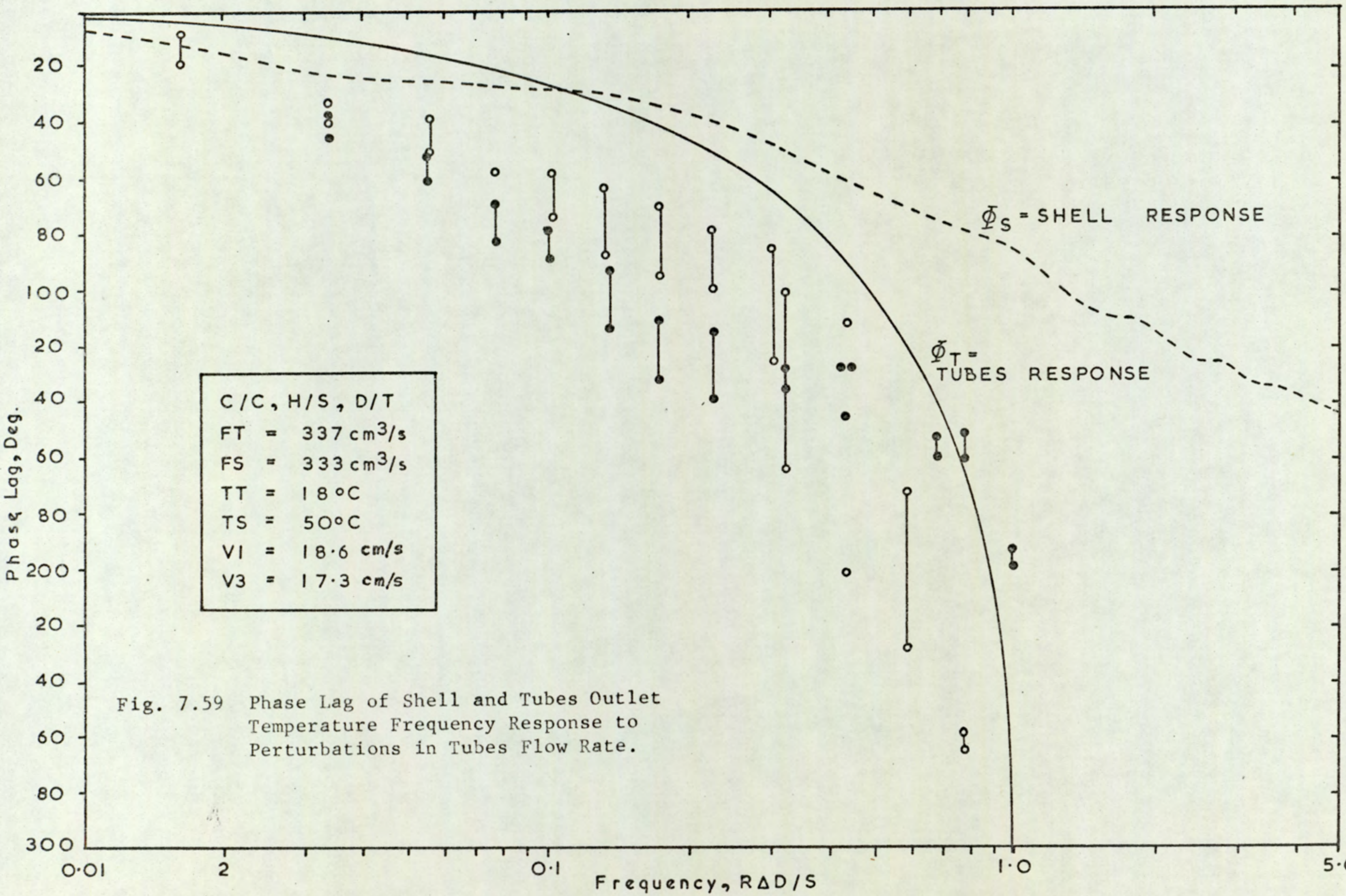

Fig. 7.59 Phase Lag of Shell and Tubes Outlet Temperature Frequency Response to Perturbations in Tubes Flow Rate.

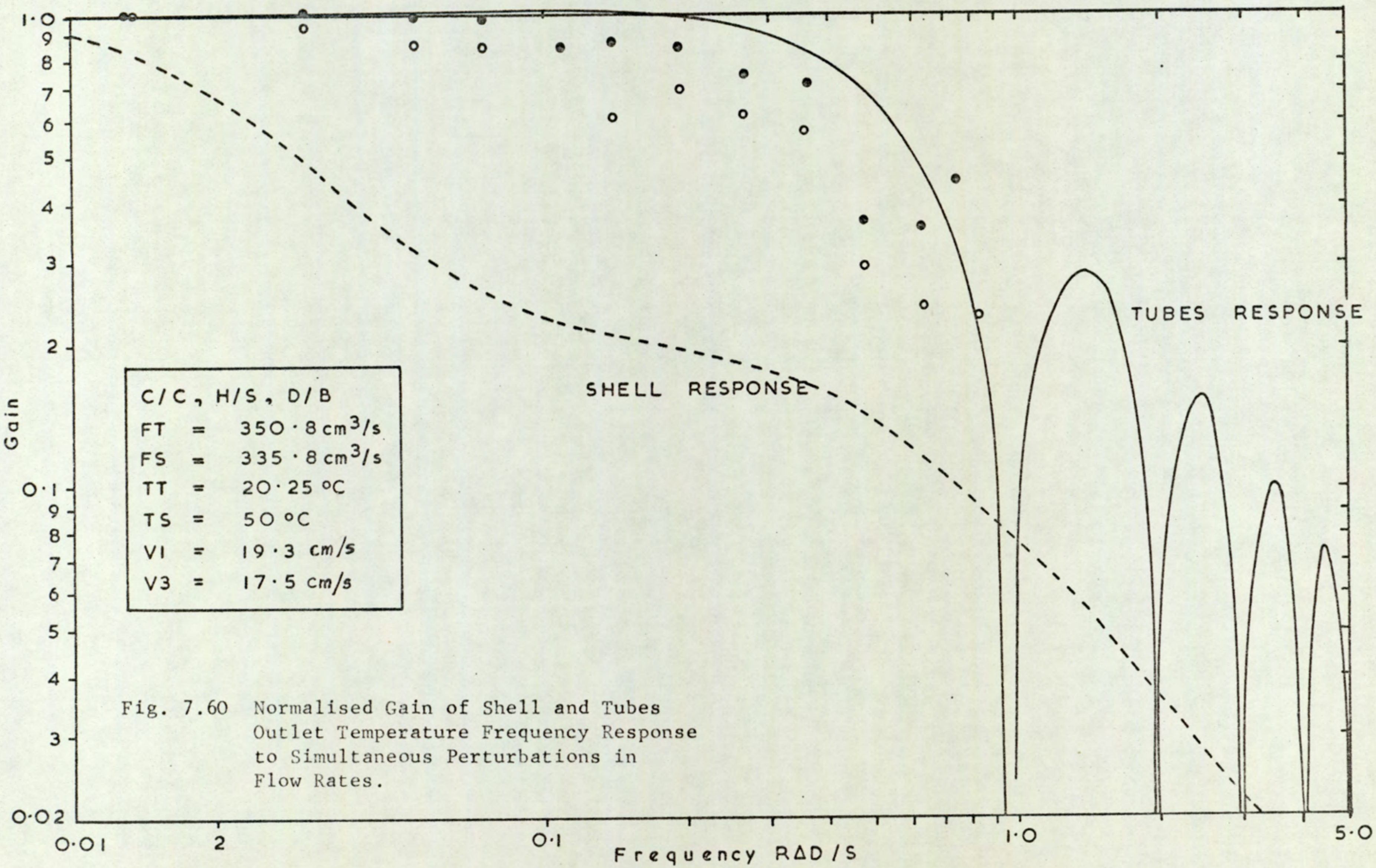

Fig. 7.60 Normalised Gain of Shell and Tubes Outlet Temperature Frequency Response to Simultaneous Perturbations in Flow Rates.

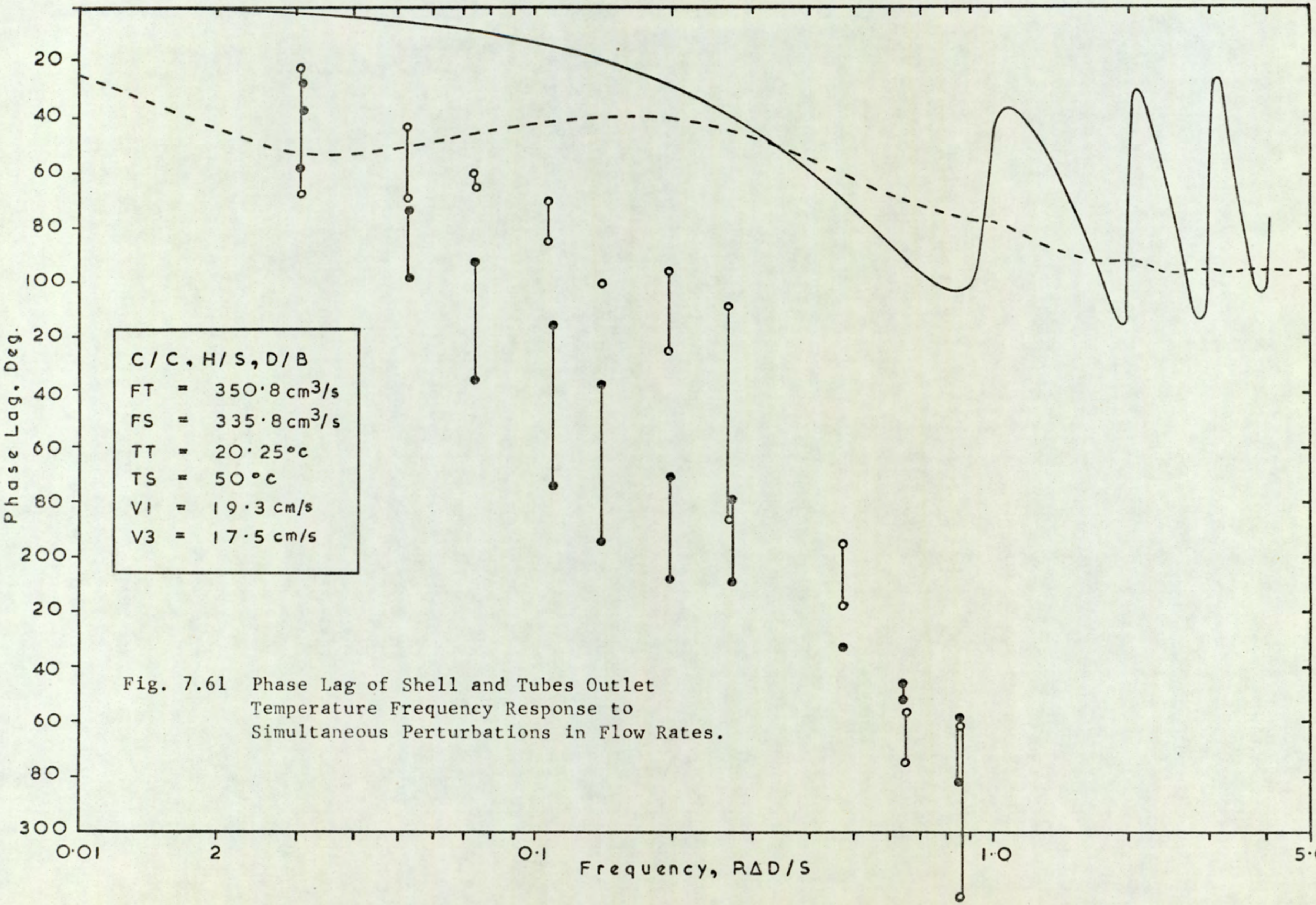

Fig. 7.61 Phase Lag of Shell and Tubes Outlet Temperature Frequency Response to Simultaneous Perturbations in Flow Rates.

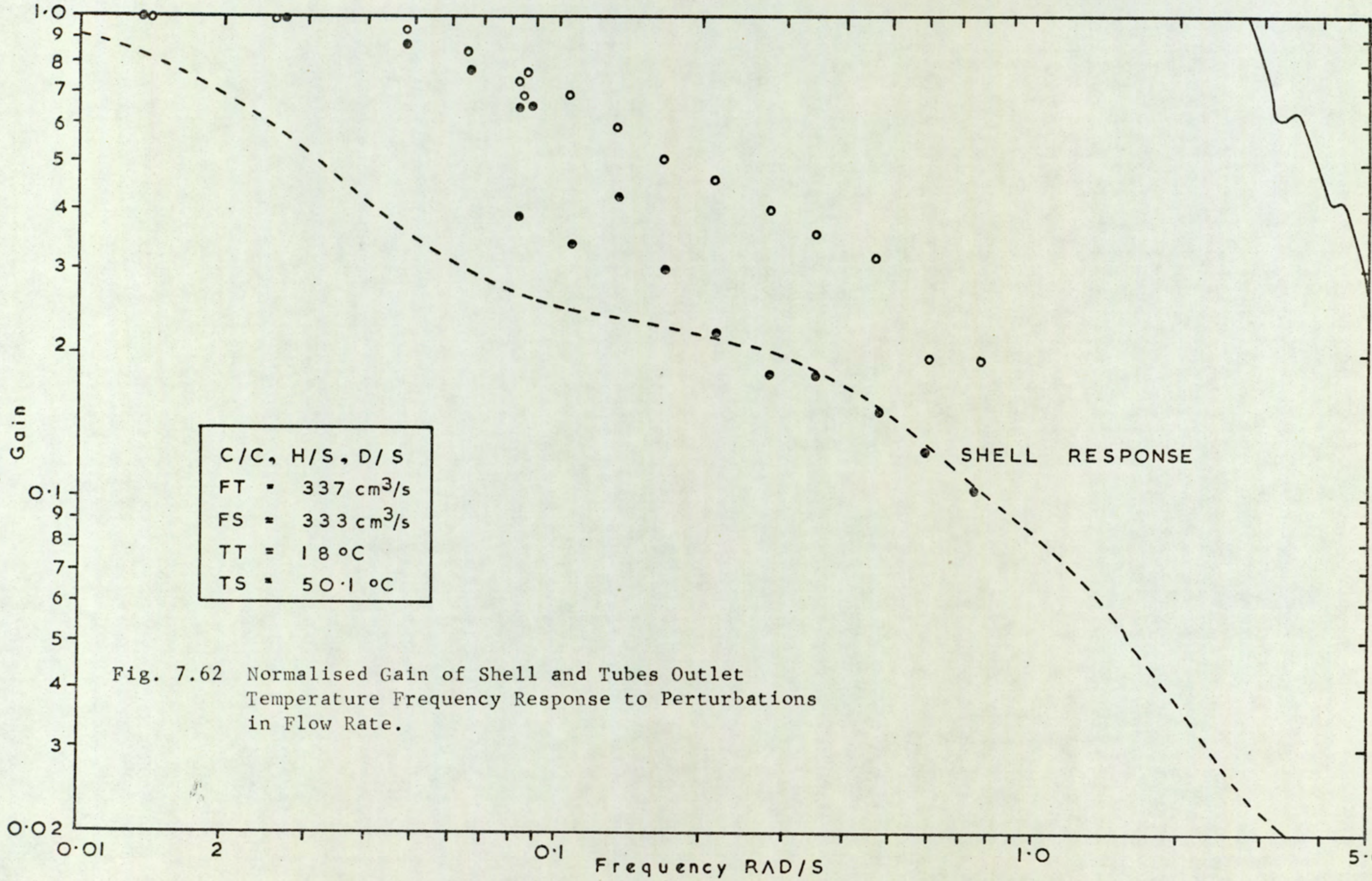

Fig. 7.62 Normalised Gain of Shell and Tubes Outlet Temperature Frequency Response to Perturbations in Flow Rate.

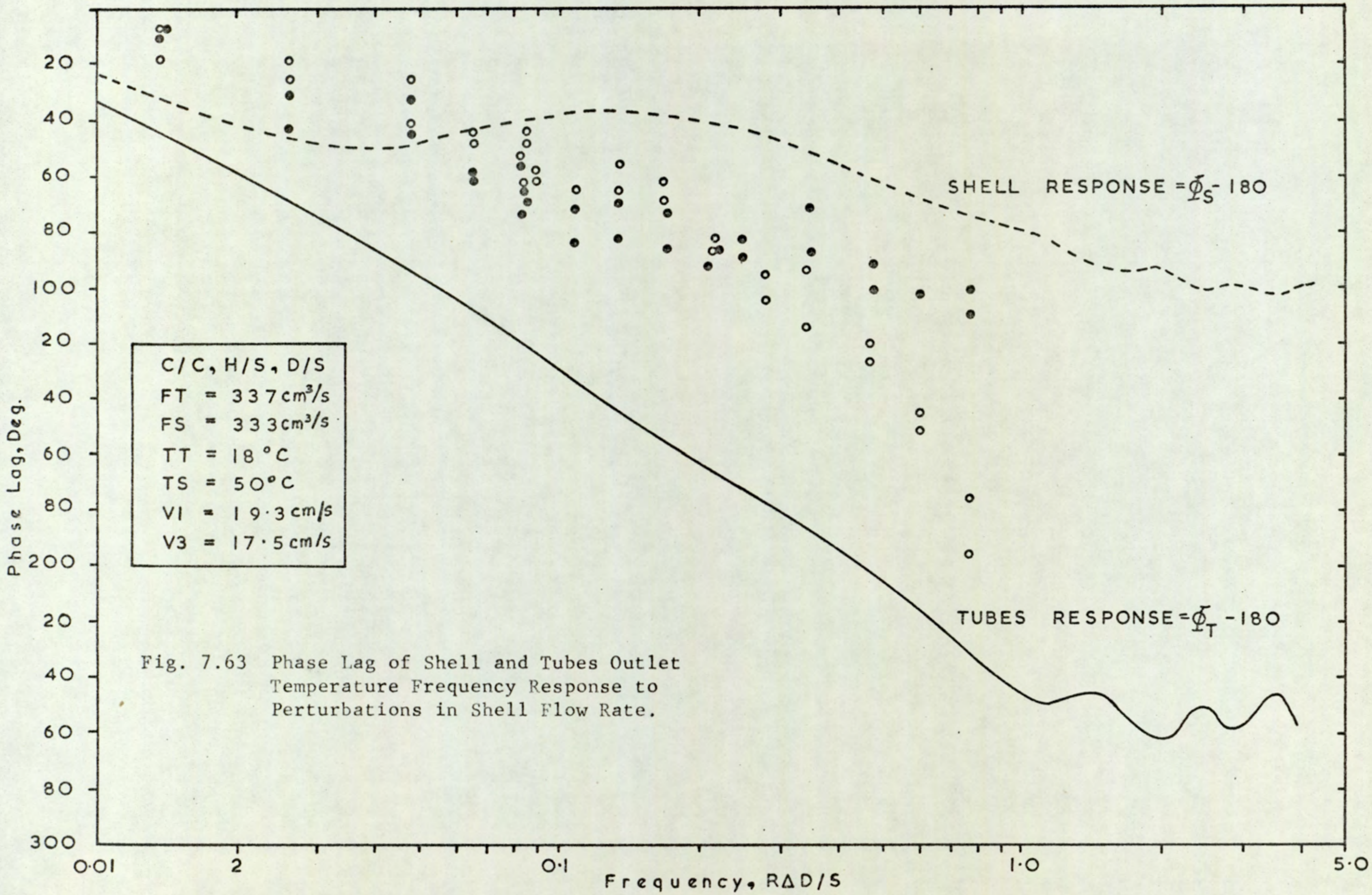

Fig. 7.63 Phase Lag of Shell and Tubes Outlet Temperature Frequency Response to Perturbations in Shell Flow Rate.

For all the conditions except those of Fig.7.50, the experimental results showed that the gain of the shell side temperature was lower than the corresponding tube side one qualitatively agreeing with the predictions. The phase lag, on the other hand, was almost always larger in absolute terms for the shell side response at most frequencies, its rate of change being rather irregular, causing it to cross over the path of the tube data, on some occasions.

It is noticeable in most cases that the tube temperature response showed the largest divergence between experimental and predicted values of gain at some intermediate range of frequencies as shown by Figs.7.40, 7.44, 7.45, 7.50 and 7.58. The best fit achieved corresponded to the conditions of Figs.7.42, 7.48, 7.52, and 7.54, which, as seen, included two sets of single variable operation and two sets of double variable operation.

The representation of the shell outlet temperature response was poor enough to render the model inadequate to represent the shell contribution to the heat exchanger behaviour in the laminar and transition region.

It is thought that the difference in the quality of the representation between the shell and the tube behaviour is related to the configuration of the two spaces, among other things, the specific area of both sides being the factor to consider.

Specific area, A_e, is here defined as the total heat transfer area divided by the total fluid mass held within the corresponding side of the exchanger,

$$A_e = \frac{A_Q}{V_F \rho_F} \qquad (7.7)$$

The smaller the specific area, the greater the importance of thermal diffusion to convey heat from the body of the fluid to the heat transfer surface and therefore the poorer the description by an algorithm which neglects such effect as the one used here.

Evidently this may seem to contradict the claim made during the analysis of transient response that the heat transfer of the shell side seems better described than the heat transfer of the tube side, but it must be emphasised that such description refers to a static condition, which does not take into account the dynamic variation of temperature gradients which occur during sinusoidal perturbation in which faster responses lead to higher gains and smaller phase lags. Obviously the process of heat transfer under sinusoidal flow velocity disturbance becomes highly complex because besides the two main mechanisms of transfer, convection and thermal diffusion as functions of the changing temperature profiles, there is also the cyclic effect introduced by the change of Reynolds number with periodic inversion of gradients . An additional cause of divergence lies in the fact that a non-linear behaviour is approximated by a linear algorithm.

Because of the experimental difficulties described in chapter 6, the data shows significant scatter, the scattering being even greater as a result of the two readings taken for each frequency. The reason for the two readings lies in the two references used to measure phase lag, corresponding to the maximum and minimum of each cycle. Since distortion due to non-linear components of the system (hysteresis, valve characteristic curve, heat transfer coefficient dependence on fluid velocity) is produced on the signal, the two references are not evenly spaced and therefore two different readings are obtained as seen in Fig.7.64. As the data show in some cases, the distortion was very large and changed with frequency.

Logically it would be expected that the inclusion of the thermal diffusion effect in the model should result in an improvement of the quality of the representation. This however cannot be taken for granted because Beckman (4) using a convection-diffusion model in the region of high turbulent flow did not achieve a representation of the experimental results as good as the one obtained by Privott (75) in the same region, using a convection model only. They both used concentric tubular heat exchangers to verify their respective models.

7.7. PULSE TESTING RESULTS

A certain amount of data was taken by the pulse testing method described in Section 4.2, with the object of speeding up the frequency response data collection. Although the analysis of this data by the Fourier transformation showed a general pattern similar to the results from pure sinusoidal data, they proved difficult to reproduce. Runs with pulses of different amplitude and durations indicated that the best results were obtained with duration in the range of 8 to 10 seconds, corresponding to the sinusoidal signal used to produce the pulsing according to the procedure described in Section 6.2.3. Using shorter pulses required a corresponding increase in the amplitude of the disturbance in order to produce a measurable response, and in the case of simultaneous perturbations, the synchronism of the signals became difficult due to their fast change. Runs repeated for the same set of conditions though producing apparently similar response curves, after data reduction yielded different Bode plots.

There are two likely causes

(i) the signal noise which affected most of the data collection, and

(ii) the low-amplitude, low-frequency cycling experienced as a result of the two partition controller used in the hot water tank (see section 6.1.1).

Because the data of the whole frequency spectrum of the Bode plots depends on the single curve generated by the transient response to the pulse disturbance, the corrupting effect of noise, which distorts local regions of the response curve, has a very strong effect on the resulting frequency response. Previously, Vincent (93) reported the importance of noise as the limiting factor of the high frequency data, in a single variable system, and the negligible effect on the results of the eye-smoothing of data. Though deletereous, the effect of noise is relatively less significant in the case of sinusoidal data because in taking them several cycles are included for each reading of amplitude, so 'averaging' and therefore reducing the effect of random noise. Furthermore, the method of measuring phase lag using the maxima and minima of the cyclic signals is less sensitive to noise.

The effect of cycling, equally present on both types of data, has also a more significant effect in the case of pulse testing because the response curve can be distorted by this spurious signal in different regions with opposite effects so producing a larger error in the results than could be inferred by the actual amplitude.

Figs. 7.64 and 7.65 present two sets of results obtained by the pulse method, together with the corresponding representation by the frequency response model. This set of results can be compared with those of

Figs. 7.44 and 7.45. In explaining the difference between the experimental results and the predictions, the limitations of the model, discussed in the previous section are equally valid.

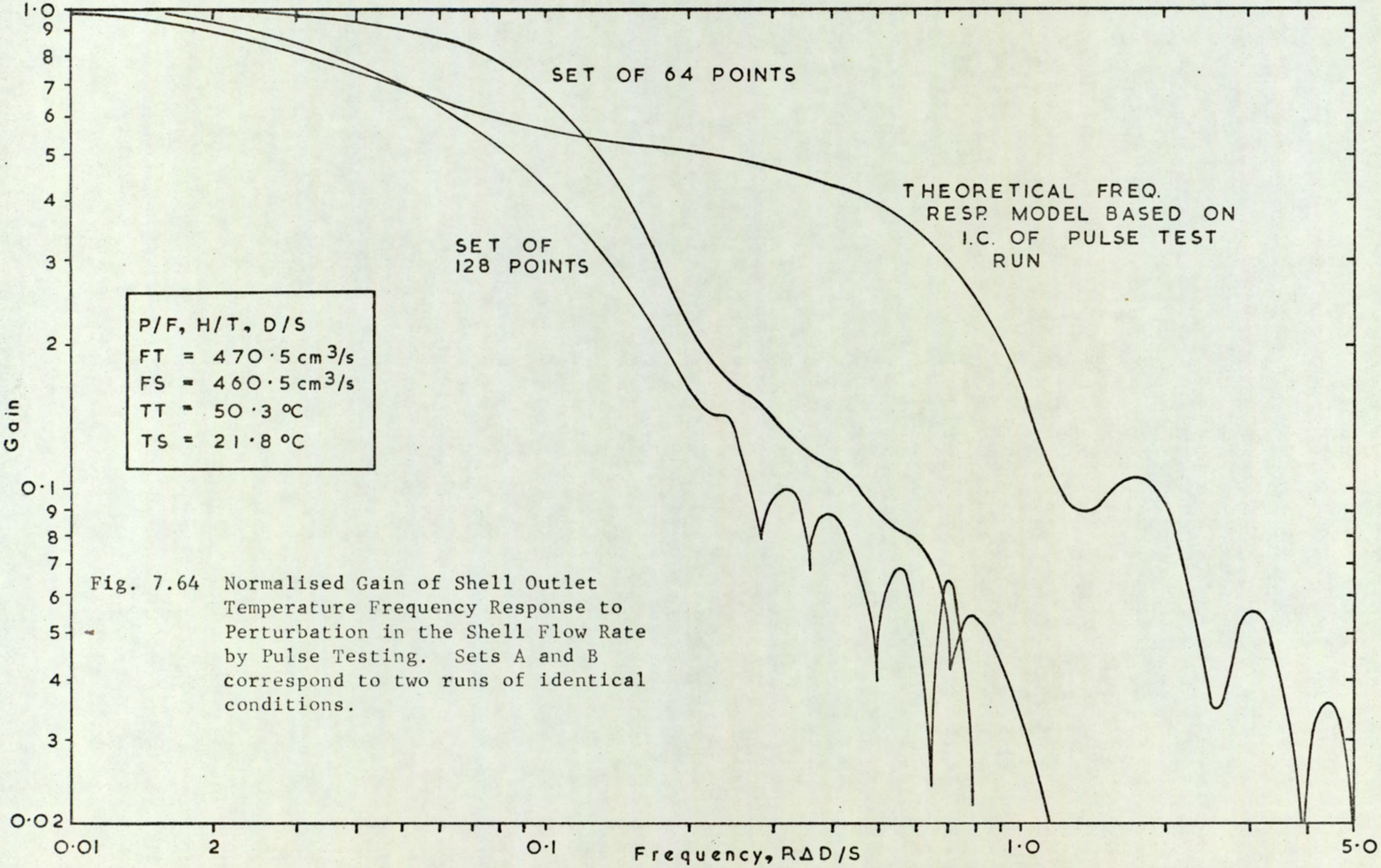

Fig. 7.64 Normalised Gain of Shell Outlet Temperature Frequency Response to Perturbation in the Shell Flow Rate by Pulse Testing. Sets A and B correspond to two runs of identical conditions.

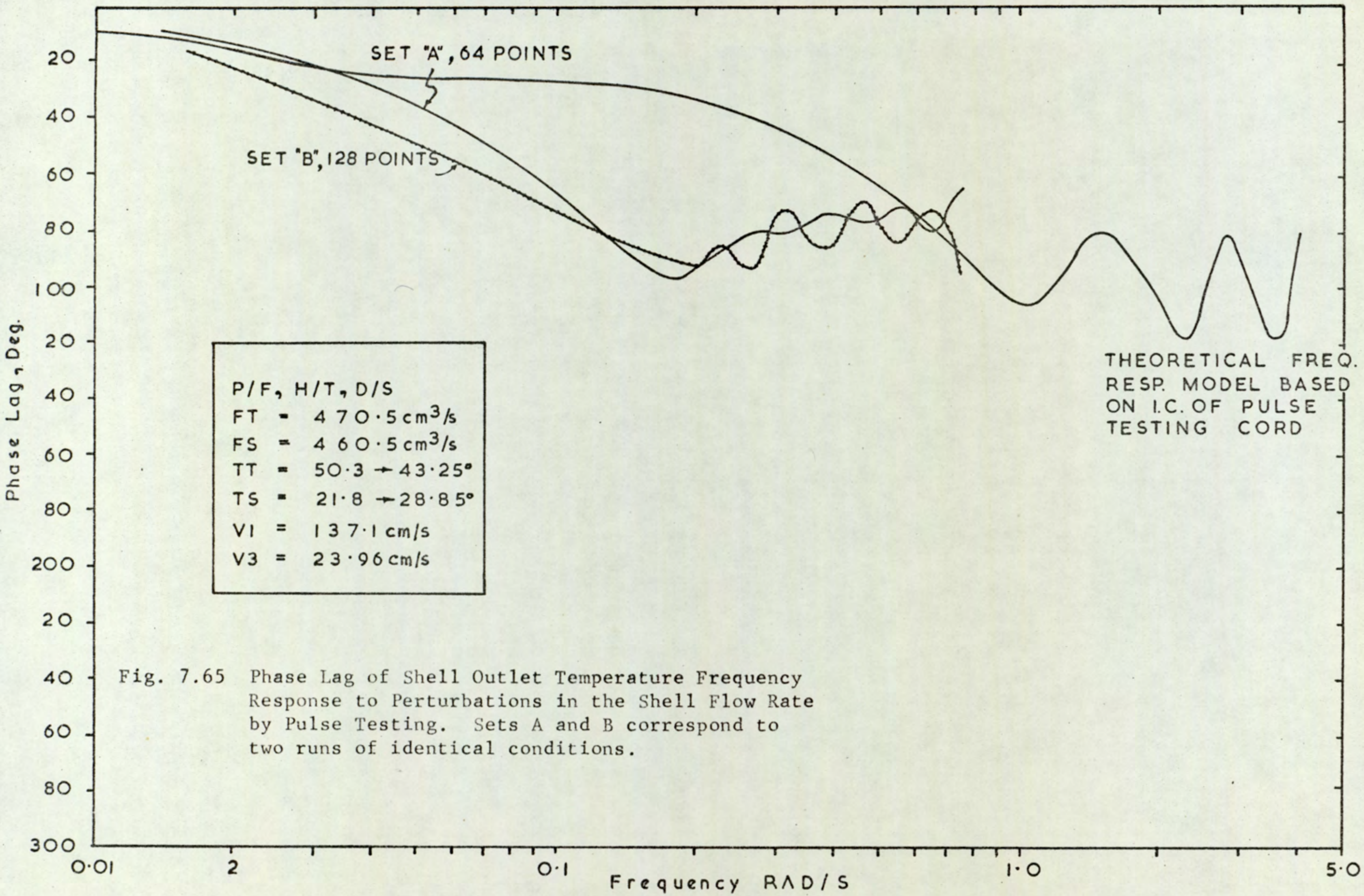

Fig. 7.65 Phase Lag of Shell Outlet Temperature Frequency Response to Perturbations in the Shell Flow Rate by Pulse Testing. Sets A and B correspond to two runs of identical conditions.

CHAPTER 8

CONCLUSIONS AND RECOMMENDATIONS

The analysis of the experimental data generated in this work and the comparison with the predictions obtained by the numerical solutions of the mathematical model of the heat transfer process between fluids has lead to the following general conclusions:

8.1 CONCLUSIONS

8.1.1 Verification of the Theoretical Principle

The multivariable heat transfer process can be represented by adaptation of single variable techniques. This representation consists of combining the simultaneous disturbances to the process and generating a response in which the individual effects are combined following the principles of linear system theory. The procedure is equally valid for the time domain and the frequency domain.

In this work the behaviour of a single-flow disturbed as well as simultaneously two-flow disturbed heat exchanger was equally simulated in the time domain and in the frequency domain without significant difference between the two types of disturbance, except for the lower static gains exhibited by the responses of the multivariable one.

8.1.2 Advantages of the Numerical Solution

The fact that the actual solution of the mathematical model is carried out by numerical methods in the time domain has permitted a more realistic representation of the process by incorporating in the model other components of the system, in this case the control valve's transient response, than would have been possible by a fully analytical solution.

8.1.3 Frequency Response Out of the Transient Non-linear Model

Because frequency response is by definition the result of relating the time response to the quasi-steady sinusoidal disturbances, any satisfactory time-domain model must be also a satisfactory way to evaluate the frequency response. The limited amount of sinusoidal data collected for that purpose indicated that, effectively, gain and phase lag can be predicted as functions of frequency, using the time domain model presented in this work. This opens the possibility of verifying the adequacy of frequency response models, developed by use of the Laplace transformation technique, by using non-linear time domain models. Since the latter can be less restricted, in the mathematical sense, than the former, they must provide a more realistic representation of the process behaviour under periodic disturbances of different frequencies. Obviously, this has to be achieved at the cost of additional work and computer time to analyse the large amount of numerical results generated in the time domain. However, the drudgery of evaluating data for the Bode plots can be avoided by including it in the computer program.

8.1.4 Time Response of the Heat Transfer Process Between Two Fluids at Low Level Reynolds Number

The dynamics of the heat transfer process between two fluids, in the region of low Reynolds number, i.e. laminar and transitional zones, is amenable to analysis by methods analogous to those used for the fully turbulent region. The results indicated that whenever the steady state was well represented by the model, so was the transient response. This implies that the degree of the prediction achieved at low Reynolds number for the transient regime depends mainly on how accurately the correlations used can predict the individual heat transfer coefficients, rather than on the heat transfer mechanism incorporated in the model.

8.1.5 Frequency Response of the Heat Transfer Process Between Two Fluids at Low Reynolds Number

The prediction of the frequency response of the heat exchange process by the model proposed is less satisfactory, especially for the shell side. Since the quasi steady state of the sustained cyclic operation of the system is hydrodynamically and thermally more complex due to the periodic change and inversion of the velocity and temperature gradients along the heat exchanger, it is apparent that the thermal diffusion becomes more important in the overall heat transfer mechanism, and is in itself differently affected by the flow patterns in both sides of the exchanger.

8.2 RECOMMENDATIONS

Several areas of interest look the obvious directions in which research in this field of heat exchange process dynamics should be directed. All the steps suggested here are closely interlinked but can be carried out independently of each other.

8.2.1 Extension of the Model to Include Temperature Disturbances

By addition of temperature disturbances to the present structure of the flow disturbed process the model can be expanded to have a multi-variable process fully disturbed in the input signal vector. This would provide a very powerful tool of analysis because the system could be simulated under all possible sets of load variations.

8.2.2 Inclusion of Thermal Dispersion in the Time Domain Model

A parallel model including the effect of thermal dispersion can be developed to compare the accuracy of the representation achieved by the fully convective and the convective-diffusive models. Only in this way can the extension of the contribution of the diffusion mechanism to the overall heat transfer process be evaluated.

8.2.3 Effect of the Thermal Dispersion on the Frequency Response Model

It is equally important to investigate the frequency response of the system using the convective-diffusive model to compare results with those obtained from the fully convective model in order to evaluate the contribution of the thermal dispersion in the frequency domain, through linearised mathematical descriptions.

8.2.4 Frequency Response Using Time Domain Models

It is very important to make a full study of the frequency response of the process using the time domain model because of its potential advantage over the conventional method of the transfer function. If the method were successful it would allow evaluation of the deviation introduced by linearisation in the prediction of frequency response of nonlinear systems.

8.2.5 Further Research in the Transitional Region

The investigation of the fluid flow steady state heat transfer in the transitional region of the Reynolds number domain still deserves a considerable amount of work. An accurate prediction of the heat transfer in this zone requires a better knowledge of its thermal characteristics. Since there is a substantial gap between the correlations used for the prediction of entry length in the laminar and the turbulent regions.

BIBLIOGRAPHY

1. Arpaci, V.S. and Clark, J.A. - 'Dynamic Response of Heat Exchangers Having Internal Heat Sources - Part II'. Trans. A.S.M.E., 80 : 625/34 (1958).

2. Ibid, 'Dynamic Response of Heat Exchangers Having Internal Heat Sources - Part III', Journal of Heat Transfer, Trans. A.S.M.E. Series C, 81 : 253/66 (1959).

3. Axon, A.G. - 'The Dynamic Behaviour and Control of a Steam-heated Multipass Exchanger', Ph.D. Thesis, Victoria University of Manchester (1963).

4. Beckman, L.V.A. - 'Unsteady State Simulation and Control Study of a Counterflow Distributed Parameter System: The Double Pipe Heat Exchanger'. Ph.D. Thesis, Tulane University, Anarbor (1969).

5. Bell, K.J. - Final Report of the Co-operative Research Program on Shell and Tube Heat Exchanger, Bulletin No.5, University of Delaware (1963).

6. Bergelin, O.P., Bell, K.J. and Leighton, M.D. - 'Heat Transfer and Fluid Friction During Flow Across Banks of Tubes - VI : The Effect of Internal Leakages Within Segmentally Baffled Exchangers'. Trans. A.S.M.E, paper No.56-A-133 : 53/60 (1956).

7. Bristol, E.S. and Peters, J.C. - 'Some Fundamental Considerations in the Application of Automatic Control to Continuous Processes', Trans. A.S.M.E., 60 : 641/50 (1938).

8. (The) British Shipbuilding Research Association - 'A Correlation of Current Data on Heat Transfer and Pressure Drop in Segmentally Baffled Shell-and-Tube Heat Exchangers'. Report No.148 (1955).

9. Bundy, A.R., M.Sc. Thesis, Tulane University, New Orleans (1960).

10.Campbell, D.P., PROCESS DYNAMICS, John Wiley and Sons, Inc., New York (1958).

11.Catheron, A.R., Goodhue, S.H. and Hansen, P.D. - 'Control of Shell and Tube Heat Exchangers', Unpublished A.S.M.E. paper 59-IRD-14 (1959).

12.Chao, Y.C. - 'The Study of Optimal Model Reference Adaptive Control of a Continuous Stirred Tank Reactor Using an On-line Hybrid Computer', Ph.D. Thesis, Aston University (1972).

13.Cima, R.M. and London, A.L. - 'The Transient Response of a Two-fluid Counterflow Heat Exchanger - The Gas Turbine Regenerator', Trans. A.S.M.E., 80 : 1169/81 (1958).

14.Clark, J.A., Arpaci, V.S. and Treadwell, K.M. - 'Dynamic Response of Heat Exchangers Having Internal and Heat Sources - Part 1', Trans. A.S.M.E., 80 : 612/24 (1958).

15.Cohen, W.C. and Johnson, E.F. - 'Dynamic Characteristics of Double-Pipe Heat Exchangers', I. & E.C., 48, N6 : 1031/4 (1956).

16.Ibid - 'Distributed Parameter Process Dynamics', Chem.Eng. Prog. Symp. Ser., 36, N57 : 86/99 (1961).

17.Coughanowr, D.R. and Koppel, L.W. - PROCESS SYSTEM ANALYSIS AND CONTROL', 87, Mc Graw Hill Book Co. - Kogakusha Co., Tokyo (1965).

18.Debolt, R.R. - 'Dynamic Characteristics of a Steam-Water Heat Exchanger', M.Sc. Thesis, University of California, Berkeley (1954).

19.Draper, C.S., Mc Kay, W. and Lees, S. - INSTRUMENT ENGINEERING - 2, Mc Graw Hill Book Co., New York (1953).

20. Dusinberre, G.M. - 'Calculations of Transient Temperature in Pipes and Heat Exchangers by Numerical Methods', Trans. A.S.M.E., 76: 421/6 (1954).

21. Eagle, A. and Ferguson, R.M. - 'On the Coefficient of Heat Transfer from the Internal Surface of Tube Walls', Proc. Roy. Soc. A127: 540/66 (1930).

22. Edwards, C.L. - 'Dynamics of a Flow Force Concentric Tube Heat Exchanger', Ph.D. Thesis, The University of Wisconsin (1960).

23. Emerson, W.H. - 'Shell-Side Heat Transfer and Pressure Drop with Turbulent Flow in Segmentally Baffled Shell-and-Tube Heat Exchangers - A Survey', N.E.L. Report No.45 (1962).

24. Finlay, I.C., - 'The Dynamic Response of Heat Exchangers to Disturbances in Flowrate', N.E.L. Report No.170 (1964).

25. Ibid - 'Determining the Dynamic Response of Heat Exchangers', C.E.P., Heat Transfer Survey : 142/50 (1966).

26. Finlay, I.C. and Dalgleish, N. - 'The Response of Single and Two-Pass Heat Exchangers to Disturbances in Flow Rate', N.E.L. Report No.206 (1965).

27. Fisher, D.G. - 'Frequency Response of Flow Forced Heat Exchangers', Ph.D. Thesis, The University of Michigan (1965).

28. Fisher, D.G. and Kadlec, R.H. - 'Effect of Reynolds and Prandtl Number on the Frequency Response of Concentric Tube Heat Exchangers', The Can. J. of Ch.Eng., 48 : 393/8.

29. Ibid - 'Frequency Response of Different Size Concentric Tube Heat Exchangers', The Can. J. of Ch. Eng., 48 : 398/404 (1970).

30. Flaherty, F.T. - 'The Transient Response of a Crossflow Heat Exchanger', M.Sc. Thesis, Massachussets Institute of Technology (1958).

31. Foust, A.S., Wenzel, L.A., Clump, C.W., Mans, L. and Andersen, L.B. - PRINCIPLES OF UNIT OPERATIONS : 162, John Wiley & Sons, Inc. (1960).

32. Friedley, J.C. - 'Asymptotic Approximations to Plug Flow Process Dynamics', Joint Automatic Control Conference, University of Pennsylvania (1967).

33. Gaither, P.H., Mc Cann, M.J. and Taft, C.K. - 'Analog and Mathematical Models of Distributed Parameter Systems', I.S.A. Conference, Reprint No.34-1-65 (1965).

34. Gay, B. and Williams, T.A. - 'Heat Transfer on the Shell-Side of a Cylindrical Shell-and-Tube Heat Exchanger Fitted with Segmental Baffles - I', Trans. of the Inst. of Chem.Eng., 46 : T95 (1968).

35. Gay, B. and Roberts, P.C.O. - 'Heat Transfer on the Shell-Side of a Cylindrical Shell-and-Tube Heat Exchanger Fitted with Segment Baffles - II', Trans. of the Inst. of Chem. Eng., 48 : T3 (1970).

36. Gould, L.A. - 'The Dynamic Behaviour and Control of Heat Transfer Processes', Sc.D. Thesis, M.I.T. (1953).

37. Ibid - 'Approximation of the Dynamic Behaviour of Heat Exchangers', Ingeniøren N30 : 825/30 (1957).

38. Ibid - CHEMICAL PROCESS CONTROL - THEORY AND APPLICATIONS, Addison-Wesley Pub. Co. (1969).

39. Gutierrez, H.J. - 'Dynamic Analysis of a Heat Exchanger Subject to Simultaneous Disturbances, M.Sc.Thesis, Aston University (1973).

40. Haigler, E.D. - 'Application of Temperature Controllers', Trans. A.S.M.E., 60 : 633/40 (1938).

41. Harriott, P. - PROCESS CONTROL, Ch.11, Mc Graw Hill Book Co., New York (1964).

42. Hearn, J.S. - 'The Dynamic Response of a Heat Exchanger to Shell-Side Flow Rate Disturbances', M.Sc. Thesis, St. Louis University (1959).

43. Herron, E.H. Jr. - 'Distributed Parameter System Dynamics - The Double Pipe Heat Exchanger', Ph.D. Thesis, Tulane University (1964).

44. Hougen, J.D. and Walsh, R.A. - 'Pulse Testing Method', Chem.Eng. Prog. Symp. Ser., 57, N36 : 74/84 (1961).

45. Hriber, E,J. - 'The Dynamic Response of a Heat Exchanger to Shell Side Fluid Temperature Disturbances', M.Sc. Thesis, St. Louis University (1960).

46. Hsu, J.P. - 'Frequency Response of a 1-2 Multipass Heat Exchanger', Ph.D. Thesis, University of Cincinnatti (1961).

47. Hsu, J.P. and Gilbert, N. - 'Transfer Functions of Heat Exchangers', A.I.Ch.E.J., 8, N5 : 593/8 (1962).

48. Iscol, L. -'Frequency Response of Shell and Tube Heat Exchangers', Ph.D. Thesis, University of Wisconsin, Madison (1959).

49. Isom, K.B. - 'The Effect of Flow Variations on the Dynamics of a Liquid-Liquid Heat Exchanger', Ph.D. Thesis, North Western University, Evanston (1963).

50. Johnson, E.C. - 'Sinusoidal Analysis of Feedback-Control System Containing Non-Linear Elements,' AIEE Trans. 71, Part II

(Applic. and Ind.) : 169/81 (1952).

51. Kamman, D.T. -'Dynamic Response of a Flow Forced Heat Exchanger to Step Changes in Velocity', M.Sc. Thesis, Purdue University, Lafayette (1966).

52. Kamman, D.T. and Koppel, L.B. - 'Dynamics of a Flow Forced Heat Exchanger - Experimental Considerations', I. & E.C. Fund., 5, N2 : 208/11 (1966).

53. Keller, R.B. - 'The Dynamic Response of a Heat Exchanger with Constant Internal Heat Generation to Several Types of Fluid Velocity Transients', Ph.D. Thesis, University of Michigan (1962).

54. Kern, D.Q. - PROCESS HEAT TRANSFER, Mc Graw Hill Book Co., New York (1950).

55. Koppel, L.B. - 'Dynamics of a Flow Forced Heat Exchanger', I. & E.C. Fund., 1, N2 : 131/4 (1962).

56. Ibid - 'Dynamics and Control of a Class of Non-linear Tubular, Parametically Forced Heat Exchangers and Chemical Reactors', I. & E.C. Fund. 5, N3 : 403/13 (1966).

57. Ibid - 'Control of Tubular Heat Exchangers and Chemical Reactors by Piecewise Constant Manipulation of Flow Rate', I. & E.C. Fund. 5, N3 : 413/22 (1966).

58. Lapidus, L. - DIGITAL COMPUTATION FOR CHEMICAL ENGINEERS, Mc Graw Hill Book Co., New York (1962).

59. Law, W.M. - 'The Dynamic Response of Shell-and-Tube Heat Exchangers to Flow Changes', Newe Technik, 4(½) : 34/44 (1962).

60. Lees,S and Hougen, J.O. - 'Pulse Testing a Model Heat Exchanger Process', I. & E.C., 48, N6 : 1064/8 (1956).

61. Leonhard, A. - 'Determination of Transient Response from Frequency Response', Frequency Response Symposium, Trans.A.S.M.E. 76, 215/36 (1954).

62. Madsen, N. - 'Design Heat Exchangers for Liquids in Laminar Flow', Chem. Eng., August 19th : 92/8 (1974).

63. Mason, C.E. - 'Quantitative Analysis of Process Lags', Trans. A.S.M.E., 60 : 327/34 (1938).

64. Masubuchi, M. - 'Dynamic Response and Control of Multipass Heat Exchangers', Unpublished paper A.S.M.E., 59-IRD-6 (1959).

65. Mc Adams, W.H. - HEAT TRANSMISSION, Mc Graw-Hill Book Co., New York (1954).

66. Mc Cann, M.J. - 'Control of Distributed Parameter Systems', Ph.D. Thesis, University of London (1963).

67. Morris, H.J. - 'The Dynamic Response of a Heat Exchanger to Inlet Temperature Disturbances', M.Sc. Thesis, St. Louis University (1959).

68. Ibid - 'Dynamic Response of Shell and Tube Heat Exchangers to Temperature Disturbances' in AUTOMATIC AND REMOTE CONTROL, 4, : 354/ , Butterworth and Co., London (1961).

69. Mozley, J.M. - 'Predicting Dynamics of Concentric Pipe Heat Exchangers', I. & E.C., 48, N6 : 1035/41 (1956).

70. Narayan, K. - 'Local and Overall Heat Transfer Coefficients in Baffled Heat Exchangers', Ph.D. Thesis, Oregon State University, (1962).

71. Nyquist, J.K., Schnidler, R.N. and Gilbert, R.E. - 'Determination of Frequency Response from Step Response', C.E.P. Symp. Ser., 59, N46 : 98/105 (1963).

72. Paschkis, V. and Hlinka, J.W. - 'Electric Analogy Studies of the Transient Behaviour of Heat Exchangers', Trans. New York Academy of Sciences, Series II, 19, N8 : 714/30 (1957).

73. Paynter, H.M. and Takahashi, Y. - 'A New Method of Evaluating Dynamic Response of Counterflow and Parallel Heat Exchangers', Trans.A.S.M.E., 78 : 749/58 (1956).

74. Perry, J.H. (Editor) - CHEMICAL ENGINEERS HANDBOOK', 3rd Edn., Mc Graw-Hill Book Co. (1950).

75. Privott, W.J. - 'Analyses of Flow Forced, Concentric Tube Heat Exchangers'. Ph.D. Thesis, University of North Carolina (1964).

76. Privott, W.J. and Ferrel, J.K. - 'Dynamic Analysis of a Flow Forced, Concentric Tube Heat Exchanger', C.E.P. Symp. Ser., 62, N64 : 200/8 (1966).

77. Profos, P. and Diss, E.T.H. - 'Die Behandlung von Regelproblem Vermittels des Frequenzganges des Regelkreises'. Zurich (1943).

78. Rizika, J.W. - 'Thermal Lags in Flowing Systems Containing Heat Capacitors'. Trans. A.S.M.E., 76 : 411/20 (1954).

79. Rodehorst, C.W. - 'A One Dimensional Dispersion Model for Transient Heat Transfer in Turbulent Flow', Ph.D. Thesis, Tulane University, New Orleans (1969).

80. Rosenbrock, H.H. - 'The Transient Behaviour of Distillation Columns and Heat Exchangers - An Historical and Critical Review'. Trans. Inst. of Chem. Eng., 40 : 376/83 (1962).

81. Short, B.E. - 'Shell and Tube Exchangers : Effect of By-Pass and Clearance Streams on the Main Stream Temperature'. A.S.M.E. paper No.60-HT-16 (1960).

82. Sieder, E.N. and Tate, G.E. - 'Heat Transfer and Pressure Drop of Liquids in Tubes'. I. & E.C., 28 : 1429/34 (1936).

83. Smith, C.L., Pike, R.W. and Murril, P.W. - FORMULATION AND OPTIMIZATION OF MATHEMATICAL MODELS, International Textbook Co., Scranton, Penn. (1970).

84. Stainthorp, F.P. and Axon, A.G. - 'The Dynamic Behaviour of a Multi-pass Steam-Heated Exchanger - I : Response to Steam Temperatures and Steam Flow Perturbations'. Ch. Eng. Sc., 20 : 107/19 (1965).

85. Stermole, F.J. - 'The Dynamic Response of Flow Forced Heat Exchangers'. Ph.D. Thesis, Iowa State University of Science and Technology, Ames (1963).

86. Stermole, F.J. and Larson, M.A. - 'Dynamic Response of Heat Exchangers to Flow Rate Changes'. I. & E.C. Fund., 2, N1 : 62/7 (1963).

87. Takahashi, Y. - ' Transfer Function Analysis of Heat Exchange Process' in AUTOMATIC AND MANUAL CONTROL (A.Tustin, Editor) : 235/45, Butterworths, London (1952).

88. Taylor, Sir Geoffrey - 'Dispersion of Soluble Matter in Solvent Flowing Slowly Through a Tube', Proc. Roy. Soc., A219 : 186/203 (1953).

89. Ibid - 'The Dispersion of Matter in Turbulent Flow Through a Pipe'. Proc. Roy. Soc. A223 : 443/68 (1954).

90. Ibid - 'Conditions Under Which Dispersion of a Solute in a Stream of Solvent can be Used to Measure Molecular Diffusion'. Proc. Roy. Soc., A225 : 473/7 (1954).

91. Thal-Larsen, H. - 'Dynamics of Heat Exchangers and Their Models', Trans. A.S.M.E., Journal of Basic Eng. : 489/504 (1960).

92. Tinker, T. - 'Shell Side Heat Transfer Characteristics of Segmentally Baffled Shell and Tube Heat Exchangers'. Reprint of Paper presented at the A.S.M.E. Annual Meeting (1947).

93. Vincent, G.C. - 'On the Dynamic Response of a Baffled Shell and Tube Heat Exchanger to Shell Flow Disturbances'. M.Sc. Thesis, St. Louis University (1960).

94. Vincent, G.C., Hougen, J.O. and Dreifke, G.E. - 'Fluid Mixing in Shell and Tube Heat Exchangers', C.E.P., 57 N7 : 48/52.

95. Whitaker, S. -'Forced Convection Heat Transfer Correlations for Flow in Pipes, Past Flat Plates, Single Cylinders, Single Spheres and Flow in Packed Beds and Tube Bundles', A.I.Ch.E. J., 18, N2 : 361/71 (1972).

96. Williams, T. and Morris, H. - 'A Survey of the Literature on Heat Exchanger Dynamics and Control', C.E.P. Symp. Ser., 57, N36 : 20/ (1961).

97. Yang, W.J. - 'The Dynamic Response of Heat Exchangers with Sinusoidal Time-Dependent Internal Heat Generation'. Ph.D. Thesis, University of Michigan (1960).

98. Ibid - 'Transient Heat Transfer in Vapour-Heated Heat Exchanger with Arbitrary Timewise-Variant Flow Perturbations'. Trans. A.S.M.E., Journal of Heat Transfer : 133/42 (1964).

99. Yang, W.J., Clark, J.A. and Arpaci, V.S. - 'Dynamic Response of Heat Exchangers Having Internal Heat Sources - Part IV'. Trans. A.S.M.E., Journal of Heat Transfer : 321/32 (1961).

NOMENCLATURE

a = Dimensionless (dl) group defined in equation (5.19); magnitude of velocity step change (Ch.3), dl.

A = Coefficient matrix, eqn. (3.18); total heat transfer area, cm^2; maximum sinusoidal amplitude, dl.

A_1, A_2 = Coefficients of the tube-side temperature, steady state analytical solution, dl.

$a_1 \ldots a_n$ = Constant coefficients of a linear mathematical description.

a_5 = Dimensionless group defined in equation (5.41).

a_6 = Heat transfer units, dl.

A_b = Net flow area through the baffled window, cm^2.

A_c = Clearance area between baffle and shell wall, cm^2.

A_e = Specific area, cm^2/g.

A_m = Maximum crossflow area between baffles, cm^2.

A_p = Minimum crossflow area between baffles, cm^2.

B = Coefficient matrix, eqn.(3.18).

B_1, B_2 = Coefficients of the shell side temperature, steady state analytical solution, dl.

C = Specific heat, cal/g. ^oC.

C_{min} = Minimum heat capacity of fluid, cal/^oC.

C_{max} = Maximum heat capacity of fluid, cal/^oC.

C_W^* = C_W/C_{min}, wall capacity ratio, eqn. (3.11), dl.

d = Tube diameter, cm.

D = Shell diameter, cm.

$\mathfrak{D}$ = Dispersion coefficient.

D_f = Driving temperature Vector, eqn.(3.18).

e = Base of natural logarithms, dl.

E_1, E_2 = Potentiometer settings defined in Fig.5.1, dl.

f = Dimensionless group defined in equation (5.14); heat transfer coefficient correction factor dl

F = Fourier transform operator

F_1 = Tube arrangement factor, eqn.(4.2d), dl.

F_2 = Clearance ratio factor, eqn.(4.2e), dl.

F_3 = End space factor, eqn. (4.2f), dl.

G = Mass flow rate, g/s.

h = Actual individual heat transfer coefficient, $cal/cm^2.s.^oC$.

H = Normalized heat transfer coefficient, dl.

i = Abscisa in distance-time plane, dl.

I = Magnitude of input signal, eqn.(3.13).

j = $\sqrt{-1}$; Ordinate in distance-time plane, dl.

k = Thermal conductivity $cal/cm.s.^oC$.

K_o = Constant group defined in equation (4.18).

l = Distance from entry point, boundary layer development, cm.

L, L_1 = Total length of heat exchanger, cm., Tag defined in page 157.

L_2 = Length between end baffles, cm.

L_3 = Space between adjacent baffles, cm.

L_e = Entry length, of boundary layer, cm.

n = Reynolds Number exponent in heat transfer coefficient correlation, dl.

N = Heat transfer units (Ch.3), dl; number of tubes in the bundle, dl.

N_u = Nusselt number, eqn.(4.2a), dl.

O = Magnitude of output signal, eqn.(3.13).

P = Pitch in tube arrangement, cm; oscillation period, s.

P_1 to P6 = P.D.E. coefficients defined in equations (4.33a) to (4.33f).

P_r = Prandtl number, eqn.(4.2c), dl.

Q = Total heat flow across the exchange surface, cal/s.

R = Tube radius, cm.

r_1, r_2 = Roots of the characteristic equation, dl.

R^* = R_{min}/R_{max}, heat transfer resistance ratio, eqn.(3.11), dl.

Re = Reynolds number, eqn. (4.2b), dl.

s = Complex Laplace transform variable, s^{-1}.

S_1, S_2 = Flow transverse area, cm^2.

t = Normalized time, dl.

T = Normalized bulk temperature, dl.

t' = Actual time, s.

T' = Actual bulk temperature, ^oC.

$\overline{T}$ = Temperature Laplace transform.

T_a = Skew time of step response relative to distance velocity lag (L_1) of tube side response, eqn.(3.6), s.

T_m = Mean delay of step response relative to L_1, eqn.(3.6, s.

T_s = Dispersion time of step response relative to L_1, eqn.(3.6), s.

U = Overall heat transfer coefficient, $cal/cm^2.s.^oC$.

v = Steady state velocity ratio, dl.

V = Normalized fluid bulk velocity, dl.

V' = Actual fluid bulk velocity, cm/s.

W = Mass flow rate (Ch.3), gm/s.

x^* = x/L, dimensionless flow length, eqn.(3.11).

Y = Normalized control valve response, dl.

z = Normalized distance along the heat exchanger, dl.

z' = Actual distance along the heat exchanger, cm.

GREEK LETTERS

α = Coefficient of skew, eqn.(3.8), dl.

δ = Static gain (s.s. change in output/s.s. change in input), equation (3.6), dl.

ρ = Density, gm/cm^3.

Δ = Fractional change.

θ^* = θ/θ_d, normalized time, eqn.(3.11).

Θ_d = $\theta_{dmin}/\theta_{dmax}$, dwell time ratio, eqn.(3.11), dl.

μ = Coefficient of variance (Ch.3), dl; fluid viscosity, gf/cm.s.

π = 3.1416

τ = Residence time, s.

Φ = Phase lag angle, deg.

ω = Angular frequency, rad/s.

SUBSCRIPTS

o = At initial point.

1 = Tube fluid condition.

2 = Shell fluid condition.

b = Bulk condition.

D = Deviation.

E = Eddy effect.

F = Related to fluid

I = Inside tube.

L = At the end point of the heat exchanger.

M = Molecular effect.

O = Outside tube.

R = Reference

S = Steam condition; shell condition.

SS = Steady state.

T = Taylor effect; tube condition.

W = Wall condition.

Note: The identification of the encoded operating conditions used in the figures of Chapter 7 is given in footnote of page 117.

APPENDIX A

CALIBRATION CURVES

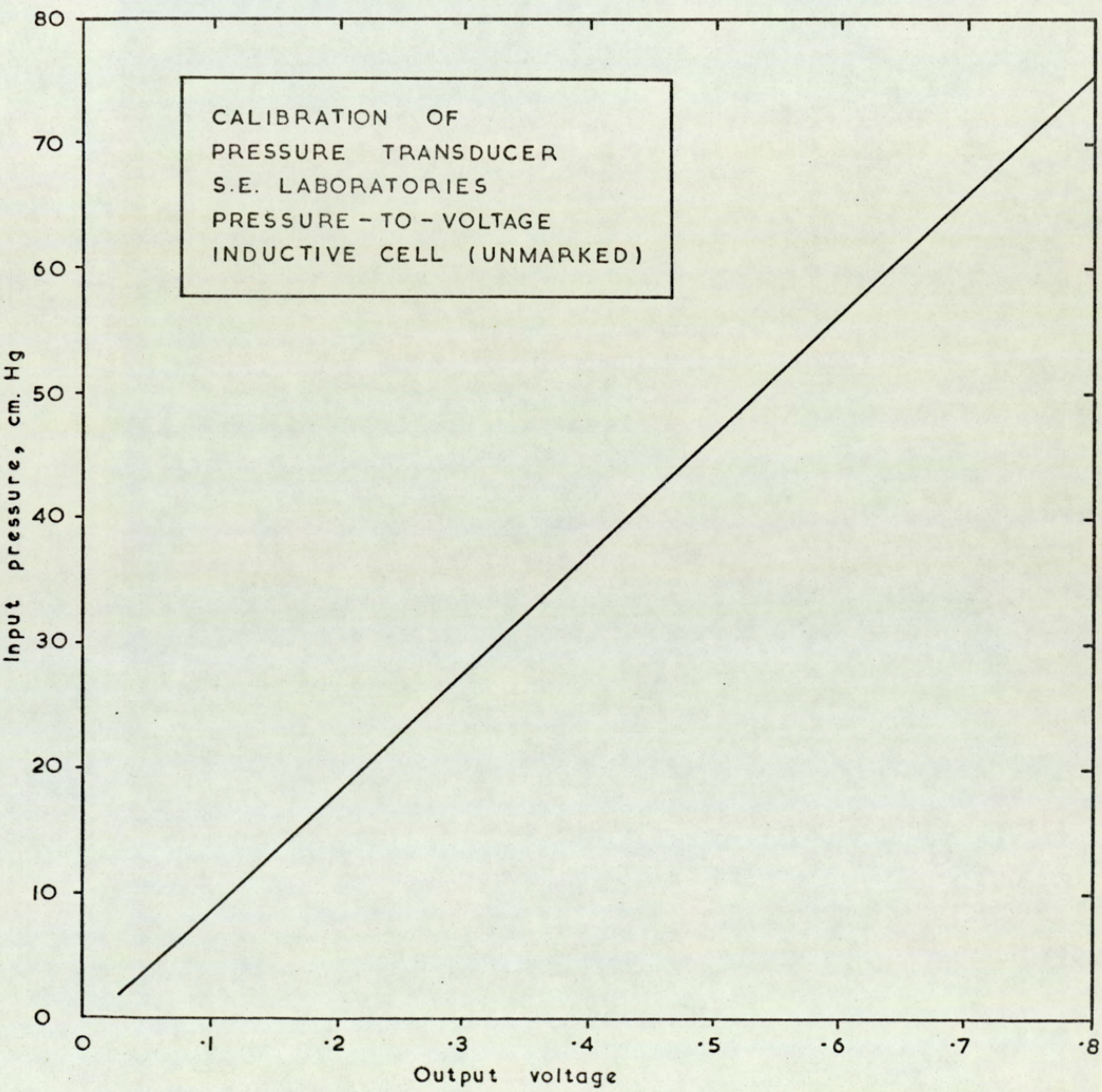

Fig. A-1 Calibration of Pressure Transducer

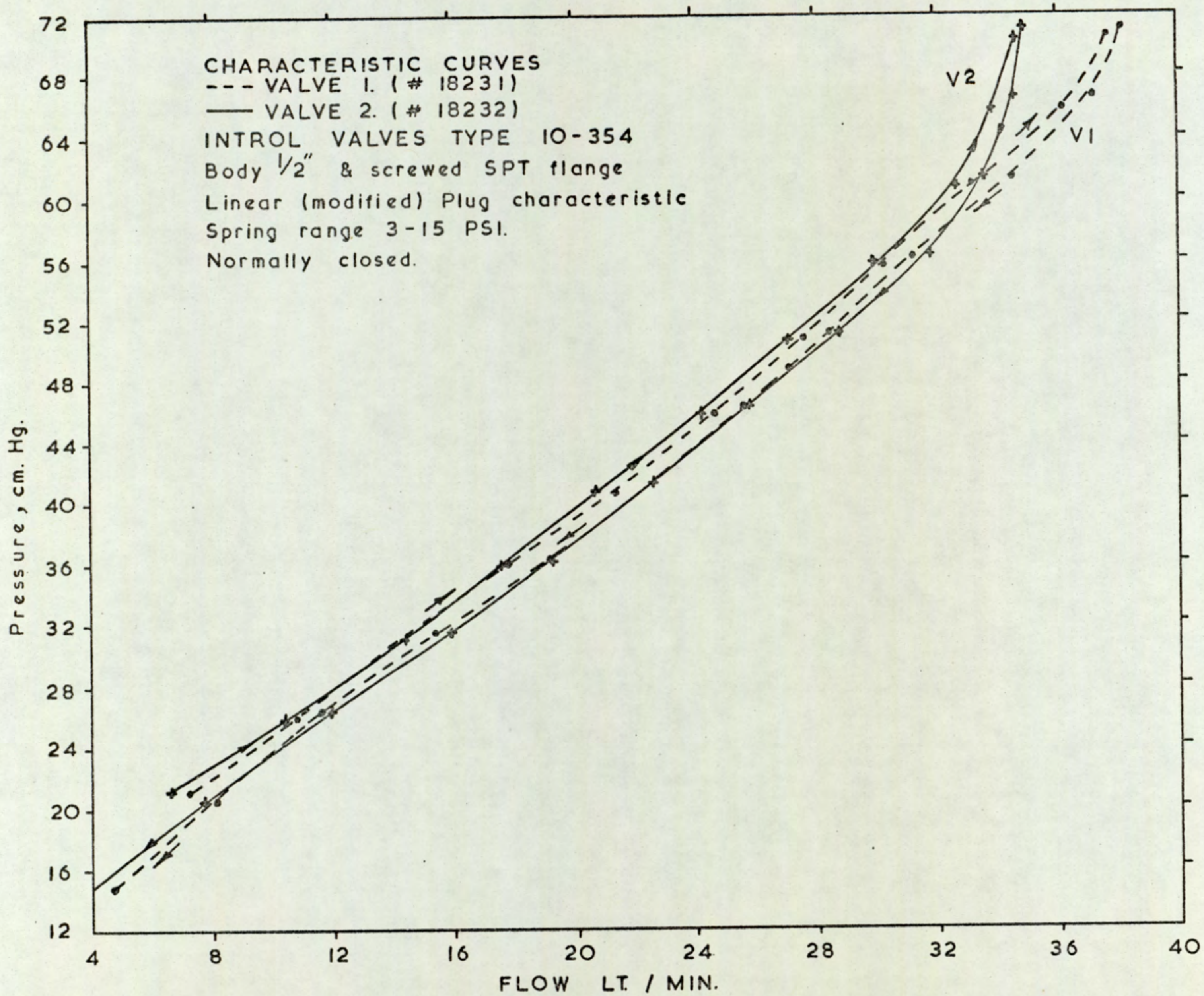

Fig. A-2 Characteristic Curves of Pneumatic Control Valves

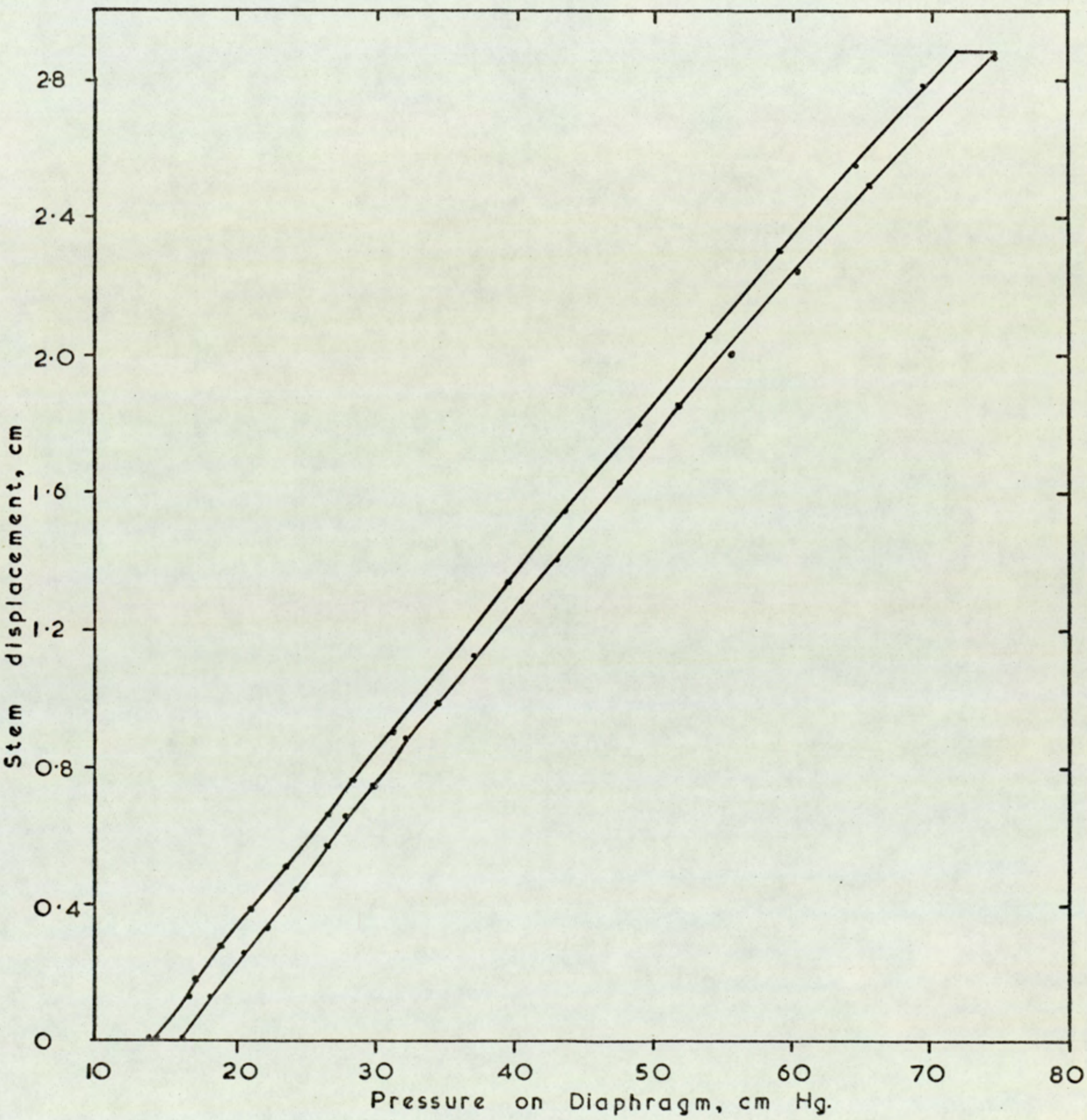

Fig. A-3 Hysteresis Curve of Control Valves

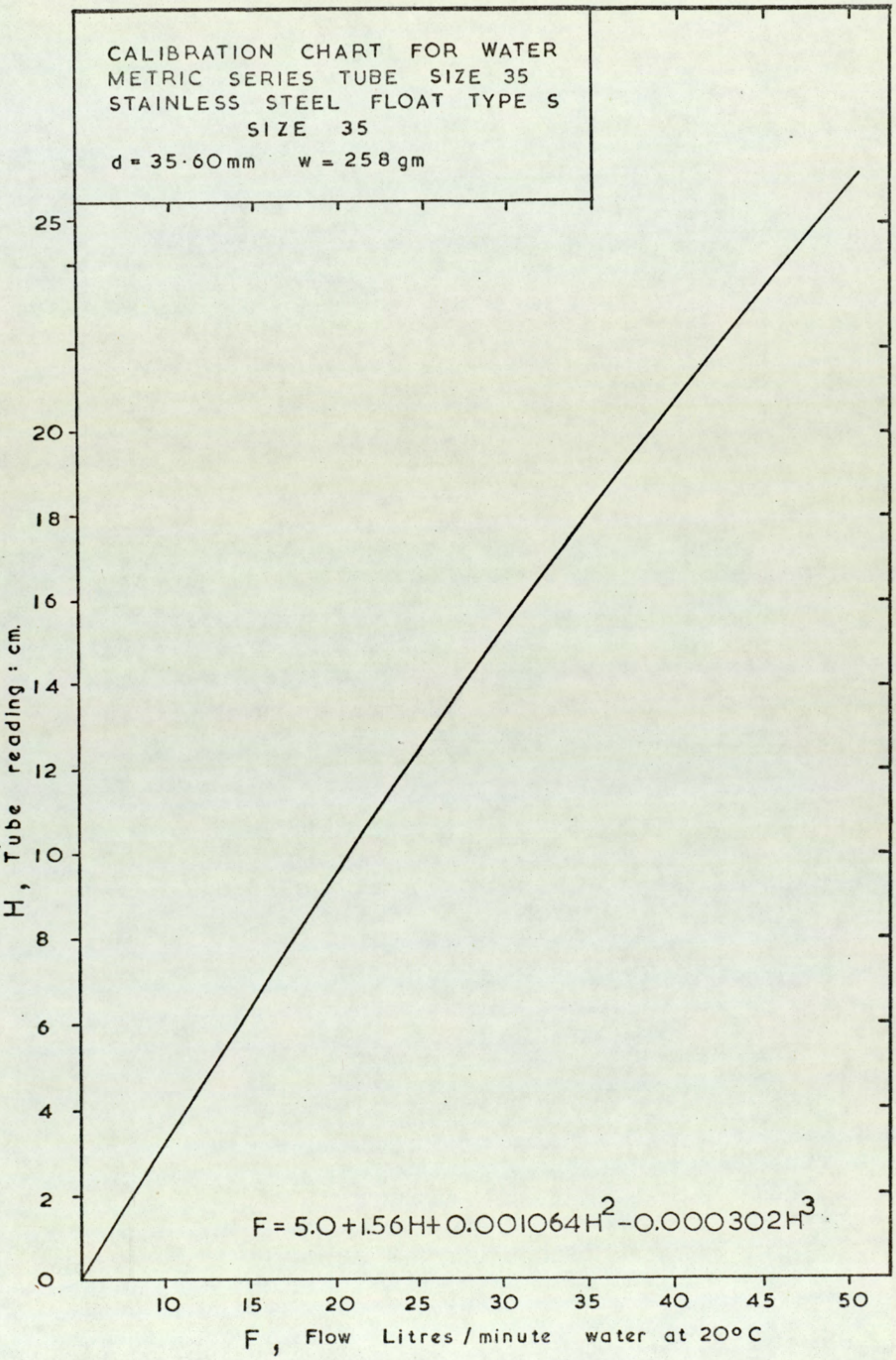

Fig. A-4 Rotameters Calibration

APPENDIX B

COMPUTER PROGRAMS

This Appendix presents the listing of the digital computer algorithm developed to simulate the heat exchange process in the time domain and in the frequency domain.

The time domain program includes the subroutines THTCØE, SHTCØE, VSCTEM and DISTURB of which the first three are also used in the frequency domain program. They have been omitted in the second listing.

Enough comment cards have been included to explain the meaning of most of the parameters and variables used, and the calculations intended; wherever possible the same nomenclature was used in both algorithms.

The listing of the time domain program corresponds to the block diagram of Fig. 5.4.

```
C     TIME DOMAIN SOLUTION OF HEAT EXCHANGER MODEL
C     SYSTEM OF FOUR PARTIAL SIMULTANEOUS DIFFERENTIAL EQUATIONS
C     CENTRAL FINITE DIFFERENCES FOR THE DISTANCE DERIVATIVES
C     FIRST ORDER BACKWARD FINITE DIFFERENCES FOR TIME DERIVATIVES
C     SUBSCRIPTS 1,2,3,4 REFER TO TUBE FLUID,TUBE WALL,SHELL FLUID
C     AND SHELL WALL RESPECTIVELY,EXCEPT WHEN AFFECTING NUMERICAL
C     GROUPS OR CONSTANTS
C     T=TEMPERATURE (STREAMS AND WALLS)
C     W=MASS FLOW
C     U=VISCOSITY
C     C=SPECIFIC HEAT (1.0 FOR WATER)
C     G=DENSITY (1.0 FOR WATER)
C     Y=CONDUCTIVITY
C     V=FLUID LINEAR VELOCITY
C     H=HEAT TRANSFER COEFFICIENT
C     D=SHELL DIAMETER ; R=TUBES RADII
C     T=NUMBER OF TUBES ; XL=TOTAL H.E. LENGTH
C     NODOSX=TOTAL OF SPACE NODES ; NODOST=TOTAL OF TIME NODES
C     KFLOW = 1 MEANS COUNTERCURRENT FLOW , OTHERWISE PARALLEL FLOW
C     KUPSET = 1 MEANS STEPCHANGE DISTURBANCE OTHERWISE SINUSOIDAL
C     KVEL=1 MEANS CHANGE IN TUBESIDE VELOCITY; IF =3,CHANGE IN
C     SHELL SIDE VELOCITY AND IF =2,CHANGE IN BOTH VELOCITIES
C
C     UNITS ARE THOSE OF THE C G S SYSTEM
C
      REAL NEXPR
      DIMENSION T1(30,3),T2(30,3),T3(30,3),T4(30,3)
    1 READ (1,* ) TOTFL1,TOTFL3,TEMTUO,TEMSHL,AMP1,FREQ,TIMAX,STEPT
      READ (1,*)AMP3,FACTOR,TTOUT,TSOUT,T
    2 READ(1,* )KFLOW,NODOSX,KUPSET,KVEL,NWRITE,LEVEL
      KVBLE=KVEL
      WRITE(2,20)
   20 FORMAT (1H1,10X,  '***** R E S U L T S *****'//'   INPUT  DATA
     1     AND  INTERMEDIATE   PARAMETERS  '//)
C
C     ..........   PRINTOUT  HEADING  .........
C
      IF(KFLOW.NE.1)GO TO 68
      WRITE(2,6)
    6 FORMAT(1H0,'COUNTERCURRENT FLOW'/)
      IF(KUPSET.NE.1)GO TO 40
      WRITE(2,26)
   26 FORMAT(1H0, 'THE DISTURBANCE IS A STEP CHANGE'/)
      IF(KVBLE-2)33,33,36
   33 WRITE(2,34)
   34 FORMAT( 1H0,'THE DISTURBANCE IS IN TUBE FLOW VELOCITY'/)
      IF (KVBLE.NE.2)GO TO  99
      WRITE(2,35)
   35 FORMAT(1H0,'THE DISTURBANCE IS IN BOTH FLUID VELOCITIES'/)
   36 WRITE(2,37)
   37 FORMAT(1H0,'THE DISTURBANCE IS IN SHELL FLOW  VELOCITY '/)
      GO TO  99
```

```
   40 WRITE(2,56)
   56 FORMAT(1H0,'THE DISTURBANCE IS A SINUSOIDAL WAVE'/)
      IF(KVBLE-2)63,63,66
   63 WRITE(2,34)
      IF(KVBLE.NE.2)GO TO  99
      WRITE(2,35)
   66 WRITE(2,37)
      GO TO 99
   68 WRITE(2,69)
   69 FORMAT(1H0,' PARALLEL FLOW (CO-CURRENT)'/)
      IF(KUPSET.NE.1)GO TO 140
      WRITE(2,26)
      IF(KVBLE-2)133,133,136
  133 WRITE(2,34)
      IF(KVBLE.NE.2)GO TO  99
      WRITE(2,35)
  136 WRITE(2,37)
      GO TO  99
  140 WRITE(2,56)
      IF(KVBLE-2)163,163,166
  163 WRITE(2,34)
      IF(KVBLE.NE.2)GO TO 99
      WRITE(2,35)
  166 WRITE(2,37)
C     ..........  END OF PRINTOUT HEADING  ..........
C
   99 CONTINUE
      R1=0.395
      R2=0.476
      RAV=0.5*(R2+R1)
      D1=10.236
      D2=10.617
      IF(T.EQ.7.) D2=11.01
      DE=1.47
      C1=1.0
      G1=1.0
      C3=1.0
      G3=1.0
      C2=0.0928
      C4=0.0928
      G2=8.92
      G4=8.92
      XL=120.0
      Y2=0.917
      Y4=0.917
C
C     PRANDTL NUMBER EXPONENT ACCORDING HEATING OR COOLING
      NEXPR=0.3
      IF(TEMTUO.LT.TEMSHL) NEXPR=0.4
C
C     SHELL SIDE TRANSVERSE AREAS FOR B.S.R.A. CORRELATION OF H3
      V1=TOTFL1/(3.1416*R1**2*T)
      S8=19.22
      V3=TOTFL3/S8
```

```
      EXPERIMENTAL OVERALL HEAT TRANSFER COEFFICIENT
      IF(KFLOW.EQ.1) GO TO  110
      X1=ABS(TEMTUO-TEMSHL)
      X2=ABS(TTOUT-TSOUT)
      GO TO 120
      DTLOG=(X1-X2)/ALOG(X1/X2)
  110 X3=ABS(TEMTUO-TSOUT)
      X4=ABS(TTOUT-TEMSHL)
      DTLOG=(X3-X4)/ALOG(X3/X4)
  120 QAVG=.5*(TOTFL1*(ABS(TEMTUO-TTOUT))+TOTFL3*(ABS(TEMSHL-TSOUT)))
      UEXP=QAVG/(297.82*T*DTLOG)
C
  122 CONTINUE
      TAV=0.5*(TEMTUO+TEMSHL)
      CALL VSCTEM(TAV,U)
      RN1=V1*2.*R1/U
      CALL THTCOE(RN1,TAV,R1,XL,U,H1,HK1,NEXPR,FACTOR)
      RN3=V3*2.*R2/U
      CALL SHTCOE(RN3,TAV,R2,U,H3,HK3)
C
C     OVERALL COEFFICIENT OF HEAT TRANSFER BASED ON INSIDE TUBE AREA
      UHINV=1./H1+(R2-R1)/(Y2*RAV/R1)+1./(H3*R2/R1)
      UH=1./UHINV
      AT=6.2832*R1*XL*T
      FGC1=TOTFL1*G1*C1
      FGC3=TOTFL3*G3*C3
      Z=FGC1/FGC3
      IF(TEMTUO.LT.TEMSHL) GO TO 74
      IF(Z.EQ.1.0) GO TO 72
      A5=EXP(UH*AT*(1.-Z)/FGC1)
      TEMT=(TEMTUO*(1.-Z)+(A5-1.)*TEMSHL)/(A5-Z)
      GO TO 73
   72 A6=UH*AT/FGC1
      TEMT=(TEMTUO+A6*TEMSHL)/(1.+A6)
   73 TEMS=Z*(TEMTUO-TEMT)+TEMSHL
      GO TO 76
   74 Z=1.0/Z
      IF(Z.EQ.1.0) GO TO 75
      A5=EXP(UH*AT*(1.-Z)/FGC3)
      TEMS=(TEMSHL*(1.-Z)+(A5-1.)*TEMTUO)/(A5-Z)
      GO TO 77
   75 A6=UH*AT/FGC3
      TEMS=(TEMSHL+A6*TEMTUO)/(1.0+A6)
   77 TEMT=Z*(TEMSHL-TEMS)+TEMTUO
   76 CONTINUE
      WRITE(2,15)KFLOW,NODOSX,STEPT,FACTOR,TEMT,TEMS,RN1,H1,RN3,H3
      TAVT=0.5*(TEMTUO+TEMT)
      TAVS=0.5*(TEMS+TEMSHL)
      CALL VSCTEM(TAVT,U)
      RN1=V1*2.*R1/U
      CALL THTCOE(RN1,TAVT,R1,XL,U,H1,HK1,NEXPR,FACTOR)
      CALL VSCTEM(TAVS,U)
      RN3=V3*2.*R2/U
      CALL SHTCOE(RN3,TAVS,R2,U,H3,HK3)
```

```
      H1EX=1./(1./UEXP-(R1/R2)/H3-.07922)
      IF(ABS(H1EX-H1).LT..0001) GO TO 88
C
      FACTOR=FACTOR*H1EX/H1
      GO TO 122
   88 UHINV=1./H1+(R2-R1)/(Y2*RAV/R1)+1./(H3*R2/R1)
C     H.T.C. BY EAGLE AND FERGUSON CORRELATION
      H1EF=0.00003035*(TAVT+70.)*V1**0.80345
      UH=1./UHINV
      UHEF =1./H1EF+(R2-R1)/(Y2*RAV/R1)+1./(H3*R2/R1)
      UHEF=1./UHEF
C
      V3SS=V3
      V1SS=V1
      V=V3SS/V1SS
      IF(KFLOW.EQ.1) V =-V
      XLT=XL
      STEPX=1.0/(NODOSX-1)
      NODOST =(TIMAX*V1/(XL*STEPT))+0.5
      NXP2=NODOSX+2
      NXP1=NODOSX+1
      NXM1=NODOSX-1
      WRITE(2,15) KUPSET,KVEL,TOTFL1,TOTFL3,TEMTUO,TEMSHL,RN1,H1,RN3,H3
      WRITE(2,15) LEVEL,NODOST,AMP1,AMP3,ITOUT,ISOUT,FREQ,UEXP ,T,UH
      WRITE(2,15)NWRITE,NODOST,A5,A6,U,H1EF,UHEF,H1EX
   15 FORMAT(1H0,2(I5),3X,8(F11.5,2X))
C
C     DIFFERENTIAL EQUATIONS COEFFICIENTS
C
      P1=2.*H1/(R1*G1*C1)
      P2=2.*R1*H1/(G2*C2*(R2**2-R1** 2))
      P3=P2*R2*H3/(R1*H1)
      P4=2.*T*R2*H3/((D1*D1/4.-37.*R2*R2)*G3*C3)
      P5=D1*H3/((D1*D1/4.-37.*R2*R2)*G3*C3)
      P6=4.*D2*H3/(G4*C4*(D2**2-D1**2))
      P7=S8/(3.1416*(D1*D1/4.-37.*R2*R2))
      WRITE(2,50)P1,P2,P3,P4,P5,P6 ,P7
   50 FORMAT (1H ,//,8(F12.6,/))
C     PARAMETER NORMALIZATION
      X=XL/V1
      PN1SS=P1*X
      PN2SS=P2*X
      PN3SS=P3*X
      PN4SS=P4*X
      PN5SS=P5*X
      PN6SS=P6*X
      V3=V3/V3SS
      V1=V1/V1SS
      XL=1.0
      DELTT=TEMTUO-TEMSHL
      IF(DELTT.LT.0.) GO TO 55
      TEMTUO=1.0
      TEMREF=TEMSHL
      TEMSHL=0.0
      GO TO 60
```

```
   55 TEMREF=TEMTUO
      TEMSHL=1.0
      TEMTUO=0.
   60 CONTINUE
      DELTT=ABS(DELTT)
C
C     COEFFICIENTS OF THE SIMPLIFIED EQUATIONS SYSTEM (S.S. CONDITION)
C
      DENOM=PN2SS+PN3SS
      A1=PN1SS*(1.-PN2SS/DENOM)
      A2=PN1SS*PN3SS/DENOM
      A3=PN4SS*(1.-PN3SS/DENOM)
      A4=PN4SS*PN2SS/DENOM
      WRITE(2,50)A1,A2,A3,A4,V1SS,V3SS,V
C
C     EVALUATION OF THE STEADY STATE SOLUTION (ANALYTIC APPROACH)
C
      ROOT= -A1-A3/(V*P7)
      IF(ABS(ROOT).LT.0.000001) GO TO 101
      IF(KFLOW.NE.1) GO TO 70
      AA2=(TEMSHL-TEMTUO)/(EXP( ROOT)*(1.+ROOT/A1)-1.)
      GO TO 80
   70 AA2=(TEMSHL-TEMTUO)/(ROOT/A1)
   80 AA1=TEMTUO-AA2
      BB2=(1.+ROOT*V1/A1)*AA2
      BB1=AA1
  101 WRITE(2,50)AA1,AA2,BB1,BB2,TEMTUO,TEMSHL,ROOT,EXPO
      WRITE(2,100)
  100 FORMAT(1H0,'*****STEADY STATE TEMPERATURE PROFILES*****'//
     1' TIMESTEP  DISTSTEP   TTUBE FLUID  TTUBE WALL     TSHELLFUID  TS
     2ELLWALL   EXPON ')
C
C     SCHEME TO EXTRAPOLATE ONE POINT AT EACH END OF THE EXCHANGER
C
      J=1
      ITREAL=J-1
      DO 200 I=1,NXP2
      IF(ABS(ROOT).LT.0.000001) GO TO 115
      EXPON=EXP(+ROOT*STEPX*(I-2))
      T1(I,J)=AA1+AA2*EXPON
      T3(I,J)=BB1+BB2*EXPON
      GO TO 130
  115 IF(TEMTUO.LT.TEMSHL) GO TO 125
      T1(I,J)=1.-(A1/(1.+A1))*STEPX*(I-2)
      T3(I,J)=(A1/(1.+A1))*(1.-STEPX*(I-2))
      GO TO 130
  125 T1(I,J)=(A1/(A1+1.))*STEPX*(I-2)
      T3(I,J)=1.-(A1/(1.+A1))*(1.-STEPX*(I-2))
  130 CONTINUE
      TI=T1(I,J)*DELTT+TEMREF
      TO=T3(I,J)*DELTT+TEMREF
      T2(I,J)=P2/(P2+P3)*T1(I,J)+P3/(P2+P3)*T3(I,J)
      TW=T2(I,J)*DELTT+TEMREF
      T4(I,J)= T3(I,J)
      TS=T4(I,J)*DELTT+TEMREF
```

```
      IREAL=I-2
      IF(NWRITE.NE.1) GO TO 193
      WRITE(2,15)ITREAL,IREAL,T1(I,J),T2(I,J),T3(I,J),T4(I,J),DELTT,TEM
     1REF,EXPON
      GO TO 200
  193 WRITE(2,15)ITREAL,IREAL,TI,TW,TO,TS,DELTT,TEMREF
  200 CONTINUE
      JUMP=60./FREQ*1./X*200./16.
C
C     SOLUTION OF TRANSIENT STATE BY FINITE DIFFERENCES APPROACH
C
      WRITE(2,250)
  250 FORMAT(1H0,'*****TRANSIENT STATE TEMPERATURE PROFILES *****'///)
      TIME=0.0
      TAU=1.3
      VRESP=1.0
      TLIMIT=20.*TAU
      NTP1=NODOST+1
      J=2
      JM1=J-1
      DO 400 K=2,NTP1
      KM1=K-1
      IF(KUPSET.NE.1) GO TO 222
C
C     INCLUSION OF CONTROL VALVE TRANSIENT RESPONSE
C     THE VALVE RESPONSE IS APPROXIMATED BY A CRITICALLY DAMPED
C     SECOND ORDER  SYSTEM WHOSE CHARACTERISTIC TIME IS =TAU
C     LEVEL=0 MEANS LINEARISED DISTURBANCE AND NO VALVE EFFECTS
C     LEVEL=1 MEANS NON-LINEAR DISTURBANCE AND NO VALVE EFFECTS
C     LEVEL=2 MEANS LINEAR DISTURBANCE PLUS VALVE EFFECTS
C     LEVEL=3 MEANS  NON-LINEARISED DISTURBANCE PLUS VALVE EFFECTS
C
      IF(LEVEL-2)  210 , 251 , 251
  251 TIME=X*KM1*STEPT
      IF(TIME.GT.TLIMIT) GO TO 258
      VRESP=1.-(1.+TIME/TAU)*EXP(-TIME/TAU)
  210 V1=1.+AMP1*VRESP
  220 V3=1.+AMP3*VRESP
      IF(K.GT.2.AND.LEVEL.EQ.0) GO TO 258
      IF(LEVEL.EQ.1.OR.LEVEL.EQ.3) GO TO 212
      GO TO 211
  222 IF(LEVEL.EQ.3.OR.LEVEL.EQ.1) GO TO 223
C     UPDATING COEFFICIENTS ACCORDING LINEARISED DISTURBANCE
      CALL DISTUR(KUPSET,STEPT,FREQ,AMP1,AMP3,V1,V1SS,V3,V3SS,XLT,KM1,
     1KVEL)
  211 CONTINUE
      V1T=1.+HK1*(V1-1.)
      V3T=1.+HK3*(V3-1.)
      GO TO 225
C
  212 IF(LEVEL.EQ.1.AND.K.GT.2) GO TO 258
      GO TO 224
  223 CALL DISTUR(KUPSET,STEPT,FREQ,AMP1,AMP3,V1,V1SS,V3,V3SS,XLT,KM1,
     1KVEL)
```

```
      UPDATING COEFFICIENTS ACCORDING NON-LINEAARISED DISTURBANCE
  224 CONTINUE
      V1T=V1**HK1
      V3T=V3**HK3
  225 CONTINUE
      P1=PN1SS*V1T
      P2=PN2SS*V1T
      P3=PN3SS*V3T
      P4=PN4SS*V3T
      P5=PN5SS*V3T
      P6=PN6SS*V3T
C
  258 CONTINUE
      DO 300 I=2,NXP1
      IM1=I-1
      IP1=I+1
      IF(I.NE.2) GO TO 260
      T1(I,J)=TEMTUO
      GO TO 270
  260 TERM1=P1*(T2(I,JM1)-T1(I,JM1))
      TERM2=V1*(T1(IP1,JM1)-T1 (IM1,JM1))/(2.*STEPX)
C
      T1(I,J)=T1(I,JM1)+STEPT*(TERM1-TERM2)
C
  270 TERM3=P2*(T1(I,JM1)-T2(I,JM1))
      TERM4=P3*(T2(I,JM1)-T3(I,JM1))
C
      T2(I,J)=T2(I,JM1)+STEPT*(TERM3-TERM4)
C
      IF(KFLOW.EQ.1.AND.I.EQ.NXP1) GO TO 280
      IF(KFLOW.NE.1.AND.I.EQ.2) GO TO 288
      GO TO 285
  280 T3(I,J)=TEMSHL
      GO TO 295
  288 T3(I,J)= TEMSHL
      GO TO 295
  285 TERM5=-V*P7*V3* (T3(IP1,JM1)-T3(IM1,JM1))/(2.*STEPX)
      TERM6=P4*(T2(I,JM1)-T3(I,JM1))
      TERM7=P5*(T3(I,JM1)-T4(I,JM1))
C
      T3(I,J)=T3(I,JM1)+STEPT*(TERM5+TERM6-TERM7)
C
  295 TERM8=P6*(T3(I,JM1)-T4(I,JM1))
      T4(I,J)=T4(I,JM1)+STEPT*TERM8
  300 CONTINUE
C
C     EXTRAPOLATED POINTS CALCULATION (OUTSIDE EXCHANGER LIMITS)
C
      T1(1,J)=2.* T1(2,J)-T1(3,J)
      T1(NODOSX+2,J)=2.*T1(NODOSX+1,J)-T1(NODOSX   ,J)
      T2(1,J)=2.*T2(2,J)-T2(3,J)
      T2(NODOSX+2,J)=2.*T2(NODOSX+1,J)-T2(NODOSX   ,J)
      T3(1,J)=2.*T3(2,J)-T3(3,J)
      T3(NODOSX+2,J)=2.*T3(NODOSX+1,J)-T3(NODOSX,J)
```

```
      T4(1,J)=2.*T4(2,J)-T4(3,J)
      T4(NODOSX+2,J)=2.*T4(NODOSX+1,J)-T4(NODOSX   ,J)
      NXP2=NODOSX+2
      IF(K.EQ.2)GO TO 290
      IF(MOD(KM1,JUMP).EQ.0)GO TO 290
      IF(K.EQ.NODOST+1) GO TO 290
      GO TO 366
  290 DO 365 I=1,NXP2
      IREAL=I-2
      IF(IREAL.EQ.0.OR.IREAL.EQ.NXM1   )GO TO 310
      GO TO 365
  310 TI=T1(I,J)*DELTT+TEMREF
      TW=T2(I,J)*DELTT+TEMREF
      TO=T3(I,J)*DELTT+TEMREF
      TS=T4(I,J)*DELTT+TEMREF
      HKM1=KM1
      TIMEN=HKM1*STEPT
      RTIME=TIMEN*X
      IF(NWRITE.NE.1) GO TO 315
      WRITE (2,15)KM1,IREAL,T1(I,J),T2(I,J),T3(I,J),T4(I,J),V1T,V3T,
     1RTIME,TIMEN
      GO TO 365
C
  315 WRITE(2,15) KM1,IREAL,TI,TW,TO,TS,V1T,V3T,RTIME,TIMEN
  365 CONTINUE
  366 DO 400 I=1,NXP2
      T1(I,1)=T1(I,J)
      T2(I,1)=T2(I,J)
      T3(I,1)=T3(I,J)
      T4(I,1)=T4(I,J)
  400 CONTINUE
      GO TO 1
      END
C
C
      SUBROUTINE THTCOE(RN1,TEMP,R1,XL,U,H1,HK1,NEXP,FACTOR)
      Y1=0.001419+0.000002216*TEMP
      IF(RN1.LT.2100.)GO TO 430
      IF (RN1.GT.2100.0.AND.RN1.LT.10000.0)GO TO 435
      IF(RN1.GT.10000.)GO TO 440
  430 H1=1.86*(RN1*U/Y1*2.*R1/XL)**.33*(Y1/(2.*R1))
      HK1=.33
      GO TO 450
  435 H1=.116*(RN1**.66-125.)*(U/Y1)**.33*(1.+(2.*R1/XL)**.66)*Y1/(2.*
     1R1)
      HK1=.66
      GO TO 450
  440 H1=.023*RN1**.8*(U/Y1)**NEXPR*Y1/(2.*R1)
      HK1=.8
  450 H1=H1*FACTOR
      RETURN
      END
```

```
      SUBROUTINE SHTCOE(RN3,TEMP,R2,U,H3,HK3)
      Y1=0.001419+0.000002216*TEMP
C     CORRELATION BY THE R.S.R.A. FOR SHELLSIDE
C     CORRECTION FACTORS LUMPED IN THE NUMERICAL COEFFICIENT
      H3=.281*RN3**.6*(U/Y1)**.333*Y1/(2.*R2)
      HK3=.6
      RETURN
      END
C
C
      SUBROUTINE DISTUR(KUPSET,STEPT,FREQ,AMP1,AMP3,V1,V1SS,V3,V3SS,XLT
     1KM1,KVEL)
      IF(KVEL-2)10,10,20
   10 V1=(1.+AMP1*SIN(FREQ*6.283185/60.*XLT/V1SS*KM1*STEPT) )
      IF(KVEL.EQ.1)GO TO 30
   20 V3=(1.+ AMP3*SIN(FREQ*6.283185/60.*XLT/V1SS*KM1*STEPT))
   30 RETURN
      END
C
C
      SUBROUTINE VSCTEM(AVT,U)
      UINV=2.148*((AVT-8.435)+(8078.4+(AVT-8.435)**2)**.5)-120.
      U= 1./UINV
      RETURN
      END
```

```
C     FREQUENCY RESPONSE SOLUTION OF HEAT EXCHANGER MODEL
C
      COMPLEX DEN,B1,B2,B3,B4,D1,D2,D3,D4,B8,AC,RAD,M1,M2,EXP1,EXP2
      COMPLEX EXP12,EXP23,EXP31,H,G,G1,G2,G3,GG,GG1,GG2,GG3,NUM1,DEN1
      COMPLEX T1V,NUM2,DEN2,T2V,E,E1,E2,E3,EE,EE1,EE2,EE3,P
      COMPLEX T1V1,T1V2,T2V1,T2V2
      REAL NEXPR,M3
C
    1 READ(1,* )TOTFL1,TOTFL3,TEMTUO,TEMSHL,OMIN,OMAX,XL,T,FCTR
      READ(1,* )KFLOW,KVEL
      WRITE(2,33)
   33 FORMAT(1H1, '*****  RESULTS  *****'//' INPUT  DATA  AND  INTERMED
     1ATE   RESULTS' //)
      WRITE(2,44) TOTFL1,TOTFL3,TEMTUO,TEMSHL,XL,T
   44 FORMAT(1H0/8(3X,F16.6/))
C
      R1=0.395
      R2=0.476
      RAV=0.5*(R1+R2)
      DI=10.236
      DO=10.617
      IF(T.EQ.7.) DO=11.01
      DE=1.47
      C1=1.0
      GL=1.0
      C3=1.0
      C2=0.0928
      C4=0.0928
      GM=8.92
      Y2=0.917
      Y4=Y2
      NEXPR=0.3
      IF(TEMTUO.LT.TEMSHL) NEXPR=0.4
C
      FACTOR=10.**.1
      V1=TOTFL1/(3.1416*R1**2*T)
      TAV=0.5*(TEMTUO+TEMSHL)
      CALL VSCTEM(TAV,U)
      RN1=V1*2.*R1/U
      CALL THTCOE(RN1,TAV,R1,XL,U,H1,HK1,NEXPR)
      H1=H1*FCTR
      V3=TOTFL3/19.22
      RN3=V3*2.*R2/U
      CALL SHTCOE(RN3,TAV,R2,U,H3,HK3)
C
C     OVERALL HEAT TRANSFER COEFFICIENT BASED ON INSIDE TUBE AREA
      UHINV=1./H1+(R2-R1)/(Y2*RAV/R1)+1./(H3*R2/R1)
      UH=1./UHINV
      AT=6.2832*R1*XL*T
      FGC1=TOTFL1*GL*C1
      FGC3=TOTFL3*GL*C3
      Z=FGC1/FGC3
      IF(TEMTUO.LT.TEMSHL) GO TO 74
      IF(Z.EQ.1.0) GO TO 72
      A5=EXP(UH*AT*(1.-Z)/FGC1)
```

```
      TEMT=(TEMTUO*(1.-Z)+(A5-1.)*TEMSHL)/(A5-Z)
      GO TO 73
   72 A5=UH*AT/FGC1
      TEMT=(TEMTUO+A5*TEMSHL)/(1.+A5)
   73 TEMS=Z*(TEMTUO-TEMT)+TEMSHL
      GO TO 76
   74 Z=1.0/Z
      IF(Z.EQ.1.0) GO TO 75
      A5=EXP(UH*AT*(1.-Z)/FGC3)
      TEMS=(TEMSHL*(1.-Z)+(A5-1.)*TEMTUO)/(A5-Z)
      GO TO 77
   75 A5=UH*AT/FGC3
      TEMS=(TEMSHL+A5*TEMTUO)/(1.0+A5)
   77 TEMT=Z*(TEMSHL-TEMS)+TEMTUO
   76 CONTINUE
      WRITE(2,15) KFLOW ,KVEL,TEMT,TEMS,H1,H3,UH,Z,A5
   15 FORMAT(1H0,/ 2(I6),3X,7(F12.6,3X) )
C
      TAVT=0.5*(TEMTUO+TEMT)
      TAVS=0.5*(TEMS+TEMSHL)
      CALL VSCTEM(TAVT,U)
      RN1=V1*2.*R1/U
      CALL THTCOE(RN1,TAVT,R1,XL,U,H1,HK1,NEXPR)
      H1=H1*FCTR
      CALL VSCTEM(TAVS,U)
      RN3=V3*2.*R2/U
      CALL SHTCOE(RN3,TAVS,R2,U,H3,HK3)
      UHINV=1./H1+(R2-R1)/(Y2*RAV/R1)+1./(H3*R2/R1)
      UH=1./UHINV
      WRITE(2,44)RN1,H1,RN3,H3,UH,V1,V3
C
      OMEGA= 0.001
      T1V1=CMPLX(0.0,0.0)
      T1V2=CMPLX(0.0,0.0)
      T2V1=CMPLX(0.0,0.0)
      T2V2=CMPLX(0.0,0.0)
      B1T=2./(R1*GL*C1)*H1
      BT1=2.0*R1/(GM*C2*(R2*R2-R1*R1))*H1
      BT2=2.*R2/(GM*C2*(R2*R2-R1*R1))*H3
      B2T=2.*T*R2/((DI*DI/4.-37.*R2*R2)*GL*C3)*H3
      BS2=H3*DI/((DI*DI/4.-37.*R2*R2)*GL*C3)
      B2S=4.*DO/(GM*C4*(DO*DO-DI*DI))*H3
      P7=19.22/(3.1416*(DI*DI/4.-37.*R2*R2))
      V2=V3
      A1 = V1*(BT1+BT2)/(B1T*BT2)
      A2 = V2*(BT2+BT1)/(BT1*B2T)
      M3=-(A1+A2)/(A1*A2)
      EXP3=EXP(M3*XL)
      IF(KFLOW.NE.1)GO TO 160
      AA1=(TEMSHL-TEMTUO)/((1.+A1*M3)*EXP3-1.)
      GO TO 180
  160 AA1=(TEMSHL-TEMTUO)/(A1*M3)
  180 AA2=TEMTUO-AA1
      WRITE(2,44)B1T,BT1,BT2,B2T,BS2,B2S,P7,M3
      WRITE(2,44)A1,A2,V2,FCTR,HK1,HK3,AA1,AA2
```

```
   10 P=CMPLX(0.0,OMEGA)
      DEN = P+BT1+BT2
      B1 = P+B1T*(P+BT2)/DEN
      B2 = BT2*B1T/DEN
      B3 = HK3*B2
      B4 = HK1*BT1*B1T/DEN + B1T*(1.-HK1)
      D1 = P*(1.+B2S/(P+BS2))+B2T*(P+BT1)/DEN
      D2 = B2T*BT1/DEN
      D3 = HK3*B2T*BT2/DEN +B2T*(1.-HK3)
      D4 = HK1*D2
C
      BB=V1*D1+B1*V2
      AC=4.*V1*V2*(B1*D1-B2*D2)
      RAD=CSQRT(BB**2-AC)
      M1=(-BB+RAD)/(2.*V1*V2)
      M2=(-BB-RAD)/(2.*V1*V2)
      EXP2=CEXP(M2*XL)
      EXP1=CEXP(M1*XL)
      EXP12=EXP1*EXP2
      EXP23=EXP2*EXP3
      EXP31=EXP3*EXP1
      F=-V1*M3*AA1/B1T
      F1=-(V2*AA1*M3)*(1.+A1*M3)/B2T
      H=(V1*V2*M3**2+BB*M3+(B1*D1-B2*D2))**(-1)
C
      IF(KVEL-2)100,100,200
  100 G=B2*D4+B4*D1
      G1=G+B4*V2*M1
      G2=G+B4*V2*M2
      G3=G+B4*V2*M3
C
      GG=B4*D2+B1*D4
      GG1=GG+D4*V1*M1
      GG2=GG+D4*V1*M2
      GG3=GG+D4*V1*M3
C
      IF(KFLOW.NE.1)GO TO 400
      NUM1=G1*(M3-M2)*EXP23+G2*(M1-M3)*EXP31+G3*(M2-M1)*EXP12
      DEN1=(B1+V1*M1)*EXP1-(B1+V1*M2)*EXP2
      T1V1=F*H*V1*NUM1/DEN1
C
      NUM2=GG1*(M3-M2)*EXP23+GG2*(M1-M3)*EXP31+GG3*(M2-M1)*EXP12
      DEN2=(B1+V1*M1)*EXP2-(B1+V1*M2)*EXP1
      T2V1=F*H*V1*NUM2/DEN2
      IF(KVEL.EQ.2) GO TO 200
      GO TO 900
C
  400 NUM1=G3*(M1-M2)*V1*(EXP3-EXP2)+(G3*(B1+V1*M2)-B2*GG3)*(EXP1-EXP2
      T1V1=F*H*NUM1/(V1*(M1-M2))
C
      NUM2=GG3*(M1-M2)*V2*(EXP3-EXP2)+(GG3*(D1+V2*M2)-G3*D2)*(EXP1-EXP
      T2V1=F*H*NUM2/(V2*(M1-M2))
      IF(KVEL.EQ.2) GO TO 200
      GO TO 900
```

```
  200 E=B2*D3+B3*D1
      E1=E+B3*V2*M1
      E2=E+B3*V2*M2
      E3=E+B3*V2*M3
C
      EE=B3*D2+B1*D3
      EE1=EE+D3*V1*M1
      EE2=EE+D3*V1*M2
      EE3=EE+D3*V1*M3
C
      IF(KFLOW.NE.1)GO TO 600
      NUM1=E1*(M3-M2)*EXP23+E2*(M1-M3)*EXP31+E3*(M2-M1)*EXP12
      DEN1=(B1+V1*M1)*EXP1-(B1+V1*M2)*EXP2
      T1V2=F1*H*V1*NUM1/DEN1
      NUM2=EE1*(M3-M2)*EXP23+EE2*(M1-M3)*EXP31+EE3*(M2-M1)*EXP12
      DEN2=(B1+V1*M1)*EXP2-(B1+V1*M2)*EXP1
      T2V2=F1*H*V1*NUM2/DEN2
      GO TO 900
C
  600 NUM1=E3*(M1-M2)*V1*(EXP3-EXP2)
      NUM1=NUM1+(E3*(B1+V1*M2)-B2*EE3)*(EXP1-EXP2)
      T1V2=F1*H*NUM1/(V1*(M1-M2))
C
      NUM2=EE3*(M1-M2)*V2*(EXP3-EXP2)
      NUM2=NUM2+(EE3*(D1+V2*M2)-D2*E3)*(EXP1-EXP2)
      T2V2=F1*H*NUM2/(V2*(M1-M2))
C
  900 T1V=T1V1+T1V2
      T2V=T2V1+T2V2
C
      EVALUATION OF GAIN AND PHASE ANGLE
      GT1V =CABS(T1V)
      GT2V =CABS(T2V)
      IF(OMEGA.EQ..001) GO TO 910
      GT1V=GT1V/GT1REF
      GT2V=GT2V/GT2REF
      GO TO 915
  910 GT1REF=GT1V
      GT2REF=GT2V
      OMEGA=OMIN
      GO TO 10
  915 FT1V =57.29578*ATAN2(AIMAG(T1V),REAL(T1V))
      FT2V =57.29578*ATAN2(AIMAG(T2V),REAL(T2V))
      WRITE(2,40)OMEGA,GT1V,FT1V,GT2V,FT2V
   40 FORMAT(1H0,5(F14.6,5X))
      IF(OMEGA.LT.1.0) OMEGA=OMEGA*FACTOR
      IF (OMEGA.GE.1.0)  OMEGA=OMEGA+0.1
      IF(OMEGA-OMAX)920,930,930
  920 GO TO 10
  930 GO TO 1
      END
```

APPENDIX C

Error in the Heat Transfer Coefficient Linearisation

Error produced by linearization of the heat transfer coefficient-fluid velocity ratio, as function of the magnitude of the velocity change and the exponent constant, n.

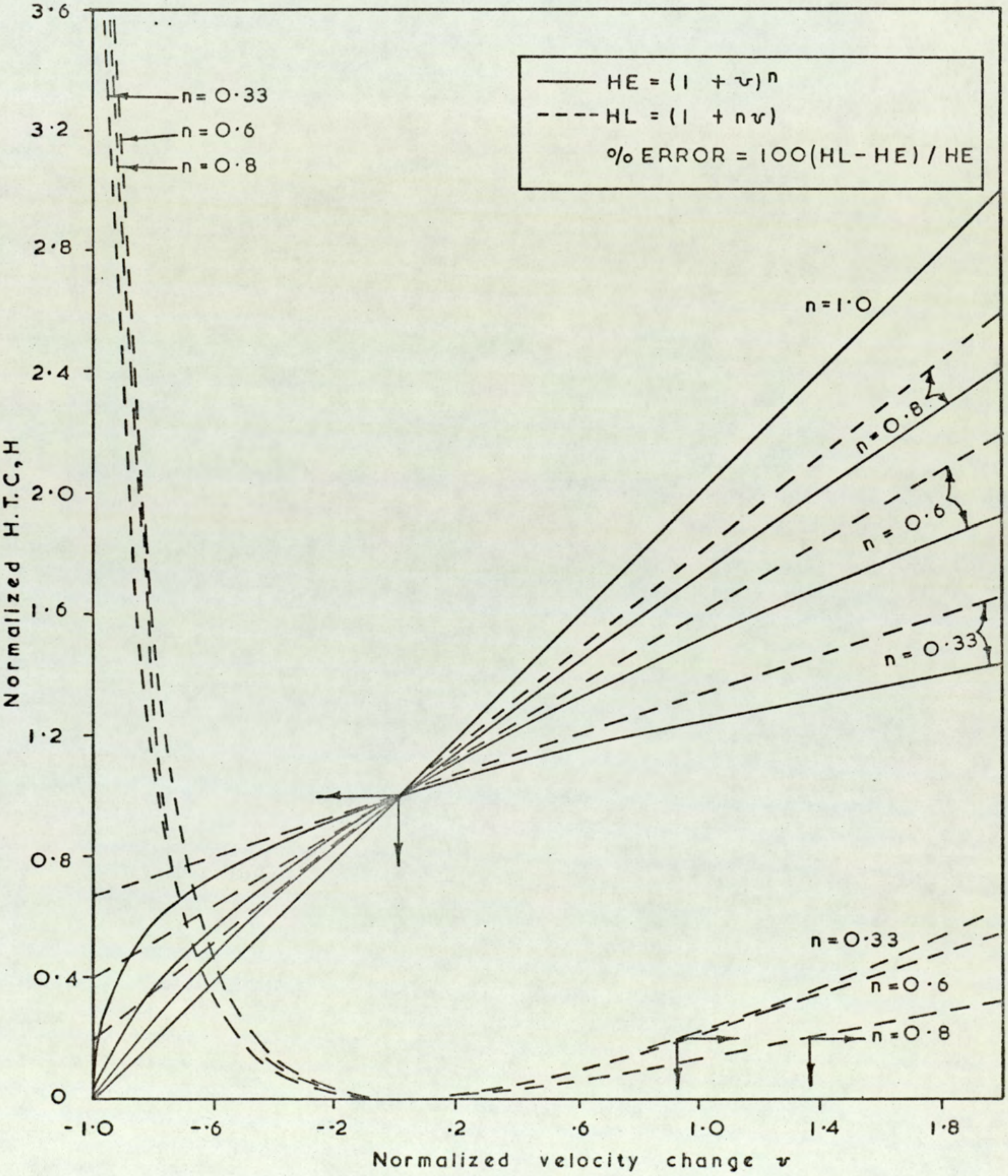

Fig. C1 Error in the Heat Transfer Coefficient Linearisation.

APPENDIX D

This Appendix demonstrates why the outlet temperatures of a heat exchanger diverge for any positive simultaneous change in both fluid velocities, and consequently converge for any negative change. The demonstration is equally valid for countercurrent and parallel flow.

Assuming T_{10} and T_{11} input and output temperatures of the hot stream; T_{20} and T_{21} input and output temperatures of the cold stream, G_1, G_2 the respective mass flows and C_1, C_2 the corresponding specific heats, for an adiabatic system the following enthalpy balance with T_{20} taken as the reference temperature, holds:

$$G_1C_1(T_{10} - T_{20}) = (T_{11} - T_{20})\, C_1G_1 + (T_{21} - T_{20})\, C_2G_2 \qquad \text{(D.1)}$$

Defining the three temperature differences as

θ_o, θ_1 and θ_2 respectively and solving the previous equation for θ_1, results in

$$\theta_1 = \theta_o - \frac{C_2G_2}{C_1G_1} \quad \theta_2 \qquad \text{(L.2)}$$

Suppose further that the ratio of fluid flows is maintained and constant when a change in flow is made,

$$\text{i.e.,}\ G_2 = K\, G_1 \qquad \text{(D.3a)}$$

and

$$(G_2 + \Delta G_2) = K(G_1 + \Delta G_1) \qquad \text{(D.3b)}$$

Obviously the increase of enthalpy of the cold stream, is equal to the heat transferred through the tube wall

$$\text{or} \quad \theta_2 . C_2 . G_2 = C_1 . G_1(\theta_o - \theta_1) \qquad \text{(D.4)}$$

and $$\theta_2 = \frac{C_1G_1}{C_2G_2}(\theta_o - \theta_1) \tag{D.5}$$

Now, if equations (.2) and (.5) are rewritten for the situation after a simultaneous change in both fluids is made, they become

$$\theta_1 + \Delta\theta_1 = \theta_o - \frac{C_2(G_2 + \Delta G_2)}{C_1(G_1 + \Delta G_1)}(\theta_2 + \theta_2) \tag{D.6}$$

and

$$\theta_2 + \Delta\theta_2 = \frac{C_1(G_1 + \Delta G_1)}{C_2(G_2 + \Delta G_2)}(\theta_o - (\theta_1 + \Delta\theta_1)) \tag{D.7}$$

Now, noticing that

$$\frac{C_2(G_2 + \Delta G_2)}{C_1(G_1 + \Delta G_1)} = \frac{C_2G_2}{C_1G_1} = K\left(\frac{C_2}{C_1}\right)$$

then by subtraction of (D.2) from (D.6)

$$\Delta\theta_1 = -K\frac{C_2}{C_1}\Delta\theta_2 = -K_1\Delta\theta_2$$

Similar procedure on (D.7) yields the same result, which shows that any change of temperature produced on one side of the exchanger as a result of simultaneous flow changes is accompanied by a proportional one but of opposite sign in the other side.

GENERAL VIEW OF THE EQUIPMENT

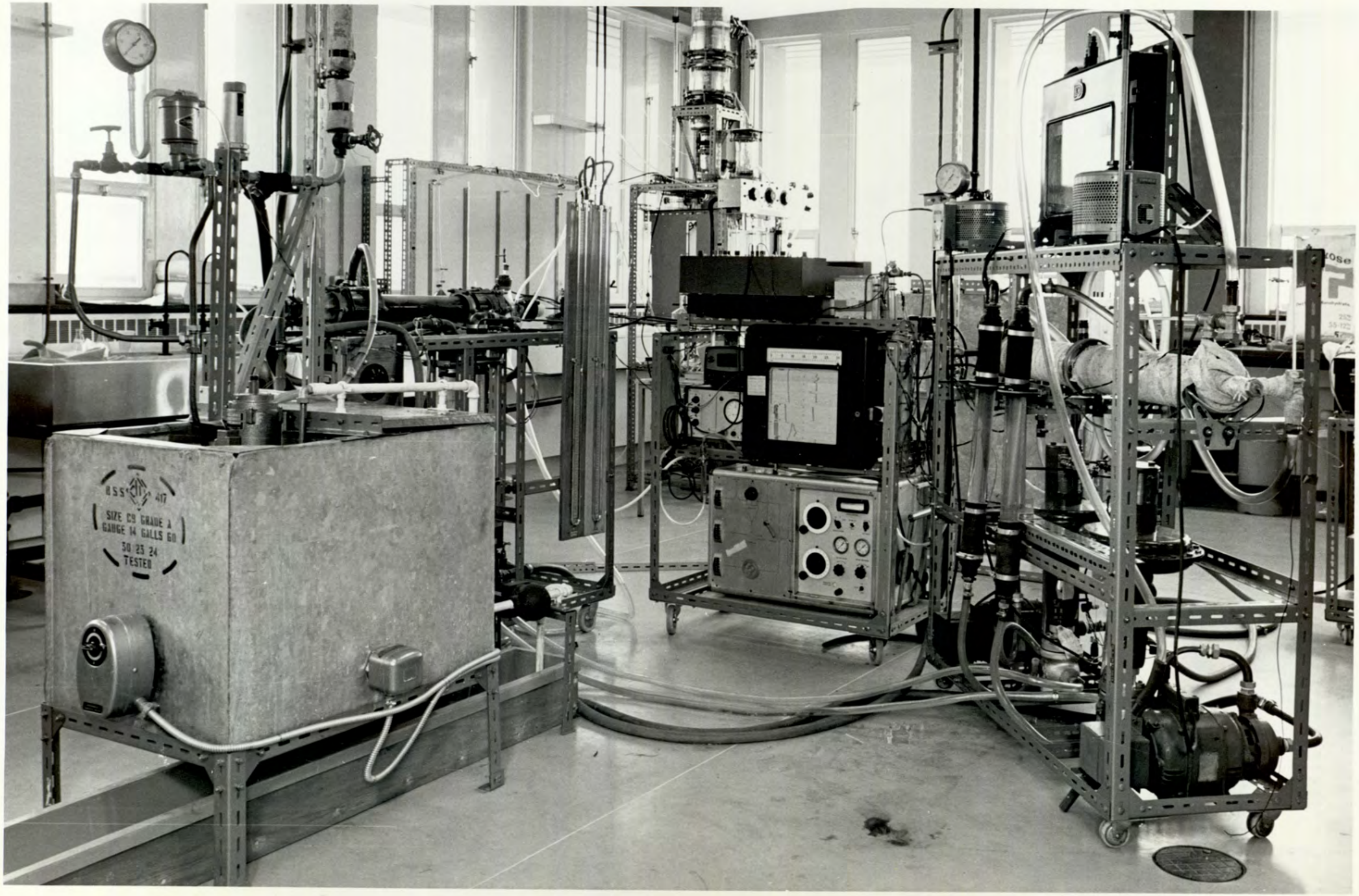
B.S.S. 417
SIZE C9 GRADE A
GAUGE 14 GALLS 60
50 25 24
TESTED

HEAT EXCHANGER

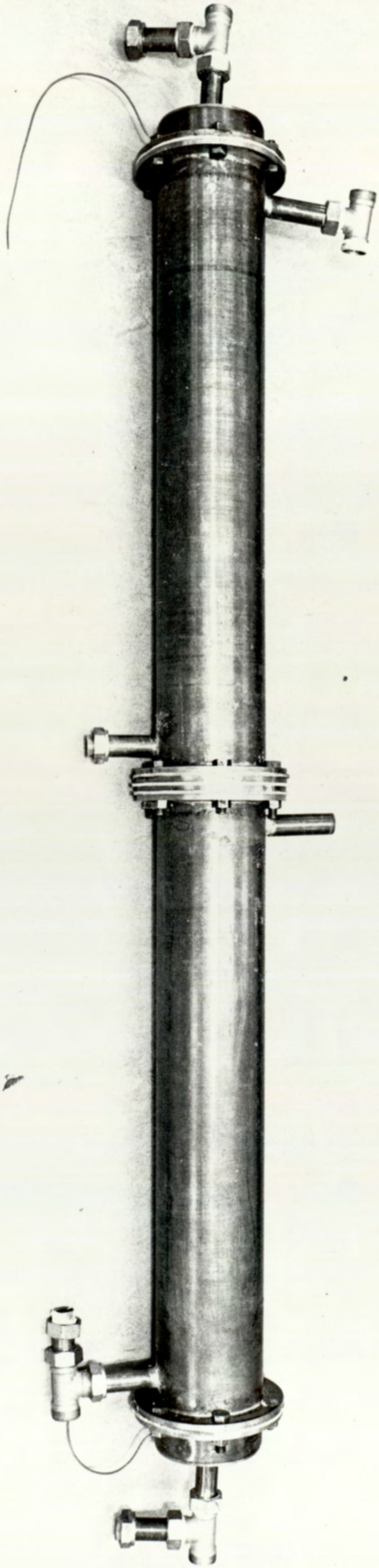

SHELL AND TUBES BUNDLE